Synthesis of Bio-lubricant Basestocks: Substitute to Conventional Lubricants

Thesis submitted in partial fulfillment of the requirements for the degree of

DOCTOR OF PHILOSOPHY

by

Venu Babu Borugadda

Department of Chemical Engineering

Indian Institute of Technology Guwahati

Guwahati - 781039, India

Synthesis of Bio-lubricant Basestocks: Substitute to Conventional Lubricants

Venu Babu Borugadda

Synthesis of Bio-Lubricant Basestocks: Substitute to Conventional Lubricants

Thesis submitted in partial fulfillment of the requirements for the degree of

DOCTOR OF PHILOSOPHY

by

Venu Babu Borugadda
Roll No.: 11610702

Department of Chemical Engineering
Indian Institute of Technology Guwahati
Guwahati - 781039, India

September, 2015

Asato maa sad-gamaya
Tamaso maa jyotir-gamaya
Mrityor-ma-amritam gamaya

"Lead me from Untruth to Truth, from Darkness to Light and from Death to Immortality"

- Brhadaranyaka Upanishad — I.iii.28

Jesus answered, "I am the way and the truth and the life. No one comes to the Father except through me"

John 14:6

For God so loved the world that he gave his one and only Son, that whoever believes in him shall not perish but have eternal life

John 3:16

Dedicated with love

To my mother Nancharamma K who lifted me from the days of my childhood. Also, to my parents, maternal uncle, sister and brother-in-law for their invaluable support and love which made me possible to come so far

&

To all my best teachers, who brought out the best in me

Department of Chemical Engineering
Indian Institute of Technology Guwahati
Guwahati - 781039, India

STATEMENT

I do hereby declare that the research findings of this thesis is the result of investigation carried out by me in the Department of Chemical Engineering, Indian Institute of Technology Guwahati, Guwahati, India, under the supervision of Dr. Vaibhav V. Goud.

In keeping with general practice of reporting scientific observations, due acknowledgements have been made wherever the research findings of other researchers have been cited in this thesis.

Date: September, 2015

Venu Babu Borugadda

Department of Chemical Engineering
Indian Institute of Technology Guwahati
Guwahati - 781039, India

CERTIFICATE

This is to certify that the thesis entitled **"Synthesis of Bio-lubricant Basestocks: Substitute to Conventional Lubricants"** submitted by **Mr. Venu Babu Borugadda (Roll No: 11610702)**, a research scholar in the Department of Chemical Engineering, Indian Institute of Technology Guwahati, for the award of the degree of Doctor of Philosophy, is a record of an original research work carried out by him under my supervision and guidance. The thesis has fulfilled all requirements as per the regulations of the institute and in our opinion has reached the standard needed for submission. The works documented in this thesis have not been submitted to any other University or Institute for the award of any degree.

(Dr. Vaibhav V Goud)
Associate Professor
Department of Chemical Engineering
Indian Institute of Technology Guwahati
Guwahati - 781039, India.

Acknowledgements

It is my immense pleasure to acknowledge my gratitude for the great help and support obtained from heaps of people in some way or another contributed to the successful completion of this endeavour. Cardinally, I am very much grateful and honor my Lord and Savior JESUS CHRIST for forgiving my sins and gave a new life which leads me to be in this conduct today. I am not a worthy person to pursue higher studies in IIT Guwahati, which is one of the premier institutes around the globe, but could achieve this position only by the abundant grace and everlasting love of Christ and His purpose for my life. However, God used many people in order to build my personal, spiritual life and academic career; in this regard, I am forever thankful to my parents (Shri Mr & Mrs. Ratnam, Shri Mr & Mrs. Subba Rao), sister and brother-in-law (Shri Mr & Mrs. Sobhan Babu), uncle (Shri Mr. Nancharaiah) and my teachers for enabling me to carry out postgraduate studies. They had never compelled me to go to employ by ceasing my studies yet in their hardships. I could certainly say, due to their constant motivation, physical and financial support, I was able to accomplish two more postgraduate degrees in my academic career.

It's my privilege to express my most sincere gratitude to my thesis supervisor Shri Dr. Vaibhav V Goud for his guidance throughout my research work. I am forever thankful to him for the way he has molded me in five constant years (2010-2015) during my academic career. I can't express in words the way he taught me, time he invested in me, opportunities and platforms he provided to me, but everyone could see that in my academic life. I entered into his research group like a mud, but he shaped me into a useful vessel throughout my academic life. I have been influenced by his guidance, valuable advices, suggestions and positive direction towards work. Without his intellectual inputs and support I might not have achieved this destination during my doctoral

research and I feel it has been a great privilege to work with him. I must also grateful to Shri Mrs. Goud and little champ Shreya for supporting Dr. Goud to spend more time in office (late nights). I am also deeply in debt with my doctoral committee members Shri Professor Pugazhenthi G, Shri Dr. Tapas Kumar Mandal of the Department of Chemical Engineering and Shri Dr. Vinayak Kulkarni, Shri Dr. Somayaji Chandramohan of the Department of Mechanical Engineering for their valuable suggestions, constructive critique time to time and contribution which helped me to improve my research work.

I express my heartfelt gratitude to Shri Professor Naik SN, Centre for rural development and technology, IIT Delhi for helping me to analyze the fatty acid composition of feedstocks and finding tribological properties for bio-lubricant basestocks. I am also thankful to Shri Professor Iyer and his research students Mr. Suresh, Mr. Bheem and Mr. Gopi from Department of Chemistry for assisting me to carry out TLC analysis and clarifying many technical doubts by sacrificing their time for me. I would like to express my sincere gratitude to Shri Dr. Mahuya De for her generous heart in allowing me to use analytical lab facilities after office hours and also to make use of various instruments with a special permission. I sincerely acknowledge the help from Shri Dr. Vimal Katiyar and his research student Mr. Arvind Gupta for providing the GPC, DSC facilities at CoE, SusPol; CIF, IIT Guwahati, for furnishing NMR facility and FIST, DST, SR/FST/ETII- 028/2010 for furnishing interfacial rheometer to Chemical Engineering Dept. IIT Guwahati. I also would love to thank all the faculty members of the Chemical Engineering Department for their kind co-operation during my stay in the department. My earnest appreciation to our department office and technical staff who had helped me in various personal and technical matters to learn and operate various instruments independently. I express my extreme thankfulness to Barak and Umiam hostel mess managers for providing feedstock (WCO, almost 20 L) at free of cost. I am pleased to thank Shri Mr. Sekhar Indupalli officer on special

duty (OSD) to the northeast and CASE constructions, Guwahati for providing different grades of conventional lubricants at free of cost.

With much appreciation and thankfulness I acknowledge the financial support from MHRD through IITG in the form of research fellowship; Department of Science and Technology (DST), New Delhi for sanctioning financial aid to attend an international conference in Brazil during August 24-28th, 2014. In regards to the Brazil trip, once again, I would like to express my heartfelt thanks to my Lord Jesus, Shri Dr. Goud, Shri Dr. Moholkar and Chemical Engineering Department; my loving and caring sister Shri Mrs. Naga Jyothi, dear brother Mr. Philip and my cheerful friends who stay in Delhi made this successful. I am also equally thankful to IITG for providing various prestigious platforms to show my research work to various renowned people in the world, such as Shri Professor CNR Rao (Bharat Ratna awardee) to whom I have presented my research work and stood as one of the ten research scholars chosen by departmental HOD's among hundreds of research scholars in IITG. Also, to be placed as one in six students chosen among six thousand students in IITG to visit various countries by Indian Youth Delegation, Government of India, Ministry of youth affairs and sports in the year of 2015.

I must thank God for giving very good friends at IITG campus who not only shared my delighted moments but also distress moments; they were always supporting me personally and professionally during my stay at IITG. My special thanks go to dear and near friends Ramu Banda, Karthik Malladi, Atlee, Adisha Aurelia Sangma, Daniel, Sandeep, Bhargav, Purabi Mazumdar, Sri Vidya, Santhiraju Pilli, Satya Anna, Dhanraj, Vikranth Volli, Mood Mohan, Sumitha Banu and Philip. It's a joy for me to thank my research group who are supportive, had a heart of helping nature and they have created a peaceful research environment during my stay in Dr Goud's lab. I am also grateful to Mrs.Swaroopa Rani, well wisher and a good friend of mine

who had an academic journey of almost eight years with memorable companionship. Very special thanks to my Christian friends, different EU units and EGF families within and exterior of the IITG campus (Dr. Prakash, Mr. Sudhir Gaddam, Mr. Edward Williams, Dr. Lyngdoh, Mr. Haokip, Mr. Sekhar Indupalli, Mr. Santosh Soren, Mr. John Sangma, Mr. James, Mr. Rambabu) who took care, prayed for me, impacted and influenced my spiritual life directly and indirectly. I also would like to thank all my best teachers (Shri Gopinath, Shri Dr. Balanarasaiah, Shri Dr. Dileep, Shri Mrs. Meenakshi, Shri Kanakaraju, Head, QRG, ISRO, SDSC SHAR, Sriharikota and Shri Mr. Ravinder), my maternal uncle Shri Mr. Nancharaiah, Scientist, DRDO, Hyderabad; Brother-in-law Shri Mr. Sobhan Babu, VAST, Scientist-F, ISRO, SDSC SHAR, Sriharikota; Sister Shri Mrs. Naga Jyothi, EE, RWS; who motivated, influenced and inspired me by explaining and showing several scientific things in various stages of my academic carrier; their love, care sacrifice and encouragement have made it possible to come so far.

Words fall short to express my thankfulness with love to my next young generation Venkateswaramma, Siva, Mukesh, Bhavani, Sameera and Mahidhar who are going to bring the change in our families and the quality of life. By concerning their future, I am passionate about research and decided to continue in the academic field in my career. I am also thankful to Mr & Mrs Prem Kiran and Ms. Prema Kanthi for their friendliness, love and care for me whom I met just few months ago, but had more memories and continue to have for rest of my life. A special thanks to Ms. Sumita Banu and Ms. Prema Kanthi for spending their time to correct my thesis.

Above all, I thank the almighty for showering his blessings upon me and for giving me good health, physical and spiritual strength which helped me to pursue my research work. This work could not have been completed without God's blessings. Finally, I hope and believe that this research experience will help me to play my role in this society.

Venu Babu B

Abstract

With the increased industrialization and modernization, the world demand of lubricants is growing at a faster rate. The rising prices of petrochemical products, depletion of oil reserves, increased environmental concerns and strict regulations on environmental pollution are the major driving forces for the development of biolubricants from renewable resources with minimum environmental impact. One of the possible alternatives to the conventional lubricants is the use of lubricants derived from the plant origins. Fatty acid alkyl esters derived from lipid feedstock such as vegetable oils can be used as biolubricants or additive for lubricity enhancement. Vegetable oil based lubricants are preferred over the conventional lubricants as they are ecofriendly, renewable, non toxic and biodegradable.

Although, vegetable oils have prominent rheological properties at higher operating temperatures and excellent biodegradability, but shows inadequate cold flow characteristics. Further, they have outstanding high temperature volatility characteristics due to the presence of triglyceride molecule, but exhibits insufficient thermal and oxidation stability at higher temperatures. These technical troubles are well known, but are not to be considered as stoppers for the use of renewable lubricant products in the industry. The lack of thermo-oxidative stability at higher temperatures and cold flow properties at lower temperatures are the major concern. In order to overcome these technical difficulties, several approaches have been tried such as chemical or structural modification of fatty acids structure, genetic modification and formulating with appropriate additives or synthetic fluids. However, this work presents the preparation, characterization and application of biolubricant basestocks derived from used cooking oil, castor oil and their methyl esters. Among various industrial applications, prepared lubricant basestocks are suitable for hydraulic and transmission applications as an alternative to conventional lubricants.

The entire work carried out in this research work is divided into five major sections:

A) Estimation of thermo-oxidative and cold flow properties of feedstocks

This chapter describes the physical and chemical changes that can occur during the frying process of edible oils (i.e. Soybean oil). Later, thermal stability (onset temperature - OT), oxidative stability (oxidative onset temperature - OOT), cold flow properties (pour point - PP) of the feedstocks were estimated by thermal analysis instruments (thermo gravimetric analysis –TGA, differential scanning calorimetry - DSC). The fatty acid composition (mixture of saturated fatty acids (SFA), mono-unsaturated fatty acids (MUFA), and poly-unsaturated fatty acids (PUFA)) of WCO/WCOFAME and CO/COFAME was determined by GC (gas chromatography) and aforementioned technical difficulties were clearly addressed in relation with the fatty acid composition of the feedstocks.

From the fatty acid composition, superior performance of CO/COFAME in terms of OT, OOT and PP was expected compared to WCO/WCOFAME. However, WCO onset temperature value was found to be higher than CO, which could be due to the presence of high molecular weight (MW) polymeric compounds in its composition. Owing to the higher content of PUFA (44.41%), WCO/WCOFAME is easily vulnerable to oxidation and degradation. The main reason for higher thermo-oxidative stability of CO/COFAME attributed to the presence of ricinoleic acid (hydroxyl groups) in its fatty acid chains (MUFA-88%) and lower PUFA content (6.6%). Higher pour point of CO/COFAME is due to the less SFA content (3.2%) and higher MUFA, PUFA content (88%, 6.6%) in its fatty acid composition.

From this chapter it could be concluded that, thermo-oxidative stability and cold flow performance properties are completely depend upon the fatty acid composition and their chemical structure. More quantity of unsaturated fatty acids enhances desirable cold flow

properties, but also affects the thermo-oxidative stability performance. In summary, to balance both the physical properties (thermo-oxidative stability and cold flow properties) higher content of MUFA in its fatty acids composition are recommended and this could be accomplished by genetic modification of plants. This chapter also concludes that thermal analysis methods (TGA, DSC) are much more accurate and reliable than conventional (ASTM) methods with respect to time of analysis, sample amount and reproducibility of experimental data to evaluate thermo-oxidative and cold flow properties.

B) Formulation of bio-lubricant base stocks via structural modifications of waste cooking oil

This chapter represent the strategies used for the formulation of bio-lubricant basestocks from WCO via series of structural modifications (epoxidation, ring opening and hexanoylation). Epoxidation of WCO was carried out and optimized using acidic ion exchange resin (AIER) IR-120 as heterogeneous catalyst to enhance oxirane oxygen content (OOC, response), thermo-oxidative stability and cold flow properties. Analysis of variance (ANOVA) of the optimization study show that, all the process parameters are highly significant to maximize the response and the best fit was noticed at 1.68 mol H_2O_2, 16.75 wt% catalyst loading, 54 ^oC reaction temperature and reaction time 11.45 h. The product confirmation was carried out by iodine value, NMR and FTIR spectral analysis. At this condition WCO epoxide OOC and conversion (unsaturation into oxirane content) was found to be 6.2 mass% and 99.54% respectively. Likewise, OT, OOT and PP were recorded as 360 ^oC, 320 ^oC and -6.2 ^oC, suggested unfavourable low temperature performance properties for prepared epoxide. Therefore, further oxirane ring was opened in presence of 2-ethyl hexanol (2-EH, Scheme 2) with sulphuric acid as homogeneous acid catalysts, followed by functionalization of hydroxyl groups with hexanoic anhydride using IR-15 as catalysts to enhance the PP. Hexanoylated product performance properties such as PP, viscosity index

(VI), tribology, biodegradability were found to be -28.45 ^{o}C, 127.98, wear scar diameter (WSD) -232 µm, friction co-efficient -0.08, film thickness -15 % and biodegradability 93.67 %. Nevertheless, all the products derived from WCO showed potential applications in various fields compared to conventional lubricants

C) Modifications of waste cooking oil methyl esters for the production of bio-lubricant base stocks

This chapter also discussed the similar study (like earlier section) using WCOFAME as a feedstock (absence of glycerol). Alkali catalysed transesterification reaction was carried out using 1:6 oil to methanol molar ratio, 1 wt% KOH as catalyst loading, 60 ^{o}C reaction temperature, and 90 min reaction time at 600 rpm. The product was confirmed by ^{1}H-NMR spectral analysis. This chapter elucidates the performance of bio-lubricant base stock prepared from WCOFAME. The optimum conditions inferred from the CCD were: temperature, 53.71^{o}C; catalyst loading, 28.17 wt%; time, 7.51 h; and H_2O_2, 1.72 mol. At this reaction condition maximum epoxide content was found to be 5.8 mass% and OT, OOT, PP was observed as 187 ^{o}C, 200 ^{o}C and, 10 ^{o}C respectively. Highly unfavourable cold flow properties were noticed for WCOFAME epoxide, hence, further structural modification was carried out to improve the PP, OT and OOT (reported in chapter 4). The characterization of WCOFAME derived biolubricant base stock exhibited excellent stability and low temperature performance in terms of OT (293 ^{o}C), OOT (247.5 ^{o}C) and PP (-27.15 ^{o}C). Thereafter, rheology of the esterified and hexanoylated products was carried out at various temperatures by varying the shear rate from 0 to 500 s^{-1} and found to be Newtonian flow behavior. The catalyst reusability study revealed that IR-120 and IR-15 can be used maximum three times without losing its catalytic activity. The tribological behaviour of WCOFAME hexanoylated product showed that WSD-209 µm, friction co-efficient-0.1, and

film thickness -81%. Correspondingly, biodegradability of the hexanoylated product holds more than 90% in 28 days signifies that all the products are eco-friendly.

D) Synthesis of bio-lubricant base stocks from castor oil containing high levels of free fatty acids

This chapter discussed about the lubricant basestocks from high FFA CO by chemical modification. The CO was extracted by Soxhlet extraction using n-hexane as an extraction solvent as per standard AOAC method. This chapter contributed the first report of its kind in literature for the preparation of bio-lubricant basestock derived from high FFA (45.6 mg KOH/g) CO. The epoxidation of high FFA CO occurred optimally at temperature, 52.81 ^{o}C; H_2O_2, 1.65 mol; catalyst loading, 15.14 wt%; and reaction time, 2.81 h. At the optimum condition, maximum epoxide content was found to be 3.85 mass%. Further, hydroxylation and hexanoylation was carried out using 2-EH and sulphuric acid, hexanoic anhydride and IR-15 as catalysts respectively. The purpose of this functionalization was to enhance the low temperature properties. The fully hexanoylated products OT, OOT and PP were found to be 236.6 ^{o}C, 235.7 ^{o}C and -27.65 ^{o}C. The resulting products contain functional groups of – CH (OR^1) CH ($OCOR^2$)-. The structural effect of functionalized groups R^1 and R^2 on pour point of the product has been systematically investigated. Notable tribological performance (WSD -257 µm, friction co-efficient -0.076, film thickness -28%) and biodegradability (95.45 %) was noticed for CO hexanoylated product. But, insignificant improvement in the thermo-oxidative stability was due to the presence of inbuilt hydroxyl groups (i.e., ricinoleic acid) in the CO triglyceride structure. From this study, it could be implicit that, higher FFA in the feedstock is not acceptable for bio-lubricant formulation and application, due to their susceptibility to thermo-oxidative degradation.

E) Preparation of biodegradable lubricant base stocks from castor oil fatty acid methyl esters

This chapter addresses the preparation of CO fatty acid methyl esters, epoxidation followed by hydroxylation and hexanoylation. Due to high FFA content, a two-step acid esterification followed by alkali transesterification was performed to synthesize methyl esters. This section investigated the preparation of bio-lubricant basestocks from COFAME via series of structural modifications with a unique fatty acid structure. At first COFAME epoxidation reaction was carried out at H_2O_2, 2.34 mol; reaction temperature, 50 ^oC; catalyst loading, 19.43 wt%; and reaction time, 5.26 h. At this optimum condition OOC was found to be 4.38 mass%, with pour point and number average molecular weight (MW) of the prepared epoxide as -10 ^oC and 846 mol/g. Further, hydroxylation and hexanoylation of COFAME epoxide showed improvement in the pour point and molecular weight as -16.4 ^oC, -28.93 ^oC and 1480 mol/g, 1750 mol/g respectively. The TG analysis of COFAME hexanoylated product showed significant hike in the OT, OOT (233.5 ^oC, 229.4 ^oC) compared to COFAME (203 ^oC, 218 ^oC). Similarly, higher biodegradability (93.75 %) and better tribological performance properties (WSD-235 µm, friction co-efficient-0.078, film thickness-13%) of COFAME hexanoylated derivative indicates that the prepared structurally modified product is in the acceptable range to use them as bio-degradable lubricant basestocks for various industrial applications.

This compilation of work done gives an overview of the current activity in the area of bio-based industrial lubricant basestocks. The work presented covers only a portion of the cutting edge technology being conducted around the globe. Based on the experimental as well as theoretical findings, it is herewith inferred that the prepared lubricant basestocks could be promising for hydraulic and transmission applications. The optimal conditions in the

epoxidation, hydroxylation and hexanoylation reactions are the key control variable to obtain a high quality lubricant basestocks. The future path towards a green environment and the eventual depletion of fossil resources requires that the research on renewable resources be continued on all fronts. Progress is being made a step at a time but will eventually result in journey to a more environmentally friendly society.

Contents

List of Tables

List of Figures

Abbreviations

2-EH	2-Ethyl 1-hexanol
AIER	Acidic ion exchange resin
ANOVA	Analysis of variance
AOAC	Association of analytical communities
AOCS	American oils chemists society
AOM	Active oxygen method
ASTM	American society for testing and materials
AV	Acid value
BP	Bharat petroleum
CAGR	Compound annual growth rate
CCl_4	Carbon tetra chloride
CCD	Central composite design
CFPP	Cold filter plugging point
CO	Castor oil
CoF	Co-efficient of friction
CSFT	Cold soak filtration test
COFAME	Castor oil fatty acid methyl esters
CNO	Canola oil
CV	Calorific value
DTG	Differential thermogravimetric
DSC	Differential scanning calorimetry
ECB	Effective composition of biodegradation
EOA	Epoxidised oleic acid

ESBO	Epoxidised soybean oil
ERSO	Epoxidised rapeseed oil
ERA	Epoxidised ricinoleic acid
EPFO	Epoxidised passion fruit oil
EPO	Epoxidised palm oil
EPOME	Epoxidised palm oil methyl esters
EMO	Epoxidised moringa oil
EN	European standard
FA	Fatty acid
FAME	Fatty acid methyl ester
FFA	Free fatty acid
FTIR	Fourier transformed infrared spectroscopy
FP	Flash point
GC	Gas chromatography
GPC	Gel permeation chromatography
HBr	Hydrogen bromide
HHV	Higher heating value
H_2SO_4	Sulphuric acid
HFRR	High frequency reciprocating rig
HOSBO	High oleic soybean oil
HOSO	High oleic sunflower oil
HPLC	High performance liquid chromatography
IOC	Indian Oil Corporation
IV	Iodine value
IIP	Indian institute of petroleum
IIT	Indian Institute of technology
JO	Jatropha oil

KBr	Potassium bromide
KOH	Potassium hydroxide
KV	Kinematic viscosity
LTFT	Low temperature flow test
MEOA	Mono-epoxidised oleic acid
MO	Moringa oil
MUO	Mustard oil
MW	Molecular weight
NaOH	Sodium hydroxide
$NaHCO_3$	Sodium bi-carbonate
NMR	Nuclear magnetic resonance
OA	Oleic acid
OS	Oxidative stability
OOC	Oxirane oxygen content
OT	Onset temperature
OOT	Oxidative onset temperature
PDSC	Pressurized differential scanning calorimetry
PAO	Poly alpha olefin
PFO	Passion fruit oil
PP	Pour point
PPD	Pour point depressant
PTSA	Para- Toluenesulphonic acid
PSU	Public sector undertaking
PO	Palm oil
POME	Palm oil methyl esters
PT	Peak temperature
RA	Ricinoleic acid

RI	Refractive Index
RT	Room temperature
RO	Ring opening
RSO	Rapeseed oil
SBO	Soybean oil
SO	Sunflower oil
TERI	The energy and research institute
TG	Thermogravimetric
TGA	Thermogravimetric analysis
VI	Viscosity index
UK	United kingdom
USA	United states of America
WCO	Waste cooking oil
WCOFAME	Waste cooking oil fatty acid methyl esters
WSD	Wear scar diameter

Notations

G_{exp}	Experimental α – glycol value
G_{the}	Theoritical α – glycol value
IV_o	Initial iodine value
A_i	Atomic weight of Iodine
A_o	Atomic weight of oxygen
A_{OH}	Atomic weight of hydroxyl group
$Cdcl_3$	Deuterated chloroform
OO_{exp}	Experimental oxirane oxygen
OO_{the}	Theoritical oxirane oxygen
R^2	Regression co-efficient

K	Flow behavior index
n	Consistency co-efficient

Units

MT/a	Metric tonnes per annum
Wt%	Weight percentage
%	Percentage
cSt	Centistoke
^{o}C	Degree centigrade
cp	Centipoise
m.Pa.s	Milli pascal second
mg KOH/g	Milligrams of KOH per gram
h	Hours Time
MHz	Mega hertz
µl	Micro litre
$gI_2/100\ g$	Grams of iodine per 100 g
psi	Pounds per square inch
$^{o}C/min$	Degree centigrade per minute
kg/m^3	Kilogram per cubic meter
kg	Kilgram
m^3	Cubic metre
ml/min	Milli litre per minute
mV	Milli volt
Ω	Ohm
Mw	Milli watt
Mass%	Percentage of mass

CHAPTER 1

Introduction and Literature Review

This chapter is divided into two sections; the former section gives a brief orientation on the introduction of conventional lubricants, need for the alternatives and their limitations were discussed. Further, this section would be discussing the current scenario and future perspectives of bio-lubricants in India, statistics of potential renewable resources available in India and their applications, chemistry, chemical composition and the limitations of renewable resources. The next section of the review is focused on some of the research and experimental work that relates to possible structural modifications for lubricant base oil production. Following this, a summary of the conclusions made in these studies will be providing further research direction and contribution of research topic to the chosen field has been elaborated. Finally, the objectives of the thesis and its organization are summarized.

1.1. Introduction

Lubricant is a substance used to facilitate relative motion of solid bodies by reducing the friction and wear between two contacting surfaces. Lubricant oils are broadly classified on the basis of their origin: mineral, synthetic and vegetable oils, in application point of view, they are categorized as the engine and non-engine lubricants (Bart et al. 2013). Among these, mineral oils are the most widely used for lubricant application, and their consumption are around 95%. Lubricants which are in the liquid form are being the predominant form for various applications as a composite mixture. Commercial lubricants are typically composite materials composed of a lubricant basestock (70-99%) formulated with an additive package (30-1%) for specific property enhancement of the resulting full lubricant formulation (Arbain and Salimon 2009). The additives are chemicals, which are used to blend with basestocks to

enhance desirable characteristics which they lack or improve existing properties. The properties considered important for lubricant application are: viscosity index (VI), pour point (PP), thermal and oxidation resistance, flash point (FP), acidity (neutralization number), friction properties and biodegradability.

Mineral oils are originated from crude oil, which is a complex mixture that contains a large array of hydrocarbon molecules and traces of nitrogen, sulphur, oxygen, metal, and salt. Synthetic oil is a mixture of compounds that are artificially made by a chemical modification of petroleum derived products; they are typically more stable to heat and oxidants than many conventional lubricant oils. Conversely, mineral and synthetic oil contains harmful substances to pollute the eco system and uncontrollable to dispose off. Gawrilow (2004) reported that annually 10-15 million tons of petroleum-based oleo-chemicals enter the biosphere. Schneider (2006) observed and described that approximately 50% of all the lubricants used to worldwide end up in the environment via total-loss applications, evaporation, spillage or accidents. The presence of these minerals based lubricants in the ecosphere pollutes the air, soil, drinking water and affect human and plant life to a great extent. On the other hand, these oils will continue to be economical, depleting at a faster rate, provide certain performance characteristics in various applications, but create a potential danger when they are not readily biodegradable and are environmentally toxic. Due to these environmental threats, mineral based lubricants are usually not considered as eco-friendly. Therefore, during the last couple of decades, the level of public awareness about environmental issues has risen considerably, thus the demand for environmentally acceptable lubricants is increasing for a pollution-free environment.

Nevertheless, replacing mineral base oils with eco-friendly products is one of the ways to decrease the unfavorable effects (low biodegradability) on the ecosystem caused

using traditional lubricants. The potential use of renewable raw materials in the lubricant industry is currently of great interest. As a result, vegetable oils/plant seed oils and their esters are perceived to be alternatives to mineral oils for lubricant base oils due to certain inherent technical properties and their ability for biodegradability. Compared to mineral oils, vegetable oils possess advantageous properties, such as higher flash point, viscosity index, lubricity, low evaporative loss, satisfactory tribological properties and biodegradability. (Erhan and Asadauskas 2000; Adhvaryu and Erhan 2002; Mercurio et al. 2004). Even though vegetable oils are contributing many advantages, but they cannot be used directly in its natural (original) form as lubricant base oils and industrial fluids due to their lower oxidative stability and inadequate thermal stability. (Becker and Knorr 1996), poor cold flow behaviour (Asadauskas and Erhan 1999) and other tribo-chemical degrading processes (i.e. oxidation, degradation) (Brophy and Zisman 1951).

In spite of the instabilities possessed by vegetable oils, there is a great necessity to use them to replace the conventional lubricant base oils. The elaborate literature survey revealed that many technical possibilities such as chemical/structural modification; additive treatment and genetic modification suggested overcoming the poor oxidative and hydrolytic stability and high-temperature sensitivity of tribological behavior of vegetable oils when used as base oils for lubricants (Soni and Agarwal 2014). Among all the possible routes, chemical modification of vegetable oils has been considered as an attractive way to formulate biodegradable lubricant base oils.

In formulating the lubricant base oil from vegetable oils, chemical (fatty acid) composition of potential feedstock is a significant feature. Chemical modifications of vegetable oils without sacrificing favourable physico-chemical characteristics and lubricity can be classified under two groups: reactions in the hydrocarbon chain (oxidative cleavage,

metathesis, radical additions, and the addition of carboxylic acids, dimerization and epoxidation) and reaction on the carboxyl group (transesterification and hydrogenation). More than 90% of chemical modifications have been occurring at the fatty acid carboxyl groups, while less than 10% have involved reactions at the fatty acid hydrocarbon chain (Bart et al. 2013). Among all the feasible chemical modifications, a reaction involved at the fatty acid hydrocarbon chain has gained much significance. From the detailed study on the structural modification of vegetable oils, it is also noticed that most of the edible oils and their esters have been used for chemical modification, which is often staple foods in human nutrition (Soni and Agarwal 2014; Borugadda and Goud 2014a). In addition to that, due to the high price of virgin oils, the end product price also remains high. Therefore, in order to minimise the end product cost, non-edible, used edible oils, which do not have any commercial value in the market can be used to prepare lubricant basestocks.

Hence, the present study was proposed with the intention of modifying the fatty acid structure to formulate lubricant base oil with improved performance properties. Prepared lubricating oil from renewable sources is also known as biolubricant base oils, due to its biodegradable nature.

1.2. Current scenario and future prospective

At present, the growth in world lubricant demand will be aided by the current expansion of an automobile industry, manufacturing and other industrialized activities. From the prior information by various lubricant industries across the globe, it was found that during the past ten years, the global lubricant market has undergone remarkable changes. International demand for lubricants has continued at around 35 million tons per year ever since 1991. It was recorded that, 37.4 million tons of lubricants were consumed worldwide during 2004, with 53% being automobile lubricants, 32% being industrial lubricants, 10% being process

oils, and 5% being marine oils (Nagendramma and Kaul 2012). Later, in 2005, 37.9 million tons, 41.8 million tons of lubricants were used in 2007 worldwide and limited data was presented to the market for 2008. However, the annual growth rate is expected to attain approximately 2% starting in 2012. The fastest growths arise in the Asia-Pacific, with China being the major gainer. Figures 1.1 (a) and (b) presented the world lubricant market partitioning by region and application wise, similarly Figure 1.2 shows the predicted consumption growth rate by region wise up to 2015. The world has approximately 1700 small and large lubricant producers, estimated 300 of these manufacturers are located in Europe (Mobarak et al. 2014). These makers are mainly petroleum companies and the main business for them is to discover, extract, and refine crude oil. 1200 self-sufficient lubricant companies focus on engine, gear, and hydraulic oils. Less than 2% of lubricant manufacturer produce more than 60% of the total volume of lubricants (Mang and Dresel 2007). **Table 1.1** shows the top ten lubricant manufacturers in the world.

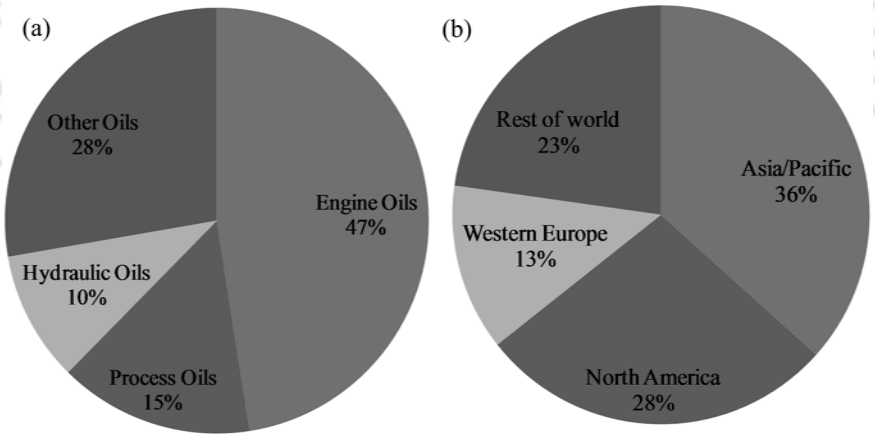

Figure 1.1: Current lubricant market worldwide, segmentation by application area (a) and geographical (b)

According to a study conducted by Ken Research (Anonymous 2013), currently the Indian lubricant market is the fifth largest in the world in terms of consumption after the US, China, Russia and Japan. The lubricant industry in India is broadly divided into three major

market sectors – automotive, industrial, and marine and energy applications. Currently, India has 44 lubricant companies in the market; however, IOC is the dominant company in the country's lubricant market, with its Servo brand of lubricants. The Indian lubricant industry is led by three major PSUs, namely, Indian Oil Corporation Ltd., Hindustan Petroleum Corporation Ltd., Bharat Petroleum Corporation Ltd., who together contribute nearly half of the market in terms of volume, while the rest is accounted by multinational companies as reported in Table 1.1 (Mobarak et al. 2014)**.** The total lubricant market in India is 1.6 billion litres, of which automotive use is about 950 million litres..

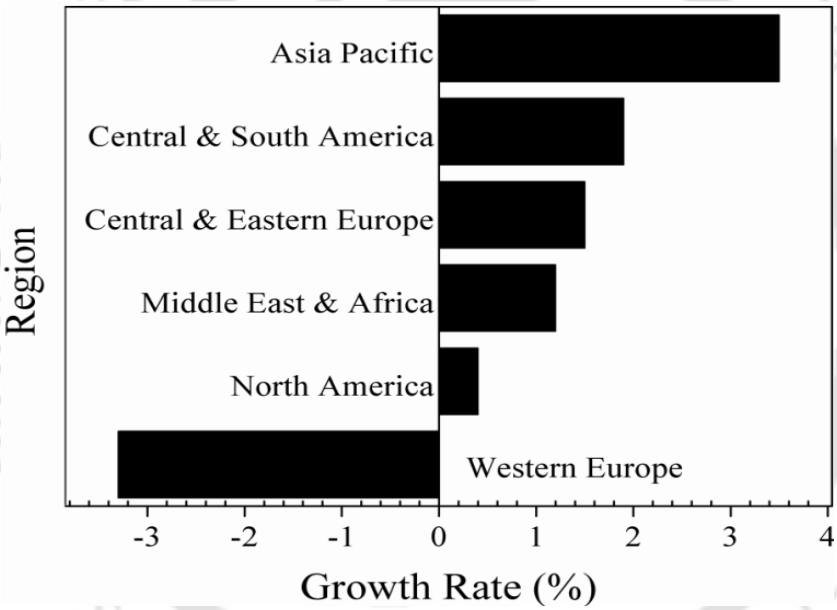

Figure 1.2: Estimated lubricants growth demand by region wise for 2005-2015

Consumption rate has been growing at 3-5 % per year, as the drainage period (longevity) has been constantly increasing. India has also become an export hub for many global players who are demanding higher specification engines and engine oils to meet more stringent international specifications. The industry revenue has increased from $1,611.7 million in 2006 at a compound annual growth rate (CAGR) of 18.6 per cent and is expected to exceed $7,713 million by 2017 due to the major push from the various sectors in the Indian lubricant market (Anonymous 2013). It is expected that these factors will result in

demand for higher-quality lubricants, leading the industry towards wider acceptance of synthetic and biodegradable lubricants due to environmental concerns. However, Indian plant-based lubricants industry, in particular, is as yet in a nascent stage, though emergent regulatory impacts on lubricants offer the potential for increasing the consumption of biolubricants over the coming decade. Thus, most of the oil majors in India like IOC, BP-Castrol, etc., as well as institutions like I.I.P., TERI, CLRI, etc., have been doing a lot of research and conducting trial runs on degradable green lubricants and would soon evolve a marketing and branding strategy for their products (Pathak 2010; Anonymous 2013).

Table 1.1: Global top ten lubricant manufacturers

Manufacturers	Name of the product	Country
Shell	Shell	Great Britain / The Netherlands
Exxon Mobil	Exxon Mobil	USA
BP	BP	UK
Chevron	Chevron	USA
Petro China	Petro China	China
Lukoil	Lukoil	Russia
Fuchs	Fuchs	Germany
Nippon oil	Nippon oil	Japan
Valvoline	Valvoline	USA
Conoco Phillips	Conoco Phillips	USA

Even though IOC has taken an initiative in 2010 to produce and introduce bio-lubricant into the market, but the commercial production is yet to commence (Anonymous 2011). On the other hand, many other countries have already commercialized and replaced 5% bio lubricant in sensitive areas such as, agricultural, forestry and transportation sectors. German

lubricant market has overall 3-4 % of biolubricants market share. Global volume consumption of biolubricants, estimated at 1.3 million pounds in 2013, valued at about US$2 billion, and forecast at 1.4 million pounds (US$2.1 billion) in 2014, is further expected to maintain a CAGR of 5.5% between 2010 and 2020 to reach a projected 1.9 million pounds, of value US$3 billion, by 2020 (Anonymous 2014). Modern bio-lubricants are technically established and undergo constant development; they are therefore, likely to be used to a greater amount in the future, particularly with regard to environmental protection and sustainability. Therefore, India needs to put a lot of efforts in order to produce multi-purpose high-quality lubricant base oils from renewable resources, which are economical.

In this regard, vegetable oils internal chemical composition and their structure, limitations need to be understood thoroughly to formulate bio-lubricants; hence the subsequent section would be addressing those issues comprehensively.

1.3. Chemical composition and chemistry of vegetable oils

1.3.1 Chemical composition

Vegetable oils can be categorized as edible and non-edible; they are part of a big family of chemical compounds known as fats or lipids. Currently, they have become more pleasing due to the fact that they are made from renewable resources, adaptability to the eco-system and compatibility to use them in diverse fields as feedstocks to synthesise value added products. Chemically speaking, vegetable oils and animal fats are triesters of glycerol with fatty acids and commonly are called as triglycerides, which are hydrophobic in nature. Triglycerides are derived from different carboxylic acids, they vary in the nature of the alkyl chain attached to glycerol and that constitutes vegetable oil matrix. All types of existing triglycerides have been used throughout the ages as foods, fuels, lubricants, and starting materials for other chemicals. This wide utility results from the unique chemical features and

physical properties of triglycerides. A generalized triglyceride structure has shown in Figure 1.3.

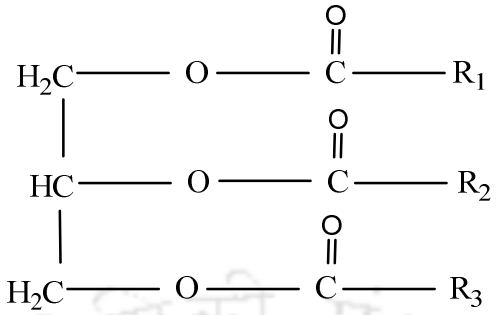

Figure 1.3: Schematic structure of triglyceride molecule

Where, R_1, R_2, R_3 are different fatty acids attached to the glycerol molecule. Thus, the physical and chemical properties of vegetable oil are mainly contributed by fatty acid composition and distribution, which holds 90% fatty acids to 10% glycerol. Fatty acids have a polar head and a hydrocarbon chain; these hydrocarbon chains of fatty acids contain one or more unsaturated double bonds. Position of double bonds and their relative position with respect to the carbon atom of the polar head group (carbonyl carbon) provide fatty acids characteristic properties. Naturally, vegetable oil triglycerides contain fatty acids that range from 14 to 22 carbons with various degrees of saturation and unsaturation (Fox and Stachowiak 2007).

Since last few years, many feedstocks have been identified in India for various practical applications and the common feedstocks available in India are edible oils, which hold the major part in human nutrition. Therefore focus needs to be shifted to feedstocks which are not edible, such as edible waste oils and non-edible oils available in India and the details of such potential non-edible oil seed plants distribution, applications, and their fatty acid composition is listed in Tables 1.2, 1.3 (a) and (b), respectively. Among the reported feedstocks, based on the availability, price and fatty acid structure, locally available

used/waste cooking oil (WCO) and castor oil (CO) are found to be the most promising raw materials with a unique fatty acid composition and much variation in their structure. Working upon these two feedstocks, can give complete insight into all the other edible and non-edible plant seed oils as feedstocks with any type of fatty acid arrangement and composition. Following paragraphs briefly discusses on these two feedstocks used in the present study.

(a) Waste cooking oil

Food cooked in reused oil has unfavourable impact on human health, but the same oil can becoming environment friendly if re-processed and used for any practical application. Patil et al. (2012) reported that about 4.1 kg of WCO is produced per person in a year. Considering the present scenario of the world population as nearly 7.18 billion, around 29 million tons of WCO will be produced in a year. All these facts indicate that used cooking oil should be recycled and can be use as a potential source for bio-fuel and bio-lubricant base oil production. Therefore, in an attempt to enhance the economic viability of bio-lubricant base oil, feedstock of edible waste oils has been considered, because it is available at a reasonable price or even free. However, during frying oil can undergo various chemical reactions such as polymerization, hydrolysis and oxidation owing to their reaction to light, heat and oxygen. As a result it form different chemical compounds which are holding higher molecular weights, such as dimer, polymer, oxidized triglycerides, diglycerides and fatty acids (Sharma et al. 2012). The cost of waste frying oil is estimated to be about half the price of virgin oil and the use of WCO significantly reduces the cost of the end product, currently in India, 1,135,000 metric tons of waste fats and oils are produced annually (Borugadda and Goud 2012; Mazumdar et al. 2012).

Table 1.2: Potential non-edible seed oil plants available in India

Botanical Name	Common Name	Distribution	Potential (MT/a)	Oil (%)	Use
Cyano Bacteria	Algae	Few places in India	157.4-629.8	20-40	Human nutrition, Animal feed, Aquaculture, Biolubricant Bio-fertiliser, Source of polyunsaturated fatty acids, and Recombinant proteins, etc
Ricinus Communis	Castor	All over India	790,000	46-55	Adhesives, Coatings, Soaps, Lubricants, Paints and Dyes, etc
Gossypium hirsutum	Cotton	All over India	851,000	18-25	Dairy cattle feeding, Alternative Bio-fuel source, etc
Jatropha Curcas	Jatropha	All over India	15,000	40–60	Biodiesel, Bio-lubricant Mineral diesel substitute, To prevent and control erosion, to Reclaim Land, Grown as a live fence, Manufacture of candles, soap, and cosmetics.
Simmondsia Chinesis	Jojoba	Few places in India	--	45-55	Cosmetics, Skin-softener, Pharmaceuticals, Lubricants and Synthesis of Biodiesel,
Pongamia Pinnata	Karanja	Maharastra, Karnataka, Assam	2,00,000	30-40	Tanning leather, Soap, Illuminating oil, lubricant, water-paint binder, and

					Pesticide.
Garcinia indica	Kokum	Western Ghats Region, Andaman and Nicobar Islands, North-Eastern region of India.	55,000		Ideal feedstock for biodiesel
Linum Usitatissimum	Linseed	Few places in India	150,000	35-45	Textiles, Oil crop, Stem fibres, Geotextiles, Filters, Absorbents, Pulp and Paper Manufacturing etc
Madhuca Indica	Mahua	Maharashtra, Gujarat, West Bengal, Karnataka, Orissa, Tamil Nadu,Kerala, and West Bengal	5,20,000	35–40	Ointment, rheumatism, illumination, lighting, soaps etc.
Moringa Oleifera	Moringa	Himalayan regions of northwest India,	--	33-41	Skin Diseases, Medicinal
Mesua ferrea	Nahor	Northeastern states of India	--	58–75	Production of biodiesel, , wood as a railway crossties, Heavy construction, Boat building, Mine props, and tool handles
Azadirachta indica	Neem	All over India	5,00,000	35±45	Preservation of stored grains, Ayurvedic Medicine, Unani and Homoeopathic Medicine, etc
Erythea Salvadorensis	Palm	--	< 70,000	20-21	Cosmetics, Sopas, Lubricant for biodiesel engine, Diesel fuel Substitute,

					Transportation fuel.
Oryza Sativa	Rice bran	Andra Pradesh, Orissa, Karnataka, West Bengal, Gujarat, Utter Pradesh	474,000	16–32	Non-edible Vegetable oil, Replacement for Mineral Diesel.
Simarouba glauca	Simarouba	Gujarat, Maharashtra, Tamilnadu, Karnataka, Orissa and Andhra Pradesh	1.1-2.2 oil/ha/yr	55–65	Manufacture of Soap, vegetable fat or margarine, Lubricant, Paint, Polishes and Pharmaceuticals
Sapindus mukorossi	Soapnut	Andra Pradesh, Karnataka, Maharashtra, Delhi, Tamil Nadu	6.61	51.8	Medicinal, Soap, Surfactant, Fabrics, Bathing, and Biodiesel, Bio-lubricant production
Citrullus colocynthis	Tumba	Few places in India	21,000 tones	--	Medicinal
--	Waste cooking oil and Animal fats	Restaurants and Households, large food processing and service facilities	11,35,000	--	Biodiesel, Bio-lubricant production

Table 1.3 (a): Fatty acid composition of oils (wt%)

Fatty acids	Castor	Cotton	Jatropha	Jojoba	Karanja	Kokum	Lin Seed	Mahua	Moringa
Myristic acid ($C_{14:0}$)	0	0.7	1.4	-	0	15.54	0	1	-
Palmitic acid ($C_{16:0}$)	1.1	28.7	15.6	1.08	14.1	2.5	5	17.8	7
Stearic acid ($C_{18:0}$)	3.1	0.9	9.7	-	10.9	56.4	2	14	4
Oieic acid ($C_{18:1}$)	4.9	13	40.8	7.22	56	39.4	18.9	46.3	78
Linoleic acid ($C_{18:2}$)	1.3	57.4	32.1	0.04	15	1.7	18.1	17.9	1
Linolenic acid ($C_{18:3}$)	0	0	0.2	-	3.6	-	55.1	<1	< 1%
Eicosanoic acid ($C_{20:0}$)	0	0	0.4	0.23	2.1	15.79	0	3	4
Eicosenoic acid ($C_{20:1}$)	0.3	0	-	-.	2.4	6.17	-	-	-
Docosanoic acid ($C_{22:0}$)	-	0	0-0.2	0.29	1.9	0.01	0	4	4
Tetracosanoic acid ($C_{24:0}$)	-	0	14	-	2.4	-	0	-	-
Unaccounted	89.6	0	1.4	14.2	4	7.42	0	-	-

Table 1.3 (b): Fatty acid composition of oils (wt%)

Fatty acids	Nahor	Neem	Palm	Rice Bran	Sal	Simarouba	Soapnut	Tumba	WCO	Micro Algae
Myristic acid ($C_{14:0}$)	2.13	0.2-0.26	1	0.4-0.6	-	-	-	-	0.5	
Palmitic acid ($C_{16:0}$)	15.3	13.6-16.2	42.6	11.7-16.5	4.5-8.6	19	4.67	13-14	20.4	12-1
Stearic acid ($C_{18:0}$)	12	14.4-24.1	4.4	1.7-2.5	34.2-44.8	14	1.45	9-10	4.8	1-2
Oieic acid ($C_{18:1}$)	53.2	49.1-61.9	40.5	39.2-43.7	34.2-44.8	63	52.64	26-28	52.9	58-60
Linoleic acid ($C_{18:2}$)	17	2.3-15.8	10.1	26.4-35.1	2.7	3	4.73	51-52	13.5	4-20
Linolenic acid ($C_{18:3}$)	-	-	0.2	0.6	-	-	1.94	-	0.8	14-30
Eicosanoic acid ($C_{20:0}$)	2	0.8-3.4	0	0.4-0.6	6.3-12.2	1	7.02	-	0.3	-
Eicosenoic acid ($C_{20:1}$)	-	-	0.1	-	-	-	23.85	0.4	0.3	-
Docosanoic acid ($C_{22:0}$)	0.5	-	0	-	-	-	1.45	0.8	0.07	-
Tetracosanoic acid ($C_{24:0}$)	-	-	0	0.4-0.9	-	-	0.47	0.3	0.04	-
Unaccounted	-	-	1.1	-	-	-	-	-	-	-

(b) Castor oil

Castor (Ricinus communis L.) is cultivated worldwide because of its commercial importance in the manufacture of various industrial chemicals. The Indian variety of castor seed has an oil content of 46-55 wt%; after the extraction of oil, residual oil cake is used as organic manure (Tongoona 1992). The oil fraction of castor seeds contains higher amount of ricinoleic acid (> 80%) as a hydroxylated fatty acid and this unique structure has given a unique identity to this biological source for the industrial synthesis of variety of compounds (Hajar and Vahabzadeh 2014). Castor plant grows well under hot and humid tropical conditions for a growing period of 4-5 months and reaching an age up to 4 years. Specially, castor plant required a temperature between 15 and 38 ^{o}C with a lower humidity throughout the growing season in order to receive maximum oil yield (Ogunniyi 2000; Borugadda and Goud 2012). The average yield of seed per hectare and oil per hectare is 1250 kg and 550 L respectively. Around the globe India is the world's largest producer and exporter of castor oil and the other major producers are China and Brazil. At present, it is cultivated around 700,000 hectares mostly in Andhra Pradesh and Gujarat under rainfall conditions. The total world production of castor seeds is estimated around one million tons and the oil extracted is about 500,000 tons with a productivity of 470 kg of oil per hectare (Santana et al. 2010). Irrespective of castor seed origin, a season in which it has grown, its fatty acid composition remains unique. However, its consumption is very less compared to production; therefore it can be considered as prospective feedstock to create bio-lubricant base oil.

1.4. Chemical structure and limitations of vegetable oils

A common representation of the triglyceride molecule is shown (Figure 1.4) along with vulnerable positions in its chemical structure. The linear and long chain structure of (un)saturated fatty compounds is quite suitable for few applications, but is frequently less ideal for lubricant base oils. Mainly, there are three positions in triglycerides where a chemical modification can most easily be effected, namely the ester moieties, β-hydrogen, and double bonds along the fatty acid (FA) chains (Figure 1.4). As reported in previous section, most of the oleochemical modifications (90%) concern the carboxyl moiety of FAs, whereas reactions of the unsaturated or saturated FA chain account only for 10%. Unsaturated fatty compounds are alkenes and contain an electron-rich double bond that can be functionalised by reactions with electrophilic reagents. The glycerol moiety of triglyceride is destructible and decomposes at high temperatures; there are two distinct modes of decomposition, namely thermolysis and autoxidation. Thermolysis occurs by β-elimination at the ester group. In addition, further weakness of vegetable oils is their tendency to hydrolyze in presence of water (Goyan et al. 1998). Hwang and Erhan (2001) described that auto oxidation of vegetable oils is originated by the formation of free radicals and peroxy radicals are formed by the reaction of free radicals with oxygen, then the peroxy radical can attack some other lipid molecule to remove a hydrogen atom to form hydro peroxide and generate another free-radical molecule to propagate the oxidation process. The complete mechanism for auto-oxidation of plant oils was well studied and reported by Moser and Erhan (2007). During oxidation compounds formed may undergo polymerisation, increasing viscosity and finally resulting in increase acidity and precipitates. Similarly, poly un-saturation in the FA chains leads to poor oxidation stability (Becker and Knorr 1996), whereas complete saturation of the double bonds results in poor low-temperature fluidity. Therefore, a limiting situation is reached beyond which further improvement in high- and low-temperature stability

(Asadauskas and Erhan 1999) cannot be obtained. This restricts the use of triglyceride molecules in industrial applications operating under a broad temperature range.

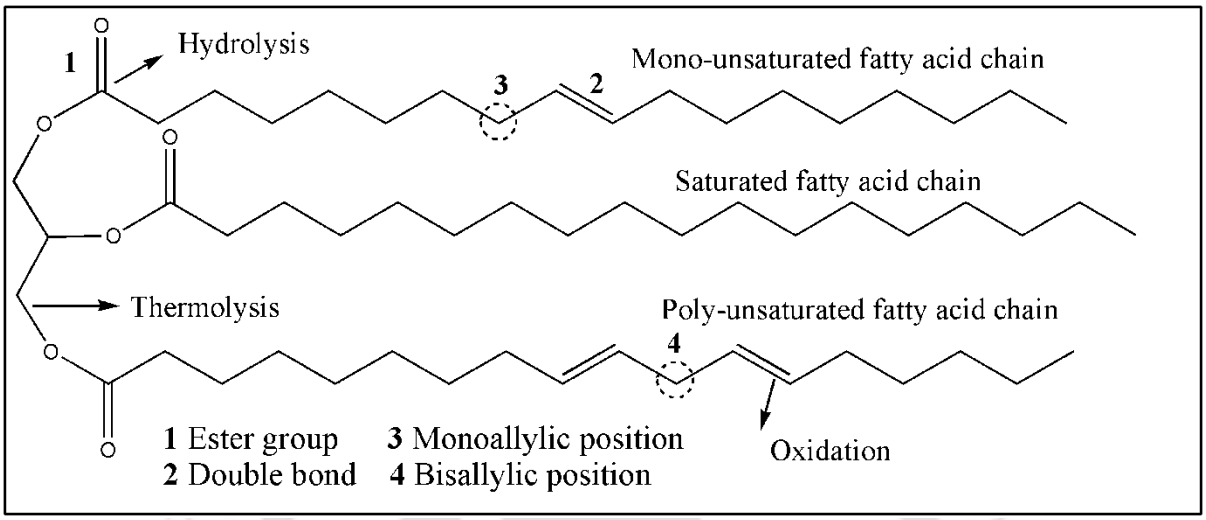

Figure 1.4: Schematic structure of triglyceride, showing positions vulnerable to chemical degradation

Therefore, in order to fix biolubricant base oils from triglycerides, chemical modification is compulsory to improve certain performance limitations of ester-based lubricant base oils without impairing their excellent tribological and environmentally relevant properties. Chemical modification of triglycerides help to build molecules with desirable properties for lubricant applications, as all the physical and chemical properties of seed oil are solely based on the molecular structure and their relative distribution. Manipulative alterations in the FA composition of vegetable oils for a specific industrial application is a challenging task and Table 1.4 shows the effect of various commercial chemical modification of oils on selected lubricant properties.

Table 1.4: Influence of chemical structure of modified triglycerides on physical properties

Chemical modification	Physical properties
High degree of branching	Excellent low-temperature characteristics
	High hydrolytic stability
	Low viscosity index
High linearity	High viscosity index
	Relatively poor low-temperature characteristics
Low saturation	Excellent low-temperature characteristics
	Limited oxidation stability
High saturation	Excellent oxidation stability
	Poor low-temperature characteristics

Modification of FA chain entails making a compromise between the following criteria: performance (tribological properties), stability towards oxidation, low-temperature behaviour, biodegradability and cost. Consecutively, various technocrats reported several modern technologies to avoid or transform the unsaturation in the FA chain to solve the issues regarding the practical application of vegetable oils as biolubricant base oils. In depth survey revealed many practical solutions, such as genetic modification (Adhvaryu and Erhan 2002), additive treatment (Sharma et al. 2008c), selective hydrogenation of unsaturated sites (Wadumesthrige et al. 2009), transesterification (Bokade and Yadav 2007) and a series of structural (chemical) modifications (Biswas et al. 2007; Campanella et al. 2008) to the FA chain.

Among the above practical solutions, this thesis addresses the series of structural (chemical) modifications to FA chain at the triglyceride molecule. Therefore, in the next section, a brief summary of the relevant state-of-the-art with respect to the chemical modification/series of chemical modifications to FA chain have been summarized.

1.5. Literature Review

The following state-of-the-art reveals the research and experimental techniques that relates to the possible chemical modifications (as a single reaction/series of reactions) on various edible, non-edible oils, merits, demerits, challenges faced to prepare bio-lubricant base oils. Subsequently, the methods used to assess and improve the oxidation, low temperature stability, biodegradability and tribological properties have also been discussed. This will provide a significant insight on the potential of bio lubricant base oils, their formulation, and its past and glorious future.

1.5.1 Epoxidation

The general process for synthesis of epoxide is known as epoxidation, it is one of the most important double bond modification reactions. There are two major reactions involved in the epoxidation, during the first stage peroxy acid is formed from the reaction of formic/acetic acid and hydrogen peroxide (Saurabh et al. 2011). Whereas in the second stage, a reaction between peracid and double bond produces epoxide, the simplified epoxidation reaction is summarised in **Scheme 1.1.**

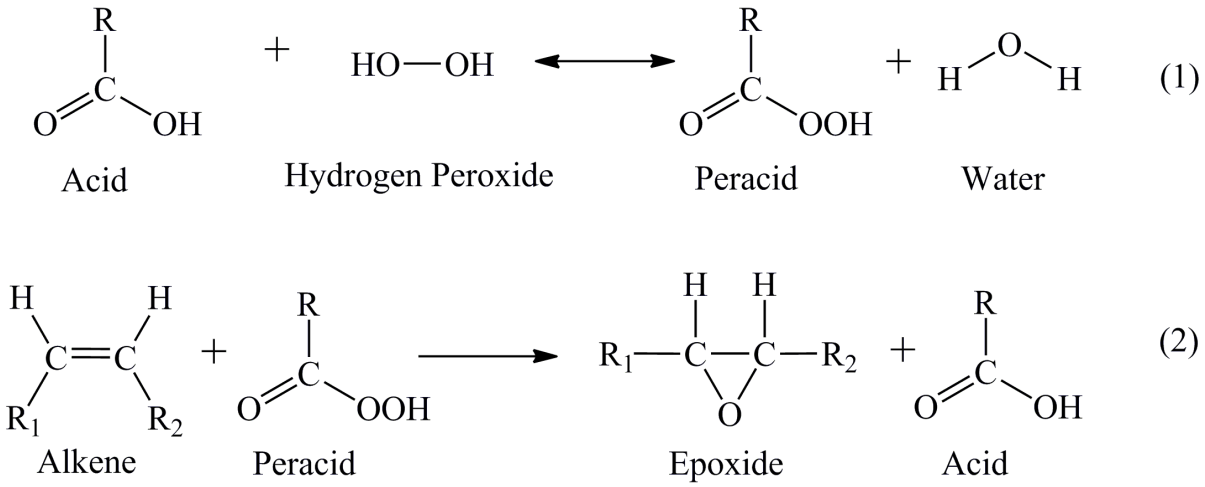

Scheme 1.1: Mechanism and reaction scheme for epoxide formation

Epoxide can be defined as cyclic ethers which consist of three membered rings, according to IUPAC norms epoxide also termed as oxirane ring (Scheme 1.1). The mechanism of epoxidation and product formation is mainly determined by oxidants and catalysts. The epoxidation of olefins, can be classified by the reaction mechanism such as, Jacobsen–Katsuki (Manganese salen complexes and iron-porphyrin catalyst), sharpless asymmetric, shi, prilezhaev reaction (peracid catalyst) and enzymatic epoxidation (Chua et al. 2012). However, every method has its own advantages and disadvantages in terms of selectivity, catalyst life, yield, and product separation and purification is still remained as a shortcoming in these systems. From the prior arts, it is noticed that, above all the process, epoxidation by prilezhaev reaction gained much significance since it is leading to low oxirane degradation, higher selectivity (depending on the catalyst and feedstock). There are four major categories of epoxidation processes based on the type of catalyst used during epoxidation: conventional sulfuric acid, acidic ion exchange resin (AIER), chemo-enzymatic, and metal-catalyzed epoxidation (Tan and Chow 2010).

Each of these processes has its own advantages and disadvantages, but the AIER process has been most often reported process in the literature, because of ease of catalyst separation and refining, few side reactions (Fiser et al. 2001).

Wu et al. (2000) studied rapeseed oil (RSO) epoxidation and significant physico-chemical properties such as viscosity, pour point, biodegradability, oxidative stability, anti-oxidant study and friction properties were estimated. They concluded that viscosity was improved for epoxidised rapeseed oil (ERSO) (86.73 cSt) compared to RSO (34.75 cSt), biodegradability of RSO and ERSO was found to be > 95%. Whereas, pour point PP was found to be -15 ^{o}C and -12 ^{o}C for RSO and ERSO respectively. It was also reported that ERSO exhibits better friction properties and improved oxidative stability. The major

observation from this report was increased PP, which was contrary to the essential performance as a biolubricant.

A study on soybean oil (SBO) epoxidation, genetically modified high oleic soybean oil (HOSBO) was conducted by Adhvaryu and Erhan (2002). Their outcomes indicated that among the epoxidised SBO, HOSBO; epoxidised soybean oil (ESBO) showed maximum oxidative stability (OS) 188.1 ^{o}C. They also investigated the oxidative stability at various additive concentrations and 0.5 wt% of additive concentration showed maximum OS. However, other important properties such as boundary lubrication, deposit forming tendency showed improved performance. Similarly, co-efficient of friction was more for ESBO than SBO, HOSBO.

Salimon et al. (2012a) and Abdullah et al. (2014) investigated mono-epoxidation of linoleic acid using Novozyme 435 as a catalyst. They have studied the influence of various process parameters on epoxidation by D-optimal design and attained optimum condition at H_2O_2-15µL, Novozyme-435 120 mg, reaction time 7 h, at this condition yield of mono-epoxidized oleic acid (MEOA) was found to be 82.14% and OOC was found to be 4.91 mass%. In this work properties of linolenic acid and MEOA were also determined and reported as PP (-2 ^{o}C, -41 ^{o}C), flash point (FP, 115 ^{o}C, 128 ^{o}C), viscosity index (VI, 224, 130.8) and oxidative stability (OS, 189 ^{o}C, 168 ^{o}C). Finally, these studies have concluded that MEOA has positive influence on PP, FP.

A recent study on epoxidation of passion fruit oil (PFO) and moringa oil (MO) by Silva et al. (2015a, 2015b) revealed the synthesis of novel biolubricants with satisfactory properties. This study also tested the additive treatment of prepared epoxides, outcomes of the study revealed that epoxides of PFO (EPFO), MO (EMO) oxidation stability (16.89 min, 204.7 min with additives; 24.57 min, 311.8 min with additives), viscosity (185.65 Cst, 80.37

cSt) was high compared to PFO (7.5 min, 31.78 cSt) and MO (28.27 min, 44.88 cSt). OOC of EPFO and EMO was found to be 4.51 and 4.23 mass% respectively, finally the study concluded that epoxidised oil showed an improvement in additive solubilisation, fluid performance, exhibited superior lubrication performance properties, film formation and lower friction co-efficient than commercial mineral base fluids.

Although a vast pool of research material is available in the literature on epoxidation of edible and non-edible vegetable oils for diverse applications. Even there are few studies on understanding the effect of process parameters on epoxidation and to determine the thermodynamic, kinematic parameters (Goud et al. 2006; Meyer et al. 2008; Dinda et al. 2008; Mungroo et al. 2008; Derawi and Salimon 2010; Meshram et al. 2011; Sun et al. 2011; Fiser et al. 2012; Monono et al. 2015). But considering the aim and objectives of current study only selected reports have been discussed here.

From the overall literature it was noted that, in the early years of research on synthesis of bio-lubricants H_2SO_4 was used as a homogeneous acid catalyst due to its acid strength, selectivity and short reaction time. Later, studies revealed about the formation of unwanted side products due to excess catalyst loading, difficulty in product purification; H_2SO_4 was not considered as an appropriate catalyst. Therefore, AIER as a heterogeneous catalyst gained much significance in *In-situ* epoxidation due to its satisfactory outcomes in terms of oxirane content, catalyst reusability and feasibility of reaction conditions. During the epoxidation, hydrogen peroxide is considered as an oxygen donor due to its high active oxygen content (47.1 wt %) and acetic acid as oxygen carrier. By examining the physico-chemical properties of epoxides from various feedstocks, it is observed that epoxides have higher pour point which is not suitable for low temperature applications; however all other properties exhibits satisfactory outcomes. Therefore, in order to enhance the PP of epoxides further

modification/s (series of structural modifications) to epoxide ring is mandatory. However, opening of the three-member oxirane ring (hydroxylation) provides a more energetically favourable site for reactions and represents a chemical intermediate for the preparation of derivatives that would be difficult to obtain directly from the unsaturated bond (Borugadda and Goud 2012). Further, functionalization of the epoxides enhances the PP compared to raw oils, epoxides and their respective esters, hence the following section discusses about the possible series of structural modifications can carry out to epoxides.

1.5.2 Ring opening/Hydroxylation

After having detailed discussion on preparation of epoxidised vegetable oils, further the use of such epoxides as substrates for the addition of alcohols and acids is described in this section. Use of various catalysts during the ring opening is discussed along with further functionalization of epoxides by ring opening to enhance the required physico-chemical properties. The term hydroxylation/ring opening (RO) reaction is used to refer to the process of introducing hydroxyl groups in the oxirane ring. Before the hydroxylation reaction occurs, the oxirane ring must be opened; there are two ways to open an oxirane ring to permit the hydroxylation reaction to occur. RO of epoxides takes place through cleavage of one of the carbon-oxygen bonds, under acidic conditions RO occurs in two key steps; firstly the epoxide is protonated, secondly, the nucleophile attacks at the most substituted position. Ring opening reaction can proceed by either S_N2 or S_N1 mechanisms, depending on the nature of epoxide and reaction conditions. There are various sources of hydroxyl groups that can be used in the hydroxylation process such as alcohols, acids and water. Special attention has been given to the addition of alcohols bearing branches in β position, because it is expected these branches will sterically hinder the new functions created by the ring opening of epoxide with the alcohols, i.e. ether and hydroxyl groups, increasing the hydrolytic and oxidative stability of the products in their application as bio-lubricants.

A number of studies have found that RO reaction is a critical step in the production of polyol or hydroxylated products. A variety of factors that may persuade in the hydroxylation are clearly discussed for process optimization. Extensive work has been carried out on RO by various technocrats using various feedstocks; the gists of few studies in the field of bio-lubricant are discussed below.

Sharma et al. (2006) prepared four hydroxy thio-ether derivatives using ESBO as a feedstock; RO was carried out in presence of perchloric acid as a catalyst, using 1-butanethiol, 1-decanethiol, octadanethiol and cyclohexyl mercaptan as alcohols. Resulted hydroxyl compounds have shown interesting oxidation stability, lubricity properties, greater affinity for metal surfaces and improved friction and wear behaviour. Onset oxidation temperature (OOT) of SBO, ESBO and RO by 1-butanethiol derivative was found to be 134, 195 and 181 ^{o}C. Later, Sharma et al. (2008a) synthesized acyl derivatives of ESBO using various anhydrides (acetic, hexanoic, propionic, butyric, isobutyric, valeric and heptanoic) in presence of BF_3 catalyst. Among all the anhydrides, hexanoic anhydride showed good lubricant properties as antiwear and PPD additive. The molecular weight of prepared ESBO and diesters was found to be 845, 883 (acetic), 887 (propionic), 884 (iso-butyric), 890 (butyric) and 905 (hexanoic). Further, Campanella et al. (2010) reported the preparation of sunflower and high oleic sunflower oil epoxidation followed by RO with methanol and ethanol using sulphuric acid, fluoroboric acid as catalyst. Crystallization temperature of SBO, sunflower oil (SO), high oleic sunflower oil (HOSO) and their epoxides was found to be -65, -35 ^{o}C; -68, -42 ^{o}C; -29, 4 ^{o}C. The rheological study of the sample showed Newtonian behaviour.

Salimon et al. (2011a) studied the optimization of epoxidized oleic acid (OA) ring opening by D-optimal design. The optimum condition of study was found to be OA/mono

epoxidized oleic acid (MEOA) 0.3:1 wt%, PTSA/MEOA 0.5:1 wt%, reaction temperature 110 ^{o}C, reaction time 4.5 h; at this optimum condition yield and OOC was found to be 84.61 % and 0.05 mass% respectively. A study on Jatropha oil (JO) epoxidation and ring opening by Daniel et al. (2011) showed that RO product PP was around -18 ^{o}C and demonstrated improvement in the oxidative stability and PP than JO and its epoxide. Patchara and Supawan (2011) prepared palm oil (PO) and their methyl esters (POME) epoxides, and further RO was studied in presence of 2-ethyl hexanol (2-EH). During the RO at various reaction conditions % transesterification was found to be 71.64 to 95.35 in epoxidised palm oil (EPO) and 51.38 to 62.86 in epoxidised palm oil methyl esters (EPOME). For both the RO products PP was found to be identical and lowest PP was found to be 9 ^{o}C for blends. Later, Arumugam et al. (2012) studied the epoxidation and RO of sunflower, palm, rapeseed and their metylesters. The oxirane ring was opened in presence of methanol and water. Among all rapeseed oil showed favourable properties as lubricants. Biodegradability of the epoxidized rapeseed oil (ERSO) and their RO products was observed to be >95%. Similarly, other significant properties such as viscosity, viscosity index and PP was found to be 90.1, 35 cSt; 160, 220; -11, -15 ^{o}C.

Similarly, Kulkarni et al. (2013) studied the epoxidation of mustard oil (MO) and further ring opening was carried out in presence of sulphuric, sulphamic and methane sulphonic acids as a catalyst using 2-ethyl hexanol. Results of the study revealed that for RO products with an increase in catalyst loading and time, viscosity index increases and PP decreases. Among all the catalysts, sulphamic acid was considered as the most suitable catalysts for the reaction. At the same time, Madankar et al. (2013) epoxidised the canola oil (CNO) and opened the ring in presence of n-butanol, amyl alcohol and 2-ethyl hexanol using IR-15 as a catalyst. Kinematic viscosity (KV), PP and onset temperatures was recorded as follows; epoxide (151cSt, 10 ^{o}C, 320 ^{o}C), butylated (251.7 cSt, -5 ^{o}C, 355 ^{o}C), amylated

(190.5 cSt, -8 ^{o}C, 361 ^{o}C) and 2-EH (85.5 cSt, -15 ^{o}C, 405 ^{o}C). This study also highlighted the catalyst reusability and found that the catalyst can be reused up to four times.

From the above investigations it was observed that alcohols and anhydrides were used in order to improve the lubricant properties and PP. However, further structural modifications such as; esterification and functionalization of various anhydrides were carried out to develop tri-esters and tetra esters which were considered to be multi grade, high quality bio-lubricants. The main focus of the following discussion is to give an overview on the synthesis of di, tri and tetra esters from the aforementioned chemical modifications. Therefore, further functionalization of the ring opened products is inquired to enhance the lubricant properties.

1.5.3 Di, tri and tetra esters formation via esterification and anhydrides addition

Further modification of ring opened product to di, tri and tetra esters need to be carried out to improve low temperature properties (PP), stability and viscosity of the products. So that high quality bio-lubricant basestocks can be obtained. In the present section a brief summary of relevant state-of-the-art with respect to bio-lubricants formulation have been summarized.

Hwang, Erhan and co-workers carried out extensive work on ESBO for few years (2001-2006), ESBO was structurally modified via ring opening and esterification reactions. In Hwang and Erhan (2001) the ESBO was esterified in presence of methanol, 1-butanol, 2-butanol, 1-hexanol, cyclohexanol, 1-decanol, 2,2-dimethyl di-propanol. The study indicates that esterification step required longer reaction time for higher molecular weight alcohols except 2,2-dimethyl di-propanol. The esterified products of methanol, 1-butanol and 1-hexanol found to exhibits pour point of -3, -6 and -9 ^{o}C respectively. Further, esterification of RO products was carried out in presence of acetic, butyric, 2-methyl propionic, hexanoic anhydrides, thereafter anhydride derivatives were additivated with 1% PPD and PP was

observed to be -39, -39 and -45 ^{o}C respectively with acetic and hexanoic anhydrides as esterification reagents. Proposed reaction scheme for the RO and esterification is depicted below (Scheme 1.2). Later Hwang et al. (2003) during their study on esterification of ESBO with 2-EH observed the formation of transesterified products, afterwards esterification with anhydrides (acetic and hexanoic) and addition of 1% PPD (PAO-4) (1.3 equiv. Mol of 2-EH) showed low temperature stability of -36 ^{o}C with high VI as 159. By additivation with 1% PPD (3 equiv. Mol of 2-EH) PP and onset temperature was observed to be -60, 165.62 ^{o}C.

Further, Hwang and Erhan (2006) examined ring opening reaction with 2-butyl octanol, decanol, 2-hexyl octanol, dodecanol, 2-octyl decanol and acetylation. Outcomes of the study revealed that, 0% and 100% transesterified products were obtained, RO products pour point without additive and with 1% additive was found to be in the range of -18 to -36 ^{o}C, -21 to -46 ^{o}C. Likewise, acetylated products PP without additive and with 1% additive were found to be in the range of -27 to -42 ^{o}C and -30 to -48 ^{o}C. Viscosity of 0 %, 100% transesterified product was found to be 232.4, 74.5 cSt; for acetylated products it was around 103.4, 41.5 cSt. From this study it was also observed that RO products have lower VI and acetylated products have higher VI and OS. The properties obtained in this study was found to be analogous with synthetic and mineral oil lubes.

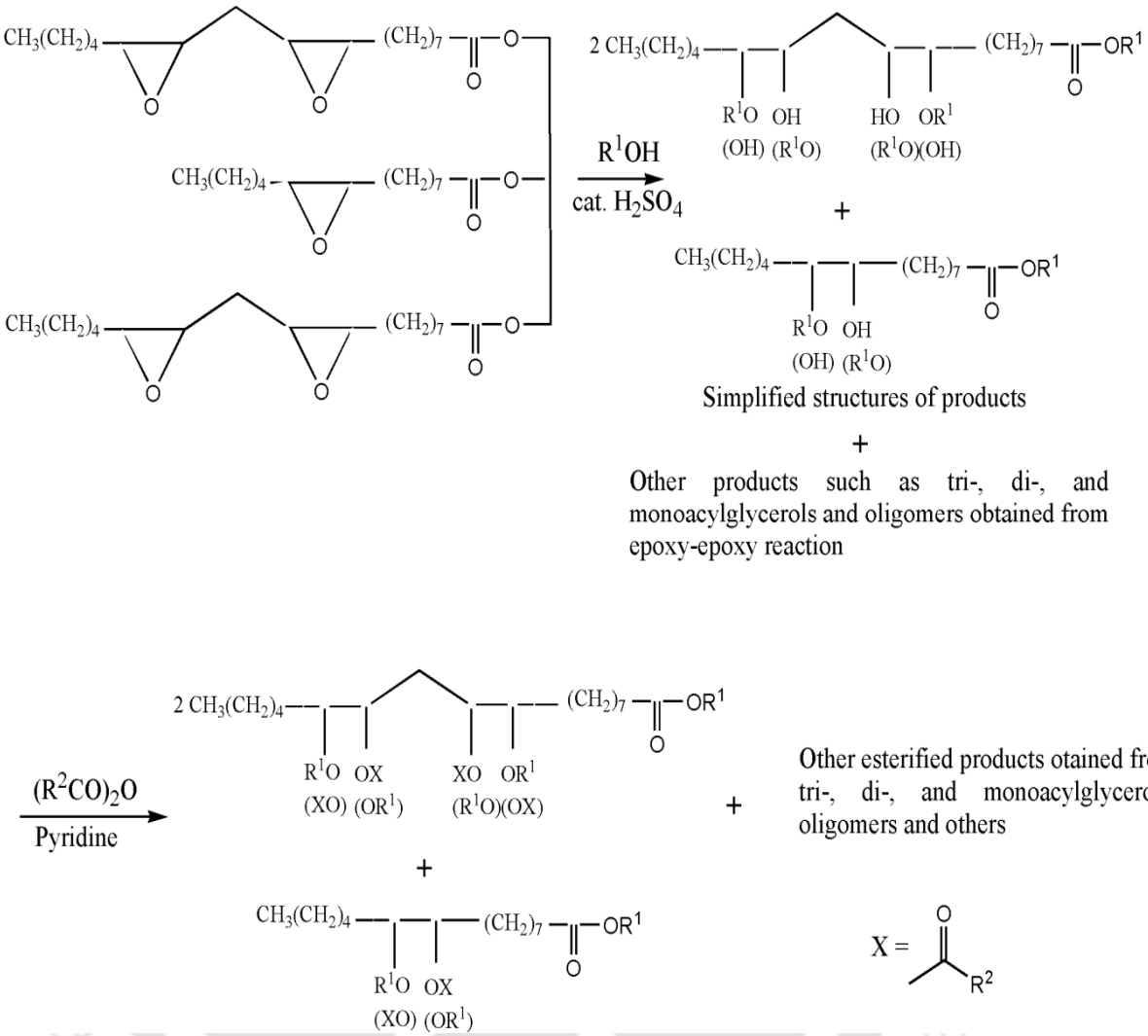

Scheme 1.2: Reaction scheme proposed by Erhan and co-workers for RO and esterification of ESBO

Sharma et al. (2006) studied the ring opening and acetylation of ESBO by using acetic, butyric, isobutyric and hexanoic anhydride. Main focus of the study was to enhance the thermo-oxidative stability of prepared anhydride derivatives. Maximum OS achieved with acetic anhydride with and without additives was 256 ^{o}C and 174 ^{o}C respectively. However, Lathi PS and Mattiasson (2007) synthesis biolubricant by ring opening reaction using IR-15 catalyst with n-butanol, isoamyl alcohol, 2-EH and further acetylation of ESBO by acetic anhydride. The results of this study revealed that 3 mol of n-butanol in esterification reaction gave maximum viscosity as 312.9 cSt, PP of the acetylated products was found to be > -5 (n-

butanol), < 0 to > -15 (isoamyl alcohol), and < -10 (2-EH). Rheology of the prepared products was examined and found to be Newtonian fluid behavior, prepared products was biodegradable and catalyst can be reused up to four times.

Salimon and Salih (2009a) studied oleic acid oxirane ring opening reaction in presence of various fatty acids (octanoic, nonanoic, lauric, myristic, palmatic, stearic, behenic) using PTSA as a catalyst. Further, esterification with octanol revealed that, improved low temperature properties can be obtained with an increase in the fatty acid chain length. The product of ring opening reaction with nonanic acid derivative showed pour point and viscosity as -30 ^{o}C, 67 cSt; further esterification by behenic acid pour point and viscosity was noticed to be -50 ^{o}C, 123 cSt (Scheme 1.3). On the other hand, similar study by Salimon and Salih (2009b) with butanol as an esterification reagent showed utmost PP and viscosity value as -56 ^{o}C, 234 cp for behenic fatty acid derivative.

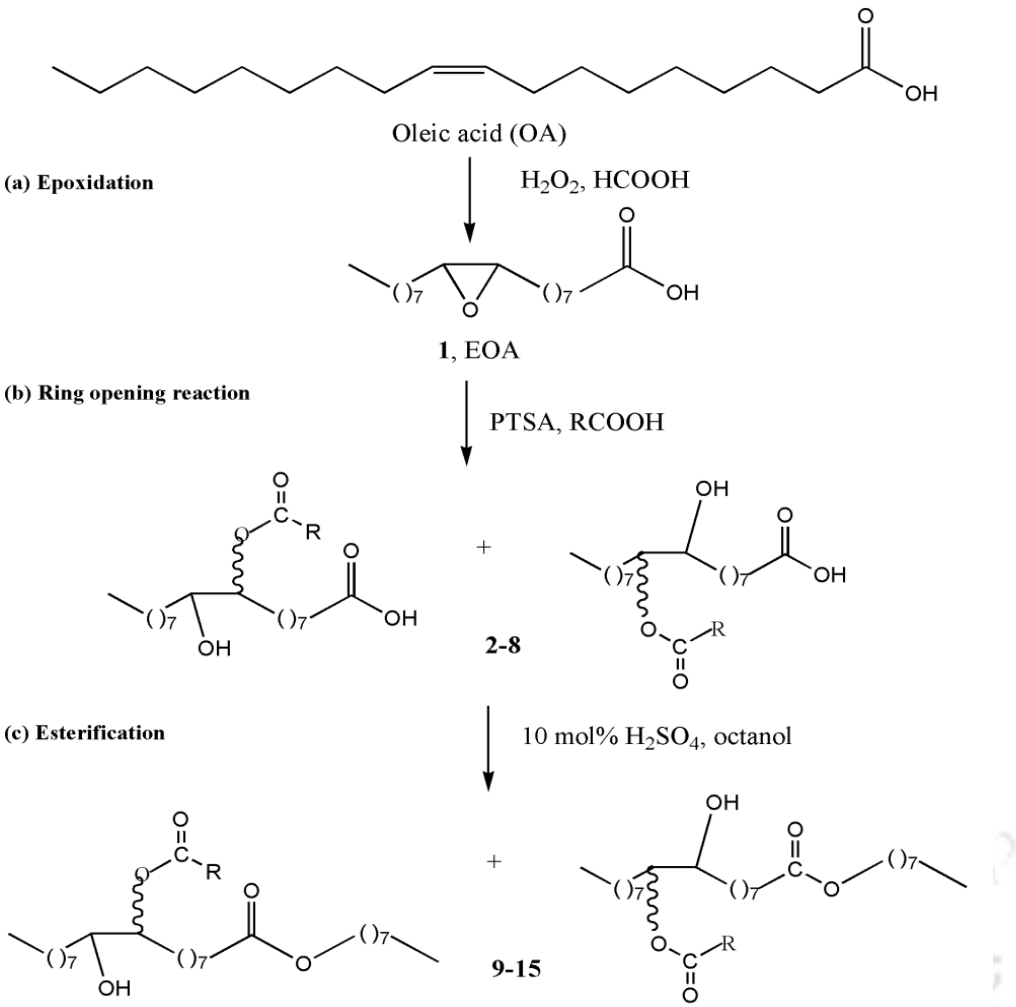

Scheme 1.3: Epoxidation of oleic acid, followed by ring opening acylation of EOA using PTSA as catalyst, RCOOH is octanoic, nonanoic, lauric, myristic, palmetic, stearic and behenic acid.

Further, Salimon and Salih (2010) studied the RO of oleic acid epoxide with octanol and 2-EH, followed by esterification of mono-esters with octanol and 2-EH, the unconverted free hydroxyl group was further reacted with oleic and stearic acid to give tri-esters. The prepared di-ester exhibits favourable cold flow properties and their PP, viscosity was found to be -23 ^{o}C, 129 cP; -28, 149 cP. Similarly, PP and viscosity of the prepared tri-esters was noticed to be -31 ^{o}C, 159 cP; -35 ^{o}C, 178 cP, from this study it could be concluded that, the tri-esters yields best performance properties.

Salimon et al. (2012b) reported a series of structural modifications (Scheme 1.4) such as epoxidation, ring opening, esterification and acetylation to prepare tri-esters of oleic acid. The significant physico-chemical properties of prepared tri-esters were measured such as PP, FP, VI and OOT. The friction and wear properties were measured by high frequency reciprocating rig (HFRR). The results showed that, mid chain esters exhibits positive influence on low temperature properties, but shows negative impact on onset temperature. The results of the study revealed that for mono, di and tri-esters maximum PP and VI was found to be -43 ^{o}C, 110 cp; -45 ^{o}C, 128 cp; -48 ^{o}C, 145 cp respectively for behenic acid derivatives. But mono, di and tri esters of all octanoic acid derivatives showed maximum OOT as 113, 131, 142 ^{o}C respectively. Acceptable friction properties were also observed for the prepared tri-esters. During the entire structural modifications yield was found to be in the range of 55-92%.

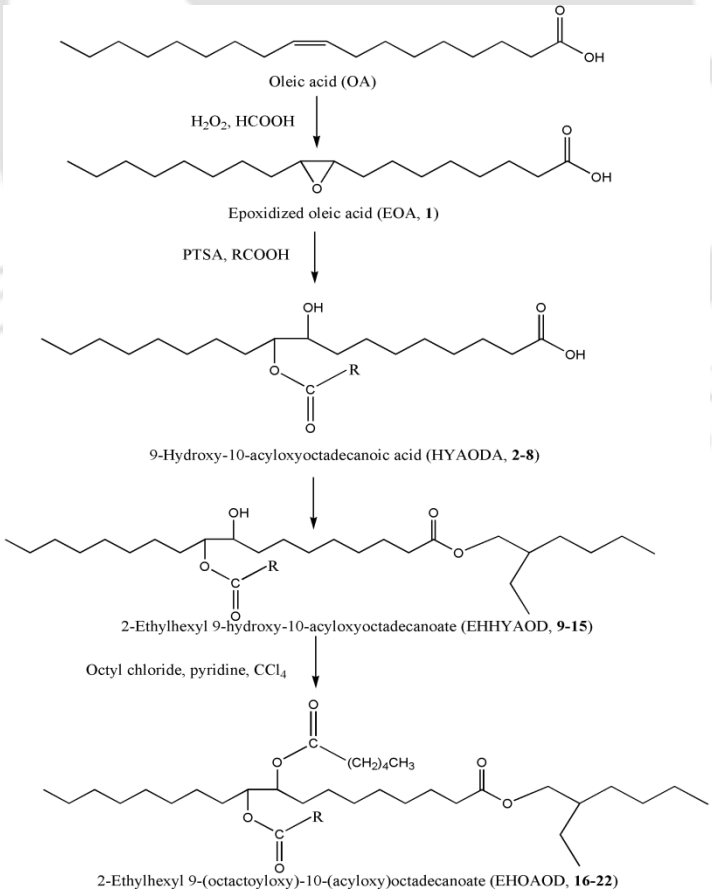

Scheme 1.4: Oleic acid based tri-esters formation

Salimon et al. (2011b) reported a series of structural modifications (RO and esterification) of epoxidised ricinoleic acid to prepare biolubricant basestocks. Epoxidation and RO reactions were carried out as per their earlier reports on oleic acid, using identical reagents and reaction conditions. Except esterification step which was carried out with butanol. The structurally modified ERA, RO and esterified products showed maximum PP and VI as 9 ^{o}C, 67; -23 ^{o}C, 171; -47 ^{o}C, 243 respectively for behenic acid derivatives. Afterwards in 2012, the same group has studied esterification in presence of 2-EH and octanol. The measured properties such as PP and VI of 2-EH derivative was found to be -42 ^{o}C, 205 and octanol derived esters PP and dynamic viscosity was observed as -53 ^{o}C, 283 mPa.s (at 25 ^{o}C). The detailed reaction path way proposed in the study s given in Scheme 1.5. From the afore mentioned chemical alterations, it was observed that, in the end product still there are two more single hydroxyl groups are present which can be functionalized further.

Salih et al. (2013) studied the functionalization of hydroxyl groups with 2 mol of stearic acid during esterification and 4-ethyl hexanol during acylation. The measured PP, VI and OOT of tri-esters and tetra esters was found to be -32 ^{o}C, 193, 245.45 ^{o}C; -44 ^{o}C, 257, 282.1 ^{o}C respectively. This study also determined the tribological properties of prepared esters. All the derivatives showed good anti-wear and friction reducing properties. From this investigation, it could be concluded that ricinoleic acid di-esters with octanol as an esterification reagent exhibits lower PP (-53 ^{o}C) compared to tetra esters of ricinoleic acid. The complete reaction pathway for the formation of tetra-esters described by Salih et al. (2013) is presented in Scheme 1.6.

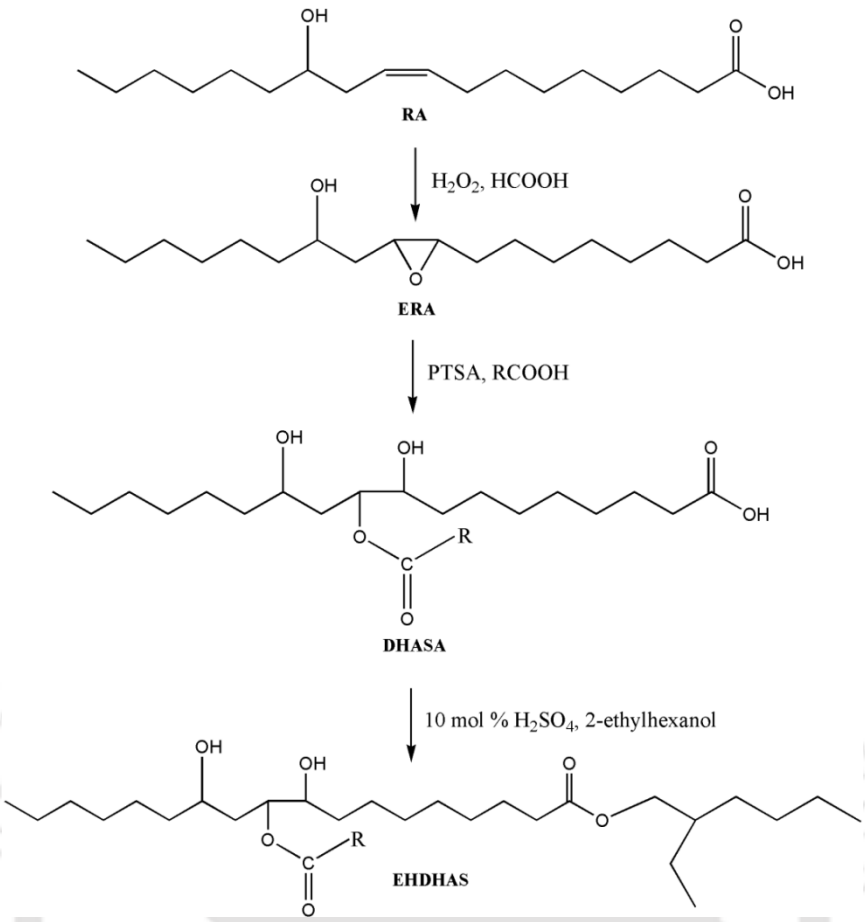

Scheme 1.5: Schematic reactions of epoxidation, ring opening and esterification of ricinoleic acid derivatives reported by Salimon et al. (2012b) (RA, ricinoleic acid; EOA, epoxidized ricinoleic acid; PTSA, *p*-toluenesulfonic acid; RCOOH, octanoic, nonanoic, lauric, myristic, palmitic, stearic and behenic acids; H_2SO_4, sulfuric acid)

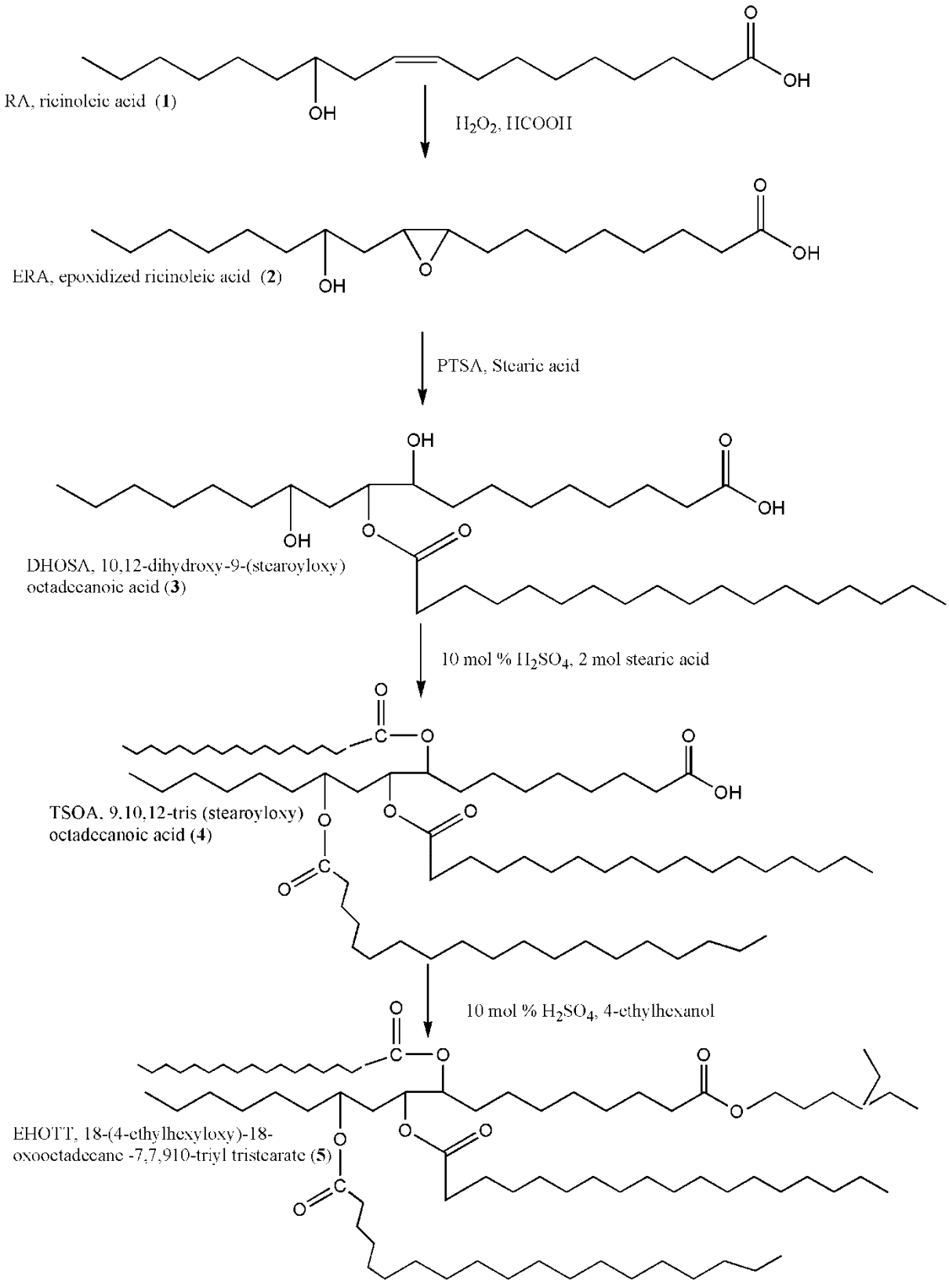

Scheme 1.6: Reaction scheme for the formation of tetra-esters

Similar manner, Salih et al. (2011a) also reported the synthesis of oleic acid based tri-esters as potential basestock for biolubricant production. The oleic acid chemical structure was altered by a series of chemical modifications such as epoxidation, RO, esterification and acetylation, synthesis process was identical to their earlier studies, but only variation in RO and acylated reagents. In this study esterification was carried out by n-pentanol (linear) and iso-pentanol (branched), further acylation was carryout by oleic and stearic acid. The pout point and dynamic viscosity of di-esters was (n-pentanol, iso-pentanol) -20 ^{o}C, 78 cp; -22 ^{o}C, 88 cp; and for tri-esters (oleic, stearic acid) it was found to be -24 ^{o}C, 105 cp and -25 ^{o}C, 113 cp respectively. Enhancement in the PP was due to increased chain length of the branching agents. Further, similar study carried out Salih et al. (2011b) using octanol as an esterification reagent and lauroyl chloride and carbon tetra chloride (CCl_4) as acylation reagent clearly claimed that hydrogen bonding was a critical parameter influencing the physico-chemical properties. Further, increase in the polar functionalities of plant oil structures showed a positive impact on wear protection due to stronger absorption potential on the metal surfaces. Among all the derivativsed products maximum PP was found to be -45 ^{o}C for behenic acid derivative. Salimon et al. (2012c) carried out RO with 2-EH and acylation by caproic, octanoic, capric, lauric and myristic fatty acids using H_2SO_4 as catalyst. The study claim that increase in the branching and chain length pour point results in a increase in the PP, esterified and acylated products PP was found to be -24.33 ^{o}C and -47.19 ^{o}C (myristic acid derivative). OS of the epoxodized, ring opened, esterified and acylated products was found to be 75.12, 112.67, 116.34 and 80.46 ^{o}C (myristic acid derivative).

Similar kind of study was carried out by Mahajan et al. (2013) on epoxidation of mustard oil and further esterification with sec-amyl alcohol and stearic acid in presence of sulphuric acid as a catalyst. The study claims that with an increase in catalyst loading and time, specific gravity and VI of RO products found to be increased. The pour point was found

to be favourable at lower catalysts loading compared to higher catalyst loading. Considerable lubricant properties were determined for the prepared esters and PP of RO product was found to be -30 ^{o}C, -26 ^{o}C respectively at 1 wt% and 2 wt% catalyst loading.

Sharma and Dalai (2013) described a green and environmentally friendly one step process for the preparation of bio-lubricant from epoxidised canola oil. In this study simultaneous epoxy ring opening and esterification was carried out in presence of acetic anhydride using a novel sulfated Ti-SBA-15(10) as catalyst. Optimal reaction conditions were found to be 130 ^{o}C reaction temperature, 4.5 g acetic anhydride, 10 wt% sulfated Ti-SBA-15 (10) catalyst loading for 5 h reaction time and stirring speed 1000 rpm. Further, effect of various catalysts on percentage conversion of epoxy canola oil to esterified product was examined and sulfated Ti-SBA-15 demonstrated 100% conversion of esterified product, reaction kinetics, catalyst reusability and lubricity properties were also determined. Finally, the study concluded that oxidative property of bio-lubricant was found to be outstanding (56.1 h), pour point -9 °C, and kinematic viscosity at 100 °C was around 670 cSt, prepared esters also demonstrated the excellent lubricity property with wear scar of 130 μm.

Recently, Li and Wang (2015) derived the bio-lubricants from waste cooking oil with improved oxidation stability and low temperature properties via epoxidation, esterification by methanol and transesterification by iso-octanol, iso-tridecanol and iso-octadecanol. Among all the transesterified product iso-octadecanol derivative showed interesting results in terms of KV, PP, OOT and was found to be 43.4 cSt, -24 ^{o}C and 194.5 ^{o}C. Investigation on the tribological properties suggested that transesterified products showed improved performance than WCO.

1.5.4 Knowledge Gap

Based on the overall literature summary it was noticed that, in recent times, number of studies have found that the series of structural modification to the epoxides getting significant attention and it has been proven to be highly efficient and effective towards the preparation of high quality bio-lubricant basestocks. Amongst various feedstocks SBO, OA, RA and few other oils has been substantially addressed, due to their availability in the local markets. However, very concise and un-detailed research was discovered for WCO, CO and their methyl esters using a series of chemical modifications for bio-lubricant application. Therefore, there is enough scope to conduct research for aforementioned feedstocks to prepare bio-lubricant basestocks from non-edible oil and edible waste oil.

1.6. Objectives

Hence, the present study was carried out with the broad objectives to prepare biolubricant base oil from locally available non-edible oil, used edible oil and their methyl esters to improve their performance compared to un-modified raw oils. Among all the performance properties, special attention was given to thermo-oxidative stability, low temperature performance, biodegradability and tribological properties. Based on the state-of-the-art presented in section 1.4, the PhD thesis targets the fulfillment of the following major objectives.

- Evaluation of the physico-chemical properties of feedstocks: waste cooking oil (WCO), castor oil (CO) and their fatty acid methyl esters (WCOFAME, COFAME)
- Epoxidation of WCO, CO and their methyl esters
  i. Optimization of reaction parameters by central composite design (CCD) technique to maximize the epoxide content
  ii. The estimation of significant physico-chemical properties of prepared epoxides

- The oxirane ring opening studies of prepared epoxides for the production of bio-lubricant base stocks (four epoxides) and their physico-chemical characterization
- Hexanoylation of ring opened products (hydroxyl groups) and evaluation of their tribological characteristics and biodegradability study of the obtained product.
- Comparative analysis of the prepared bio-lubricant basestocks

1.7. Organization of the thesis

The PhD thesis is organized in nine chapters.

Chapter 1 addressed the state of art, possible scope for further research, objectives and organization of the thesis.

Chapter 2 dissertated the synthesis procedures of methyl esters by transesterification, epoxides by in-situ epoxidation, hydroxylated products by ring-opening and di-esters by hexanoylation. Further, this chapter has given main emphasis on various product confirmation methods; correspondingly, physico-chemical characterization techniques used to evaluate the significant product performance properties were reported.

Chapter 3 addressed the possible physico-chemical changes in cooking oil during frying process. Further, thermo-oxidative stability and cold flow properties of the feedstocks examined thoroughly, which were considered as limitations to use feedstocks as lubricant basestocks.

Chapter 4 describes three different structural modifications (epoxidation, hydroxylation and hexanoylation) carried out to various fatty acids, with glycerol in the feedstock (WCO) to improve the performance limitation properties. Further, significant physico-chemical properties were estimated at every stage after each chemical modification.

Chapter 5 similar study was carried out like Chapter-4 with WCOFAME as a feedstock without glycerol.

Chapter 6 presents series of chemical modifications carried out to CO in presence of glycerol, along with one excess hydroxyl group in its structure to enhance limiting properties. Upon, every chemical modification significant physico-chemical properties were evaluated and compared with the properties of un-modified feedstock at every step.

Chapter 7 analogous study was carried out like Chapter-6 with COFAME as a feedstock without glycerol.

Chapter 8 performance limitation properties (thermo-oxidative and cold flow properties) of feedstocks, epoxides, hydroxylated and hexanoylatd products were compared with the conventional hydraulic lubricants collected from the local market of Guwahati, India. Based on the obtained results, this chapter proposed the potential applications for the lubricant basestocks prepared in the present study.

Chapter 9 presents several conclusions drawn from the research work and it also provides the potential directions for future work.

CHAPTER-2

Experimental and Characterization

This chapter dissertated methyl esters synthesis procedure by transesterification, epoxide by in-situ epoxidation, hydroxylated products by ring-opening, di-esters by hexanoylation and oil extraction process from castor seeds also discussed in detail. During epoxidation of all the feedstocks, central composite design (CCD optimization technique was implemented and experimental design, statistical analysis also explored. Further, this chapter has given the main emphasis on various product confirmation methods such as NMR (^{1}H, ^{13}C), FTIR, iodine value, oxirane oxygen content (OOC) and α-glycol content. Correspondingly, physico-chemical characterization techniques used to evaluate the significant product performance properties were reported. These techniques had shown that, all the products can act as impending potential candidates for biolubricant basestock application.

2.1. Materials

2.1.1 Soxhlet extraction of castor oil (CO) and preparation of its methyl esters

In this study castor seeds were obtained from Cherukupalli, Andhra Pradesh, India. Collected castor seeds were de-hulled and one hundred grams of grinded (using mixer grinder) castor seeds were used to extract oil. CO was extracted from grinded castor seeds by soxhlet apparatus for eight hours as per AOAC standard method. Hexane was used as an extraction solvent near to its boiling point to avoid loss of solvent *via* evaporation. Extraction time was considered when the first drop of solvent recycled in to the thimble. Finally the extract was concentrated in rotary evaporator (BUCHI, R-200, Germany) for complete removal and recovery of the solvent; residual oil was cooled and weighed to estimate the extraction yield and further physico-chemical properties of extracted CO was evaluated.

In the process of preparing methyl esters from CO, acid value (AV) performs a major role. Since the AV of extracted CO was very high (45.6 mg KOH/g), a two-step acid esterification process followed by alkali transesterification was performed for the preparation of CO fatty acid methyl esters (FAME). Esterification was carried out in a 500 ml special glass reactor (3 mm thick), sealed tightly and fitted with a condenser at the top. The reaction glass vessel was placed in a temperature controlled water bath at 1:10 oil to methanol molar ratio, with 5 wt% of catalyst concentration (sulphuric acid - H_2SO_4), 90 min reaction time, and a stirring speed of 600 rpm. At these conditions, AV was reduced from 45.6 mg KOH/g to 3.01 mg KOH/g.

Similarly, transesterification was carried out in the same setup using 1:6 oil to methanol molar ratio and 1 wt% potassium hydroxide (KOH) as a base catalyst. Initially, esterified oil was charged into the reactor and heated up to 60 ^{o}C; because, beyond this temperature evaporation of methanol was observed when methanol was used as transesterification reagent. The alkali catalyst (KOH - 1 wt%) was dissolved in methanol to form sodium methoxide solution, and it was prepared freshly in order to avoid moisture absorbance and to maintain the catalytic activity. The prepared sodium methoxide solution was slowly added to the preheated oil. The system was totally closed to the atmosphere to prevent the loss of methanol, and stirred for 90 min. After completion of reaction, the mixture was cooled and transferred into a separating funnel and allowed to settle overnight for product separation. The upper layer contains methyl esters, residual methanol and catalyst, whereas the lower layer contains glycerol and impurities. The glycerol layer was drawn off using separating funnel and FAME layer was washed with warm millipore water (40 ^{o}C) until the pH of washing water reached equal to that of millipore water. The FAME was dried at 60 ^{o}C under the vacuum by using rotary evaporator to remove the water content, the obtained yield of castor oil fatty acid methyl esters (COFAME) was recorded as 95%.

2.1.2 Base catalysed transesterification of WCO

Waste cooking oil (fish fried soybean) was collected from hostel mess, IIT Guwahati, Guwahati, India. After collection, oil was used without any further purification to prepare FAME. The obtained oil was measured for its AV and was recorded to be 1.46 mg KOH/g. Hence single step transesterification procedure was followed at 1:6 oil to methanol molar ratio, 1 wt% catalyst loading, 600 rpm stirring speed for 90 min at 60 ^{o}C reaction temperature to prepare waste cooking oil fatty acid methyl esters (WCOFAME) (Borugadda and Goud 2014b).

After transesterification, the methyl esters conversion was confirmed by ^{1}H, ^{13}C NMR spectral techniques. The physico-chemical properties of prepared methyl esters were determined using standard ASTM, AOCS official methods and discussed in the respective chapters (4, 5, 6 and 7).

2.2. Preliminary studies on epoxidation process variables and experimental design

During the epoxidation of all feed stocks (CO, WCO and their FAME), four reaction variables such as, substrate molar ratio i.e. mole ratio of C=C bonds to H_2O_2 (mol), catalyst loading (wt%), temperature (^{o}C) and reaction time (h) were chosen to optimise and understand the effect of these variables, which were highly responsible for maximum OOC. Prior to the optimization experiments, a set of preliminary experiments have been performed by adopting a single parameter optimization approach to set the optimum range of chosen process parameters. Initially, reaction time was optimized by withdrawing the sample at regular 1 h interval to estimate iodine value (IV) and oxirane oxygen content (OOC). During the progress of reaction, a linear increase in epoxide content and decrease in IV was observed up to certain time period, beyond which gradual decrease in OOC was noticed. A similar trend was noticed for all other reaction variables (H_2O_2, temperature and time).

Hence, depending on the preliminary studies, range (lower (-1), medium (0) and higher (+1) levels) of the process variables were chosen for all the feedstock's and coded in the respective chapters according to equation 2.1. Throughout this study, optimization was performed only for epoxidation reaction to maximize the oxirane oxygen content, as oxirane rings are considered as reactive sites for further study. However, the optimization of hydroxylation and hexanoylation was carried out by preliminary study approach.

Upon deciding the range of each process variable, a set of experimental design matrix was generated using 2^4 full factorial CCD for four independent variables, by giving a total number of 30 ($=2^n+2n+6$) experiments, where 'n' is the number of independent variables. During the optimization, the value of α (alpha) was fixed at level 2 ($\alpha = 2^{4/4}$), further, eight axial experiments and sixteen factorial runs were carried out with six extra replications at the centre of design to estimate the pure error.

$$X_i = \frac{X_{i-}X_0}{\Delta X_i} \qquad (2.1)$$

All epoxidation reactions were carried out in 250 ml three necked glass reactor equipped with five blade glass stirrer to maintain proper mixing among the reactants and to avoid the reaction mass transfer resistance. Additionally, the condenser was inserted to reflux the gases evolved during reaction, the whole setup was immersed in the heating oil bath. Initially, unit quantity of oil/FAME was transferred into the reaction vessel, consequently heated to a required reaction temperature, then 0.5 mol of glacial acetic acid with respect to mole ratio of C=C bonds and other reaction variables i.e. hydrogen peroxide, catalyst were considered from CCD experimental design matrix. During the preliminary studies, process parameters overall optimum range was observed to be 45–70 ^oC reaction temperature, hydrogen peroxide molar ratio 1–2.5, catalyst loading 10–30 wt% and reaction time 2 - 14 h. All the experiments were carried out in an identical setup and process parameters used are

mentioned in experimental design matrix (Appendix). The addition of hydrogen peroxide to the reaction mixture was carried out drop wise in the first half an hour, when the temperature was 5 ^{o}C below the reaction temperature to avoid explosion, 1500 rpm stirring speed was maintained to assure consistent mixing. After the complete addition of hydrogen peroxide, reaction was continued for desired time duration as mentioned in Appendix. Upon completion of epoxidation, prior to analysis prepared epoxides were washed repeatedly with sodium bicarbonate followed by warm millipore water (40 ^{o}C) until all the catalyst and other reactants were removed to make it neutral, finally rotary evaporator was used to distilled off solvent and trace water. OOC was determined for the final epoxide product after each experimental run. All the experimental runs were carried out in duplicate and the average values were reported during the entire study. Experimental design and detailed statistical analysis carried out is clearly described in Appendix using prior reports on RSM (Mahalik et al. 2010; Abnisa et al. 2011; Borugadda and Goud, 2014a; Mubarak et al. 2014).

2.3. Epoxide ring opening studies

The epoxide prepared at optimized condition was used further to study the ring opening reaction. Initially various alcohols (i.e. methanol, propanol, butanol and 2-EH) were used in order to determine the PP of ring open (RO) products with sulphuric acid (homogeneous acid) and IR-120 (heterogeneous acid) as catalysts. Ring opening reaction was carried out with WCO epoxide as a feedstock under different operating conditions to improve the cold flow properties and to bypass the transesterification of fully ring opened product. The reaction was carried out in a three neck round bottom flask equipped with over head motor, reflux condenser and other two necks for withdrawing the sample and to monitor the reaction temperature. A known amount of epoxidised oil/FAME was taken into a reactor followed by alcohol (mol) and catalyst (wt%), the effectiveness of process parameters was studied thoroughly for 100 % ring opening reaction to takes place. The catalyst loading was altered

between 0.5 - 2 wt%, similarly reaction time was varied from 2 min to 24 h depends up on the catalysts used and reaction temperature was varied from room temperature to 70 ^{o}C. During the course of reaction samples were withdrawn at regular intervals, washed with 5% $NaHCO_3$ solution followed by drying with sodium sulphate. The residual alcohol was removed by a short path distillation column under reduced pressure at 80 ^{o}C to obtain the pure ring opened product. Among selected alcohols and catalysts 2-EH, sulphuric acid was found to be most effective combination and exhibited 100% conversion to ring opened products, hence for further ring open reaction with other epoxides (i.e. CO, COFAME and WCOFAME) same reactants were used.

2.4. Hexanolyation of resulting hydroxyl group in the ring opened products

During hexanolyation, identical reaction setup as described in RO section was used. In order to fully functionalize hydroxyl groups in the ring opened product, process parameters were varied and optimized. Hexanoic anhydride molar ratio was varied in the range 1 - 3 mol, catalyst loading 0.5 - 3 wt%, temperature 30 to 110 ^{o}C, reaction time 3 - 15 h and stirring speed 1000 - 1500 rpm was maintained. During functionalization of anhydride groups, after every one hour sample was withdrawn, washed with 5% $NaHCO_3$ solution followed by drying with sodium sulphate. The removal of residual anhydride was accomplished in a short path distillation column under reduced pressure at 80 ^{o}C to recover the di-ester derivatives (hexanoylated products) from RO products.

2.5. Product confirmation methods

2.5.1. (Alpha) α- glycol content

α - glycol content enables to know the presence of hydroxyl groups in epoxide/RO product. It was determined by the method reported by May (1973) and Weiss (1970), based on the oxidation of glycol with benzyltrimethylammonium periodate in a non-aqueous medium. The succeeding expression was used for the estimation of α - glycol content of epoxide/RO product.

$$\alpha\text{-Glycol content (moles/100 g)} = \frac{(V_B - V_S)*N}{20*w} \qquad (2.2)$$

Where V_B , volume of $Na_2S_2O_3$ solution consumed for the blank test, ml;

Vs, volume of $Na_2S_2O_3$ solution consumed by the oil/FAME epoxide or ring opened sample, ml;

N, normality of $Na_2S_2O_3$ solution;

W, weight of epoxide/RO product, g

The relative percentage conversion to α - glycol was calculated from the following expression:

Relative percentage conversion to α – glycol = $(G_{exp}/G_{the})*100$

Where, G_{exp} is the experimentally obtained α - glycol and G_{the} is the theoretically obtainable maximum α - glycol, which was determined from the following expression:

$$G_{the} = \left[\frac{(IV_0/2*A_i)}{100+(IV_0/2*A_i)2*A_{OH}}\right]*100 \qquad (2.3)$$

Where, A_{OH} (= 17) is the atomic weight of hydroxyl group.

2.5.2. ^{1}H, ^{13}C Nuclear magnetic resonance (NMR) Spectroscopy

^{1}H, ^{13}C NMR spectrum was recorded using 500 MHz NMR spectrometer (Oxford, AS400, China) using a 5 mm broad band inverse probe head equipped with shielded z-gradient accessories. Samples were dissolved in 400 µl deuterated chloroform ($CdCl_3$) and transferred to 5-mm NMR tube. The deuterated chloroform chemical shift peak at 7.26 ppm was taken as internal reference. Typical parameters used were, spectral width: 4800 Hz; time domain data points: 32 K; flip angle: 90 ^{o}C; relaxation delay: 5s; spectrum size: 32 K points; and line broadening for exponential window function; 0.3 Hz.

2.5.3 Fourier transformed infrared spectroscopy (FTIR)

The FTIR spectra were recorded on a Shimadzu FTIR spectrophotometer (IR Affinity 1, Shimadzu, Japan) equipped with a KBr beam splitter. A normal scanning range of 400 – 4000 cm^{-1} was employed for 30 repeated scans at a spectral resolution of 4 cm^{-1} with a pair of KBr crystals in thin film. The spectras was recorded in transmittance mode.

2.5.4 Iodine value (g I_2/100 g)

The iodine value (IV) can be defined as mass of iodine in grams consumed by 100 grams of oil/FAME/epoxide, it measures the amount of unsaturation (double bonds) present in the sample. IV greatly influences the oxidation and aging process, IV was determined according to the Wijs method (AOCS Tg 1-64, 1997), higher iodine value signifies more unsaturation content.

2.5.5 Oxirane oxygen content (OOC)

The oxirane oxygen content was determined by AOCS Method (Cd-9, 120) II.D.20 (HBr Method) using hydrobromic acid solution in glacial acetic acid. Theoretical oxirane oxygen (OO_{the}) and relative percentage conversion to oxirane was calculated from the following expressions

$$OO_{the} = \left[\frac{(IV_0/2*A_i)}{100+(IV_0/2*A_i)*A_0} \right] A_0 \times 100 \qquad (2.4)$$

Where, A_i (126.9) and A_0 (16) are the atomic weights of iodine and oxygen respectively, and IV_0 is the initial iodine value of the oil/FAME.

$$\text{Relative percentage conversion to oxirane} = \left[\frac{OO_{exp}}{OO_{the}} \right] \times 100 \qquad (2.5)$$

Where, OO_{exp} is the experimentally determined content of oxirane oxygen in 100 g of epoxide. Duplicate measurements were made and the average values were reported. All the product confirmation analysis was run in duplicate, and the average values are presented.

2.6. Product physico-chemical characterization techniques

2.6.1 Acid value and free fatty acid content

Acid value is defined as the amount of potassium hydroxide (in mg) required for neutralizing 1 g of sample. Half of the AV is always considered as free fatty acid content in the sample (FFA), AV and FFA were calculated according to AOCS official method (Te TA-64,1997). Phenolphthalein solution was used as an indicator for titration. Acid value was calculated using the following expression: $\text{Acid Value} = \frac{\text{Volume of the titrant (ml)*N*56.10}}{\text{Mass of the sample (g)}}$ (2.6)

Where, N is the normality of accurately standardized sodium hydroxide solution.

2.6.2 Biodegradability study

The bio-degradability was predicted according to bio-kinetic model ASTM D7373-12 method. ASTM D 7373-12 method was used to evaluate the effective composition of biodegradation (ECB) products and predicts the cumulative biodegradation of prepared di-esters. The biodegradation tests were repeated twice for di-esters and average values were recorded.

2.6.3 Calorific value (CV, MJ/kg)

The calorific value (CV) or higher heating value (HHV) can be defined as the energy released in the form of heat when one gram of testing substance undergoes complete combustion with oxygen under standard conditions. The CV was determined according to ASTM D2015-85 standard method. The calorific value is a characteristic for each substance, higher the calorific value, more the heat energy produced when unit amount of oil/FAME is burnt.

2.6.4 Chemical (fatty acid) composition of feedstocks by gas chromatography

The fatty acid composition of CO and WCO was determined using Nucon 5765 gas chromatograph equipped with a flame ionization detector (Nucon Engineers, Delhi, India) and fused silica capillary column BPX-70, 60 m × 0.25 mm × 0.25 µm (SGE, India). The column temperature was programmed to increase from 180 ^{o}C to 240 ^{o}C at 4 ◦C/min. The detector and injector temperatures were fixed at 240 ^{o}C and 230 ^{o}C, respectively. The carrier gas used was nitrogen (40 psi) at a flow rate of 45 ml/min, air and hydrogen flow rates were 30 ml/min and 300 ml/min, respectively. The sample injection volume was 1.0 µl with a split flow of 60 ml/min. The fatty acid composition of COFAME and WCOFAME is shown in Table 2.1.

Table 2.1: Fatty acid composition of feedstocks

Name of fatty acid	WCO/ FAME	CO/ FAME	Chemical name of fatty acid	Structure (xx:y)*	Formula
Palmitic	14.20	1.4	Hexadecanoic	16:0	$C_{16}H_{32}O_2$
Stearic	4.07	1.8	Octadecanoic	18:0	$C_{18}H_{36}O_2$
Oleic	23.96	4	*cis*-9-octadecenoic	18:1	$C_{18}H_{34}O_2$
Linoleic	39.16	6	*cis*-9,*cis*-12-octadecadienoic	18:2	$C_{18}H_{32}O_2$
Linolenic	5.25	0.6	*cis*-9,*cis*-12,*cis*-15-octadecadienoic	18:3	$C_{18}H_{30}O_2$
Ricinoleic	-	84	12-hydroxy-(*cis*)-9-octadecenoic acid	18:1-OH	$C_{18}H_{34}O_3$

*xx - number of carbons and y-number of double bonds in the fatty acid chain

2.6.5 Cloud point and pour point by ASTM method

Cloud point (CP, ^{o}C) is defined as "the lowest temperature at which a cloud or haze of wax crystals appear at the bottom of the test jar when the test substance is cooled under prescribed conditions". Pour point (PP, ^{o}C) can be defined as the lowest temperature at which the test substance ceases to flow from a tilted jar under prescribed conditions. CP, PP values were measured according to ASTM D2500/66-IP 219/67 method using Cryostat (Model SSI 01080 A, Southern Scientific Lab, Chennai) equipment. CP, PP measurements are done with a difference of 1 ^{o}C, 3 ^{o}C raise in temperatures, generally lubricants with lower CP and PP exhibit improved fluidity at low temperatures than those with higher CP and PP.

2.6.6 Cold flow properties by differential scanning calorimetry (DSC)

PP was measured to determine the low temperature flow properties, and it was a rough indication of the lowest temperature at which sample is promptly pumpable. In this study, PP was also determined by adopting differential scanning calorimetry technique (DSC, 1 star e-system, Mettler Toledo). Three to five milligrams sample was taken in a 40 µl sealed pan under the nitrogen flow rate of 40 ml/min. A temperature program with four sequential active steps was used, in which the sample was heated from room temperature (RT) to 50 ^{o}C at 5 ^{o}C/min at constant heating rate, then it was hold at 50 ^{o}C for 5 min (isothermal condition) to homogenise the sample. Then sample was cooled from 50 ^{o}C to (-30 ^{o}C) at 5 ^{o}C/min and continued at the same temperature to 5 min for complete crystallization. Thereafter sample was heated from (-30 ^{o}C) to 50 ^{o}C at a heating rate of 5 ^{o}C/min, DSC measurements repeated twice and the average values are reported here.

2.6.7 Density (kg/m^3)

The density (ρ) of a material is defined as its mass per unit volume, densities were determined at 25 °C using a specific gravity bottle according to ASTM D4052 method. Density was calculated using the following expression:

$$\text{Density (kg/m}^3\text{)} = \frac{\text{Mass (kg)}}{\text{Volume (m}^3\text{)}} \qquad (2.7)$$

2.6.8 Gel permeation chromatography

The gel permeation chromatography (GPC) profiles were obtained on a PL-gel Mixed D GPC column, Shimadzu (Japan), equipped with an auto sampler. GPC was calibrated using polystyrene (MW range 300–500,000) in the HPLC-grade chloroform at room temperature and HPLC-grade chloroform was used as an eluent at 1 ml/min.

2.6.9 Kinematic viscosity

Kinematic viscosity (KV, cst) is a measure of resistance to gravity flow of a fluid. KV was determined using Anton-Paar interfacial rheometer (MCR-301, Austria). Flat plate geometry was used for analysis, parallel plate 35 Ti sensor, HAAKE DC 50 thermo controller was chosen for this analysis. Shear stress vs shear rate, viscosity vs shear rate, and viscosity vs temperature measurements were carried out at variable shear rates (ranging from 0 to 500 s^{-1}). Around 100 data points were recorded over a time period of 3 min at an interval of 1.8 s and viscosity measurements were carried out at 25, 40, 60, 80, and 100 ^{o}C. A thermostatic water bath was used to control the working temperature within a set point range of 0.1^{o}C. Rheological behavior was also determined at an identical condition. All rheology experiments were performed twice and average values are reported.

2.6.10 Moisture content

Moisture content was determined using Karl fisher auto-titrator, it is a qualitative parameter which influences the storage life. High moisture content may serve as a medium for microbial growth. Microbial growth in the oil may lead to damage of fuel/storage tank and supports emulsion formation.

2.6.11 Thermal and oxidative stability by thermo gravimetric analysis

Thermal and oxidative stability study was carried out in a non-isothermal mode in a Mettler Toledo (TGA 851) thermo gravimetric analysis (TGA) instrument to identify the temperature regimes where predominant weight losses (and hence transformations) occur. TGA was conducted in two unlike atmospheres (N_2 and O_2/air), thereby, an insight could be gained to analyze the effect of atmosphere on various temperature regimes. The conventional heating rate (10 ^oC/min) was adopted and temperature programming is from room temperature (25 ^oC) to 700 ^oC. Less than ten milligrams of sample was taken in a silica crucible (900 µl) and was heated in an inert atmosphere (Nitrogen, 40 ml/min) to determine thermal stability and oxygen/air atmosphere (100 ml/min) was used to define oxidative stability. The onset temperature (thermal stability, OT, ^oC) and oxidation onset temperature (oxidative stability, OOT, ^oC) were calculated from a plot of weight % versus temperature (^oC) for each run.

2.6.12 Oxidative stability by DSC

The oxidative stability of the samples were estimated using DSC (METTLER TOLEDO, Star e-system) at a constant heating rate (10 ^oC/min) in an oxygen/air atmosphere. DSC analysis was performed by heating samples from room temperature to 350 °C in oxygen/air atmosphere (100 ml/min) using nitrogen (40 ml/min) as a purging gas. OOT was estimated from temperature versus heat flow thermo-gram.

2.6.13 Refractive index (RI)

The RI was measured using refracto meter (ABBE Refracto meter), it is the degree of deflection of a beam light that occurs when it pass from one medium to the other. The refractive index value increases with the degree of unsaturation. This value indicates the presence of long chain un-saturated fatty acids in the sample.

2.6.14 Tribological Properties

The lubricity testing was carried out using high frequency reciprocating rig (HFRR) apparatus (ASTM D6079 – 04). The test sample (6 ml) sample was placed in a sample container onto a metal surface. The ball was in contact with the metal surface at 50 Hz for 75 min and the diameter of resulting wear scar on the ball surface was then measured using a microscope (with 20 × magnification). Anti-wear and friction reducing properties of prepared di-esters from CO, WCO and their FAME derivatives were estimated. The HFRR method decides the ability of prepared di-esters to affect friction and wear between the surfaces in relative motion under the load. The three major parameters, wear scar diameter (WSD), co-efficient of friction (CoF), and film thickness are the indicative parameters of assessing the lubricity of any fluid. Before the test, instrument (HFRR) was calibrated for fluid A (high lubricity reference) and fluid B (low lubricity reference fuel) as recommended by ASTM D 6079 - 4 Method. After calibrating the instrument, lubricity effect of di-esters from CO, WCO and their FAME derivatives were tested. The HFRR test is a computer-controlled reciprocating friction and wears test rig system. During test A, 2 ml of fuel is placed in the test reservoir of HFRR and adjusted to the standard temperature of 60 ± 0.2 °C. As per the ASTM D 6079 - 4 method, the standard and preferred temperature prescribed for evaluating lubricity is 60 ± 0.2 °C. Once the fuel temperature is stabilized, a vibrator arm holding a horizontally mounted non-rotating steel ball and loaded with 200 g mass is lowered until it contacts a test disk completely submerged in the fuel. The test ball is oscillated at a fixed frequency (50±1Hz) with a fixed stroke length (1±0.02 mm). After 75 min, the test ball is removed from the vibrator arm and cleaned. The spot (wear scar) formed on the surface of the ball was measured; the size of the spot is associated with the lubrication qualities of the sample being tested. In addition to the WSD, CoF, film thickness of the data also correlated for tested samples.

Wear scar diameter: Lubricity is the ability of a material to provide boundary lubrication to prevent wear between moving parts. After the test is completed, the spot (wear scar diameter) on the 6 mm steel test ball was measured with the help of 100 × magnification photomicroscope and recorded. The wear scar on the test sample was measured in x and y directions (dimension across the direction of the test sample specimen motion is x, y dimension). The average wear scar diameter (in micrometers) is the mean of addition of wear on x and y direction.

Friction co-efficient (μ): When one surface moves over another, there is always some resistance to movement and the force that opposes movement is called friction. If the friction is proportional to the load, the friction co-efficient (μ) can be calculated from equation given below.

$$\mu = F/P \quad (2.8)$$

where, F is the friction force and P is the applied load in Newtons. A high friction co-efficient is normally indicative of poor lubricant, with significant metal-to-metal contact and wear. The co-efficient of friction depends mainly on the materials that are in sliding contact and can vary from 0.003 to 3.0 or more.

Film Thickness (%): The film thickness (%) was measured by HFRR machine; in this, the contact resistance circuit applies a 15 mV potential across the specimen contact and a balance resistor series. The contact and balance resistor thus form a potential divider circuit. The 10 Ω default series resistance was set by the electronic unit. The potential drop across the contact is thus a measure of contact resistance, as compared to the balance resistor. A low or zero film reading means that the potential drop across the contact, and hence the contact resistance is very low; i.e., there is significant metal-to-metal contact taking place between the tests specimens. This is usually associated with a high friction force and high wear. A

high film reading means the metal surfaces are being separated; this may be by a chemical film formed. The lubricity tests run were carried out twice to ensure repeatability in the data.

2.7. Summary

Present chapter discussed the detailed experimental procedures for preparation of FAME, epoxides, hydroxylated and hexanoylated derivative from the feedstocks. Further, various product confirmation and physico-chemical characterization techniques are also discussed thoroughly.

CHAPTER-3

Thermo-oxidative and cold flow properties of feedstocks

This chapter addresses the possible physico-chemical changes occur in cooking oil during frying process. Further, thermo-oxidative stability and cold flow properties of the feedstocks examined thoroughly, which were considered as limitations to use feedstocks as lubricant basestocks. Onset temperature (OT) and oxidative onset temperature (OOT) were estimated by TG analysis and cold flow properties were determined by DSC thermal analysis. In summary, estimated thermo-oxidative stability and cold flow properties behaviour was examined with respect to the fatty acid composition and realized the effect of chemical composition and structure on estimated properties.

3.1. Physico-chemical changes occur in cooking oil during frying

Waste oil is defined as any oil based on edible, non-edible, petroleum or synthetic oils, through use or handling it becomes unsuitable for its original purpose, due to the presence of impurities or loss of original properties. Worldwide the production of oils and fats is about 154 million tonnes, this figure referring to the production of 17 major fats (butter, lard, tallow, grease and fish oil) and vegetable oils (i.e. soybean, cotton seed, ground nut, sunflower, rapeseed, sesame, corn, olive, palm, palm kernel, coconut, linseed and castor). Most of these vegetable oils are used as edible, since frying improves the taste of food, in the present scenario it is a common method in food preparation. In the present study, fish fried (500–600 pieces) soybean oil which was exposed to a high temperature (230–250 ^{o}C) and heated up to 5 - 6 h continuously was used. Frying can be defined as, a process of immersing food in hot oil contact with air, oil, food, and frying pan at an elevated temperature. During frying, oil undergoes hydrolysis, thermo-oxidative degradation, produces volatile and non-

volatile commodities. In addition to this, the same oil is used several times because of economical reasons.

However, continuous use of same oil for frying could cause various physical and chemical changes in the oil. Some physical changes observed in vegetable oil after frying are an increase in viscosity, specific heat, surface tension and colour. If the same oil is used repeatedly many undesired and harmful reactions takes place such as thermolytic, oxidative and hydrolytic. Most of the volatile compounds vaporize in the atmosphere with steam and remaining non-volatile compounds in the oil undergoes further chemical reactions and produces free fatty acids, peroxides, polymeric materials, large amounts of diglycerides and tends to cause gumming in the fryer (Mazza and Qi 1992; Gordon and Kourimska 1995; Romero et al. 1998; Xu et al. 1999; Tompkins and Perkins 2000). The toxicological effects of these compounds upon human consumption are still not completely known, and also these used frying oils could cause disposal problem. Frankel et al. (1984a) reported that during the fish frying process major components formed are diglycerides, dimers, trimers and high molecular weight polymeric compounds. The formation of aforementioned products depends on time of frying, surface area of food, type and composition of frying oil. Choe and Min (2007) noticed that the dimers and polymers are larger molecules with molecular weight ranging from 692 to 1600 daltons and formed by a combination of -C-C-, -C-O-C-, and -C-O-O-C- bonds. They have also noticed that dehydroxydimer, ketodehydrodimer, monohydrodimer, dehydrodimer of linoleate, and dehydrodimer of oleate are dimers found in soybean oil during frying at around 195 ^{o}C.

From Table 2.1, it can be seen that WCO contains more polyunsaturated fatty acids than monounsaturated and saturated fatty acids. Takeoka et al. (1997), Bastida and Sanchez (2001) observed that oil rich in un-saturated fatty acids polymerizes more easily during deep frying than the oil rich in monounsaturated and saturated fatty acids. From the above

discussion, it was clear that WCO used in this study may contain higher molecular weight polymeric compounds.

3.2. Thermal stability of CO and WCO

TG analysis was used to study the thermal stability of oils/FAME and it gives the result in terms of percentage weight loss against temperature. Thermal stability of oils/FAME was determined from onset temperature of thermal decomposition under nitrogen atmosphere. Onset temperature can be defined as the temperature at which decomposition of oils/FAME starts. From the literature, it was observed that the heating rate of 10 ^{o}C/min provides better information about thermal behavior (Santos et al. 2004; Dweck and Samapio 2004). Therefore, in the present study, same heating rate was adopted; TG was also performed at 20 ^{o}C/min for comparison purpose.

Comparison of TG, DTG curves of CO and WCO at a constant heating rate of 10 and 20 ^{o}C/min under nitrogen atmosphere are shown in Figures. 3.1 and 3.2. The DTG curve provides detail information about initial and final temperatures of a particular decomposition process. The decomposition of CO took place in three consecutive stages; on the other hand, in case of WCO single stage decomposition pattern was noticed. The first phase of decomposition in case of CO was initiated at 180 ^{o}C and extended up to 300 ^{o}C. During this stage, low boiling point (high volatile), unstable compounds like oxygenated compounds, hydroperoxides, and polyunsaturated fatty acids undergo decomposition (Knothe 2005; Farias et al. 2002; Sricharoenchaikul and Atong 2009). In the second phase, decomposition was initiated from 300 ^{o}C and extended up to 420 ^{o}C, during this temperature range, monounsaturated fatty acids including ricinoleic acid get decomposed. In the third phase, decomposition of saturated fatty acids was occurred between 420 ^{o}C and 456 ^{o}C. The final stage was extended from 456 ^{o}C to 700 ^{o}C, where the decomposition of pyrolyzed product

occurred. DTG curves of CO showed three steps of mass loss attributed to the decomposition and/or volatilization in various temperature ranges. Similar behavior of CO decomposition was also noticed by Marta et al. (2007) and agrees well with the present study.

Table 3.1: Onset temperatures (thermal stability) of CO and WCO

Oil	Heating rate (°C/min)	Onset temperature (°C)
CO	10	310
CO	20	320
WCO	10	360
WCO	20	370

Table 3.2: Mass loss (%) data for CO and WCO under N_2 atmosphere

Oil	Heating rate (°C/min)	Temperatures (°C) of mass loss at		
		10 %	50 %	90 %
CO	10	273	365	415
CO	20	300	378	440
WCO	10	345	397	435
WCO	20	365	410	445

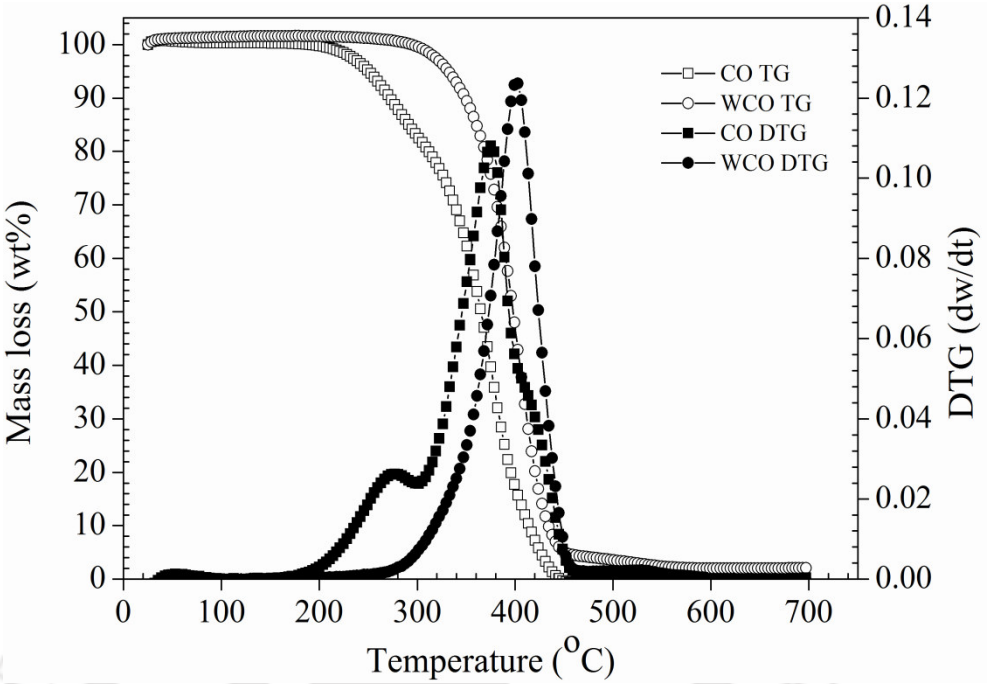

Figure 3.1: TG/DTG thermo-grams of CO and WCO at 10 °C/min under N_2 atmosphere

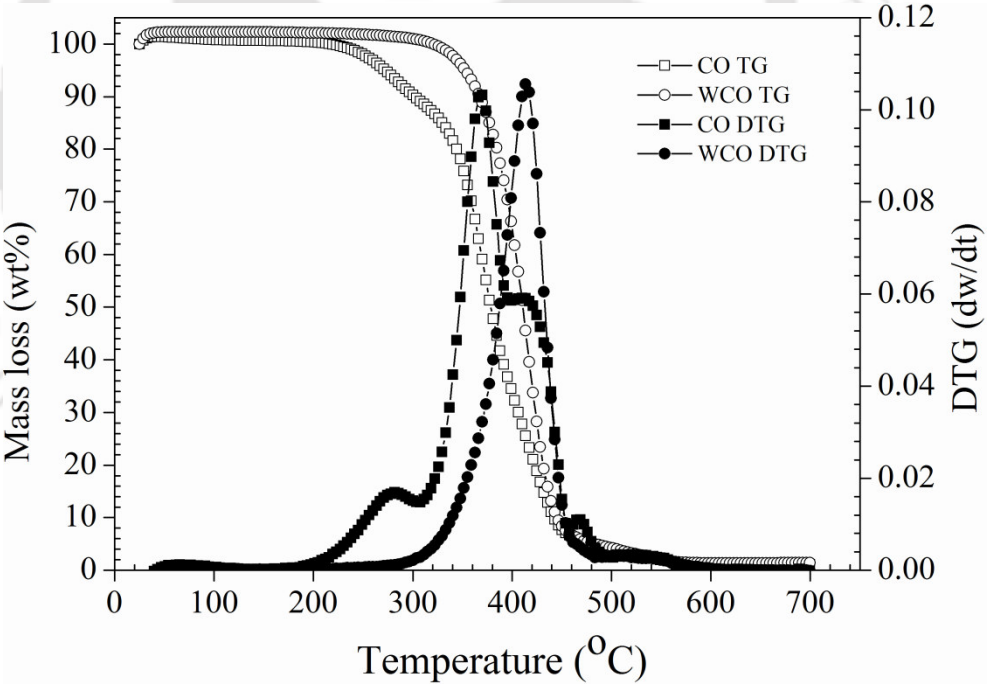

Figure 3.2: TG/DTG thermo-grams of CO and WCO at 20 °C/min under N_2 atmosphere

Similarly, DTG curves of WCO (Figures. 3.1 and 3.2) showed a single continuous step of thermal decomposition in the temperature range of 260–460 °C, which indicates the

breakdown of heavier hydrocarbons into lower molecular hydrocarbons, carbon dioxide, and carbon monoxide. Similar kind of thermal decomposition pattern was noticed in the literature for other oils which agrees well with the present study (Jayadas and Nair 2006; Diniz et al. 2008; Garcia et al. 2007; Siddharth and Sharma 2011).

These results revealed that in the inert atmosphere, CO and WCO were thermally stable up to temperature 310 and 360 ^{o}C, respectively. The thermal stability results of oil can be paired to its fatty acid composition in order to understand their degradation behavior. Generally, higher the unsaturation content in oils/FAME, lower the thermal stability. This can be explained by high boiling point of saturated fats compared to its un-saturated equivalents (Farias et al. 2002; Sricharoenchaikul and Atong 2009). However, Imahara et al. (2006) in their study clearly demonstrated that polyunsaturated fats are more unstable to thermal treatment than monounsaturated fatty acids. From Table 2.1, it can be seen that the saturated, monounsaturated, and polyunsaturated fatty acids of WCO was found to be 18.27%, 23.96%, and 44.41%, respectively; similarly, for CO it was found to be 3.2%, 88%, and 6.6%, respectively. Therefore, from the above discussion and the fatty acid composition profile, CO was expected to show more thermal stability than WCO (Imahara et al. 2006; Marta et al. 2007; Garcia et al. 2007; Park et al. 2008; Diniz et al. 2008; Refat 2009; Siddharth and Sharma 2010, 2011; Anonymous 2011). But the present study contradicts the earlier findings and showed that WCO was thermally more stable than CO. This can be explained with the help of Section 3.1, that deep frying process forms higher molecular weight polymeric compounds which decomposes at elevated temperatures; this attributed to the higher thermal stability of WCO than CO. The study also reveals that the process of decomposition of CO initiated and completed within a temperature range inferior to WCO. Similarly, data in Tables 3.1 and 3.2 further supports that WCO was thermally more stable

and less volatile compared to CO. The study of thermal stability is an important factor to define the useful span and storage condition for bio-fuels/bio-lubricants (Marta et al. 2007).

3.3. Oxidative stability of CO and WCO

Oxidative stability can be defined as the resistance of oils/FAME against oxidation. To measure the oxidative stability, TG analysis was performed under oxygen atmosphere. Oxidative stability is the quality indicative parameter for oils/FAME and it gives information about shelf life of oils/FAME in ambient or oxidative atmosphere. Figures 3.3 and 3.4 show weight loss (TG thermo-gram) and first derivative (DTG thermo-gram) of mass loss with respect to temperature for CO and WCO. Oxidation process is principally an exothermic reaction which occurs between oils/FAME and oxygen. Conventionally, active oxygen method (AOM), ASTM D5308, ASTM D2274, ASTM D3241, ASTM D5483, EN 14112 (Rancimat), and pressurized DSC methods were used to evaluate the oxidative stability based on the formation of insoluble sediments after an accelerated aging process (Dunn 2006; Sharma et al. 2008a, 2008b; Garcia et al. 2010; Siddharth and Sharma 2010; Saldaria et al. 2013). In the present study, TG analysis was adopted for fast, better results, reproducibility, and ease of analysing the experimental data.

In general, it was observed that oxidative stability is strongly depends on polyunsaturated fatty acids in the oils/FAME rather the amount of saturated or monounsaturated fatty acids (Knothe 2002, 2003; Park et al. 2008; Ramos et al. 2009). That means greater the degree of unsaturation, greater the susceptibility to oxidation (Sherwin 1978; Frankel 1984b; Hamilton et al. 1997). As per earlier discussion and also from the fatty acid composition profile, it was noticed that WCO contains more polyunsaturated fatty acids than CO. Due to this high degree of poly unsaturation, WCO exhibits poor oxidation stability than CO. This behavior is supported by earlier reported literature, where many researchers

(Schober and Mittelbach 2004; Knothe 2005) investigated how the oxidative stability of a mixture of alkyl esters depends on their fatty acid profile. A higher oxidative stability of CO attributed due to the presence of hydroxyl groups. Further, TG and DTG curves (Figures 3.3 and 3.4) indicate that oxidative degradation takes place in three distinct steps. Each step corresponds to the decomposition of polyunsaturated, monounsaturated, saturated fatty acids, and oxidation of carbon residue in the oxygen environment (Adhvaryu and Erhan 2002; Marta et al. 2007).

Table 3.3: Oxidative onset temperatures (oxidative stability) of CO and WCO

Oil	Heating rate (°C/min)	Oxidative onset temperature (°C)
CO	10	308
CO	20	312
WCO	10	298
WCO	20	309

Table 3.4: Mass loss (%) data for CO and WCO under O_2 atmosphere

Oil	Heating rate (°C/min)	Temperatures (°C) of mass loss at		
		10 %	50 %	90 %
CO	10	340	386	500
CO	20	355	395	512
WCO	10	330	375	485
WCO	20	345	386	493

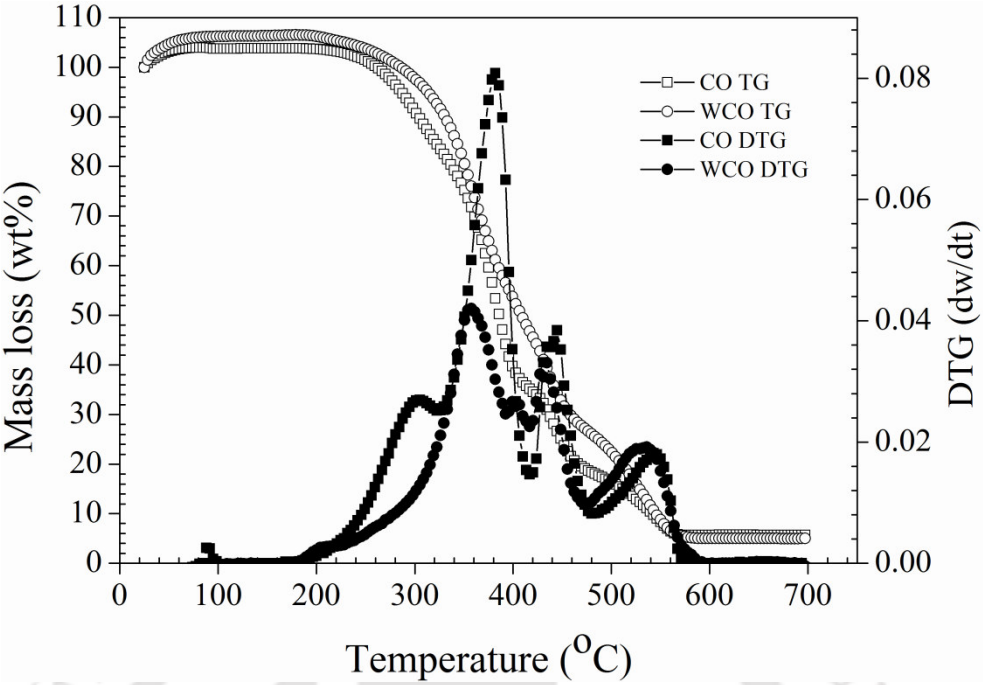

Figure 3.3: TG/DTG thermo-grams of CO and WCO at 10 °C/min under O_2 atmosphere

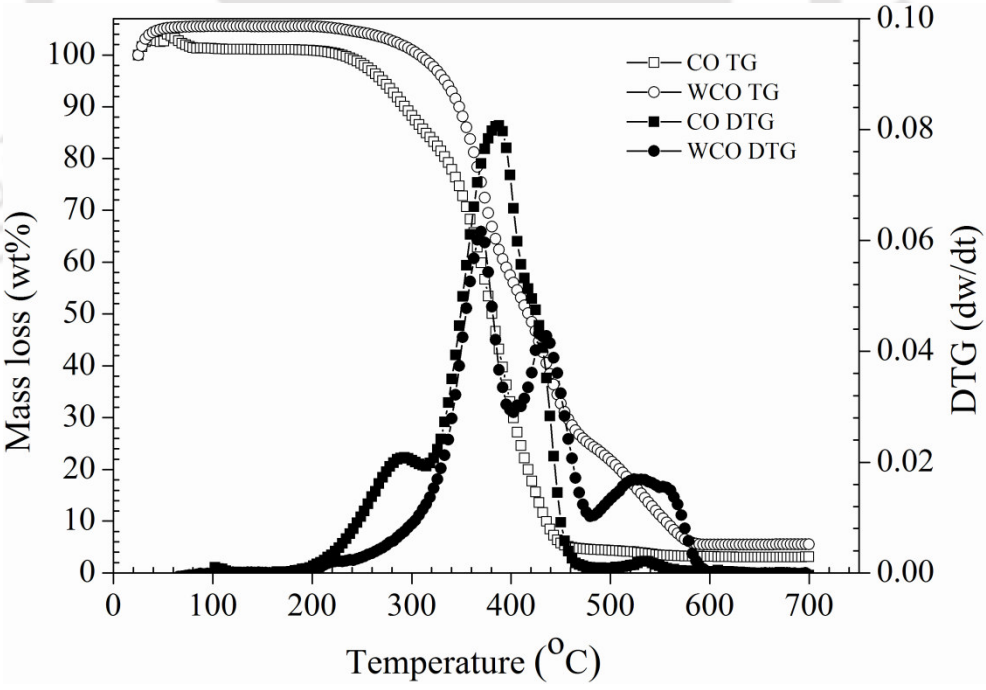

Figure 3.4: TG/DTG thermo-grams of CO and WCO at 20 °C/min under O_2 atmosphere

Figure 3.4 shows TG analysis results at 20 ^{o}C/min heating rate. Investigation on the effect of onset temperature (thermal stability) at various heating rates revealed that, for both the samples higher onset temperature was noticed at a heating rate of 20 ^{o}C/min than 10 ^{o}C/min. The oxidation onset temperature was increased from 308 ^{o}C (10 ^{o}C/min) to 312 ^{o}C (20 ^{o}C/min) for CO; similarly, for WCO it was increased from 298 ^{o}C (10 ^{o}C/min) to 309 ^{o}C (20 ^{o}C/min). The data in Tables 3.3 and 3.4 further confirm that CO shows more oxidative stability compared to WCO. The study of oxidative stability is a highly considerable factor to define useful span and storage condition of oils/FAME (Marta et al. 2007).

3.4. Cold flow properties

Pour point is one of the most important properties of any oils/FAME used as a fuel or lubricant in low temperature climatic conditions (Jayadas and Nair 2006). Conventional low temperature properties such as PP, CP and cold filter plugging point (CFPP) can be determined using ASTM methods (Jayadas and Nair 2006; Marta et al. 2007; Garcia et al. 2010; Ramalho et al. 2012). In the present study PP of CO and WCO was determined using two different methods such as the ASTM standard method and DSC analysis, the obtained results are compared and tabulated in Table 3.5. Curently, DSC received a substantial assistance in finding the cold flow properties (Claudy et al. 1988; Dunn 1999; Coutinho and Daridon 2005; Garcia et al. 2010). DSC curves show plots of heat flow (mw) against temperature (^{o}C); the experimental procedure is well explained in Chapter-2 (Section 2.6.5 and 2.6.6). The vegetable oils/FAME are composed of mixed triglyceride esters of different fatty acids, i.e., saturated, monounsaturated, and polyunsaturated. Normally oils/FAME solidifies over a range of temperatures. However, Dunn (1999) described that the results obtained with characteristic temperatures received during cooling better predicted the cold flow properties than the correlations obtained with heating thermo-grams. During the cooling

cycle PP was determined, since cooling is an exothermic reaction heat flow gains as solidification starts.

From earlier reported literature (Soriano et al. 2006; Ramos et al. 2009; Papadopoulos et al. 2010), it was found that quantity and the fatty acid composition of oils/FAME are directly responsible for the operating conditions of oils/FAME at lower temperatures. From the literature (Soriano et al. 2006; Ramos et al. 2009; Papadopoulos et al. 2010), it was also noticed that more the saturated fatty acids in the oils/FAME, poorer its cold flow properties. Dunn (1999) claimed that saturated compounds are responsible for the unfavorable cold flow properties. Therefore, from the above discussion, it was clear that more the unsaturated fatty acids in the oils/FAME better the cold flow properties. The saturated fatty acids content of castor oil was 3.2%, whereas in case of WCO it was 18.27%. Therefore, from the comparative evalution of fatty acid composition, CO was expected to show favourable cold flow properties than WCO and the same was noticed in the present study. This may be because of the higher unsaturation content (mono - 88%, poly - 6.6%) in the CO. Park et al. (2008) reported that for favorable low temperature properties, higher amount of monounsaturated fatty acids are desirable in the oils/FAME composition.

Table 3.5: Pour points of CO, WCO by ASTM and DSC methods, comparison

Oil	ASTM	DSC
Castor	-21	-22
Waste cooking	-3	-7

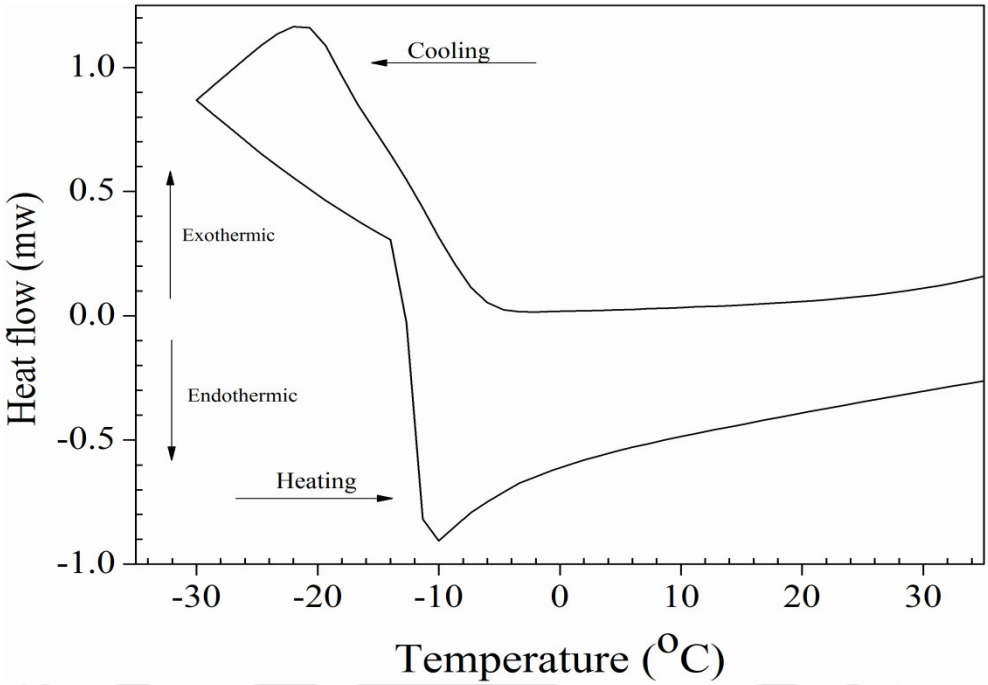

Figure 3.5: DSC cooling thermo-gram of castor oil

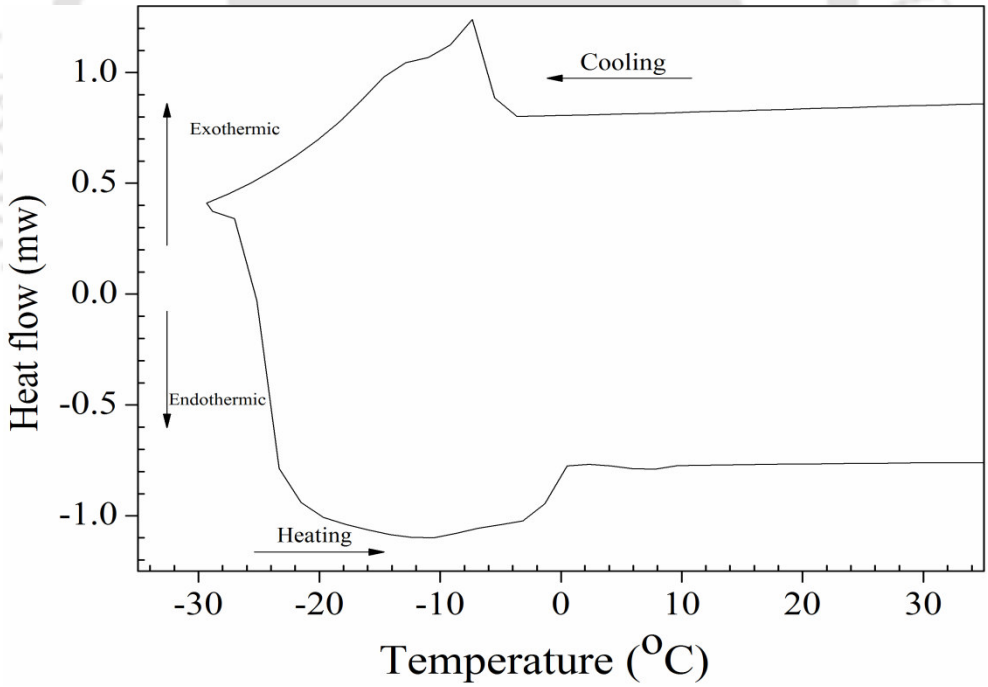

Figure 3.6: DSC cooling thermo-gram of waste cooking oil

Figures 3.5 and 3.6 show DSC cooling thermo-grams of CO and WCO, there was a single broadened exothermic peak associated with the change in phase from liquid to solid, during such phase change oil/FAME sample undergoes crystallization and releases more

amount of heat energy with a sharp exothermic curve. The temperature at which exothermic peak occurs that point was considered as a PP of oils/FAME (Table 3.5). DSC offers a quick and easy method to determine PP, it requires very less quantity of oil/FAME as well to find the cold flow properties (Angel et al. 2010). Jayadas and Nair (2006) in their study reported that these methods are suitable and contributes better results to determine cold flow properties than conventional methods. An alternative to CFPP is the low-temperature flow test (LTFT). Recently, the U.S. Department of Enegy has introduced a novel method to evaluate the cold flow properties of biodiesel, named cold soak filtration test (CSFT). But above all PP is the conventional and widely used measurement technique to determine the cold flow properties (Dunn 2005a).

3.5. Thermal stability of COFAME and WCOFAME

The comparison of TG and DTG thermo-grams of COFAME and WCOFAME at constant heating rate 10 and 20 ^{o}C/min in the nitrogen atmosphere is shown in Figures 3.7 and 3.8. The plots show that FAME were thermally degraded in a single continuous step and it was in agreement with the study conducted by Marta et al. (2007); Siddharth and Sharma (2011). The compositional features of fatty acid esters that influence the thermo-oxidative properties of fatty ester molecule include chain length, the degree of unsaturation and branching of the chain. Esters with high unsaturated fatty acids content are less stable than the saturated ones (Garcia et al. 2004, 2010; Nik et al. 2005; Refaat 2009). While comparing the thermal decomposition profile at 10 and 20 ^{o}C/min for FAME, it was observed that with increased heating rate, degradation rate was found to be increased and the onset temperature was increased from 203 (10 ^{o}C/min) to 222 ^{o}C (20 ^{o}C/min) and 178 (10 ^{o}C/min) to 198 ^{o}C (20 ^{o}C/min) for COFAME and WCOFAME, respectively (Table 3.6). A similar type of

behaviour was noticed by Ledakowicz and Stolarek (2002) during their study on biomass decomposition.

Low onset temperature of WCOFAME was due to the physical and chemical differences between the derived methyl esters and also due to its fatty acid composition profile. This can be better explained from the weight loss profile (Figures. 3.7 and 3.8, Table 3.7) of COFAME and WCOFAME. For COFAME, 10% weight loss was observed at 200 ^{o}C while in case of WCOFAME, it was at 170 ^{o}C which includes moisture loss and decomposition of mono and polyunsaturated fatty acids (oleic, ricinoleic, linoleic and linolenic). All the components of COFAME which accounted for almost 50% weight loss were decomposed at 243 ^{o}C, whereas for WCOFAME 50% weight loss was at 212 ^{o}C, it includes the breakdown of saturated fatty acids (i.e. palmitic and stearic). Similarly the components of COFAME which accounted for almost 90% weight loss were decomposed at around 310 ^{o}C and for WCOFAME 90% weight loss was observed at 233 ^{o}C. The remaining 10% was mostly pyrolysis products which were highly viscous liquids and undergoes secondary decomposition up to 310–700 ^{o}C for COFAME and 233–700 ^{o}C for WCOFAME, it is also representative of decomposition of polymeric materials formed during degradation (Adhvaryu and Erhan 2002). Similar observations were drawn by Garcia et al. (2010) in their study on bio-oil. In the present study, COFAME and WCOFAME residue was completely burnt out after being heated up to 700 ^{o}C.

Table 3.6: Onset temperatures (thermal stability) of COFAME and WCOFAME

FAME	Heating rate (°C/min)	Onset temperature (°C)
CO	10	203
CO	20	222
WCO	10	178
WCO	20	198

Table 3.7: Mass loss (%) data for COFAME and WCOFAME under N_2 atmosphere

FAME	Heating rate (°C/min)	Temperatures (°C) of mass loss at		
		10 %	50 %	90 %
CO	10	200	243	310
CO	20	220	265	325
WCO	10	170	212	233
WCO	20	185	235	258

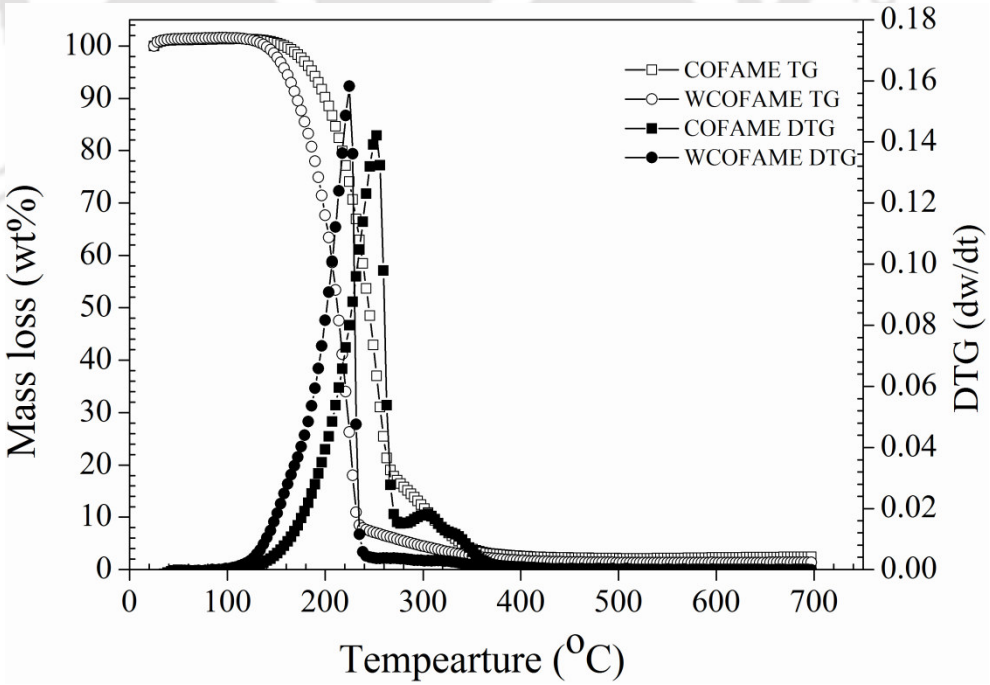

Figure 3.7: TG/DTG thermo-grams of COFAME and WCOFAME at10 °C/min under N_2 atmosphere

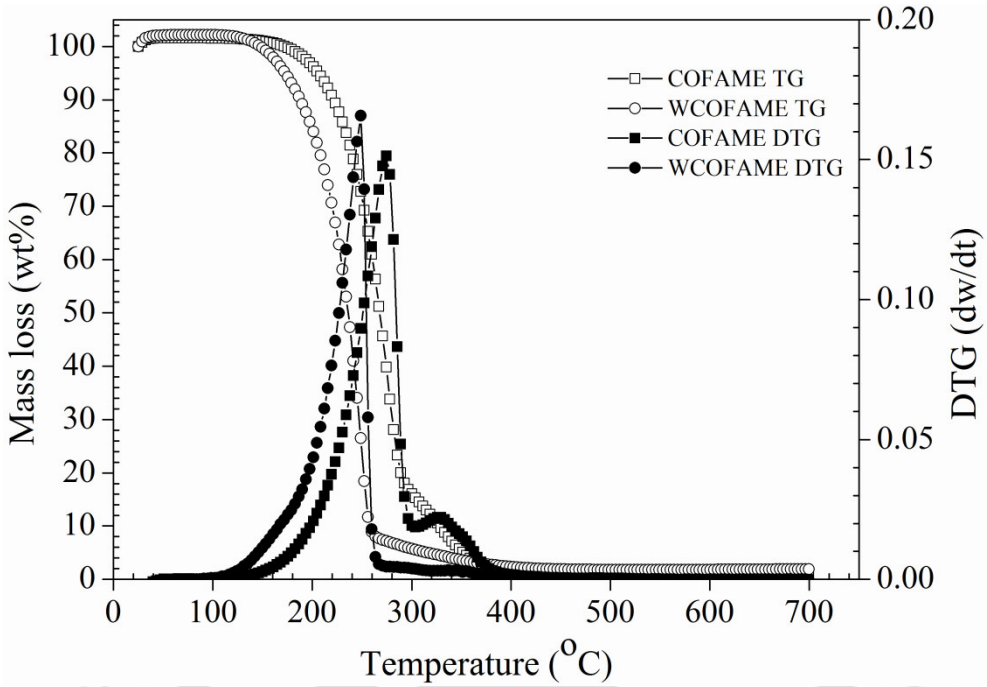

Figure 3.8: TG/DTG thermo-grams of COFAME and WCOFAME at 20 °C/min under N_2 atmosphere

From the above discussion, it was clear that initiation and completion of the thermal degradation of WCOFAME was within a temperature range inferior to COFAME, which may be due to higher polyunsaturated fatty acids present in WCOFAME (44.41%) compared to COFAME (6.6%). The polyunsaturated fatty acids were responsible for thermal stability i.e. higher the polyunsaturation in the ester, lower the thermal stability. This attitude of fatty esters could be explained by lower boiling point of unsaturated fatty acids compared to saturated fats. The works carried out by various researchers on thermal stability of esters have reported alike results (Farias et al. 2002; Park et al. 2008; Sricharoenchaikul and Atong 2009) and remarked in Tables 3.6 and 3.7. The study of thermal stability is an important factor to define the useful life time and storage condition (Conceicao et al. 2007). Thermal stability also reveals that how long the fuel/lubricant can be stored and used potentially in inert atmosphere.

3.6. Oxidative stability of COFAME and WCOFAME

Figures 3.9 and 3.10 show typical TG thermo-grams (weight loss versus temperature) and the first derivatives of mass loss with respect to temperature (DTG) for COFAME and WCOFAME under oxygen atmosphere. As shown in Figures 3.9 and 3.10 DTG curves indicate that oxidative degradation occurred in a single continuous step in the temperature range of 140 - 360 ^{o}C, 100 - 400 ^{o}C for COFAME, WCOFAME respectively. A single continuous step in the degradation of COFAME and WCOFAME under oxygen atmosphere attributed to decomposition and/or volatilization of methyl esters contents (i.e. saturated fatty acids, unsaturated fatty acids, and oxidation of carbon residue in the oxygen environment) (Adhvaryu and Erhan 2002; Marta et al. 2007). In general, DTG analysis of oil under oxygen atmosphere gave three distinct peaks and each peak has its own significance in the decomposition or combustion process of unsaturated fatty acids, saturated fatty acids and oxidation of carbon residue. However, in case of methyl esters a single continuous peak was observed (Santos et al. 2004; Marta et al. 2007; Garcia et al. 2010).

Table 3.8: Oxidative onset temperatures (oxidative stability) of COFAME and WCOFAME

FAME	Heating rate (°C/min)	Oxidative onset temperature (°C)
CO	10	218
CO	20	230
WCO	10	187
WCO	20	200

Table 3.9: Mass loss (%) data for COFAME and WCOFAME under O_2 atmosphere

FAME	Heating rate (°C/min)	Temperatures (°C) of mass loss at		
		10 %	50 %	90 %
CO	10	215	258	325
CO	20	222	268	330
WCO	10	188	230	263
WCO	20	200	240	274

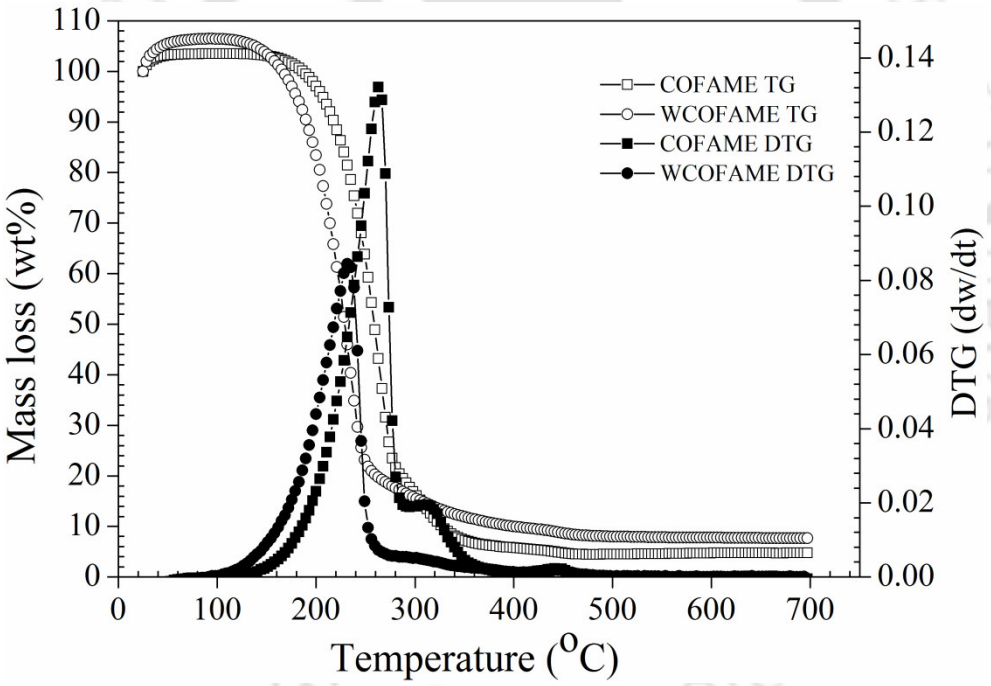

Figure 3.9: TG/DTG thermo-grams of COFAME and WCOFAME at 10 °C/min under O_2 atmosphere

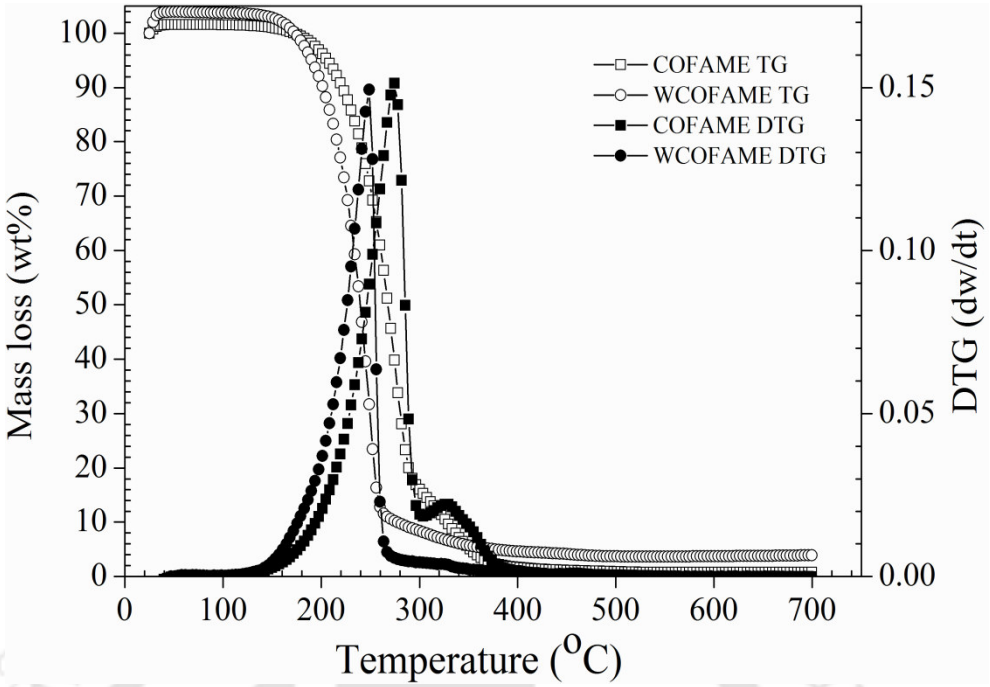

Figure 3.10: TG/DTG thermo-grams of COFAME and WCOFAME at 20 °C/min under O_2 atmosphere

During transesterification, high molecular weight by-product glycerol was removed resulting a substantial change in TG and DTG characteristic curves. Similar kind of behavior was noticed by Siddhart and Sharma (2011) during their study on oxidative stability of corn biodiesel under the air atmosphere. Apart from that, TG analysis was also performed at the heating rate of 20 °C/min and the characteristic thermo-grams are shown in Figure 3.10. A similar trend in the decomposition pattern was attributed, but only difference was due to a high heating rate, decomposition was faster at 20 °C/min compared to 10 °C/min. Therefore, oxidation onset temperature was increased from 218 °C (10 °C/min) to 230 °C (20 °C/min) for COFAME and 187 °C (10 °C/min) to 200 °C (20 °C/min) for WCOFAME (Table 3.8).

From the fatty acid composition and chemical structure of COFAME and WCOFAME, it was clear that WCOFAME were more sensitive to oxidative decomposition than COFAME, as it contain more amounts of polyunsaturated fatty acids. Knothe (2006, 2007) and other researchers (Nadal et al. 2006; Refaat 2009) observed that polyunsaturated

fatty acids are highly responsible for estimating the oxidative stability and they are more susceptible to auto oxidation or oxidation during its contact with the atmosphere. The unsaturation in the fatty acid chain is the structural basis of auto-oxidation mechanism, as the methylene groups adjacent to double bonds turn out to be specifically prone to radical attack as the first step of esters oxidation (Dunn 2005a). Dunn (2005b) also claimed that the saturated compounds show significantly higher melting points than unsaturated fatty acid compounds.

In the present study, from the fatty acid compositional analysis (Table 2.1) it was observed that WCOFAME contains more polyunsaturated (44.41%) compounds in its composition than COFAME (6.6%), hence it was easily vulnerable to oxidative degradation than COFAME. Further, fatty acid composition, thermal and oxidative stability analysis data in Tables 2.1, 3.8 and 3.9 confirms that COFAME was oxidatively more stable compared to WCOFAME due to higher monounsaturated fatty acids content in its composition (i.e. ricinoleic acid, 84%). But, the significant difference was observed when the heating rate was increased to 20 ^{o}C/min, which may be due to shift in onset temperature to higher temperature range (i.e. 20 ^{o}C/min). More unsaturation leads to oxidation which results in the formation of polymerization products (Adhvaryu and Erhan 2002).

3.7. Cold flow properties of COFAME and WCOFAME

One of the major problems associated with the biodiesel/methyl ester is poor low temperature flow properties and due to that operating engine at cold climate regions is often challenging. Therefore, low temperature flow properties of the fuel need to be monitored closely. The cloud point is the temperature at which FAME becomes cloudy due to the formation of wax crystals. Further decrease in temperature below CP causes wax crystals to grow rapidly and prevent fuel to flow and causes major operational problems (Dunn 2005a;

Dunn 1999; Lang et al. 2001). The lowest temperature at which fluid still flows is known as pour point (Kaya et al. 2009).

Biodiesel is a mixture of long-chain fatty acid methyl esters that differ in carbon chain length and degree of saturation. The crystallization temperature of esters depends on the fatty acids chain length and interactions between the molecules (Rodrigues et al. 2006). These FAME are miscible with each other at room temperature, and therefore show no heat change when mixed. However, crystallization or a polymorphic transition of a given ester could exhibit the heat change, which can be monitored using DSC. There are reports in the literature about the estimation of triglycerides enthalpy and crystallization using DSC (Small 1986). Lee et al. (1995) in their study reported that branched chain esters have the lower crystallization temperature than that of conventional straight chain esters. Knothe (2005) reported that biodiesel with the higher amount of saturated fatty acids in the range of carbon chain C_{16}–C_{18} and low concentration of low melting point unsaturated mono-alkyl esters exhibits poor cold flow properties.

Table 3.10: Pour point of COFAME and WCOFAME by ASTM and DSC methods, comparison

FAME	ASTM	DSC
Castor oil	-12.5	-13
Waste cooking oil	1	-1

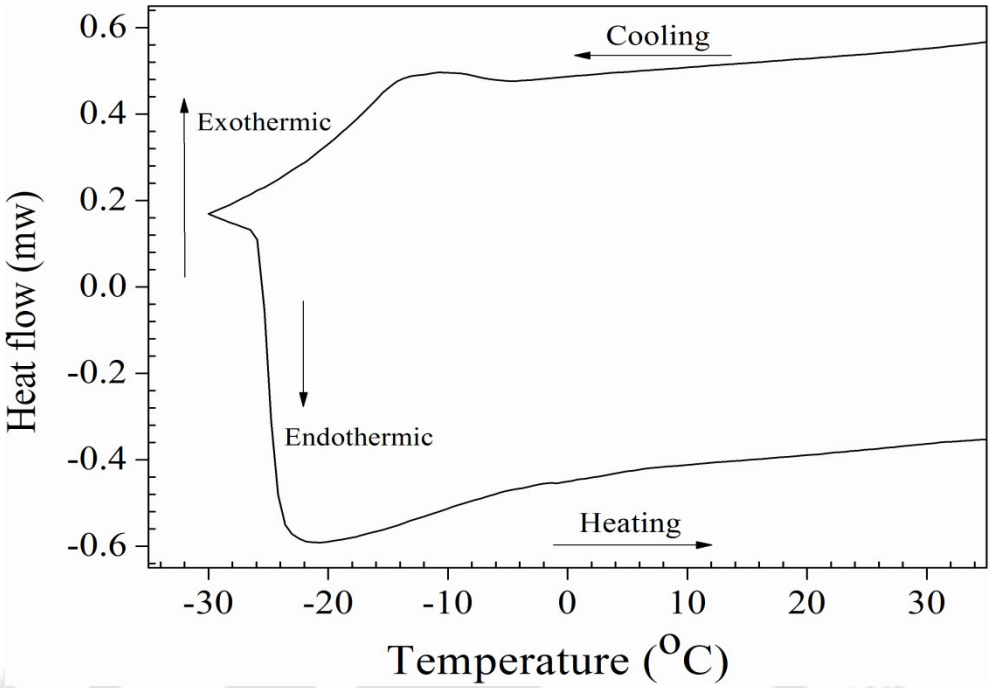

Figure 3.11: DSC cooling thermo-gram of COFAME

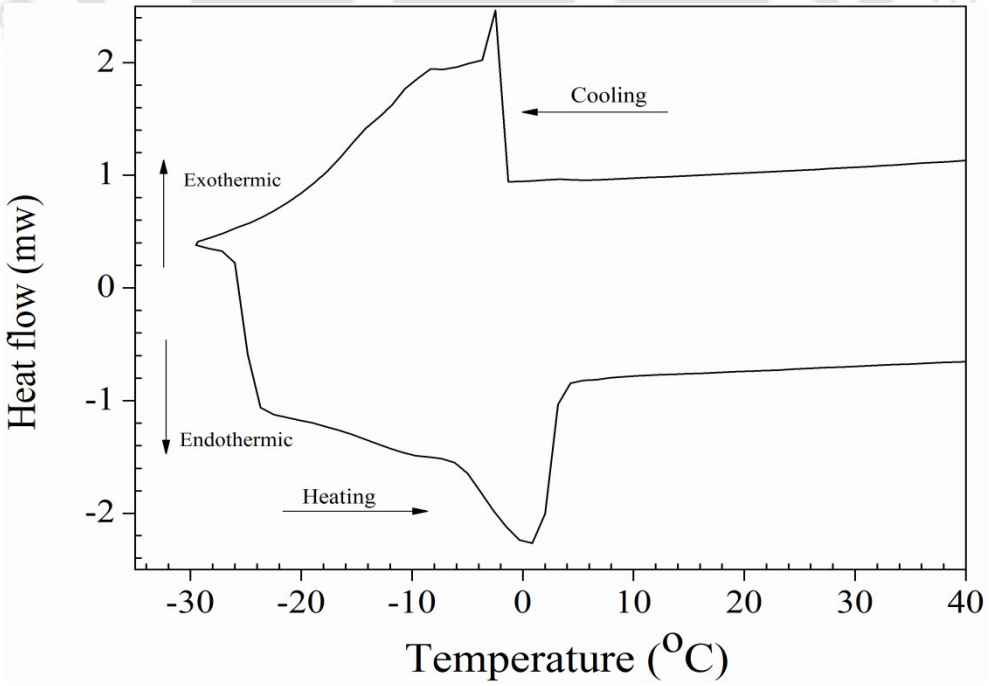

Figure 3.12: DSC cooling thermo-gram of WCOFAME

In this study PP of WCOFAME and COFAME were estimated according to ASTM D97 and DSC method and comparative results are tabulated in Table 3.10. Typical DSC thermo-grams of COFAME and WCOFAME are shown in Figures 3.11 and 3.12 and the fatty acid composition of methyl esters are represented in Table 2.1. The PP of esters was noticed as a sharp increase in the heat energy flow due to the exothermic nature of increasing reaction. The temperature at which exothermic peak occurs that was considered as a PP (Table 3.10) and results obtained from the DSC method correlates well with the PP estimated by the ASTM D97 method (Nik et al. 2005; Quinchia et al. 2012). The difference in the PP of methyl esters sample can be explained from the fatty acid profile (Table 2.1). Zuleta et al. (2012) described that unsaturated esters crystallizes at a lower temperature than saturated esters, this attributed to the different three-dimensional conformations. Saturated ester molecules are in its minimum energy when fully extended and are well stacked, thereby strengthening intermolecular attraction force.

Unsaturated ester molecules, especially cis-formation have weaker intermolecular interactions and therefore crystallize at lower temperature. For WCOFAME 18.27 wt% of medium chain saturated compounds were responsible for its weak performance, whereas in COFAME saturated fatty acids was 3.2 wt%. As a result, the COFAME with higher percentage of total unsaturated fatty acids (94.6%) showed lower pour point than WCOFAME (68.37%). These observations are consistent with those reported in the literature (Jayadas and Nair 2006; Norris 2007; Park et al. 2008; Angel et al. 2010) in which crystallization temperature of saturated fatty acids was higher than that of unsaturated fatty acids (Tables 3.5 and 3.10). From these findings it can be seen that DSC provides accurate means of monitoring the crystallization.

3.8. Summary

In the present chapter, thermo-oxidative stability and cold flow properties of CO, WCO and their FAME was studied using TGA and DSC thermal analysis techniques. Thermal analysis results revealed that the triglycerides alkyl chain structure showed a significant impact on the thermo-oxidative stability of CO and WCO. The chromatographic analysis of COFAME and WACOFAME exposed the fatty acid composition, stability and cold flow properties data was justified according to their fatty acid profile. Thermo-oxidative stability and cold flow properties of the CO/COFAME was found to be superior to WCO/WCOFAME due the presence of higher monounsaturated fatty acid (ricinoleic acid) in CO/COFAME composition. The decomposition behavior of oils and FAME was also studied at two different heating rates (10 and 20 ^{o}C/min), decomposition patterns were found to be identical at both the heating rates. However, due to the increased heating rate, onset temperature was found to be high at 20 ^{o}C/min than 10 ^{o}C/min for all the feedstocks. Similarly, CO/COFAME demonstrates improved cold flow properties (PP) than WCO/WCOFAME, due to less saturated fatty acids content and higher monounsaturation content in CO/COFAME composition.

Comparative evaluation between ASTM and DSC methods disclosed that these methods can be used alternatively for the estimation of thermo-oxidative stability and pour point. In addition to that DSC offers simple technique with good repeatability and reproducibility of experimental data to analyze the PP in less amount of time and by consuming a small quantity of the test sample (< 10 mg). During the analysis of stability and pour point data fatty acid composition plays a vital role. Finally from this study it could be concluded that TGA/DTG and DSC thermal analysis techniques found to be an efficient and

effective methods to determine the degradation behavior and cold flow properties of test samples.

Therefore from the study on thermo-oxidative stability and low temperature properties of feedstocks, it was noticed that, these properties need to be improved in order to apply them as lubricant basestocks. Hence, the following chapters (4 - 7) deals with various structural (chemical) modifications carried out to fatty acids present in the feedstocks to overcome performance limitations and to enhance the thermo-oxidative stability and low temperature properties of end products.

CHAPTER-4

Formulation of bio-lubricant basestocks via structural modifications of waste cooking oil

This chapter addresses the different structural modifications carried out to unsaturated fatty acids present in the WCO. The primary section of the chapter discussed the optimization results of WCO epoxidation such as, analysis of variance (ANOVA) and impact of the process variables to maximize OOC. Further, the significant physico-chemical properties of prepared epoxide was estimated at an optimum condition and compared with un-modified WCO. The outcomes of WCO epoxide analysis in terms of cold flow property was found to be un-favourable, thus the ring opening of epoxide in presence of 2-EH followed by functionalization of hexanoic anhydride was carried out to enhance the low temperature properties of prepared basestocks. Important physico-chemical properties are determined along with the thermo-oxidative stability and cold flow properties of hydroxylated and hexanoylated products, further WCO derived hexanoylated product tribological properties and biodegradability was also found out.

4.1. Optimization of WCO epoxidation: ANOVA analysis and fitting of quadratic model

To optimize the epoxidation process parameters for maximum OOC, preliminary studies were carried out for four process variables (Figure 4.1), the range of each process variable is identified and reported in Table 4.1. ANOVA as a multivariate technique was considered to explore the entire optimization process. Based upon the preliminary studies data (Table 4.1 and Figure 4.1) of process variables, their experimental matrix is prepared and presented in the Appendix (Table A.1) for CCD analysis. All the 30 designed experiments were

performed at laboratory conditions (experimental procedure was well explained in Chapter-2, section 2.2), and results are analysed by multiple regression analysis. A quadratic polynomial Eq. (1) is received from the design experimental data to predict higher OOC as shown below in terms of coded variables.

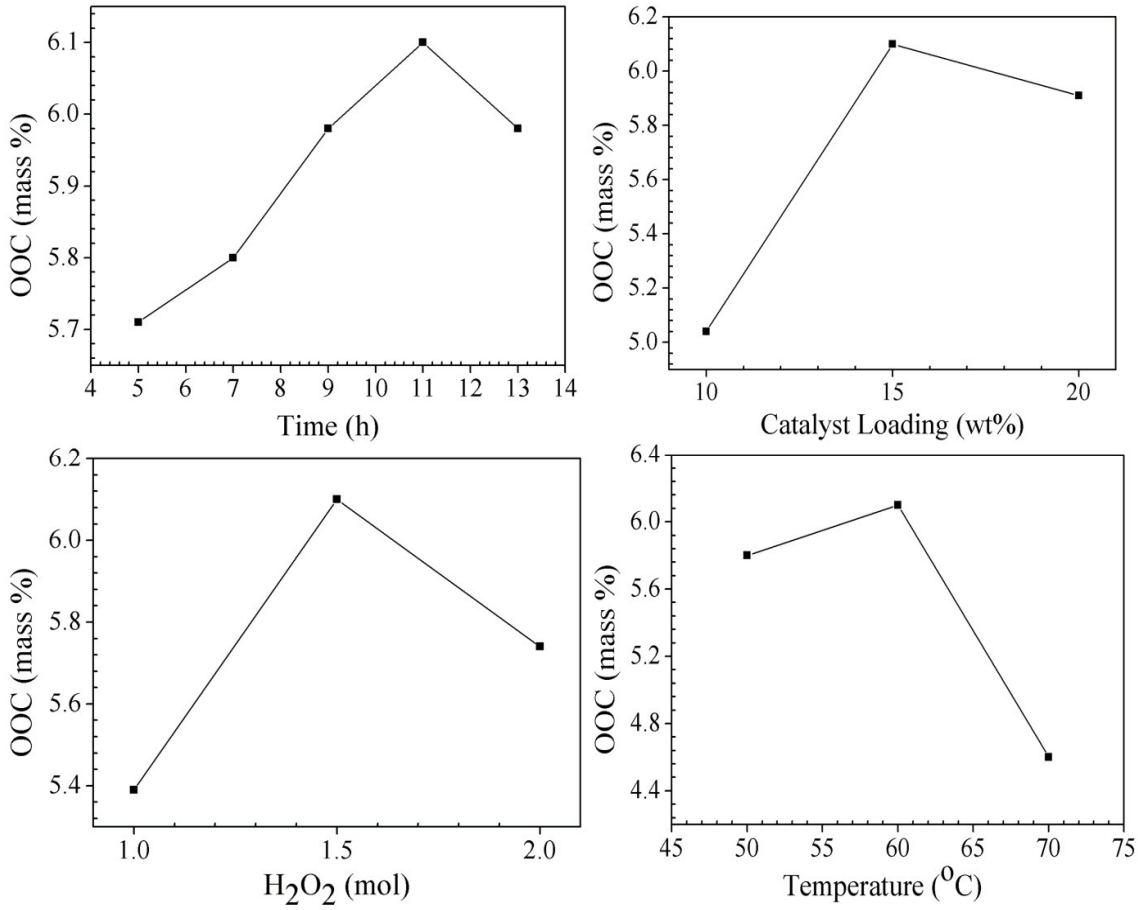

Figure 4.1: Effects of reaction variables such as time, catalyst loading, hydrogen peroxide and temperature on epoxidation of WCO (preliminary studies)

Table 4.1: Independent process variables and their optimum levels for WCO epoxidation

Independent Variables	Symbol	Unit	Variable Levels		
			-1	0	+1
Time	A	hr	8	11	14
Catalyst Loading	B	wt%	11	16	21
Temperature	C	^{o}C	45	55	65
Hydrogen Peroxide	D	mol	1.1	1.6	2.1

Response (OOC) = 6.17 + 0.048 A + 0.18 B – 0.17 C + 0.27 D – 0.039 AB – 0.14 AC + 0.055 BD + 0.029 CD – 0.24 A^2 – 0.16 B^2 – 0.33 C^2 – 0.26 D^2 (4.1)

In order to ensure a good model and to evaluate the analysis of variance on individual model co-efficients the test for lack of fit need to be performed. The lack of fit is an assessment of the failure as a model to represent the data in the observational domain at which the points are not included into the regression or variations in the model that can't be reported by random error. Generally, significant factors can be graded based on the F -value or p-value (also known as the probability of error value or "prob > F" value). Greater the magnitude of F-value and correspondingly smaller the "prob > F" value, more significant (important) is the corresponding co-efficient (Sahu et al. 2010; Mahalik et al. 2010; Cronje et al. 2011; Prabhakar and Raja 2012). The effects of a second order response surface model in the form of ANOVA for higher epoxide content is summarized in Table 4.2. It can be observed (Table 4.2) that F-value of the model is found to be 215.01 and the corresponding P-value (prob >F) is very small, i.e. < 0.0001, ensures that model is highly significant. The p-values are adopted as a tool to assure the significance of each co-efficient. Further, the effect of linear variables, such as catalyst loading (B), temperature(C), hydrogen peroxide molar ratio (D); cross variables such as, the effect of time and temperature i.e. AC and the

quadratic effects of all four process variables (i.e. A^2 , B^2 ,C^2 , D^2) are highly significant, since P-value is very low (<0.0001). Other model terms of linear variable time (A) cross variable catalyst loading and hydrogen peroxide molar ratio, i.e. BD, time and catalyst loading i.e. AB are also significant (since P-value is >0.0001and <0.05). Similarly, other model cross variable terms, temperature and hydrogen peroxide molar ratio i.e. CD, time and hydrogen peroxide molar ratio, i.e. AD, catalyst loading and temperature i.e. BC is said to be in-significant due to greater P-value, i.e. > 0.005. To improve the quality of model, highly in-significant cross variables AD and BC were omitted from the model. The lack of fit F-value 1626 entails that lack of fit is extremely significant relative to the pure error. This signifies that model is extremely accurate without any noise, and results are reproducible. Furthermore, the observed values are very much close to the predicted values as shown in Figure 4.2.

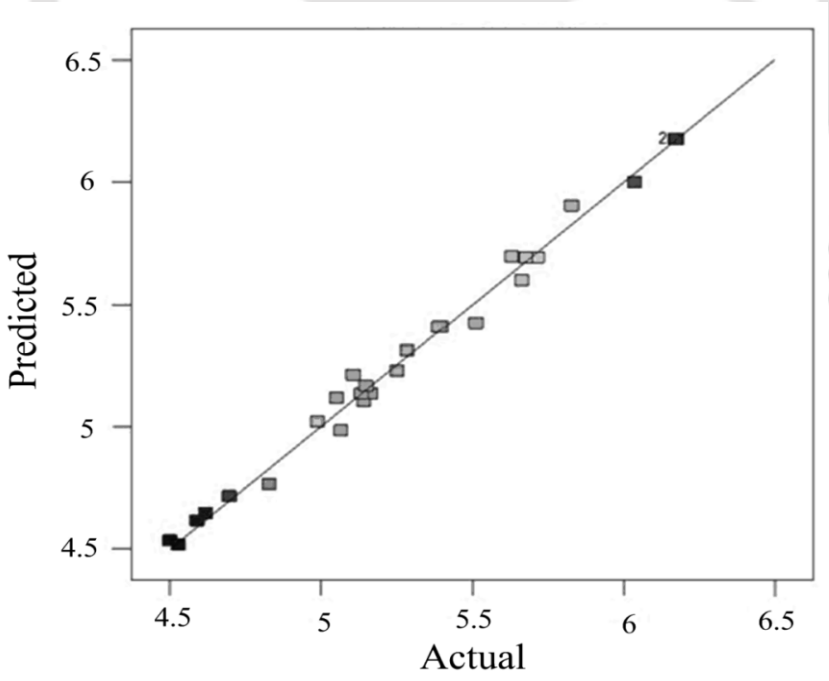

Figure 4.2: Predicted versus actual plot of response (OOC) for WCO epoxide

Table 4.2: Regression co-efficients of predicted and quadratic polynomial model for response variable (OOC) for epoxidised WCO

Source	Sum of Squares	Degrees of Freedom	Mean Square	F Value	p-value (prob > F)
Model	8.842	12	0.736	215.01	< 0.0001
A-Time	0.055	1	0.055	16.27	0.0009
B-Catalyst Loading	0.817	1	0.817	238.45	< 0.0001
C-Temperature	0.723	1	0.723	211.05	< 0.0001
D-H_2O_2	1.738	1	1.738	507.25	< 0.0001
AB	0.024	1	0.024	7.01	0.0169
AC	0.329	1	0.329	96.01	< 0.0001
BD	0.048	1	0.048	14.07	0.0016
CD	0.013	1	0.013	4.03	0.0607
A^2	1.578	1	1.578	460.72	< 0.0001
B^2	0.703	1	0.703	205.22	< 0.0001
C^2	2.948	1	2.948	860.42	< 0.0001
D^2	1.784	1	1.784	520.71	< 0.0001
Residual	0.058	17	0.003		
Lack of Fit	0.058	12	0.004	1626	< 0.0001
Pure Error	1.49E-05	5	2.99E-06		
Cor Total	8.9	29			
R^2	0.9935				

The preciseness of a model can be evaluated by the regression co-efficient, i.e. R^2. The R^2 value is always between 0 and 1, and its order of magnitude intimates the aptness of the model. For a good statistical model, the R^2 value should be close to 1. The regression value for higher epoxide content is presented as 0.9935, which is close to 1 and it signifies that the variation of 99.35% for higher epoxide content is assigned to the independent variables and only about 0.65% of the full variance cannot be explained by the model. This signifies that accuracy and the general ability of a polynomial model are well. The predicted R^2 value (i.e. 0.97) is in reasonable agreement with the adjusted R^2 value (0.98), which recommended an eminent co-relational statistic between the observed and predicted values. Therefore, the regression model provides an excellent explanation of the relationship between independent process variables and response variables.

4.2. Influence of the process variables for maximum oxirane oxygen content

To investigate the interactive effects of four process variables on the response, three dimensional (3D) response surface plots and two dimensional (2D) counter plots are drawn by considering the two variables at a time while keeping others at a central level (0). These plots are graphical representations of the quadratic polynomial equation (Equation 4.1) and drawn using design expert software trial version (8.0.7.1, Stat-Ease, Inc., MN, USA).

4.2.1 Effect of time (A) and catalyst loading (B)

The combined effect of time and catalyst loading on the conversion of ethylenic unsaturation into oxirane oxygen was investigated, and obtained results have been shown in the form of 3D response surface, and 2D counter plots (Appendix, Figure A.1 (a) and (b)). From the figures (Figure A.1 (a) and (b)), it can be seen that OOC increased (i.e. from 5.05 to 6.17 mass%.) almost linearly with an increase in catalyst loading from 6 wt% to 16 wt% and

reaction time from 5 h to 11 h. Outcomes of this study indicate that, time and catalyst loading are highly significant as linear and cross variables. With the increased catalyst loading and time, OOC increased and then decreased gradually. Therefore, from this investigation it was observed that maximum OOC of 6.17 mass% can be achieved at 16 wt% of catalyst loading and 11 h reaction time. Meshram et al. (2011) investigated and reported alike outcomes between catalyst loading and reaction time during their study on epoxidation of wild safflower oil.

4.2.2 Effect of time (A) and temperature (C)

Figure A.2 (a) and (b) shows the 3D response surface plot and corresponding counter plot for time and temperature to maximize OOC. From figures (Figure A.2 (a) and (b)), it could be observed that OOC increased with an increase in reaction time from 5 h to 13 h, and similar trend was noticed when reaction temperature increased from 48 ^{o}C to 57 ^{o}C. However, with further increase in reaction time and temperature, OOC was found to be decreased in WCO epoxide. Fiser et al. (2012) during their study on epoxidation of castor oil revealed that the rate of epoxidation increases with respect to temperature upto a limited reaction time and temperature, but beyond that oxirane cleavage was observed. It has been also reported that (Fiser et al. 2012) stability of oxirane ring decreases at higher temperatures. Therefore, based on the reported literature (Fiser et al. 2012) and from the present study, it was revealed that temperature had a major impact on formation of stable oxirane ring. This suggests that time and temperatures are highly significant as linear and cross variables. Similarly, it has been reported that when oxirane ring is exposed to higher temperature for longer duration, it leads to oxirane cleavage and thus form an un-wanted side reactions (mechanism is shown in Scheme A.1). Thus, it can be said that the use of optimum operating temperature and reaction time can give safe and economically favourable conditions to prepare lubricant

basestocks. The maximum OOC of 6.17 mass% was obtained at 55 ^{o}C and 11 h of reaction time.

4.2.3 Effect of catalyst loading (B) and hydrogen peroxide molar ratio (D)

Figure A.3 (a) and (b) shows the effect of catalyst loading and hydrogen peroxide to ethylenic unsaturation molar ratio on maximization of OOC. It can be observed that the extent of unsaturation (iodine value) conversion increased with an increase in the molar ratio of hydrogen peroxide molar ratio from 0.6 to 1.6 mol and catalyst loading from 6 to 16 wt%. The increased hydrogen peroxide molar ratio and catalyst loading in the reaction mixture enhances the rate of peracid formation and consequently, the rate of epoxidation. The maximum OOC obtained was 6.17 mass% at 1.6 mol of hydrogen peroxide and 16 wt% catalyst loading. However, with an increase in the molar ratio beyond 1.6 mol and 16 wt% catalyst loading, considerable decrease in the OOC was observed, which may be due to oxirane cleavage (mechanism) as mentioned in Scheme A.1. Fiser et al. (2012) have shown the strong dependency of hydrogen peroxide on OOC and epoxide selectivity during their study on epoxidation of castor oil using optimum hydrogen peroxide molar ratio of 1.5. Therefore, the catalyst loading and hydrogen peroxide molar ratio shows a significant impact on OOC as linear and interaction variables.

4.2.4 Effect of temperature (C) and hydrogen peroxide molar ratio (D)

The effect of temperature and hydrogen peroxide molar ratio for maximum OOC at constant time and catalyst loading is shown in Figure A.4 (a) and (b). From the results it has been observed that the combination of medium temperature (55 ^{o}C) and medium hydrogen peroxide molar ratio (1.6 mol) gave increased OOC compared to the combination of higher temperature and lower hydrogen peroxide molar ratio. This is due to the fact that the excess hydrogen peroxide molar ratio (> 1.6 mol) and higher temperature leads to more oxirane

cleavage (Madankar et al. 2013). From Figure A.4 (a) and (b) it is clear that slightly higher hydrogen peroxide molar ratio (i.e. 1.68 mol) than the central value (1.6 mol) and lower temperature (55 ^{o}C) was desirable for maximum OOC of 6.17 mass%.

4.2.5 Attaining optimal conditions to maximize OOC for WCO

Counter plots (2D) and response surface plots (3D) indicates the effects of interaction on process variables of the epoxidation reaction. Apart from that, 2D and 3D plots also contributed information about the various trusted combinations of variables that gives higher OOC in epoxidised WCO, which offers a variety of choices when the practical aspects are regarded in actual commercialization of the process. From the optimization study, various experimental conditions were suggested as the optimum value, among them the following set of experimental conditions are followed i.e. H_2O_2, 1.68 mol; catalyst loading, 16.75 wt%; temperature, 54 ^{o}C; and reaction time, 11.45 h for higher OOC. Under these experimental conditions, OOC of epoxidised WCO was expected to be 6.25 mass% (predicted value).

4.2.6 Model validation and confirmation

To validate the optimal combination of process variables and adequacy of the predicted model, confirmatory laboratory experiments were executed at the predicted condition reported in section 4.2.5. The OOC of 6.2 mass% was observed, and this value is almost close to the predicted value with 0.008 error%, which suggests that the formulated model was believed to be precise and authentic. In the present study, all 30 experiments (Table A.1), including confirmatory experiments were conducted in a duplicate at laboratory conditions and the average values are reported.

4.3. Physico-chemical characterization of WCO epoxide

4.3.1 FTIR spectroscopy

The conversion of ethylenic unsaturation into oxirane oxygen and their subsequent fictionalization were observed under FTIR spectra. The disappearance of double bonds at 3002 - 3008 cm^{-1} and formation of epoxy groups at 838 cm^{-1} were confirmed by the transformation of double bonds into a three-member oxirane ring via epoxidation reaction. Lee et al. (2009) reported that FTIR is not only used to confirm the formation of product but also to monitor potential side reactions. The FTIR spectra of WCO and its epoxide are shown in Figure 4.3 along with its functional groups in Table 4.3. The appearance of an epoxy peak at 820 - 843 cm^{-1} provided evidence of that epoxidation reaction occurred with ion-exchange resin as catalyst. Salih et al. (2011b) described the characteristic signals in the FTIR spectrum of oleic acid at 830, 845 cm^{-1} which represent the quaternary carbons of the oxirane ring. The complete disappearance of C=C bonds in the WCO epoxide FTIR spectra (Figure 4.3) at 3010 cm^{-1} further supported the almost complete conversion of double bonds to oxirane oxygen (i.e. 95%). Farias et al. (2010) identified that via oxirane ring opening reaction -OH functional groups can be derived from epoxy functional groups. In this study, FTIR spectra exhibited no trace of -OH absorption peak at approximately 3000 - 3500 cm^{-1} represents no oxirane cleavage during WCO epoxidation.

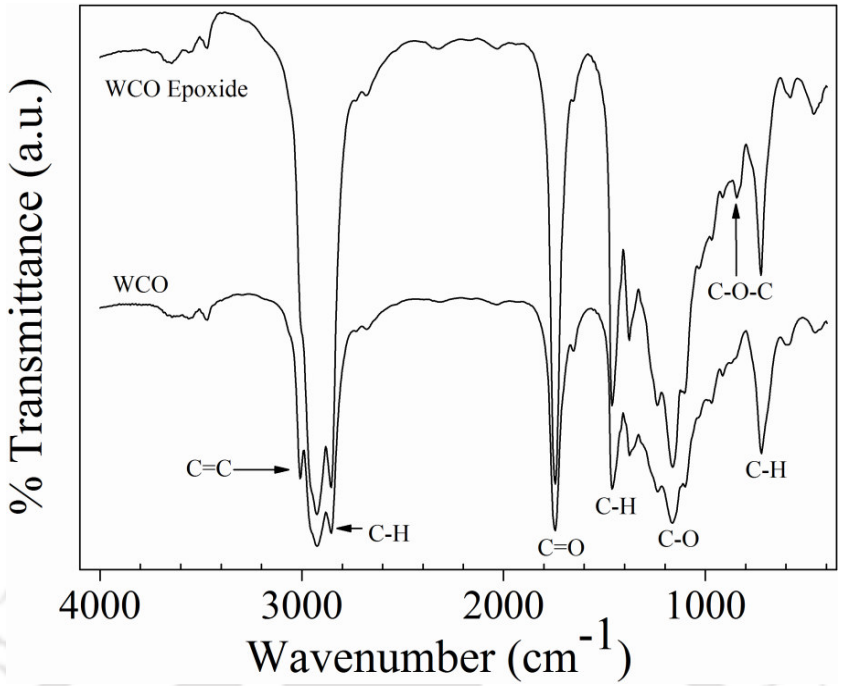

Figure 4.3: FTIR spectra of WCO and WCO epoxide

Table 4.3: The main functional groups present in FTIR spectra's of WCO and WCO epoxide

WCO	WCO epoxide	Functional Group
3009	-	C=C bending vibration
2930, 2850	2930, 2850	C-H stretching vibration (aliphatic)
1720	1720	C=O stretching vibration
1455	1455	C-H scissoring and bending
1285	1285	C-O stretching asymmetric
-	823	C-O-C oxirane ring
725	725	C-H group vibration (aliphatic)

4.3.2 Product confirmation by NMR spectroscopy

^{1}H-NMR spectra (Figure 4.4 (a) and (b)) confirms the main signal's assignments in WCO and its epoxide as shown in Table 4.4. The olefinic hydrogens (-CH=CH-) of WCO is present at δ 5.25 - 5.37 ppm region. These have been disappeared in epoxidised WCO spectra, which suggests that unsaturated double bonds (CH=CH) are transformed into

oxirane (-CH-O-CH) during the epoxidation reaction. From Figure 4.4 (b), it can be observed that epoxy group (-CH-O-CH) is present at δ 2.77 - 2.9 ppm region. The characterization of reaction products by ^{1}H-NMR revealed that no hydroxylation reaction occurred during the epoxidation, i.e. no peaks were observed at δ 3.4 - 4 ppm region. Therefore, from the ^{1}H-NMR spectrum of WCO and its epoxide, it could be verified that WCO conversion into epoxide was confirmed and agrees well with the reported literature (Farias et al. 2010).

Table 4.4: The main functional groups present in ^{1}H-NMR spectra's of WCO and WCO epoxide

WCO	WCO epoxide	Functional Group
0.88-0.95	0.7-0.8	$-CH_3$
1.1-2.8	1-2.1	$-CH_2$
4.1-4.3	3.8-4.1	-CHOCOR
5.2-5.55	-	-CH=CH-
-	2.81-3	-CH-O-CH-

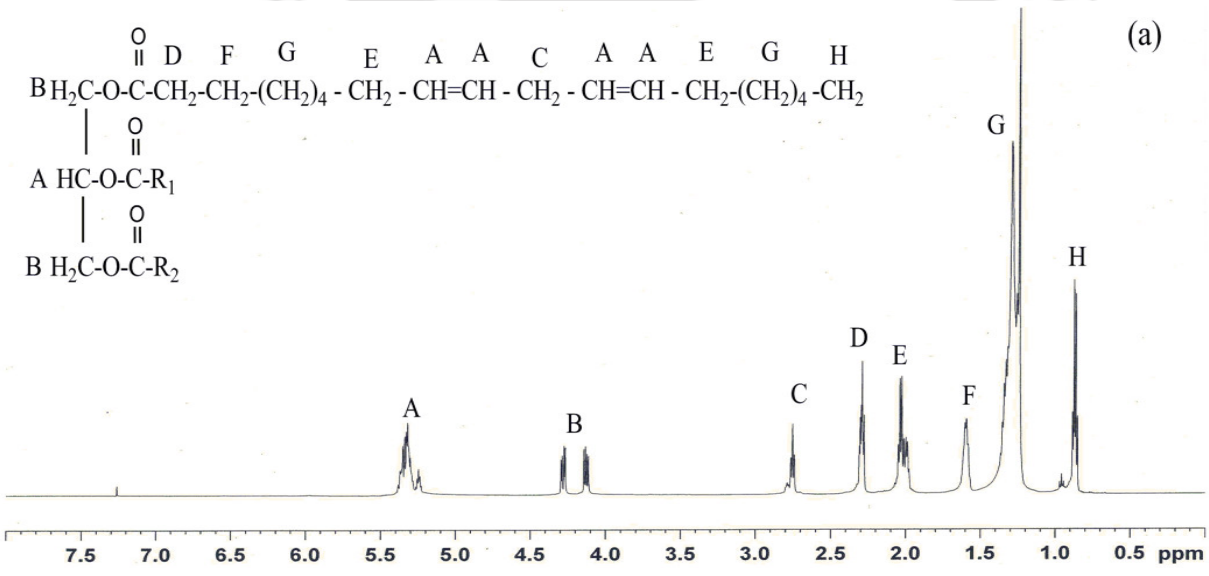

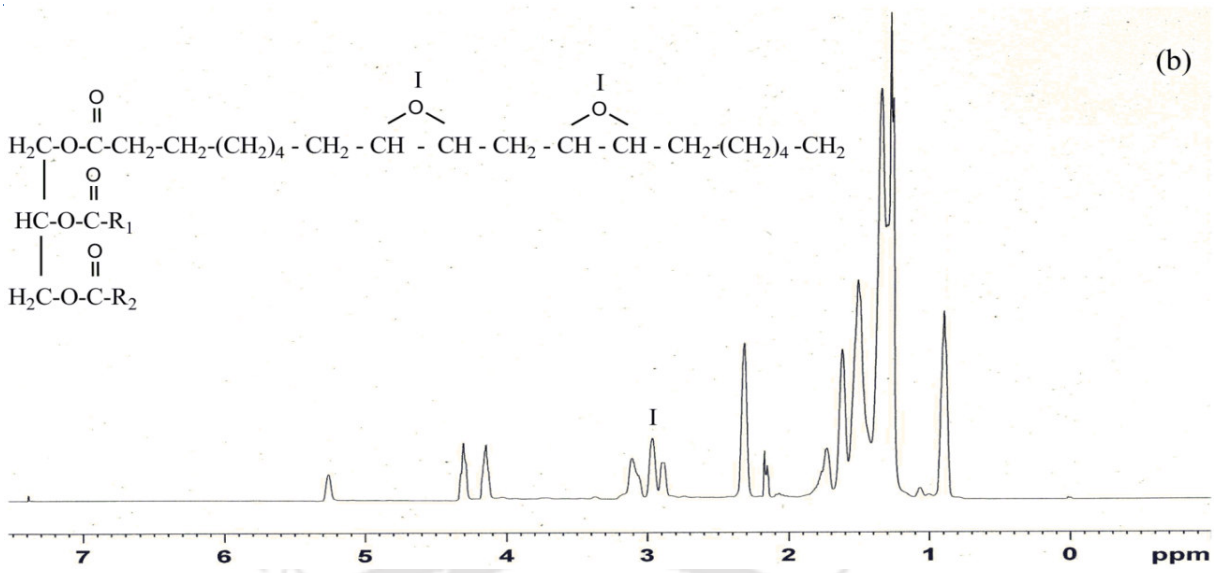

Figure 4.4: ^{1}H-NMR spectra's of WCO (a) and WCO epoxide (b) represented by triglyceride of linoleic acid

4.3.3 Low-temperature properties

The ability of epoxide to continue in a liquid state at lower temperature is a highly significant property for many of the industrial materials, such as lubricants, surfactants and fuels. Pour point (PP) reveals the lowest temperature at which epoxide can be used in various applications. Lower the PP, more useful the epoxide in cold climatic conditions, in the present study DSC technique was adopted to determine the PP (Figures 3.6 and 4.5). From the results it was observed that WCO epoxide offers higher PP (-6.2 ^{o}C) compared to that of un-modified WCO (-7 ^{o}C) and agrees with the earlier report by Erhan et al. (2000). From these outcomes it is clear that structural modification can alter the cold flow properties (PP). Soriano et al. (2006) reported that, unsaturation content plays a major role in low temperature properties; more the unsaturation content better the cold flow behaviour. The increase in PP of WCO epoxide was due to the removal of unsaturation content. Wadumesthrige et al. (2009) in their study reported that epoxidation did not enhance the cold flow properties considerably, and the same is noticed in the present study as well.

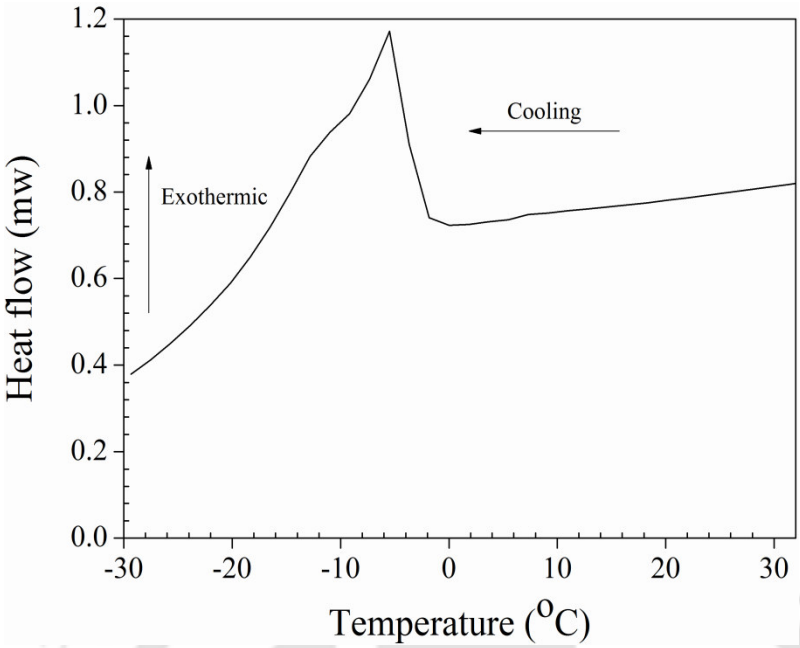

Figure 4.5: DSC thermo-gram for WCO epoxide for pour point determination

4.3.4 Thermo-oxidative stability

The ability to resist thermal and oxidative degradation is another significant factor for many industrial materials such as polymers, fuels and lubricants. Therefore, in this study TG analysis was used for evaluating the thermo-oxidative stability of WCO and its epoxide. Thermo-oxidative stabilities are estimated from thermal and oxidative onset temperatures respectively (Borugadda and Goud 2013). Onset temperature corresponds to the minimum temperature at which sample decomposition starts; in other words, maximum temperature up to which sample can be stable without any weight loss. From Figures 3.1 and 4.6 it can be observed that WCO is thermally more stable (onset temperature of 360 ^{o}C) compared to WCO epoxide (330 ^{o}C). In general thermal stability of WCO epoxide is anticipated to be high compared to WCO, but in the current study, opposite trend was noticed. This can be explained with the help of WCO source, as mentioned in Chapter-3, section 3.1 fish fried soybean oil was collected and used as received without any further purification.

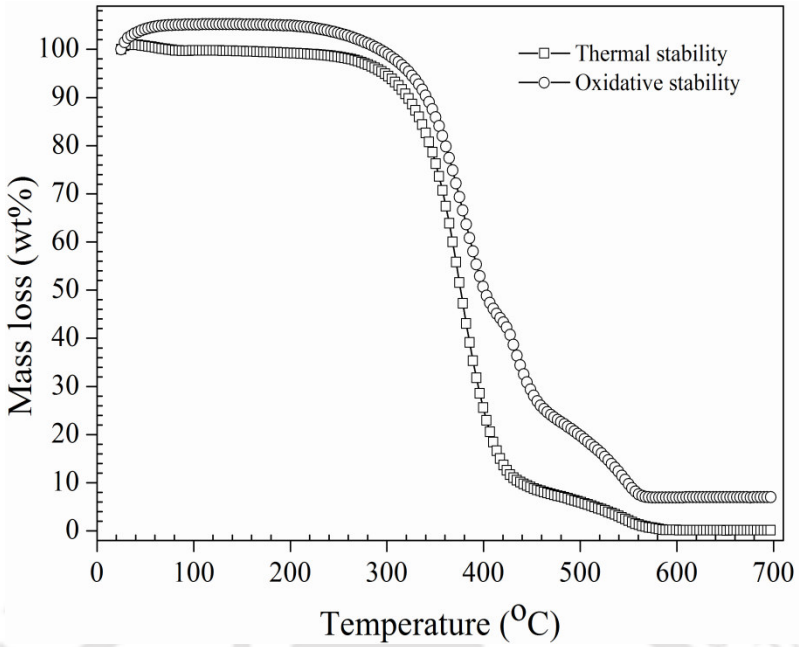

Figure 4.6: TGA thermo-grams for WCO epoxide under nitrogen atmosphere (Thermal Stability) and air atmosphere (Oxidative Stability)

From section 3.1, it was clear that WCO used in this study must be containing high molecular weight polymeric compounds, which could be the reason for exhibiting higher thermal stability than WCO epoxide. In order to clarify this, thermo-oxidative stability, cold flow properties were evaluated for refined soybean oil and it was found to be 305 ^{o}C, 240 ^{o}C and -9.43 ^{o}C respectively (Figures A.5 and A.6). Therefore, from the present study it was clear that, if WCO used in this study would have been pre-treated before undergoing epoxidation reaction, results would have been different.

Oxidative stability is the quality indicative parameter for the epoxide in real-life application. Oxidation of epoxide results in decreasing shelf life along with increase viscosity and acid value simultaneously (Romeu et al. 1998). Oxidative stability of WCO and its epoxide is measured by oxidative onset temperature (Figures 3.3 and 4.6). From Figure 4.6, it is clear that WCO epoxide exhibits more oxidative stability (i.e. 320 ^{o}C) than WCO (i.e. 280 ^{o}C). Since, unsaturated compounds are more susceptible to oxidation than saturated compounds with the same hydrocarbon chain length. Apart from that, poly-

unsaturated compounds are more reactive than mono-unsaturated compounds. Therefore, from the present study on oxidative stability of WCO and its epoxide, it was noticed that epoxidation of WCO decreases the unsaturation content thereby enhances its oxidative stability.

4.3.5 Rheological behaviour

The rheological behaviour of WCO epoxide was studied at various temperatures and shown in Figure 4.7. From Figure 4.7, it is observe that shear rate increases with respective to shear stress, in spite of temperature variation. This linear relation between shear stress versus shear rate suggests Newtonian type fluid behaviour for WCO epoxide. It can also notice from the Figures 4.7 and 4.8, as temperature increases shear stress decreases gradually and increased in shear rate was observed (Figure 4.8). In the present study, rheological behavior of WCO epoxide is found using power law model (Eq. 4.2).

$$\tau = K\gamma^{n} \qquad (4.2)$$

The values of flow behavior index 'k' and consistency co-efficient 'n' were obtained according to the power law relation. Taking the logarithms of power law relation (Eq. (4.2)) it gives following form of the equation,

$$\ln(\tau) = \ln(k) + n \ln(\Upsilon) \qquad (4.3)$$

According to Eq. (4.3), plot between ln(τ) and ln(Υ) is expected to show a straight line relationship (Figure 4.9) with slope 'n' and intercept ln(k). The ln(τ) dependence of ln(Υ) for WCO epoxide at various temperatures, ranging from ambient to 100 ^{o}C is shown in Figure 4.8, indicating that at various temperatures a linear relationship exists between ln(τ) and ln(Υ). From this dependency ln(k) and 'n' values were evaluated by linear regression

analysis, and the results are reported in Table 4.5 and shown in Figure 4.9, which express that flow behaviour index decreased with temperature and consistency co-efficient always remains constant and close to one irrespective of temperature variation. Yen and Yang (2003) studied and reported similar kind of results in their study on rheological behavior of polyacrylamide solution. This behaviour of epoxide signifies that WCO epoxide adopting the Newtonian fluid behaviour (Hwang et al. 2003), therefore, based on the aforementioned rheological characterization; it could be predicted that WCO epoxide provides a smooth performance during its usage without any operational difficulties.

Table 4.5: WCO and WCO epoxide rheological properties with power law model

Temperature (^{o}C)	WCO Epoxide DV (K, Pa.s)	WCO Epoxide KV (cSt)	n	R^2	WCO DV (Pa.s)	WCO KV (cSt)
28	0.38	486.29	0.98	0.99	0.04	59.94
40	0.22	282.38	0.98	1	0.02	35.00
60	0.09	123.73	0.97	0.99	0.01	18.50
80	0.04	58.07	0.98	0.99	0.008	11.39
100	0.02	33.33	0.98	0.99	0.006	8.10

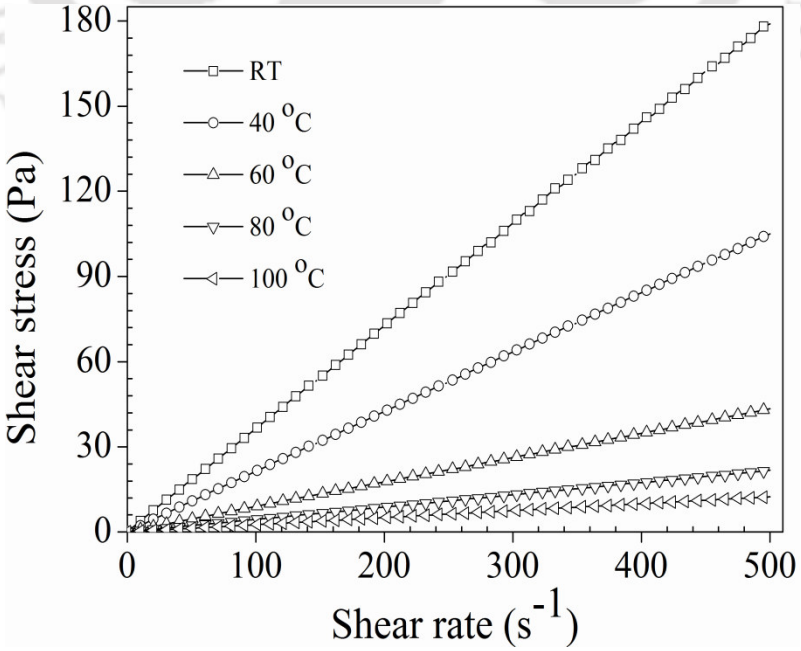

Figure 4.7: Shear stress versus shear rate relation for WCO epoxide

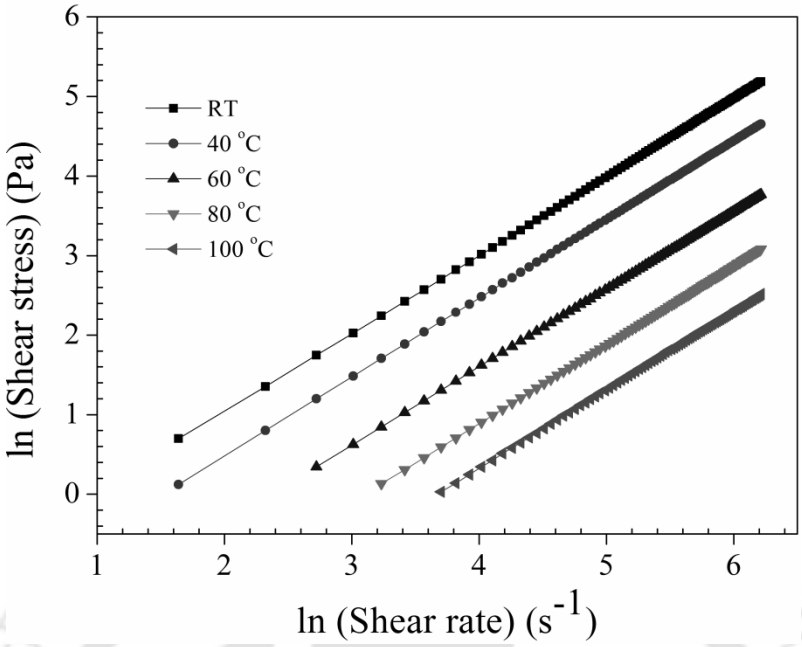

Figure 4.8: Logarithmic plot of shear stress versus shear rate for WCO epoxide

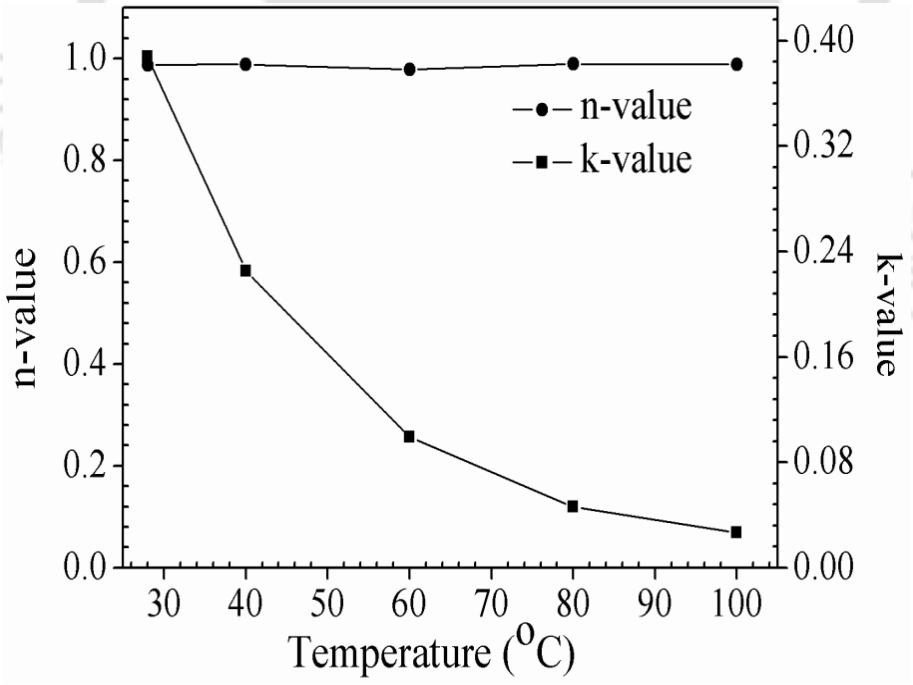

Figure 4.9: Plot of experimental value of n and k for WCO epoxide

4.3.6 Viscosity and viscosity index

The detailed knowledge of viscometric properties of WCO and chemically modified WCO (epoxide) is of particular importance whenever lubrication is their intended use. Both the dynamic and kinematic viscosities at various temperatures (28, 40, 60, 80 and 100 ^{o}C) for WCO and its epoxide are presented in Table 4.5. In the present study viscosity of WCO was found to be 35 cSt and 8.1 cSt at 40 ^{o}C and 100 ^{o}C respectively. After structural modification (epoxidation) the viscosity increased to 282.38 cSt and 33.33 cSt at 40 ^{o}C and 100 ^{o}C respectively. From the comparison of WCO and its epoxide viscosities at 40 ^{o}C it was evident that for WCO epoxide viscosity (282.38 cSt) was almost eight times higher than WCO (35 cSt), similarly at 100 ^{o}C viscosity was four times higher than that of un-modified WCO. In the present work it is anticipated that, improvement in the viscosity of epoxide is attributed to the inclusion of oxygen molecule in the midst of unsaturation, thereby molecular weight and viscosity of the epoxide improved. Recently, Gorla et al. (2013) studied the properties of lubricant basestocks from epoxidised karanja oil and its alkyl esters and they have reported the similar kind of results on viscosity of karanja oil and its epoxide. Generally, in the absence of lubricant, moving parts inside these systems (i.e. gears, pistons, hydraulic brakes, any two moving parts) would grind together and releases heat, generates stress and wear. Therefore, in order to avoid the aforementioned negative effects and improve the life time of equipments, epoxides must have the higher viscosity to keep a good lubricant film between two moving parts.

Similarly, viscosity index of WCO and its epoxide is estimated in order to find out the variation of viscosity over a wide range of temperatures. Viscosity index of epoxidised WCO was found to be higher (217) compared to its un-modified WCO (159). These results are in well agreement with the outcomes reported by Gorla et al. (2013) during their study on

epoxidised karanja oil. Hwang et al. (2003) reported that lubricant is considered to have a stable viscosity, temperature relation and in the present study it is confirmed from rheological behaviour (Section 4.3.5) of epoxide with power law model. This implies that prepared WCO epoxide serves better lubricant properties compared to its un-modified WCO.

4.3.7 Physico-chemical characterization

The physico-chemical properties of WCO and its epoxide are summarized in Table 4.6. The acid value of WCO epoxide was found to be 0.4 mg KOH/g. Lower acid value (AV) signifies that WCO epoxide does not create any trouble or damage (due to corrosion) to the equipment during its usage. Free fatty acid (FFA) content is always half of the AV, which indicates the formation of soap when it is mixed with water; the estimated FFA value is very less (0.2 mg KOH/g). Similarly, density of WCO was found to be 752 kg/m^3, after chemical modification it reached to 798.14 kg/m^3. This may be due to increased molecular weight, polarity and intermolecular forces in the epoxide after reaction.

Measure of IV (i.e. unsaturation sites) after epoxidation reaction is one of the ways to confirm completion of epoxidation reaction. Initial IV of WCO was found to be 132.9 (gI_2/100 g of oil), whereas after the reaction, it was observed to be 0.60 (gI_2/100 g of epoxide). From Table 4.6 it is confirmed that 99.54% double bonds are transformed into oxirane ring via epoxidation, and the conversion is calculated based on initial and final IV's. These three membered rings of oxirane could form a smooth layer due to tribo-polymerization which is tribologically effective to reduce friction during usage (Wu et al. 2000). Similarly, relative percentage conversion to oxirane was found to be 80.31% (Eq. (2.3)). Likewise, α-glycol content (theoretical and experimental) found to support the presence of hydroxyl groups (Eq's. (2.2) and (2.4)) in WCO epoxide, and the relative percentage conversion of α-glycol is computed according to Eq. (2.3) and reported in Table

4.6. One of the considerable properties of epoxide is moisture content, which indicates the presence of water in the epoxide. In general, presence of moisture encourages the bacteria to grow; this leads to an increased AV, viscosity and free radical compounds via oxidation (Sharma et al. 2008a and 2008b). In this study epoxide moisture content was found to be 0.2 wt% (Table 4.6) which again favours to the usage of WCO epoxide without any trouble. Refractive index of WCO and its epoxide was found to be 1.47 (Table 4.6), which shows that very less amount of heat energy can pass through the oil and epoxide, which is the desired property for lubricants to maintain their rheological properties. Lower refractive index lubricants are preferred to avoid thermal variations in the application point of view during usage.

Table 4.6: Physico-chemical properties of WCO and WCO epoxide

Physico-chemical properties	**WCO epoxide**	**WCO**
Acid Value (mg KOH/g)	0.4	3
Density (kg/m^3)	798.14	752
Iodine Value (g I_2/100 g)	0.6	132.94
Kinematic Viscosity (cSt) at 40 ^oC	282.38	35
Kinematic Viscosity (cSt) at 100 ^oC	33.33	8.1
Moisture Content (weight %)	0.2	0.38
Pour Point (^oC)	-6.2	-8.6
Refractive Index (at 27.6 ^oC)	1.47	1.47
Specific Gravity	0.8	0.75
Oxirane Content (% by mass, Experimental)	6.2	-
Oxirane Content (% by mass, Theoretical)	7.72	-
Relative percentage conversion of oxirane (% by mass)	80.31	-
Glycol content (mol/100 g, Theoretical)	0.44	-
Glycol content (mol/100 g, Experimental)	0.18	-
Relative percentage conversion α-Glycol (mol/100 g)	58.34	-

4.4. Acid catalyzed oxirane ring opening studies of epoxidised waste cooking oil with various alcohols and catalysts

The effectiveness of alcohols such as, methanol, 2-Propanol, 1-Butanol and 2-EH as ring opening reagents; sulphuric acid (homogeneous) and ion-exchange resin (IR-120) (heterogeneous) as catalysts for oxirane ring opening and corresponding structural, physico-chemical changes were studied thoroughly. Initially, ring opening (hydroxylation) was carried out with methanol (5 - 20 mol) in presence of IR-120 (1 - 5 wt%) as a catalyst at room temperature to 70 ^{o}C, samples were withdrawn from 10 min to 9 h of reaction time. During first 1 h samples were withdrawn for every 10 min, thereafter for every 1 h ring opening products were withdrawn to determine the extent of the ring opening by determining OOC. From the ring opening investigations it was found that, only 61 % ring opening could be achieved (based on OOC) with methanol even at higher molar ratios (20 mol), at elevated temperature (70 ^{o}C), and for longer reaction time (9 h) using IR-120 as catalysts. Alike experiments were repeated for sulphuric acid and similar kind of observations were found, but > 90% ring opening was achieved at lower reaction condition such as time < 30 min at room temperature, and 1500 rpm compared to IR-120.

Based on the through study on WCO hydroxylation, optimum condition was found to be 1.5wt% sulphuric acid, 10 moles of alcohol, 1500 rpm for 30 min at room temperature, at his condition PP and molecular weights (number average and weight average) of the ring opened product was found to be 3.3 ^{o}C and 995, 1164 respectively. Since the molecular weight and small chain length of methanol, unsatisfactory PP was noticed, but during the study, sulphuric acid was found to be an efficient catalyst for hydroxylation. In addition to that, reaction time was less at ambient temperature for the complete ring opening reaction to

takes place with sulphuric acid as a catalyst compared to IR-120. Hence, further all experiments were preceded with sulphuric acid as a catalyst at room temperature.

Improved cold flow properties of the basestocks was one of the principle objectives in the current study, therefore assorted alcohols with variation in molecular weight, structure and boiling point were tested to enhance the PP of WCO hydroxylated product. Hence, 1-Butanol, 2-Propanol and 2-EH were also tested as ring opening alcohols to observe the enhancement in PP and molecular weight at identical reaction conditions (room temperature, 10 moles of alcohol, 1.5wt% of sulphuric acid, 1500 rpm stirring speed for 30 min). Upon completion of the hydroxylation with other alcohols, the product was purified by washing with sodium bicarbonate and dried with sodium sulphate; further, purified products PP was found to be -2 ^{o}C (2-Propanol), -4 ^{o}C (1-Butanol) and -16 ^{o}C (2-EH) respectively (Figure A.7). Besides PP, molecular weight (number average and weight average) of the hydroxylated product was found to be 1026, 1189 for 2-Propanol; 1154, 1345 for 1-Butanol and 1528, 1793 for 2-EH respectively. Among all the alcohols attempted in the present study, 2-EH showed interesting results in terms of low temperature properties and average molecular weight to maintain the viscosity and thermo-oxidative stability, therefore 2-EH was used for hydroxylation throughout the study.

Up on conducting hydroxylation experiments with 2-EH few observation are discovered in the sequence of adding the reactants (alcohol and sulphuric acid) to epoxidised cooking oil. In the first case catalyst was added (sulphuric acid) drop wise, followed by the addition of alcohol and vice-versa, in the second case catalyst and alcohol was pre mixed in a small beaker and added drop wise to epoxidised cooking oil. In first case, lower ring opening conversion was obtained, and this step demands higher reaction temperature and time. The sulphuric acid as a high acidic strength catalyst when added directly (drop wise) to

epoxidised cooking oil, catalyst was burning the epoxide, fatty acids and forming a micro crystals and reducing the catalytic activity by forming a solid crystals of epoxide reacted with sulfuric acid. Hence, the first case was demanding higher reaction temperature and time for complete conversion from oxirane ring to hydroxylated product (ring opened product).

Whereas, in the second case (pre-mix addition), within a short span of time (15 min) at room temperature 100% conversion was achieved. During the addition of 2-EH to sulphuric acid (dilution) it was found that both are completely soluble and thereby concentration of acid reduced, but not sulphuric acid strength, when this pre-mix acid and alcohol was added to epoxide, reaction took place in a short time span. Similar way experiments were carried out with different alcohols such as methanol, 1-butanol and 2-propanol having different molecular structure, weights and boiling points. During the pre-mixing phenomena it was also noticed that, catalyst (due to higher acid strength) is evaporating the alcohol due to its high acid strength, therefore it could be reasoned that a pre-mixing type of reaction is possible only with higher molecular weight alcohols such as 2-EH.

However, to find out the exact optimum condition for complete ring openings, preliminary studies were carried out with 2-EH as ring opening reagent using sulphuric acid as a catalyst, by varying one parameter at a time and keeping the other reaction variables (alcohol molar ratio, catalyst loading and reaction time) at a constant value. The results of sequential addition and pre-mix addition are shown in Figure 4.10. From the figure it can be seen that at 6 mol of 2-EH and 3 wt% of catalyst loading transesterification was not observed, but with further increase in the alcohol moles beyond 6 mol the rate of transesterification increases along with conversion (Figure A.8). The ring opening reaction was monitored by determining epoxy content and reaction was stopped when the OOC

content in the hydroxylated product was ≤ 0.01 mass%. Further, product was confirmed by FTIR spectra which indicates the disappearance of a epoxy group at 822 cm^{-1} and appearance of hydroxy peaks at 3450 cm^{-1} (Figure 4.11). Further, ring opening and % transesterification of hydroxylated WCO was calculated using ^{1}H-NMR spectra (Patchara and Supawan 2011). However, extent of transesterification was found to be less than 10% at 1, 2 and 3 wt% of catalyst loadings (Figure A.8). From the ring opening study, finally it could be concluded that 100 % ring opening can be accomplished at 10 mol of 2-EH, 3 wt% catalyst loading, 30 min reaction time and temperature as room temperature and this is the best reaction condition for complete ring opening of epoxides. During the hydroxylation with various alcohols, it was observed that, for 100% ring opening with an increase in the alcohols molecular weight, reaction time also increases. However, during the entire study, all the end products acid values were observed to be less than 0.5 mg KOH/g.

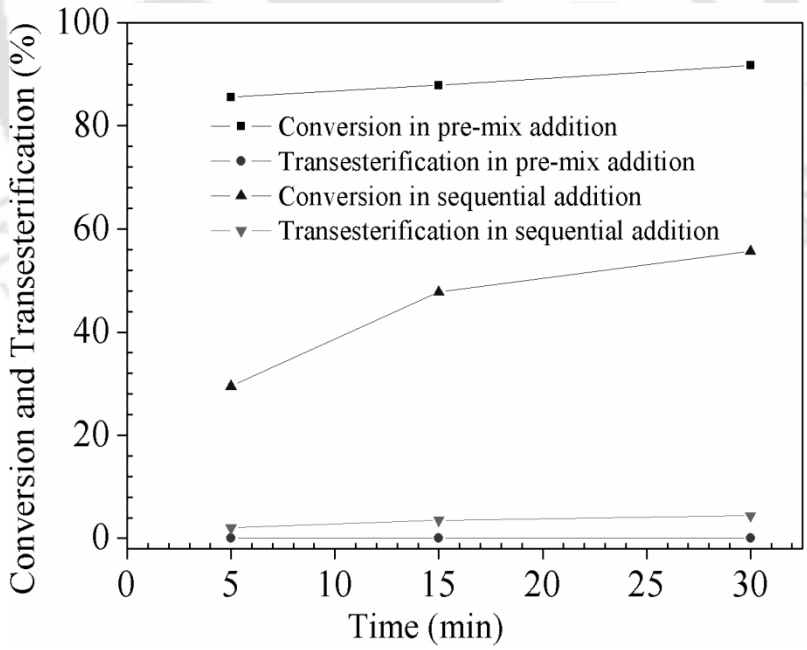

Figure 4.10: Conversion and transesterification outcomes of sequential and pre-mix addition for WCO at 6 mol of 2-EH, 3 wt% of H_2SO_4, at room temperature

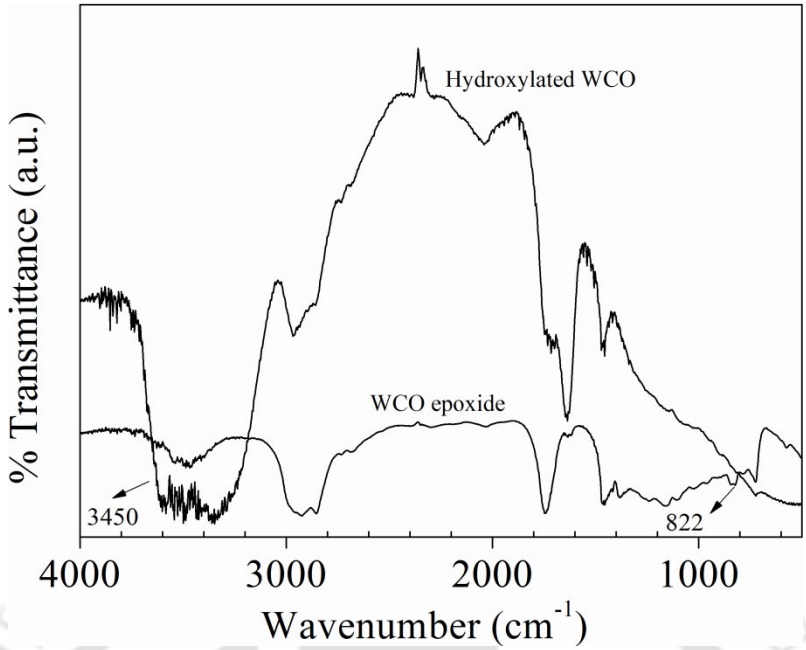

Figure 4.11: Product confirmations by FTIR spectra of WCO epoxide and hydroxylated product

4.5. Hexanoylation of resulting hydroxyl groups in the ring opened product

In order to improve the cold flow properties, the hydroxylated product was further reacted with hexanoic anhydride to functionalize the hydroxyl groups. The progress of hexanolyation at varied reaction conditions was monitored by withdrawing the aliquots of reaction mixture at every 1 h interval. During the course of reactions (Figure 4.12, Figure A.9), it was noticed that hexanoylation requires higher reaction temperature, lower anhydride molar ratio and catalyst loading. The formation of hexanoylated product was confirmed by FTIR spectroscopy. The disappearance of hydroxyl absorption band (at 3400 - 3500 cm^{-1}) and change in the relative intensities of 1725 cm^{-1} in the ester fingerprint region provided evidence of hexanoylation reaction. Among all the attempted reaction conditions, best reaction condition was found to be 2 mol of anhydride, 70 ^{o}C temperature, 2 wt% of catalyst loading and 9 h of reaction time. During the study it was observed that beyond 70 ^{o}C temperature end product turned into black color (poor product quality). Therefore, in order to

maintain the product quality and structural integrity of hexanoylated product the reaction temperature was limited to 70 ^{o}C.

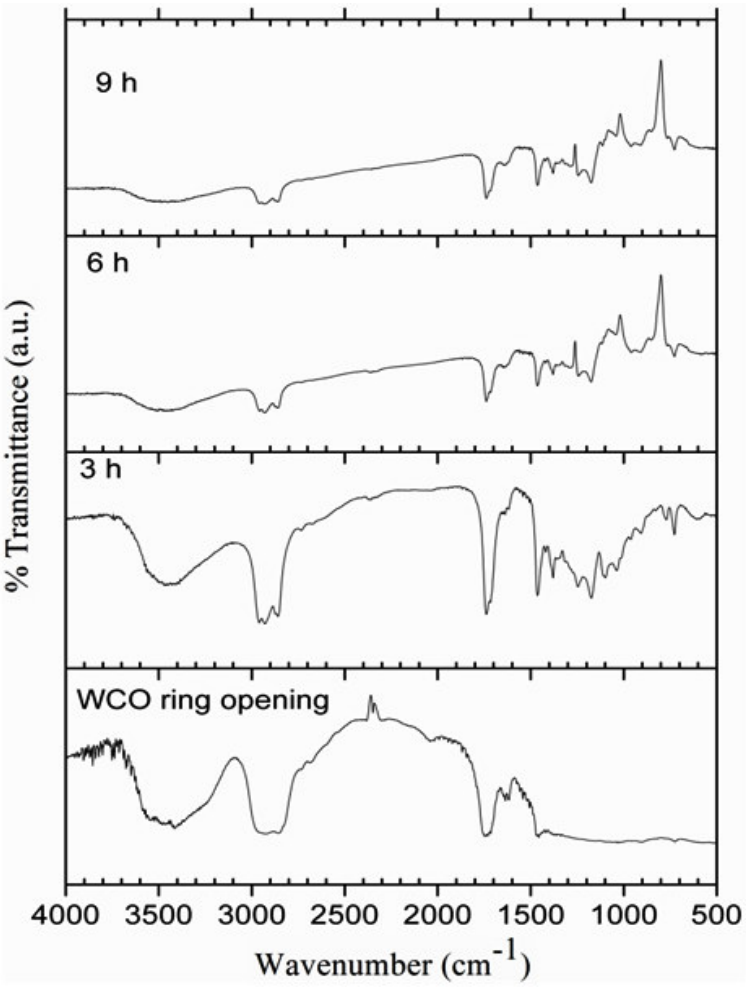

Figure 4.12: Product confirmations by FTIR spectra of various reaction conditions for hexanoylation of WCO hydroxylated product at 2 mol, 2 wt% and room temperature

4.6. Physico-chemical characterization of hydroxylated and hexanoylated derivatives from WCO

4.6.1 Product confirmation by NMR spectral analysis and GPC

The hydroxylation and hexanoylation reactions progress was closely monitored by analyzing the sample using FTIR and ^{13}C-NMR spectroscopy. From ^{13}C-NMR spectra (Figure 4.13 (a)) of WCO epoxide, the intense peak at δ 50 - 60 ppm indicates the presence of epoxy carbon in

the sample. After hydroxylation (Figure 4.13 (b)) disappearance of peaks at δ 50 - 60 ppm confirmed the transformation of oxirane ring into ring opened product. Further, functionalization of hydroxylated products with hexanoic anhydride was confirmed by appearance of high intense ester peak at δ 175 ppm and increased intensity of carbons at δ 20 - 40 ppm range (Figure 14.3(c)). The same was confirmed by FTIR spectra of WCO epoxide and hydroxylated product. Figure 4.11 shows the disappearance of epoxide peak at 824 cm^{-1} and appearance of broad hydroxyl peak at 3250-3700 cm^{-1} range which was earlier absent in the epoxide spectra.

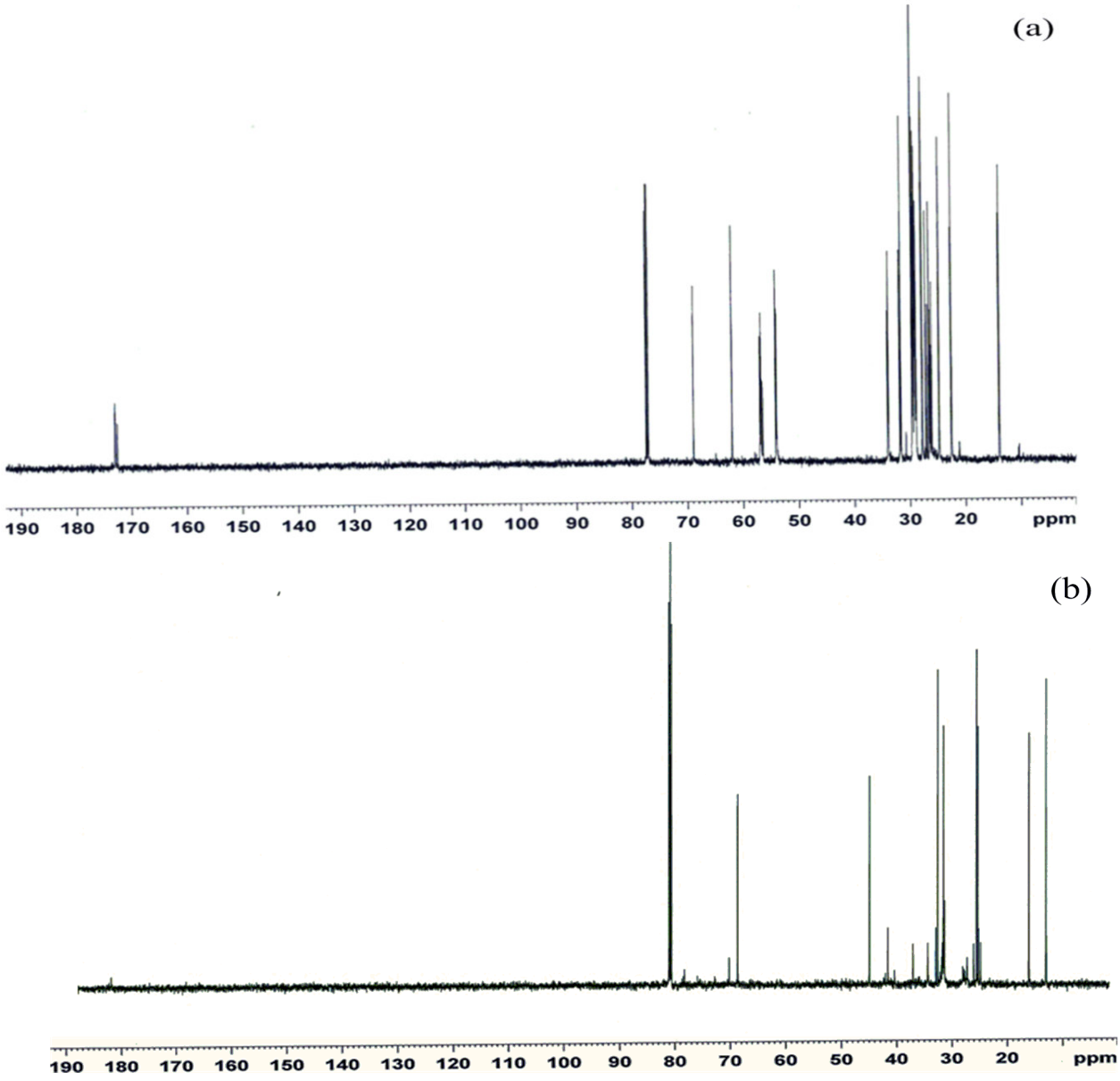

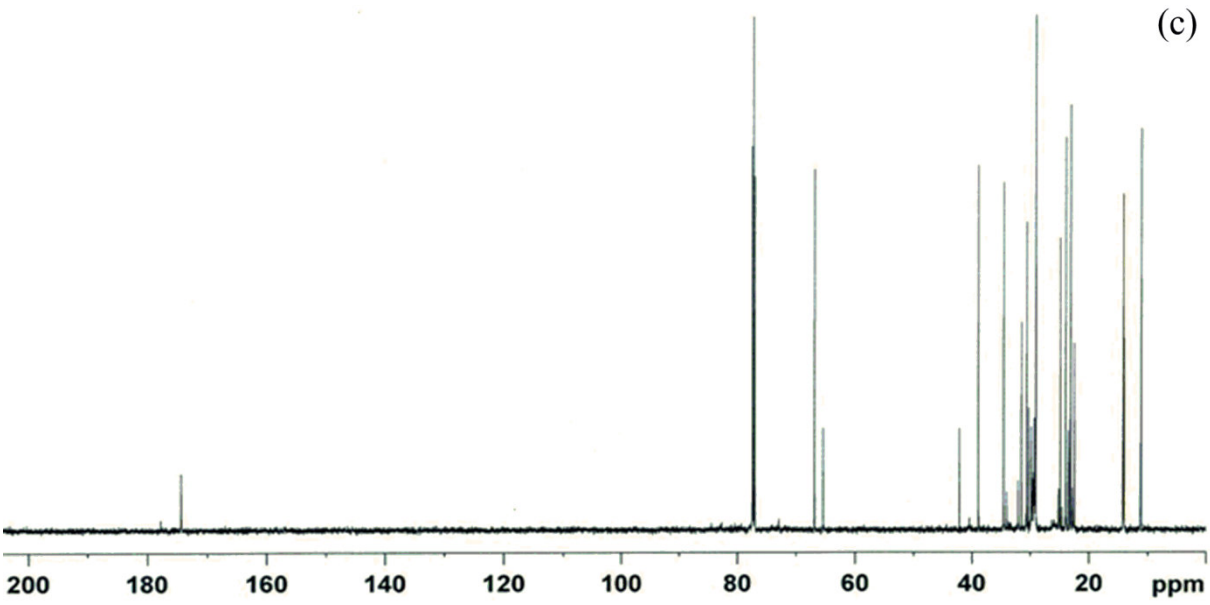

Figure 4.13: Product confirmation by ^{13}C-NMR spectra of WCO epoxide (a), hydroxylation (b) and hexanoylation (c)

Similarly, hexanoylation was confirmed by complete disappearance of hydroxyl groups at 3250-3700 cm^{-1} range and increased ester peak at 1725 cm^{-1} in FTIR spectra as shown in Figure 4.14. In addition to the product confirmation, functionalizations of the alcohol and anhydride groups are supported by determining the end products molecular weights using gel permeation chromatography (GPC). As reported in Table 4.7, molecular weight of hydroxylated and hexanoylated products were increased compared to the starting material (i.e. epoxide), which signifies that the functionalization is taking place in the fatty acid chain by extending the chain length and branching, thereby enhancing the PP of the functionalized products.

Table 4.7: Molecular weights of the WCO epoxide, hydroxylated and hexanoylated products

Sample	Number Avg. Mol. Wt.	Weight Avg. Mol. Wt.
WCO epoxide	945	1053
WCO hydroxylation	1528	1793
WCO hexanoylation	1740	1980

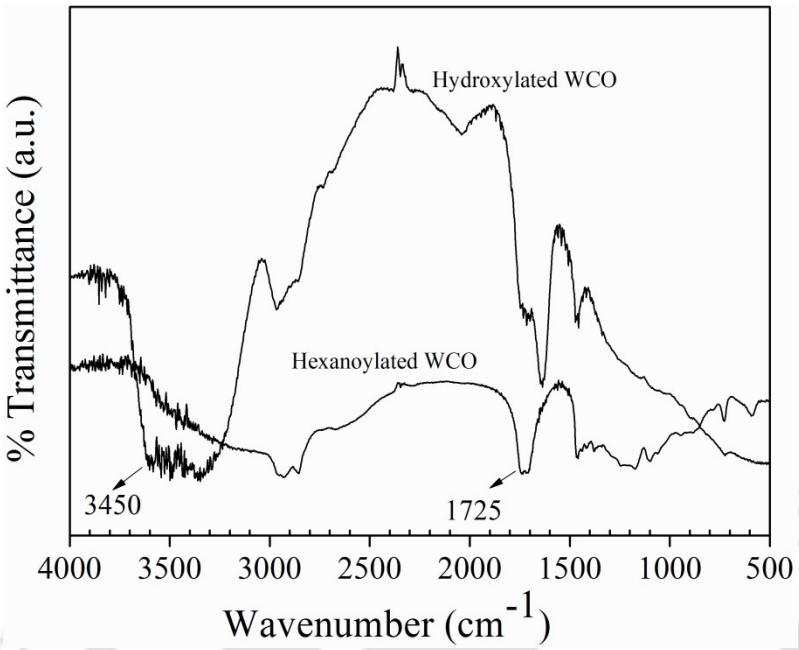

Figure 4.14: Product confirmation by FTIR spectra of WCO hydroxylation and hexanoylated product

4.6.2 Viscosity, viscosity index and rheological properties of prepared hydroxylated and hexanoylated products

As per the application part is concern rheology, viscosity and viscosity index plays a major role for all lubricant basestocks. Kinematic viscosity and viscosity index of prepared hydroxylated and hexanoylated products are evaluated and the results obtained are depicted in Table 4.8. From the table it was observed that with an increase in the branching (i.e. formation of mono-esters to di-esters) viscosity decreased and VI increased. Mahajan et al. (2013) also observed similar results during their study on chemically modified epoxidised mustard oil for bio-lubricant application. Viscosity index is the measure of change in viscosity with respect to temperature and it is very much dependent on attached terminal groups. As reported in Table 4.8, it was observed that viscosity decreases with functionalization, whereas viscosity index increases. Yao et al. (2010) claimed that, VI

increased with molecular weight and in the present study VI of WCO hydroxylated product is found to be 337.32, similarly for hexanoylated product it is found to be 127.98.

Table 4.8: Kinematic viscosity and viscosity index of hydroxylated and hexanoylated products

Sample	Kinematic Viscosity (cSt)		Viscosity Index
	@40 °C	@100 °C	
WCO epoxide	282.38	33.33	162
WCO hydroxylation	29.63	9.65	337.32
WCO hexanoylation	10.57	2.9	127.98

The rheological behavior of used cooking oil derived di-esters determined using interfacial rheometer by varying the shear rate (0 – 500 S^{-1}) at various temperature (25, 40, 60, 80 and 100 °C) is presented in Figure 4.15 (a) and (b). From Figure 4.15 (a) it can be seen that in spite of temperature variations, shear stress vs. shear rate relation was found to be linear and signifies Newtonian fluid behaviour and Figure 4.15 (b) shows that sample viscosity decreased with an increase in the temperature which is due to the higher thermal movement among molecules

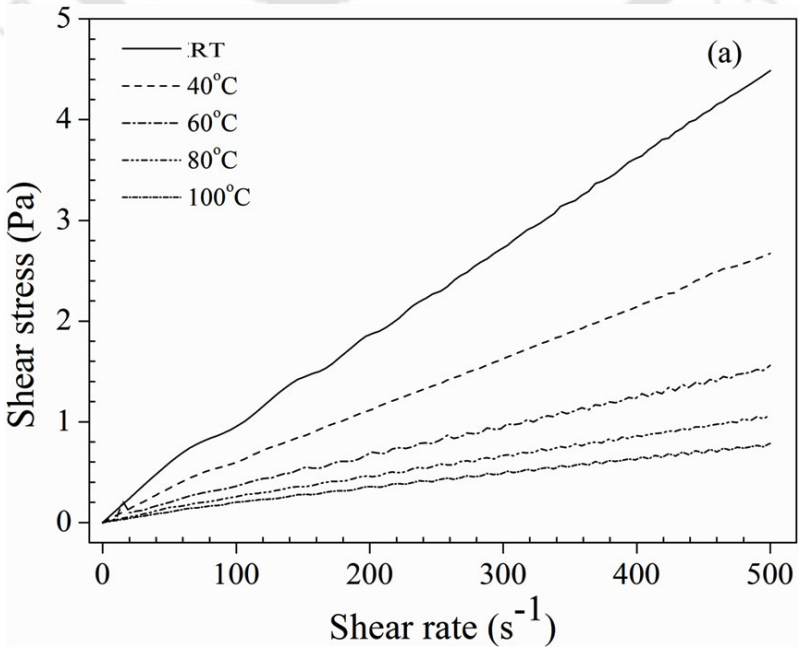

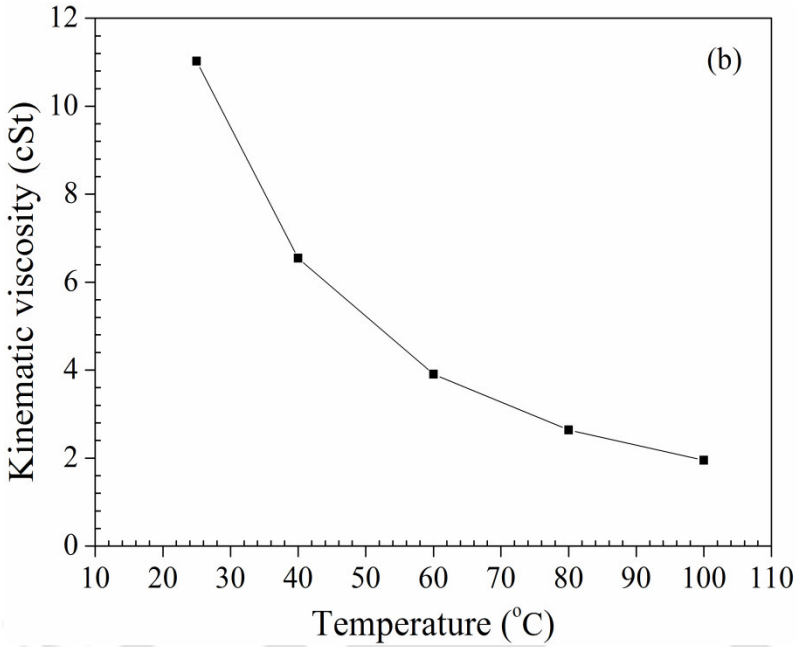

Figure 4.15: Shear stress versus shear rate (a) and temperature versus kinematic viscosity (b) relation for WCO derived di-esters

4.6.3 Determination of thermo-oxidative stability of hydroxylated and hexanoylated products

The thermal and oxidative stability of prepared hydroxylated and hexanoylated product was determined by measuring the onset and oxidative onset temperature in nitrogen and oxygen atmospheres using TG analysis technique. The higher onset and oxidative onset temperature suggest better thermal and oxidative stability (Figure 4.16). The DTG plot of hydroxylated product which contains traces of 2-EH showed two stage decomposition pattern, which indicates the presence of un-reacted 2-EH (18 wt%) in hydroxylated product. Therefore, for further purification of hydroxylated product, a short path distillation column technique was followed to remove the traces of 2-EH in the sample. The purified sample was then subjected to TG analysis and almost single stage degradation was noticed from TGA/DTG thermo-grams (Figure 4.16). However, even after removal of 2-EH by short path distillation column, small peak was detected in the DTG thermo-gram of hydroxylated product, which signifies the presence (2%) of 2-EH, similar kind of result was encountered with hexanoic anhydride.

This trace level of hexanoic anhydride and 2-EH in the end product (around ≤ 2 wt%), might show negligible effect during the performance. The thermo-oxidative stability, peak temperatures (maximum degradation temperatures) of hydroxylated and hexanoylated products (Figure A.10) obtained during TG analysis of used cooking oil are reported in Table 4.9. From the stability results it could be concluded that as the branching increases (from mono esters to di-esters) stability of the sample decreases and similar observation was reported by Guo et al. (2011) during oxirane cleavage of epoxidised palm oil.

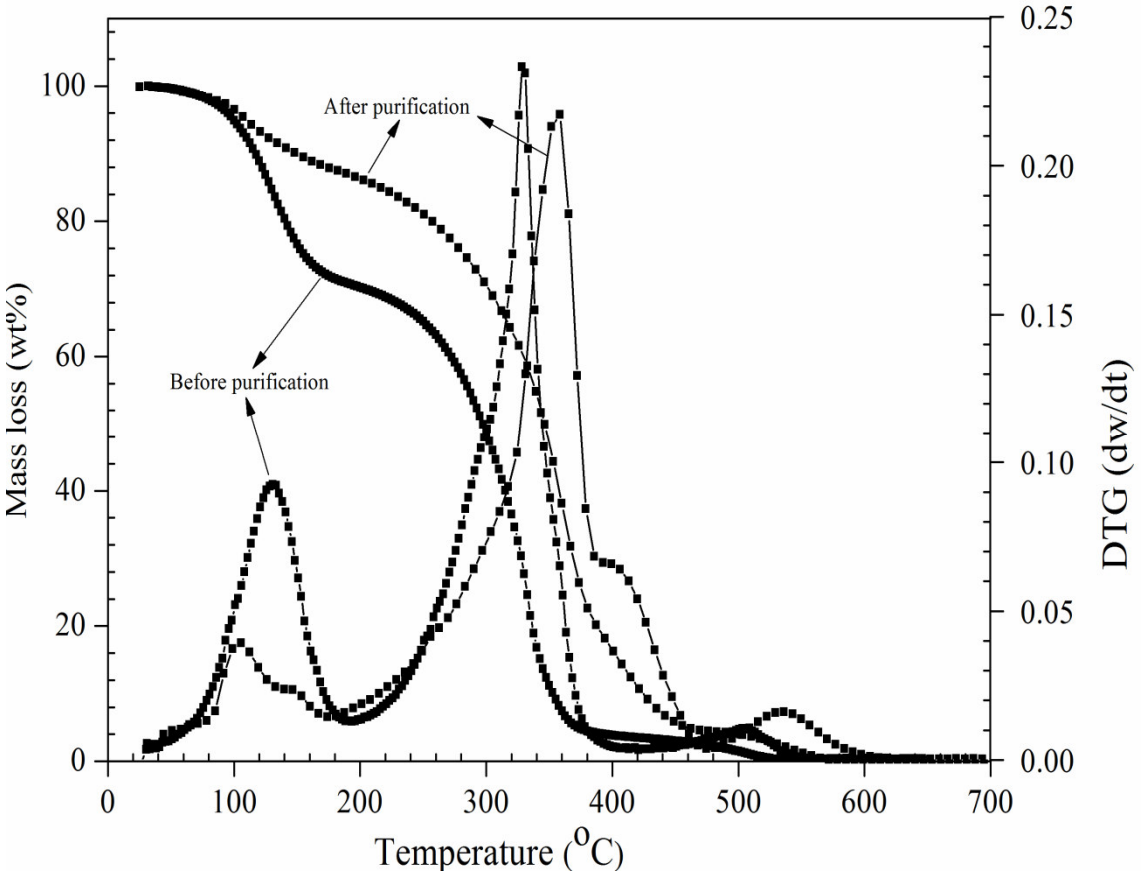

Figure 4.16: TG/DTG thermo-grams of WCO ring opened product, before and after purification

Table 4.9: Onset temperature (OT), oxidative onset temperature (OOT), peak temperatures (PT) and pour point temperatures of prepared hydroxylated and hexanoylated products

Sample	Thermal stability (^{o}C)		Oxidative stability (^{o}C)		Pour Point (^{o}C)
	OT	PT	OOT	PT	
WCO hydroxylation	325.5	361.1	239.3	279.3	-14.93 ± 0.61
WCO hexanoylation	286.3	326	230.7	270	-28.45 ± 0.25

4.6.4 Low temperature study

The low temperature properties of bio-lubricant basestocks are monitored by measuring the sample's PP and CP. As reported in the literature unmodified plant seed oils can't be used at sub-zero temperatures due to their poor cold flow behavior (Mahajan et al. 2013; Kamalakar et al. 2014; Borugadda and Goud 2013, 2014b). Therefore, structural modification of plant seed oils is an essential step to prepare good quality bio-lubricant basestock. Castro et al. (2006) reported that branching on the fatty acid chains improves the cold flow properties. In their work modification was carried out by the attachment of oxygen, alkyl group of 2-EH and ester group from hexanoic anhydride at the midst of fatty acid chains as shown in Scheme A.2. Further, Hwang and Erhan (2001) disclosed that the addition of ester side chain at 9 or 10 position of fatty acid chain could enhance the PP significantly. In the present study pour point of used cooking oil epoxides was estimated to be -6.2 ^{o}C, further hydroxylation and hexanoylation (Figure 4.17) of epoxide products results in much better PP (Table 4.9). The functionalization of 2-EH and hexanoic anhydride to the fatty acid chains demonstrated the most effective reduction in PP and this could be attributed to the presence of a large branching group at the mid-point of a fatty acid chain, that makes a steric barrier around individual molecules and suppresses crystal growth which resulted in lower PP of the sample (Table 4.9).

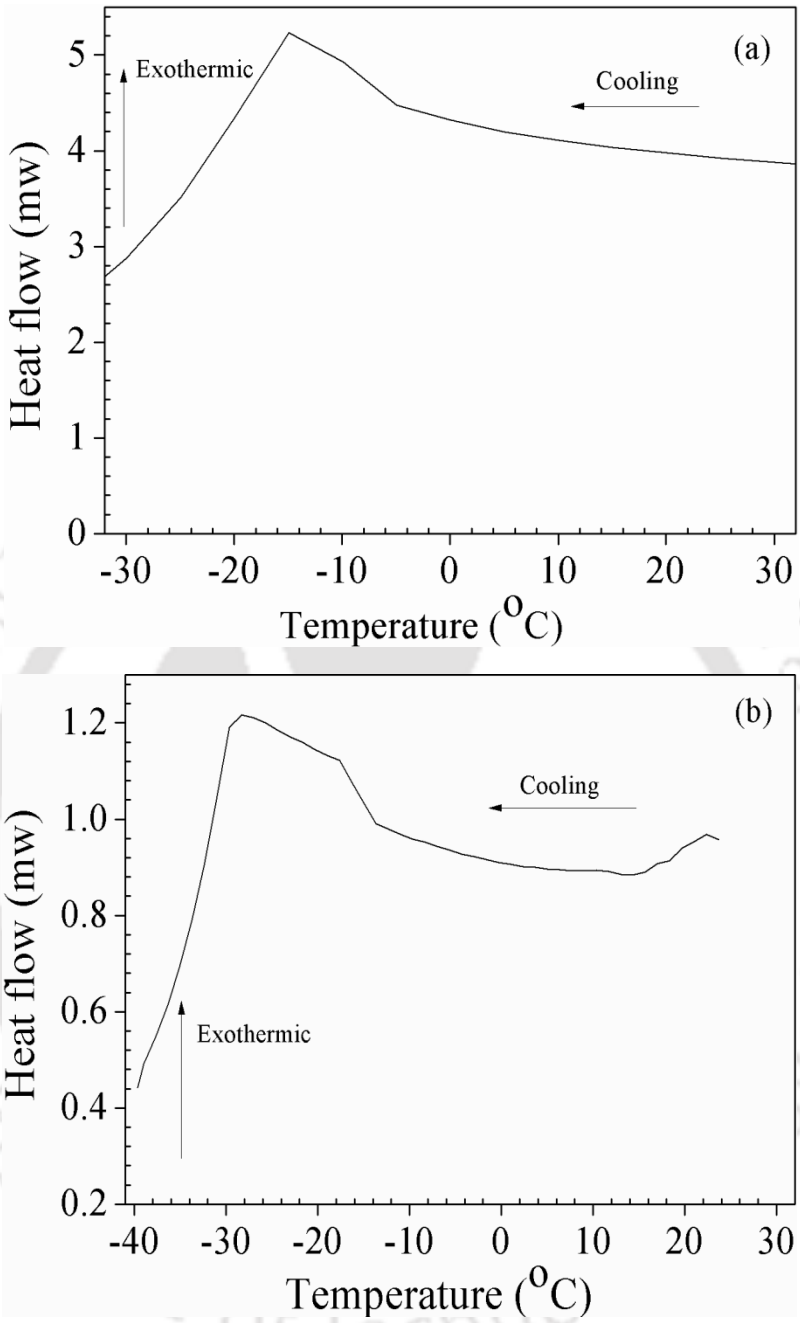

Figure 4.17: DSC thermo-grams for WCO hydroxylation (a) and hexanoylation (b)

4.6.5 Tribological measurements

The anti-wear and friction reducing properties of prepared di-esters was evaluated using HFRR lubricity tester. The HFRR method decides the ability of prepared di-esters to affect friction and wear between the surfaces in relative motion under a load. During the test average wear scar diameter of 232 µm (x-axis-272 µm, y-axis-192 µm, Figure 4.18), film

thickness of 15% and co-efficient of friction (CoF) 0.08 was noticed. From these outcomes it could be observed that branching of 2-EH and hexanoic anhydride derivatives could enhance the wear scar diameter (WSD), which results in improved tribological performance. In addition to that, hydroxyl and ester functionalities at 9 and 10 carbon positions of the fatty acid chain assist di-esters compounds stick to the metal surface and reduce friction. The dynamic branching structure of di-esters compounds initiates working for the metal to metal contact process and molecules formulated anti frictional film, thereby reducing friction and wear (Madankar et al. 2013). Similarly, lower CoF could be due to the higher viscosity of the sample after structural modification.

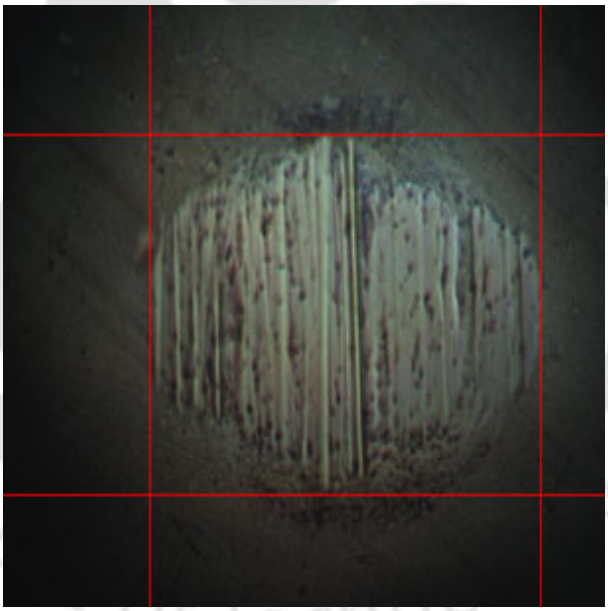

Figure 4.18: Microscopic wear scar image for WCO derived di-ester

4.6.6 Biodegradability study

Bio-kinetic model was used as per ASTM D 7373-12 to evaluateing the effective composition to biodegradation (ECB) and predicts the cumulative biodegradation of prepared di-esters. The estimated biodegradation profile of duplicate tests run carried out for used cooking oil di-esters was found to be 93.67 % ± 2.13. From the biodegradability test it

was found that the prepared di-esters are biodegradable and showed good reproducibility among the duplicate test runs. The cumulative biodegradation of used cooking oil derived di-esters was found to be 1.06.

4.7. Summary

This chapter dealt with the series of structural modifications (epoxidation, ring opening and hexanoylation) carried out to the unsaturated fatty acids present in the waste cooking oil. The optimization was carried out for WCO epoxidation reaction for maximum epoxide content; further preliminary studies were carried out for the hydroxylation and hexanoylation to establish the optimum conditions. After each chemical modification, significant physico-chemical properties were estimated, main emphasis was on the performance limitations of the feedstocks. The outcomes of WCO epoxidation reaction revealed that the epoxide product exhibits superior oxidative stability than WCO, whereas thermal stability and PP was found to be low. Therefore, to improve the PP functionalization of 2-EH and hexanoic anhydride was carried out. The thermal onset, oxidative onset and PP temperatures of WCO hexanoylated products were found to be 286.3 ^{o}C, 230.7 ^{o}C and -28.45 ± 0.25 ^{o}C respectively. Among all the performance limitation properties studied in this chapter, only the cold flow property i.e. pour point showed improvement after functionalization (WCO - (-8.6 ± 0.32 ^{o}C) and WCO hexanoylation-(-28.45 ± 0.25)), whereas thermo-oxidative stability was found to be decreased. Nevertheless, all the products derived from WCO showed potential applications in various fields compared to conventional lubricants. Further the comparative evaluation of thermo-oxidative stability and cold flow properties of lubricant basestocks prepared in the present study with conventional hydraulic lubricants are clearly described in Chapter-8.

CHAPTER-5

Modifications to waste cooking oil fatty acid methyl esters for production of bio-lubricant basestocks

Unlike the previous chapter, this chapter also studied the chemical modifications of various unsaturated fatty acids present in the WCOFAME, after the removal of glycerol in its fatty acid structure. Initial sections of this chapter discussed the optimization of WCOFAME epoxidation, validation of the model and evaluation of significant physico-chemical properties of the epoxide at an optimum condition. Main emphasis was on the performance limitation properties of esters for their usage as bio-lubricant basestocks. Outcomes of the thermo-oxidative stability and cold flow properties (performance limitation properties) revealed that, thermo-oxidative stability was enhanced, but the PP obtained was higher after epoxidation. Therefore, further to enhance the PP, WCOFAME epoxide was functionalized with 2-EH and hexanoic anhydride. Admirable thermo-oxidative stability and cold flow properties were found for hydroxylated, hexanoylated WCOFAME derived products with excellent biodegradability of di-esters.

5.1. Optimization of WCOFAME epoxidation

In order to optimize the WCOFAME epoxidation process parameters, preliminary analysis was carried out for four process variables by single factor optimization technique (Figure 5.1), the optimum range of each process variable is known and reported in Table 5.1. Depending on the preliminary studies data (Table 5.1, Figure 5.1) experimental matrix was generated based on CCD and presented in (Table A.2). All 30 designed experimental runs were executed at laboratory conditions, and results were analyzed by multiple regression analysis and shown in Table A.2. Further, ANOVA technique was considered to explore the

entire optimization process to construct a relationship between response variable OOC and input process variables for maximum OOC. Through ANOVA a quadratic polynomial equation obtained from the experimental data to predict the higher epoxide content in terms of coded variables is presented in Equation 5.1.

$$\text{Response (OOC)} = 5.833 - 0.013\,A - 179\,B + 0.11\,C + 0.4\,D - 0.108\,AB + 0.036\,AC - 0.216\,AD - 0.029\,BC - 0.185\,BD - 0.018\,CD - 0.193\,A^2 - 0.418\,B^2 - 0.433\,C^2 - 0.149\,D^2 \quad (5.1)$$

Results of a second order response surface model in the form of ANOVA for the maximum epoxide content are summarized in Table 5.2. It can be seen that F-value of the model is found to be 3385.9, and corresponding p-value (prob > F) is very small, i.e. < 0.0001 indicates that the model is highly significant. The p-values are adopted as a tool to ensure the significance of each co-efficient in the model. In this study, the main linear effects of temperature (B), hydrogen peroxide molar ratio (C) and catalyst loading (D); cross and quadratic effects of all the four process variables (i.e. AB, AC, AD, BC, BD, A^2, B^2, C^2 and D^2) are highly significant since p-value is < 0.0001. Similarly, rest of the linear variable time (A), cross variable hydrogen peroxide molar ratio and catalyst loading (CD) are also significant, since p-values are lying in between 0.002 and 0.001. In the present model, the absence of insignificant parameters indicates that all the linear, cross and quadratic terms are highly considerable and are playing a major role to maximize epoxide content. The lack of fit F-value of 5.65 indicates that lack of fit is considerably significant relative to the pure error, and this signifies that the model is extremely accurate without any noise, and the results are reproducible. Furthermore, observed (actual) values are very close to the predicted values as shown in Figure 5.2.

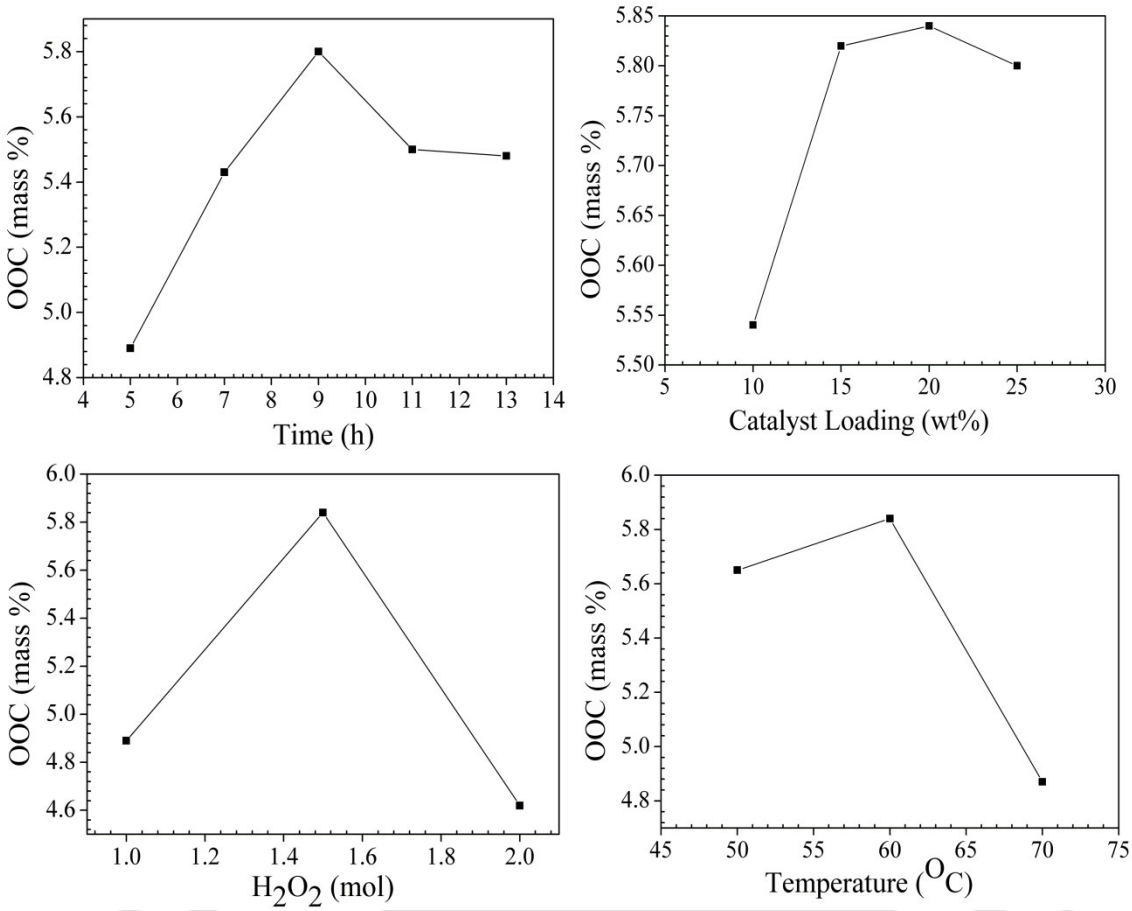

Figure 5.1: Effects of reaction variables time, catalyst loading, hydrogen peroxide and temperature on epoxidation of WCOFAME (preliminary studies)

Table 5.1: Independent process variables and their optimum levels for WCOFAME epoxidation

Independent Variables			Variable Levels		
	Symbol	Unit	-1	0	+1
Time	A	h	7	9	11
Temperature	B	^oC	50	60	70
Hydrogen Peroxide	C	mol	1	1.5	2
Catalyst Loading	D	wt%	10	20	30

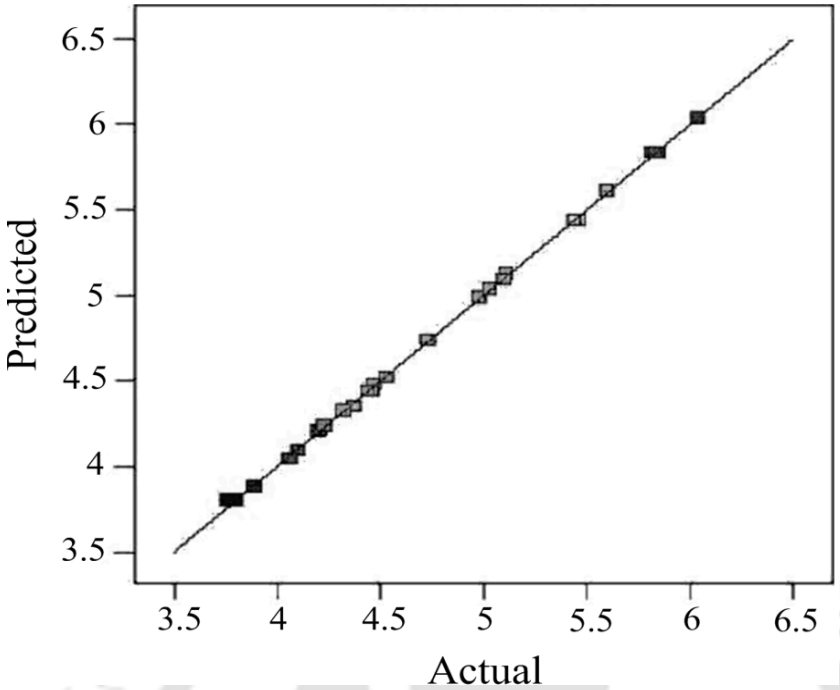

Figure 5.2: Predicted versus actual plot of response (OOC) for WCOFAME epoxide

The precision of a model was evaluated by the regression co-efficient i.e. R^2. For a good statistical model, R^2 value should be close to 1. The regression value for maximum epoxide content is presented as 0.9996, which is close to 1, and this signifies that the 99.96% model behavior can be interpreted for higher epoxide content, while only about 0.04% of the full variance can't be explained by the model. This represents that accuracy and the general ability of a polynomial model is good. The predicted R^2 value 0.9996 is reasonably co-ordinating with the adjusted R^2 0.9993, which had recommended prominent co-relational statistics between experimental and predicted values. Therefore, the regression model provides an excellent explanation of relationship between the independent process variables and the response variable.

Table 5.2: Regression co-efficients of the predicted, quadratic polynomial model for response variable (OOC) for epoxidised WCOFAME

Source	Sum of Squares	Degrees of Freedom	Mean Square	F Value	p-value (prob > F)
Model	15.39114	14	1.099367	3385.909	< 0.0001
A-Time	0.004537	1	0.004537	13.97492	0.0020
B-Temperature	0.774004	1	0.774004	2383.833	< 0.0001
C-H_2O_2	0.292604	1	0.292604	901.1832	< 0.0001
D-Catalyst Loading	3.848004	1	3.848004	11851.36	< 0.0001
AB	0.187056	1	0.187056	576.1092	< 0.0001
AC	0.021756	1	0.021756	67.00645	< 0.0001
AD	0.752556	1	0.752556	2317.776	< 0.0001
BC	0.013806	1	0.013806	42.52147	< 0.0001
BD	0.551306	1	0.551306	1697.952	< 0.0001
CD	0.005256	1	0.005256	16.18857	0.0011
A^2	1.021907	1	1.021907	3147.343	< 0.0001
B^2	4.792907	1	4.792907	14761.54	< 0.0001
C^2	5.14305	1	5.14305	15839.93	< 0.0001
D^2	0.611157	1	0.611157	1882.286	< 0.0001
Lack of Fit	0.004475	10	0.000447	5.659781	0.0348
Pure Error	0.000395	5	$7.91*10^{-05}$		
R^2	0.9996				

5.2. Influence of the process variables to maximize OOC

In order to decide the best reaction condition under which epoxidation was favourable for maximum epoxide content, the linear, cross and quadratic effect of process parameters on response was examined. The factorial design consists of sixteen factorial points; eight axial points, six replicates at the central level. Three dimensional (3D) response surface plots and two dimensional (2D) counter plot are graphical representation of the regression equation, which was received from the design expert software (trial version 8.0.7.1, Stat-Ease, Inc., MN, USA) to understand the interaction between the process variables. These plots were drawn by varying two process parameters at a time while keeping others at a central level (0). Statistical analysis of the process was executed to assess the analysis of variance and p-test.

5.2.1 Effect of time (A) and temperature (B)

Figure A.11 (a) and (b) describes the interactive effects of time and temperature on maximum epoxide content. From Figure A.11 (a) and (b), it could be observed that with an increase in reaction time from 7 h to 13 h, oxirane content was increased (5.8 mass%) up to a certain time period, i.e. 9 h and beyond which oxirane content decreased. The decrease in OOC can be attributed to the fact that higher reaction time results in the oxirane cleavage. Similarly, temperature was varied from 50 to 80 ^{o}C to understand the effect of temperature on OOC with respect to time. The results showed in Figure A.11 (a) and (b) revealed that OOC increased with an increase in temperature up to 60 ^{o}C and decreased thereafter. A careful analysis of the figure also reveals that higher temperatures favor the conversion of unsaturation to OOC, but also lead to increased oxirane cleavage, which is not favorable commercially. The behaviour of 2D and 3D figures revealed that higher temperature and longer reaction time lead to decrease the OOC (Niederhauser and Koroly 1949). The

optimum OOC of 6.04 mass% was obtained at medium temperature 60 ^{o}C and 9 h of reaction time.

5.2.2 Effect of time (A) and hydrogen peroxide molar ratio (C)

The sensitivity of response to interacting variables (time and hydrogen peroxide molar ratio) can be examined by 3D graphs while holding the other variables at central level (temperature (B), catalyst loading (D) at 60 ^{o}C, 20 wt%). The influence of two different process variables on the response (i.e. OOC) is shown in 3D response surface plot, and 2D counter plots (Figure A.12 (a) and (b)). From figure (Figure A.12 (a) and (b)), it can be seen that OOC increased almost linearly with the hydrogen peroxide molar ratio. Although the maximum conversion of double bonds to oxirane ring was achieved at 1.5 mol of H_2O_2, but this ratio also tends to destroy the oxirane ring when reaction was prolonged for longer reaction time (Borugadda and Goud 2014a). For a lower H_2O_2 molar ratio (Table A.2, Run No 21), the maximum OOC and rate of epoxidation was considerably low as compared to that obtained at 1.5 molar ratio and similar findings were noticed and patented by Niederhauser and Koroly (1949) during their study on esters of oleic and linoleic fatty acids. This may be attributed to an insufficient amount of H_2O_2 in the reaction mixture to transform the unsaturation content into epoxide. On the other hand, higher molar ratios of H_2O_2 assist the OOC to form undesirable by-products. In addition, Meshram et al. (2011) reported that epoxide formed at 1.5 hydrogen peroxide molar ratios contributed better stability; therefore, 1.5 mol of H_2O_2 to unsaturation was considered as the optimum molar ratio for further experimentations.

5.2.3 Effect of time (A) and catalyst loading (D)

Figure A.13 (a) and (b) shows the combined effect of varying catalyst loading and reaction time on maximum OOC. Increase in the catalyst loading from 0 to 40 wt% leads to a linear

increase in the OOC from 5 to 6.04 mass%. These findings were ascribed to the availability of active surface area of the catalyst which enhances the rate of peracetic acid formation thereby oxirane content. However, more catalyst loading aroused additional problems of agitation and decreased the mass transfer rate; hence, higher catalyst loading lowers the OOC. Sun et al. (2009) during their study observed limitation in mass transfer with the use of excess catalyst in the reaction mixture. Further, higher catalyst loading and reaction time provides the platform for oxirane rings to react with excess catalyst, acetic acid and by-product water formed during epoxidation (Sun et al. 2009).

5.2.4 Effect of temperature (B) and hydrogen peroxide molar ratio (C)

The effect of reaction temperature and substrate ratio (mol ratio of H_2O_2/C=C-bonds) on maximum oxirane content was investigated. The reactions at various molar ratios (0.5, 1, 1.5, 2 and 2.5) were performed at five different temperatures (40, 50, 60, 70 and 80 ^oC). From Figure A.14 (a) and (b), it is evident that, with an increase in the reaction temperature epoxide content was found to increase linearly. However, maximum epoxide content (6.04 mass%) was noticed at 60 ^oC at reaction time of 9 h. From Figure A.14 (a) and (b), it can also be also noticed that further increased in the temperature beyond 60 ^oC, the OOC content found to decrease. Therefore, epoxidation at higher temperatures (> 60 ^oC) acts as a medium to open oxirane ring (Meshram et al. 2011). Likewise, with an increase in the hydrogen peroxide molar ratio from 0.5 to 2.5 mol, OOC was found to be increased up to 1.5 mol ratio. However, beyond 1.5 molar ratio OOC decreased due to excess H_2O_2 concentration which can leads to oxirane cleavage. Therefore, to obtain the maximum oxirane, medium level of H_2O_2 concentration and temperature should be used where both the effects were optimized.

5.2.5 Effect of temperature (B) and catalyst loading (D)

The influence of catalyst loading, temperature and their combined interaction on epoxidation at constant H_2O_2 molar ratio and reaction time was represented by the 3D response surface plot and its corresponding 2D contour plot in Figure A.15 (a) and (b). From figure (Figure A.15 (a) and (b)), it can be depicted that OOC increased with an increase in the temperature and catalyst loading, this fact indicates that both the variables had significant interaction between each other, but decrease the OOC beyond 60 ^oC. From the preliminary studies, it was noticed that the optimum value for the maximum OOC lies somewhere in between 20 - 30 wt% catalysts loading. But during the optimization experiments, 40 wt% catalysts loading showed maximum OOC as 6.04 mass%. This may be attributed to the different interaction effects of process variables during the preliminary studies and optimization experiments. From Figure A.15 (a) and (b), increased OOC can be observed with an increase in the temperature and catalyst loading from 50 - 60 ^oC and 0 to 40 wt% respectively. Further, increase in the temperature and catalyst loading resulted in decreased OOC. Finally, from the interaction of these variables it can be seen that medium reaction temperature was favourable for maximum oxirane formation. However, at higher temperatures OOC decreases, which indicates that the reaction temperature had a negative interaction effect with increased catalyst loading. These observations were in agreement with the results shown in Figure A.15 (a) and (b).

5.2.6 Effect of hydrogen peroxide molar ratio (C) and catalyst loading (D)

Figures A.16 (a) and (b) demonstrates the effect of hydrogen peroxide molar ratio and catalyst loading on the course of oxirane formation at various catalyst loadings and H_2O_2 molar ratios. It was anticipated that with an increase in catalyst loading and hydrogen peroxide molar ratio peracetic acid formation increases. As discussed in the aforementioned sections, higher catalyst loading and H_2O_2 molar ratio showed the negative effect on epoxide

content and same behavior has been noticed during this interaction as well. Thus, the experimental range explored in this work, furnished the optimum condition at 1.5 moles of hydrogen peroxide per mol of ethylenic unsaturation and 40 wt% catalysts loading. Petrovic et al. (2002) reported that higher hydrogen peroxide molar ratio resulted more oxirane cleavage, and same behavior was noticed in the present study.

5.2.7 Attaining optimal conditions, model validation and confirmation

Optimization was performed based on desirability function to determine the optimal synthesis conditions for maximum OOC. The optimum conditions to maximize OOC was found to be substrate ratio 1.72 mol, catalyst loading 28.17 wt%, reaction time 7.51 h and reaction temperature 53.71 ^{o}C. The optimum solution was selected from the proposed multiple solutions given by RSM optimization tool. The anticipated maximum OOC from the model at this condition was 6.04 mass%. The model verification was done by conducting the experiments in triplicate at identical condition and the maximum OOC of 5.8 mass% was obtained. The good agreement between the model predicted, and experimental value of OOC confirmed that the formulated model was believed to be precise and authentic.

5.3. Physico-chemical characterization of prepared WCOFAME epoxide product

In the present section, various spectral analysis techniques such as FTIR, NMR are discussed in detail to confirm the epoxide product. Similarly, cold flow properties, thermo-oxidative stability, catalyst re-usability and physico-chemical characterization of the WCOFAME and its epoxide are discussed in detail and compared. Finally, rheology of the WCOFAME epoxide also studied in order to determine its flow behaviour and all the analytical procedures are clearly described in Chapter-2.

5.3.1 FTIR spectroscopy

FTIR spectroscopy is an appropriate and sensitive technique to monitor the WCOFAME epoxidation process (Lee et al. 2009). WCOFAME FTIR spectra is also identical to the WCO epoxide FTIR spectra as shown in Figure 4.3, the characteristic peak in the range 3002 - 3008 cm^{-1} attributed to the stretching of double bonds (i.e. unsaturation). Further, similar findings were observed for WCOFAME epoxidation as well. The complete disappearance of the double bonds signifies that almost all the double bonds are converted in to epoxy group via epoxidation. The new peaks at 838 cm^{-1} attributed to epoxy group and alike results were also reported in the literature (Sharma et al. 2008a). Lee et al. (2009) reported that FTIR was not only practised to confirm the formation of epoxy product, but also to monitor the potential side reactions, i.e. ring opening (esterification or hydroxylation). Meyer et al. (2008) described that via oxirane ring opening reaction; -OH functional groups can be derived from epoxy groups. In this study, WCOFAME epoxide spectra exhibited with no trace of -OH absorption peak approximately at 3000 - 3500 cm^{-1}, which indicates that no oxirane cleavage was observed during epoxidation (Figure 4.3).

5.3.2 Product confirmation by NMR spectroscopy

The proton (^{1}H-NMR) spectroscopy was one of the significant spectral techniques to identify the products and to monitor reaction progress. The ^{1}H-NMR spectrum of WCOFAME and its epoxide is shown in Figure 5.3 (a) and (b). The disappearance of olefinic hydrogen (δ 5.299 - 5.388 ppm range) bond in the WCOFAME epoxide spectra suggests that unsaturation was converted into epoxide. Likewise, the corresponding formation of epoxide product (-CH-O-CH-) peak at δ 2.868 - 3.109 ppm range was noticed in the WCOFAME epoxide spectra which was absent in WCOFAME. From Figure 5.3 (b), it can be also pointed out that disappearance of unsaturation content ensures the complete conversion of double bonds in to

epoxide as discussed in the FTIR study. Further, characterization of epoxide products by ^{1}H-NMR revealed that no oxirane cleavage occurred during the epoxidation, i.e. no extra peaks were observed at δ 3.4 - 4 ppm region. Whereas, in both the spectra (Figure 5.3 (a) and (b)) singlet was observed at δ 3.6 ppm along with very tiny peaks on the either side of the singlet which signifies methyl esters peak and apart from that no other peaks are noticed in this region. Finally, from ^{1}H-NMR spectra of epoxide conversion is verified and confirmed.

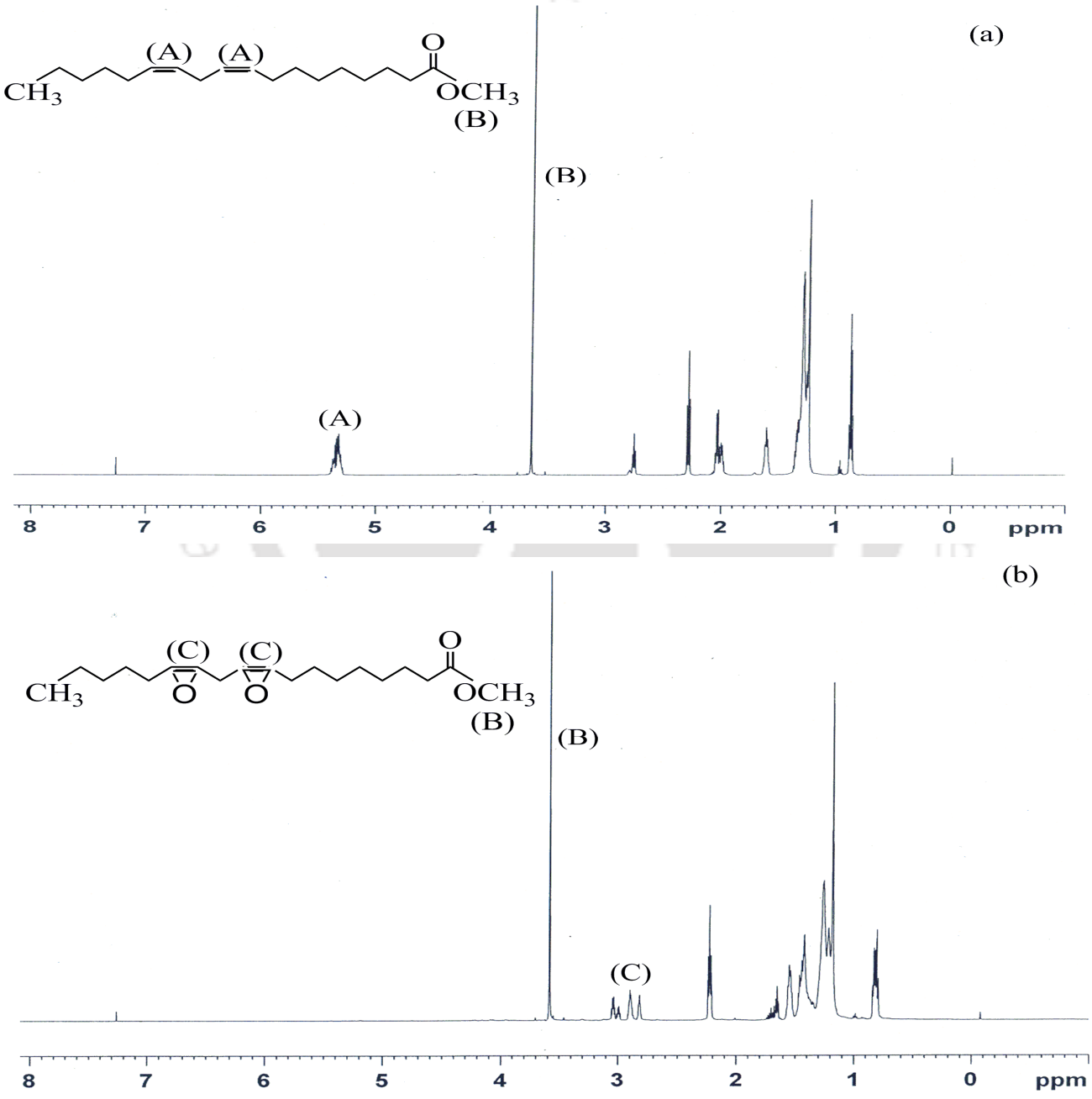

Figure 5.3: ^{1}H-NMR spectrums of WCOFAME (a) and its epoxide (b) represented by linoleic acid

Similarly, ^{13}C-NMR spectra of WCOFAME and its epoxide are shown in Figure 5.4 (a) and (b). Figure 5.4 (b) ^{13}C-NMR spectra showed the complete removal of olefinic carbons between δ 125 - 135 ppm range in the epoxide product and the additional peaks at δ 53 - 59 ppm are absent in WCOFAME spectra (Figure 5.4 (a)), which belongs to epoxy carbons.

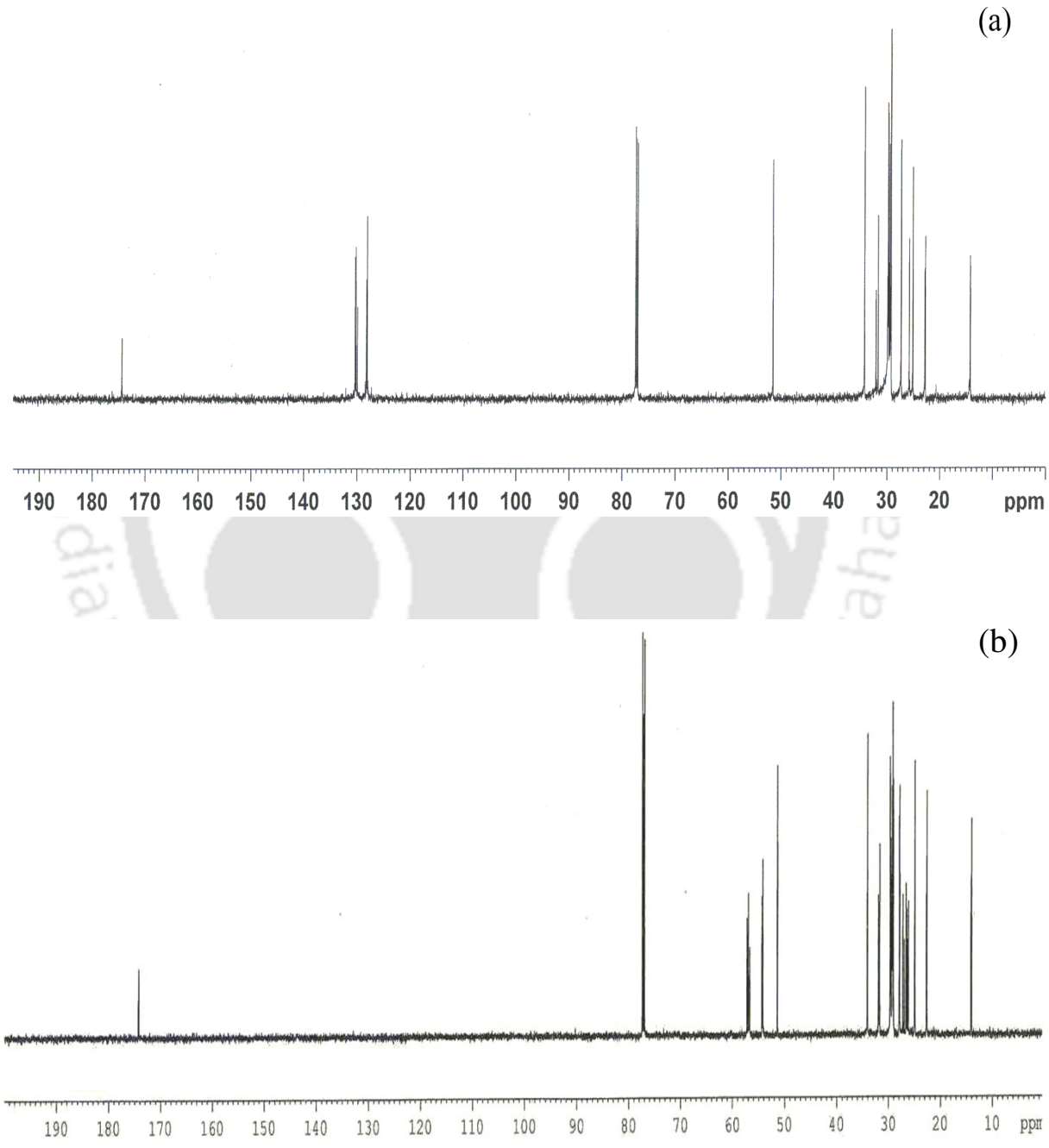

Figure 5.4: ^{13}C-NMR spectrums of WCOFAME (a) and its epoxide (b)

5.3.3 Pour point determination by DSC

The low temperature performance of vegetable oils and their derivatives is one of the major concerns to use them as lubricant basestocks compared to conventional basestocks. DSC thermal analysis was performed to determine heat flow versus temperature profile of WCOFAME and its epoxide cooling thermo-grams (Figures 3.12 and 5.5). The exothermic peaks in Figures 3.12 and 5.5 indicate the crystallization temperatures as -1 ^{o}C and 10 ^{o}C for WCOFAME and its epoxide respectively. The structurally modified (i.e. epoxide) WCOFAME displayed PP as 10 ^{o}C (Figure 5.5) and for WCOFAME, it was found to be -1 ^{o}C (Figure 3.12), indicates significant increase in PP after structural modification which might be due to the removal of unsaturation. This tendency was due to the complete conversion of unsaturation into epoxide. Various researchers have noticed similar trends with respect to the unsaturated fatty acid composition of oils and esters (Farias et al. 2010). From this study, it could be seen that the structural modification of WCOFAME can alter the low-temperature properties, thus they can be used in cold climatic conditions.

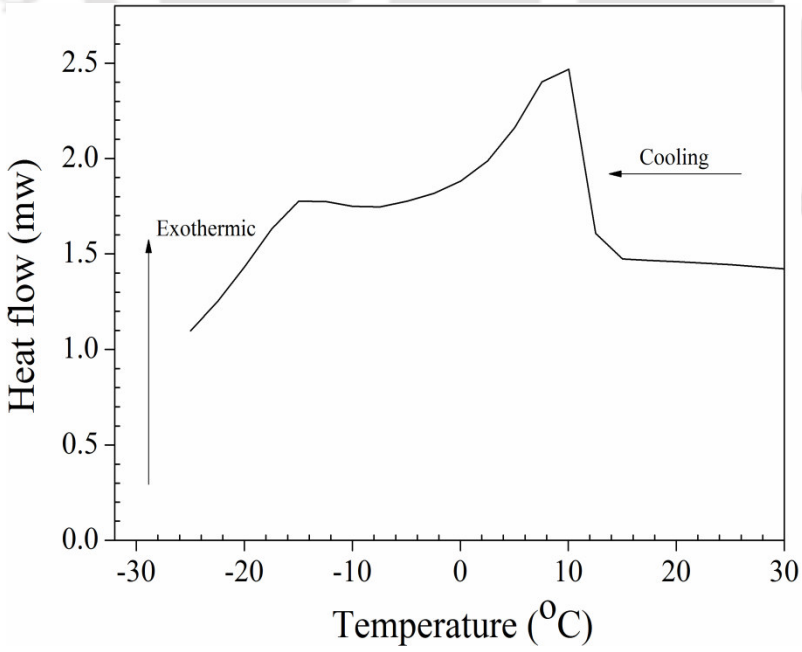

Figure 5.5: DSC thermo-gram for WCOFAME epoxide for pour point determination

5.3.4 Thermo-oxidative stability

The basic knowledge of thermo-oxidative properties of prepared lubricant basestocks is essential to predict the long term thermo-oxidative stability of epoxide, which is one of the highly significant properties of lubricants. Thermal analysis experiments were carried out using computer-controlled thermogravimetric analyser. The TGA thermo-grams of WCOFAME and its epoxide in inert atmosphere (N_2) are shown in Figures 3.7 and 5.6. From the figure it can be seen that WCOFAME and its epoxide were stable up to 178 ^{o}C and 187 ^{o}C (onset temperatures) relatively in an inert atmosphere. Similarly, maximum decomposition temperature corresponds to the temperature at which maximum weight loss occurred i.e. at 224.5 ^{o}C and 245.5 ^{o}C for WCOFAME and its epoxide respectively. The higher thermal stability of epoxide attributed to the absence of unsaturation content in WCOFAME epoxide. During epoxidation, double bonds were transformed into oxirane ring, hence it was anticipated that epoxide could give higher thermal stability than un-modified WCOFAME (Borugadda and Goud 2014c). Madankar et al. (2013) reported that any feedstock with saturated fatty acids and monounsaturation content has a positive influence and also thermally more stable than polyunsaturation content. Thermal stability of epoxide is highly considerable factor for various industrial applications and it depends on chemical structure, density of the basestocks.

Similarly, oxidative stability is determined as a quality indicative parameter in oxygen atmosphere to predict the actual lubricant service life at higher or extreme temperature and pressure conditions. Figures 3.9 and 5.6 depicts the thermo-grams of WCOFAME and its epoxide, from the TGA thermo-grams, oxidative onset temperatures was found to be 187 ^{o}C and 200 ^{o}C, likewise maximum decomposition temperatures was around 228 ^{o}C and 263 ^{o}C respectively. Even though the onset temperatures are very close,

maximum amount of the epoxide decomposed at 263 ^{o}C signifies that WCOFAME epoxide is oxidatively more stable than WCOFAME.

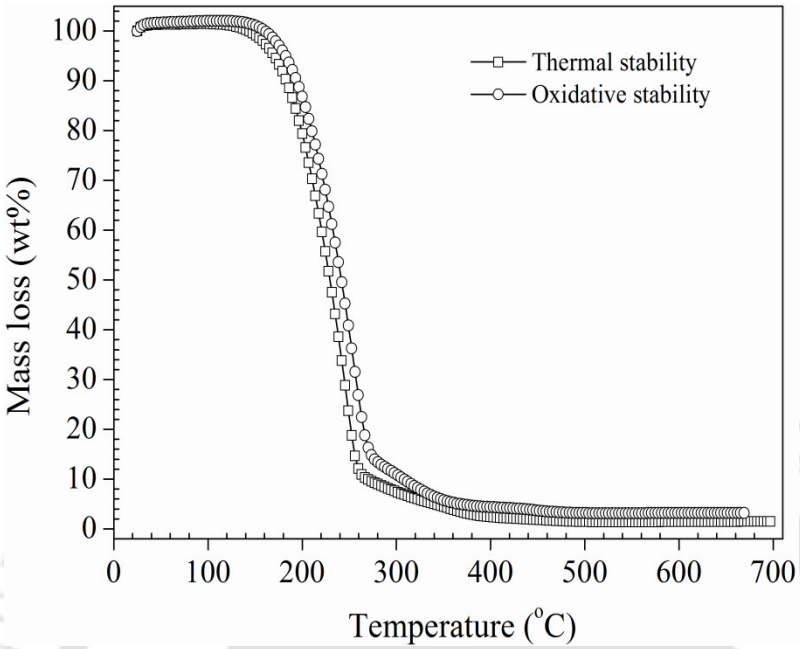

Figure 5.6: TGA thermo-grams for WCOFAME and its epoxide under nitrogen atmosphere (Thermal Stability) (a) air atmosphere (Oxidative Stability) (b)

5.3.5 Catalyst re-usability

The catalyst used in the epoxidation reaction was tested for its reusability and stability at optimum condition. The recovered catalyst after first usage in epoxidation was further washed with diethyl ether, refluxed with alcohol to remove any absorbed material from the pores of a catalyst surface and then dried in an oven for 3 h at 80 ^{o}C. After complete drying it was reused at optimum condition for four times, and OOC was determined after each run. The OOC data showed that recovered catalysts retained its activity up to three runs at optimum condition. However, after a third run marginal decrease in the OOC was observed and during the entire re-usability study no makeup catalyst was added (Figure 5.7). Salih et al. (2013) studied and reported that, IR-120 catalysts could be used maximum four times for canola oil epoxidation at un-optimized condition. But, in the present study, it was found that

IR-120 can be re-used maximum three times to make use of its catalytic activity at optimum condition. In the present study similar observations were made for other feedstocks as well for catalyst re-usability analysis.

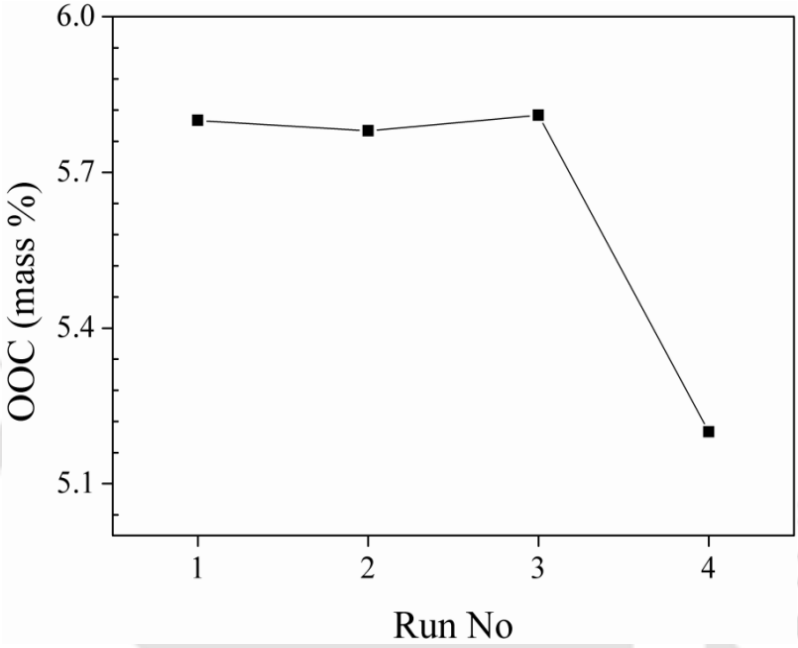

Figure 5.7: Catalyst re-usability plot for IR-120 during epoxidation

5.3.6 Rheological behavior

The rheological measurements were carried out using interfacial rheometer to study the bulk rheological properties of WCOFAME epoxide by varying shear rates from 0 to 500 s^{-1} at different temperatures such as 28, 40, 60, 80 and 100 ^{o}C. From Figures 5.8 and 5.9, it can be seen that in spite of temperature variations, shear stress versus shear rate relation was found to be linear and signifies Newtonian fluid behavior. Similarly, Figure 5.10 illustrates epoxide viscosity variation as a function of temperature over a temperature range varying from room temperature to 100 ^{o}C (i.e. 28, 40, 60, 80 and 100 ^{o}C). Likewise, Figure 5.10 shows that epoxide viscosity decreased with an increase in the temperature which was due to the higher thermal movement among molecules (Salih et al. 2013). A favourably good agreement was

found when the results were compared with the other studies on ozonized vegetable oil as pour point depressant for neat biodiesel (Soriano et al. 2006).

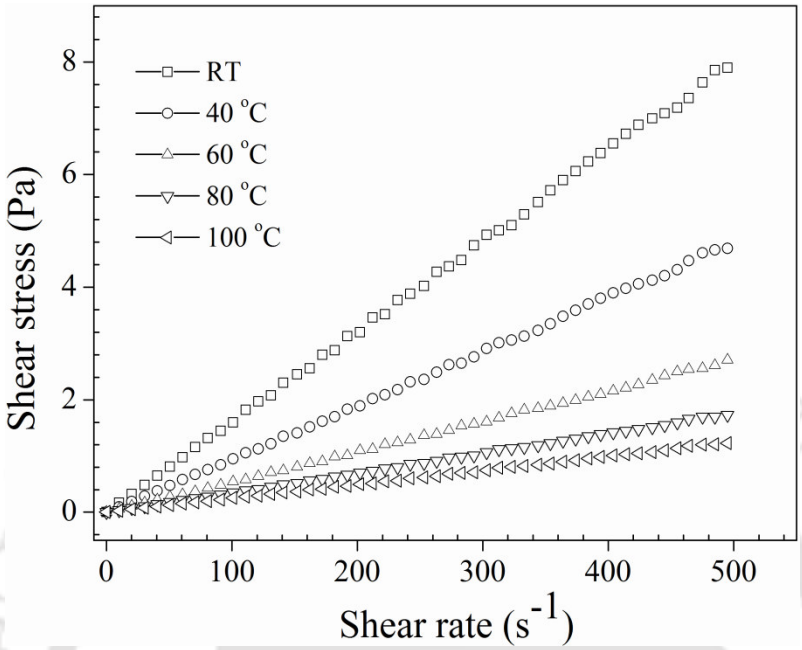

Figure 5.8: Shear stress versus shear rate relation for WCOFAME epoxide

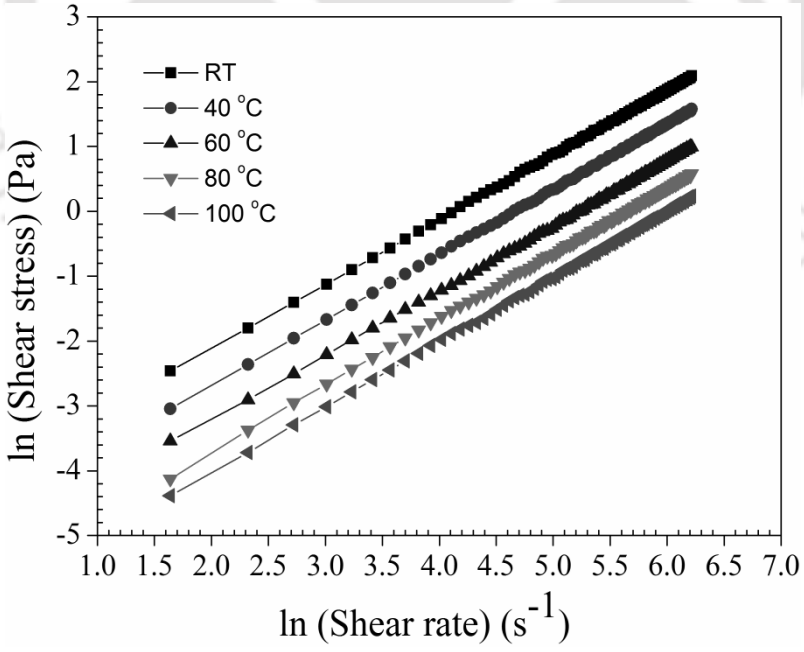

Figure 5.9: Logarithmic plot of shear stress versus shear rate for WCOFAME epoxide

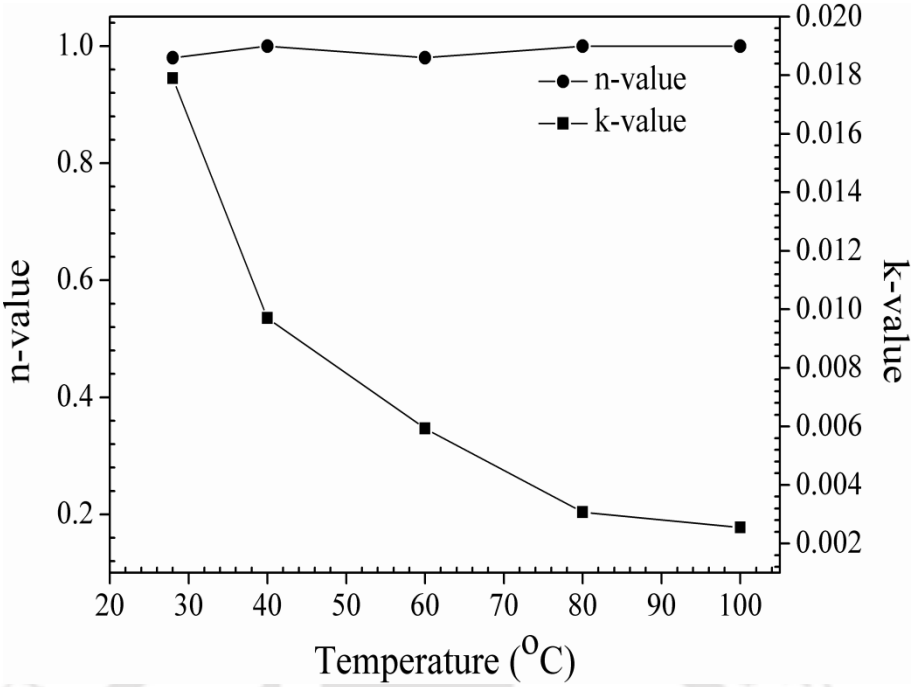

Figure 5.10: Plot of experimental value of n and k for WCOFAME epoxide at various temperatures

5.3.7 Physico-chemical characterization

All the significant physico-chemical properties of WCOFAME and their corresponding epoxide are given in Table 5.3. Iodine value (IV) estimation after epoxidation is one of the ways to confirm and support completion of epoxidation reaction. Initial IV of WCOFAME was found to be 132.94, (gI_2/100g of esters) whereas after epoxidation it was observed to be 0.253 (gI_2/100g of epoxide). Very less IV value implies that almost all the unsaturation was transformed into epoxide, and conversion was calculated according to initial and final IV of the samples. From Table 5.3, it can be seen that 99.8 % of double bonds were transformed into oxirane ring. The experimental (5.8 mass%) and theoretical (7.72 mass%) values of OOC were calculated as per the method described by Santos et al. (2005) and reported in Table 5.3. Relative percentage conversion of oxirane was found to be 76.42 %.

Likewise, AV of WCOFAME epoxide was found to be 0.96 mg KOH/g, lower AV signifies that epoxide does not raise any operational problems to the engine and other parts

of the equipment by corrosion during usage. α-Glycol content was determined to confirm the presence of hydroxyl groups. Theoretical and experimental values of α-glycol content along with the relative percentage conversion of α-glycol are calculated and depicted in Table 5.3. The density and kinematic viscosity (KV) of WCOFAME was found to be 703 kg/m^3, 4.71 cSt respectively, whereas for epoxide it was 773.82 kg/m^3, 10.42 cSt respectively. Improved density and KV of WCOFAME epoxide attributed to increase in molecular weight, polarity and intermolecular forces during the structural change via epoxidation.

One of the most important properties of epoxide is moisture content, which indicates the presence of water in epoxide sample. The presence of moisture in epoxide supports the bacterial growth, which leads to an unwanted performance during usage thereby increases AV, viscosity and free radical compounds via oxidation. Always lower moisture content is preferred for epoxide. In the present study, WCOFAME epoxide moisture content was found to be 0.16 wt% (Table 5.3) which was very low and indicates smooth performance of WCOFAME epoxide without any trouble during usage. The refractive indexes of WCOFAME and its epoxide were found to be 1.45 (Table 5.3), which expresses that minute quantity of heat energy can pass through the esters and epoxide samples, which is desirable to avoid degradation of the products.

Table 5.3: Physico-chemical properties of WCOFAME and WCOFAME epoxide

Physico-chemical properties	WCOFAME Epoxide	WCOFAME
Acid value (mg KOH/g)	0.96	0.38
Density (kg/m^3)	773.82	703
Iodine value (g I_2/100 g)	0.25	132.94
Kinematic viscosity (cSt) at 40 ^oC	10.42	4.71
Kinematic viscosity (cSt) at 100 ^oC	3.29	
Moisture content (wt%)	0.16	0.15
Pour point (^oC)	10	-3
Refractive index (at 27.6 ^oC)	1.45	1.45
Oxirane content (Experimental, mass%)	5.8	-
Oxirane content (Theoretical, mass%)	7.72	-
Relative percentage conversion of oxirane (%)	76.42	-
Glycol content (mol/100g, Theoretical)	0.44	-
Glycol content (mol/100g, Experimental)	0.14	-
Relative percentage conversion α-glycol (%)	47.24	-

5.4. Hydroxylation of WCOFAME epoxide

Chapter-4 described and discussed the WCO epoxide hydroxylation followed by hexanoylation. Hence, to avoid the repeatability this chapter only discussed about the optimization of reaction conditions for the WCOFAME ring opening (RO) i.e. hydroxylation and hexanoylation, followed by their physico-chemical characterization. The prepared WCOFAME epoxide at an optimum condition was used to study the oxirane ring opening with 2-EH using sulphuric acid as a homogeneous acid catalyst. Hydroxylation was carried out in an identical setup as discussed earlier in Chapter-4. A requisite amount of epoxidised WCOFAME was added into a reactor followed by pre-mixed solution of 2-EH and H_2SO_4

catalyst, the effectiveness of process parameters was studied thoroughly for the complete ring opening (100 %). The preliminary studies were carried out to decide the optimum condition for complete ring opening by varying significant process parameters. During hydroxylation, catalyst loading and 2-EH moles were altered between 0.5 - 3 wt% and 4 - 10 mol respectively, similarly reaction time was varied from 2 - 30 min at room temperature (Figure A.17). The final optimum condition was found to be 8 mol of 2-EH, 3 wt% of H_2SO_4 catalyst loading, 15 min of reaction time at room temperature and 1500 rpm stirring speed.

The comparative analysis of optimum reaction conditions for WCO and its methyl esters hydroxylation, WCOFAME consumed less time and reactants. The difference in the consumption of alcohol and reaction time for methyl esters is ascribed to the absence of higher molecular weight glycerol in the feedstock (WCOFAME). The glycerol also consumed some amount of alcohol in transesterification during hydroxylation of WCO epoxide, therefore more quantity of alcohol and time needed for complete conversion of oxirane oxygen to hydroxyl groups. But, during the hydroxylation of WCOFAME absence of glycerol reduced the consumption of 2-EH and reaction time.

5.5. Hexanoylation of WCOFAME hydroxylated product

The hexanoylation of WCOME hydroxylated product was carried out to enhance the cold flow properties. The hydroxyl group in the ring opened product was fully functionalized by using hexanoic anhydride in presence of IR-15 as a heterogeneous strong acid catalyst. During hexanoylation, process parameters varied were, hexanoic anhydride molar ratio was altered by 1 - 2 mol, 2 - 3 wt% of IR-15 catalyst loading, reaction temperature by 50 - 60 ^{o}C, reaction time 1 - 9 h at 1500 rpm stirring speed was used throughout the study to avoid mass transfer resistance. Based on the above range of each process variable, the optimum condition was established as, 2 mol of hexanoic anhydride, 50 ^{o}C reaction temperature and 2

wt% of catalyst loading at 2 h of reaction time. Further, the product was confirmed by FTIR analysis and was found to be indistinguishable to WCO hydroxylation and hexanoylation FTIR spectra (Figure 4.14). The difference in the consumption of reactants and reaction conditions for hexanoylation of WCOFAME is identical to WCO and this phenomenon was clearly explained in section 5.4.

During the functionalization study samples were withdrawn at regular intervals and washed with 5% $NaHCO_3$ solution followed by diethyl ether. Further, the removal of residual solvent and anhydride was accomplished by a short path distillation column under reduced pressure at 80 ^{o}C to recover the functionalized product. However, during the entire study, acid value all the end products was found to be less than 0.5 mg KOH/g, which is acceptable range for commercial application.

5.6. Effect of chemical modification (hydroxylation and hexanoylation) on physico-chemical properties

5.6.1 Product confirmation by NMR spectral analysis and GPC

The progress of WCOFAME hydroxylation and hexanoylation reactions was closely monitored by FTIR and ^{13}C-NMR spectral analysis. (Figure A.18) The disappearance of peaks at δ 50 - 60 ppm range indicates the transformation of epoxy groups into hydroxyl groups. Subsequently the hexanoic anhydride was functionalized to enhance the pour point of end product and was confirmed by the increased intensity of ^{13}C-NMR peaks at δ 20 - 40 ppm range (Figure A.19) and singlet ester peak at δ 175 ppm. The same was confirmed by FTIR spectra of WCO epoxide and hydroxylated product (Figure 4.11). The results of spectral analysis are identical to that obtained with ^{13}C-NMR spectra's of WCO hydroxylation and hexanoylation (Figure 4.13 (b) and (c)). Therefore Figure 4.3 can be considered as the reference spectra to identify and confirm the product formation.

Further, WCOFAME derived hydroxylated product was reacted with hexanoic anhydride to functionalize the hydroxyl groups with anhydride groups. The formation of di-esters (hexanoylated) product was confirmed by the complete disappearance of hydroxyl groups and increased ester peak of WCOFAME derived hexanoylated product (Figure 4.14).

In addition to the product confirmation by spectral analysis, functionalization of the 2-EH and anhydride groups were supported by determining the end products molecular weights by GPC analysis. As reported in Table 5.4, molecular weights of the hydroxylated and hexanoylated products were increased compared to WCOFAME epoxide, which signifies that the ester groups were attached to the nucleophilic sites and extending the branching at fatty acid chains of methyl esters.

Table 5.4: Molecular weights of WCOFAME epoxide, hydroxylated and hexanoylated products

Sample	Number Avg. Mol. Wt.	Weight Avg. Mol. Wt.
WCOFAME epoxide	989	1017
WCOFAME hydroxylation	1498	1720
WCOFAME hexanoylation	1680	1850

5.6.2 Viscosity, viscosity index and rheology of hydroxylated and hexanoylated products

The kinematic viscosity and viscosity index of prepared WCOFAME hydroxylated and hexanoylated products were evaluated and the results are presented in Table 5.5. The viscosity analysis results revealed that, kinematic viscosity of WCO derived products (29.63, 9.65 cSt) almost double than that of WCOFAME derived products (16.76 and 4.99 cSt at 40 ^{o}C and 100 ^{o}C). The functionalization of sample indicates that, as branching is increases from mono-esters to di-esters, KV and VI decreases. Mahajan et al. (2013) also noticed alike findings during their study on chemically modified epoxidised mustard oil for bio-lubricant

properties. As reported in Table 5.5, it was observed that viscosity drops with functionalization but, VI of the hydroxylated product is enhanced (257.8) compared to WCOFAME epoxide (188), but when it is compared to hexanoylated product VI is reduced and found to be 133.01 (Table 5.5).

Table 5.5: Kinematic viscosity and viscosity index of hydroxylated and hexanoylated products

Sample	Kinematic Viscosity (cSt)		Viscosity Index
	@40 °C	@100 °C	
WCOFAME epoxide	23.23	5.5	188
WCOFAME hydroxylation	16.76	4.99	257.8
WCOFAME hexanoylation	8.33	1.09	133.01

The rheological behavior of WCOFAME derived di-esters determined using interfacial rheometer by varying the shear rate (0 – 500 s^{-1}) at different temperatures (25, 40, 60, 80 and 100 °C) is demonstrated in Figure 5.11 (a) and (b). From the figure it was noticed that, in spite of the increase in temperature, shear stress vs. shear rate relation was found to be linear and signifies Newtonian fluid behaviour.

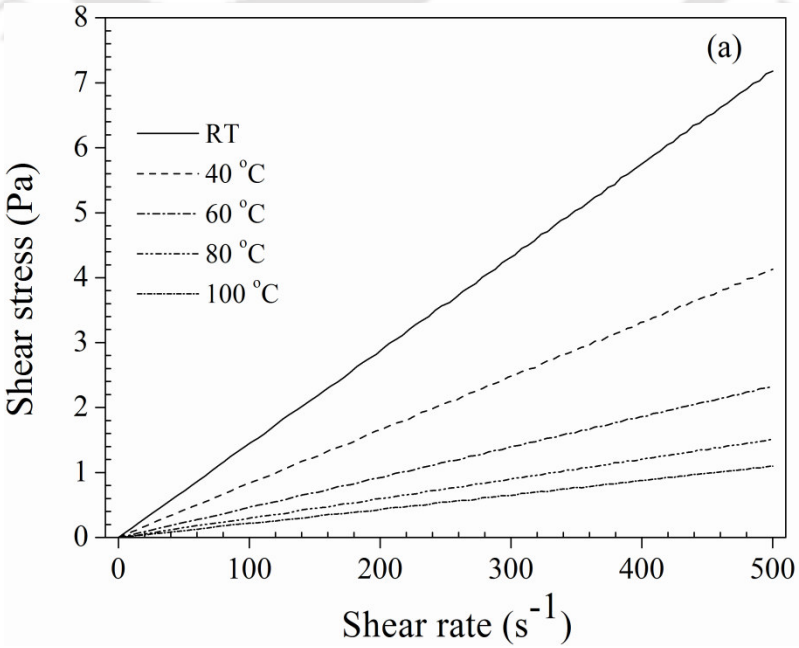

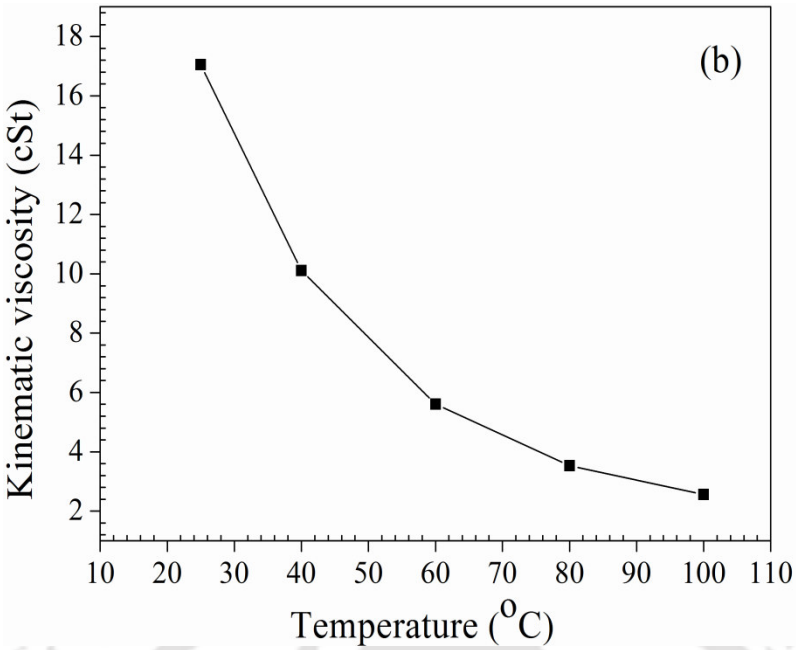

Figure 5.11: Shear stress versus shear rate (a) and temperature versus kinematic viscosity (b) relation for WCOFAME derived di-esters

5.6.3 Thermo-oxidative stability, cold flow properties of the WCOFAME derived hydroxylated and hexanoylated products

From the TGA study, thermo-oxidative stability and peak temperatures (maximum degradation temperatures) of WCOFAME hydroxylated and hexanoylated products are reported in Table 5.6. The thermal stability analysis of the chemically modified samples after each step revealed an increase in the onset temperatures. The thermal stability (OT) of WCOFAME, hydroxylated and hexanoylated products was found to be 175 ^{o}C, 265.9 ^{o}C and 293 ^{o}C respectively (Figures 5.6, A.20 and A.21). Likewise, oxidative stability (OOT) was in the range of 180 ^{o}C, 246.8 ^{o}C and 247.5 ^{o}C respectively (Figures 5.6, A.20 and A.21). From the comparative analysis of OT and OOT data it can be concluded that chemical modification of WCOFAME enhances its thermal and oxidative stability. However, reverse trend was noticed in case of WCO and its functionalization products (Table 4.9). Enhancement in the stability of the samples attributed to the absence of -OH or glycerol in the chemical structure and fatty acid composition of the feedstock (i.e. WCOFAME).

Table 5.6: Onset temperature (OT), oxidative onset temperature (OOT), peak temperatures (PT) and pour points of prepared WCOFAME derived hydroxylated and hexanoylated products

Sample	Thermal stability (^{o}C)		Oxidative stability (^{o}C)		Pour Point (^{o}C)
	OT	PT	OOT	PT	
WCOFAME hydroxylation	265.9	327.3	246.8	268.4	-13.97 ± 0.45
WCOFAME hexanoylation	293	337.2	247.5	279.6	-27.15 ± 0.39

Apart from that, samples are also analyzed to estimate its cold flow properties, the pour point of WCOFAME derived hydroxylated and hexanoylated products was found to be -13.97 ± 0.45 ^{o}C (Figure 5.12 (a)), -27.15 ± 0.39 ^{o}C (Figure 5.12 (b)) respectively. Form the table it can be seen after hydroxylation significant increase of -24 ^{o}C in the PP temperature was noticed (i.e. WCOFAME epoxide, 10 ^{o}C; hydroxylated product, -13.97 ^{o}C), this could be attributed to the absence of glycerol or -OH group in the chemical structure of the feedstock (WCOFAME) as explained in the earlier section. Further, hexanoylation also showed significant enhancement in the PP temperature of -13 ^{o}C (hydroxylated product, -13.97^{o}C; hexanoylated product, -27.15 ^{o}C). Altogether from the feedstock (WCOFAME, 10 ^{o}C) to the end product (WCOFAME hexanoylated, -27.15 ^{o}C) the increased in the PP temperature was around - 37.15 ^{o}C. From the comparative evaluation of feedstock used in the present study, cold flow properties of WCOFAME derived products (hydroxylated and hexanoylated) showed significant improvement in the PP than the other feedstocks (Table 5.6). The functionalization of 2-EH and hexanoic anhydride to WCOFAME fatty acid chains demonstrated the most effective reduction in the PP temperature and this could be attributed to the presence of large branching group at the midst of fatty acid chain and it makes a steric barrier around the individual molecules and suppresses formation of crystal growth which results in lowering samples PP .

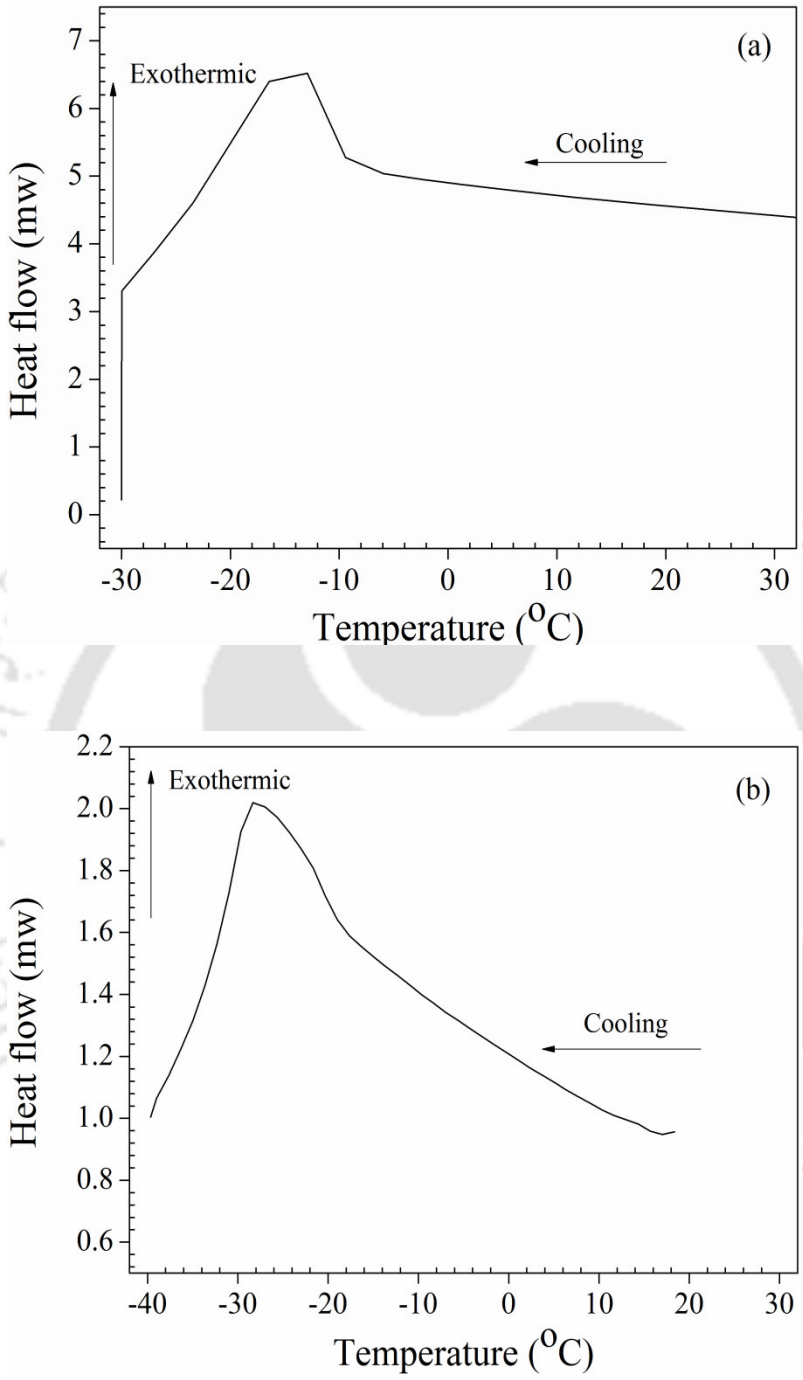

Figure 5.12: DSC thermo-grams for WCOFAME hydroxylation (a) and hexanoylation (b)

5.6.4 Tribology and bio-degradability of WCOFAME hexanoylated product

The anti-wear and friction reducing properties of prepared WCOFAME derived hexanoylated product was evaluated using HFRR lubricity test. Details about the experimental and

analysis part are well explained in Chapter-2 in section 2.6.14. For the WCOFAME derived hexanoylated product wear scar diameter was found to be 231 µm, 187 µm and 209 µm (x-axis, y-axis and average, Figure 5.13), with film thickness of 81 % and co-efficient of friction (CoF) as 0.1. The higher film thickness ascribed to the absence of glycerol or -OH in WCOFAME composition. The obtained tribological properties were within the acceptable range to use them as lubricant basestocks (Madankar et al. 2013).

Biodegradation profile of duplicate test runs carried out with WCOFAME derived hexanoylated product was found to be 90.82 % ± 1.98, which indicates that the prepared WCOFAME derived di-esters are biodegradable and showed good reproducibility among the duplicate test runs. The cumulative biodegradation values by bio-kinetic model and biodegradability of WCOFAME derived di-esters was found to be 1.04 and 90.82. The comparative evaluation of feedstock used in the present study, the biodegradability of WCO derived di-esters was found to be 93.6 % compared to WCOFAME derived di-esters (i.e. 90.82 %).

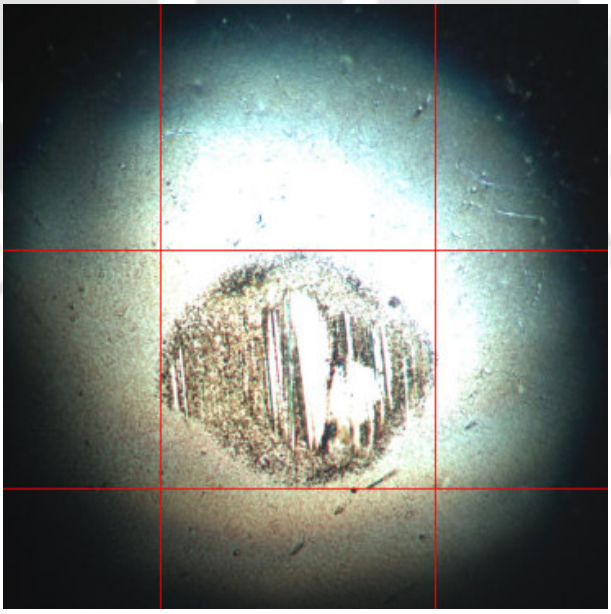

Figure 5.13: Microscopic wear scar image for WCOFAME derived di-ester

5.7. Summary

The current work has demonstrated the synthesis of biodegradable bio-lubricant basestocks from WCOFAME via series of chemical modifications, known as epoxidation, hydroxylation and hexanoylation. Furthermore, epoxy groups of methyl esters were selectively reacted with 2-EH and hexanoic anhydride by nucleophilic reactions to give hydroxyl, hexanoylated derivatives using sulphuric acid and IR-15 as catalysts. This investigation established the optimum conditions for epoxidation, hydroxylation and hexanoylation followed by finding the significant physico-chemical properties after every chemical modification step. Interesting findings were observed in case of thermo-oxidative stability and pour point temperatures of the hydroxylated and hexanoylated products. Through a series of chemical modifications, thermo-oxidative stability and cold flow properties were enhanced and this could be attributed to the absence of -OH or glycerol molecule in the fatty acid chain or fatty acid profile of the feedstock. Besides to the stability and pour point; rheological and tribological performance features provides the retention of lubrication performance even at high temperatures. Correspondingly, biodegradability of the hexanoylated product holds more than 90% in 28 days signifies that all the products are eco-friendly.

CHAPTER-6

Bio-lubricant basestocks preparation from high free fatty acids castor oil: Process optimization and product characterization

The main objective of this chapter is to develop a biodegradable lubricant basestocks from high FFA castor oil (CO) via epoxidation. The compositional analysis of castor oil indicates higher amount of ricinoleic acid as a hydroxylated fatty acid in its composition and hence considering this as a unique identity, the feedstock was selected for the structural modifications. Optimization of castor oil epoxidation process was carried out to maximise the OOC and found the interactions, effects of process parameters on response by ANOVA. Further, validation of model and significant physico-chemical characteristics of the prepared CO epoxide was studied thoroughly. Product confirmation and physico-chemical characterization revealed that, due to higher free fatty acids content; lower OOC and more oxirane cleavage was noticed, along with unsatisfactory cold flow properties. However, further hydroxylation and hexanoylation was carried out to increase the branching and chain length of the ricinoleic fatty acid structure, thereby increases the cold flow properties. Major aim the study was also to enhance the performance limitations of high FFA CO along with biodegradability of the end product compared to feedstock. Therefore, subsequent sections of this chapter elaborated upon the experimental investigations carried out to realize the performance limitations and tribological properties, biodegradability of the end product.

6.1. Optimization of high FFA CO epoxidation

In order to optimize the CO (high AV) epoxidation process variables for maximum epoxide content, preliminary studies (Figure 6.1) were carried out to find the optimum range of each

process variable and shown in Table 6.1. Further, the experimental matrix was generated (Table A.3) to decide exact optimum condition. All the experiments were carried out at laboratory conditions and results were analyzed by multiple regression analysis and shown in Table 6.2. Following the OOC responses in design matrix, further ANOVA sought the entire optimization process to build relationship between a response variable (OOC) and input process variables for maximum OOC. A quadratic polynomial equation was obtained from the experimental data to predict higher epoxide content and shown below in terms of coded variables.

$$\text{Response (higher OOC)} = 3.82 + 0.038\,A - 0.82\,B - 0.19\,C + 0.068\,D - 0.37\,AB - 0.16\,AC + 0.022\,AD - 0.15\,BC - 0.33\,BD + 0.16\,CD - 0.21\,A^2 - 0.56\,B^2 - 0.56\,C^2 - 0.58\,D^2 \quad (6.1)$$

In order to ensure a thorough model fit and to measure the analysis of variance on individual model, co-efficients test for lack-of-fit need to be estimated. The lack of fit is an assessment of failure of a model to represent the data that can't be reported by random error (Tabrizi and Nassaj 2011). The results of a second order response surface model in the form of ANOVA for the maximum epoxide content is summarized in Table 6.2. It can be seen from Table 6.2 that F-value of the model is 2261.27 and the corresponding P-value (prob > F) is very small i.e. < 0.0001, implying that the model is highly significant. The P-values are adopted as a tool to ensure the importance of each co-efficient. In this study, main linear effects of time (A), temperature (B), catalyst loading (C) and hydrogen peroxide molar ratio (D), cross and quadratic effects of all four process variables (i.e AB, AC, BC, BD, A^2, B^2, C^2, D^2) are highly significant, since the P-value is very less (< 0.0001).

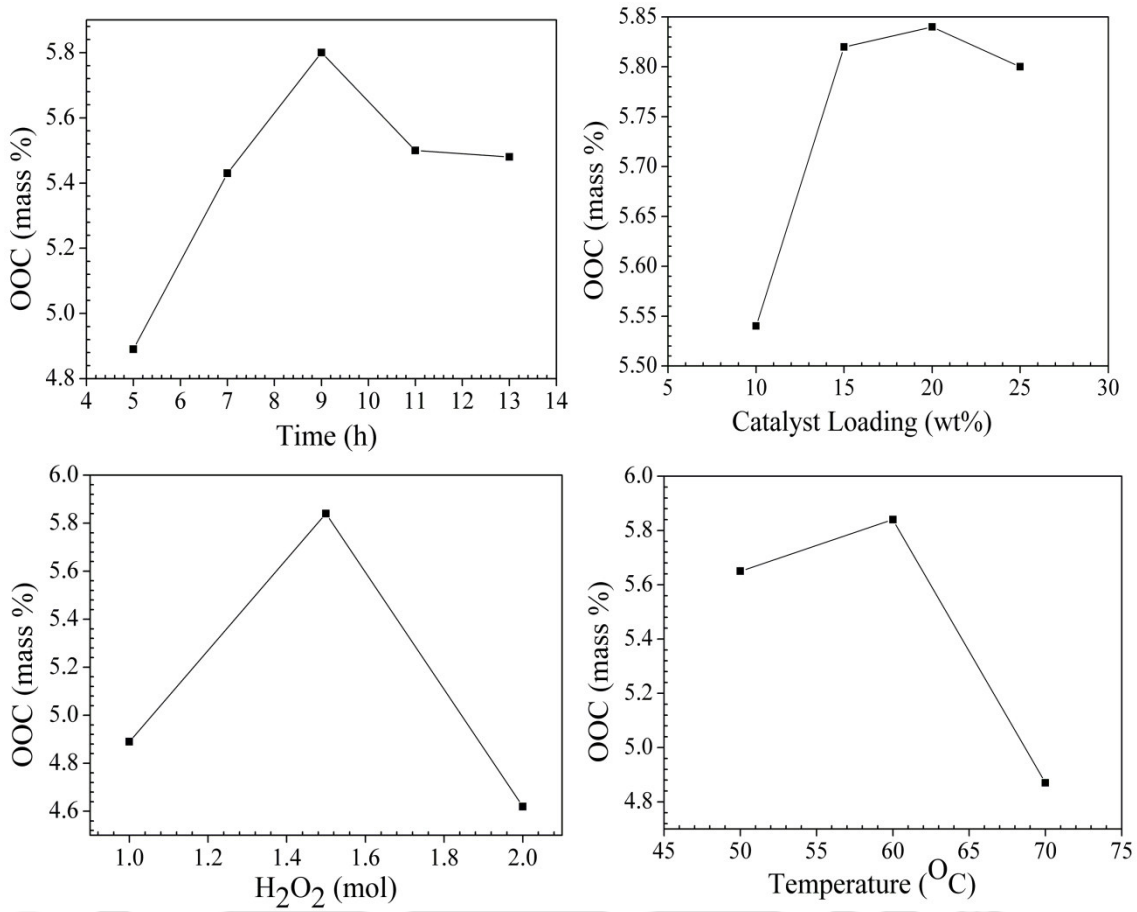

Figure 6.1: Effects of reaction variables time, catalyst loading, hydrogen peroxide and temperature on epoxidation of high FFA CO (preliminary studies)

Table 6.1: High FFA castor oil epoxidation process variables and their optimum levels

Independent Variables	Symbol	Unit	Variable Levels		
			-1	0	+1
Time	A	h	2	3	4
Temperature	B	^{o}C	50	60	70
Catalyst Loading	C	wt%	10	15	20
Oil: Hydrogen peroxide (H_2O_2)	D	mol	1	1.5	2

The other model term (cross variable) time and hydrogen peroxide molar ratio (AD) are also significant variable, since the P-value is 0.0309 (< 0.05). In the present model absence of insignificant parameters intending that all the liner, cross and quadratic terms are

highly significant for maximum epoxide content. The insignificant lack-of-fit F-value of 4.26 entails that lack of fit is considerably significant relative to the pure error, which signifies that the model is extremely accurate without any noise and the results are reproducible. Furthermore, the actual values are very much close to the predicted values as shown in Figure 6.2.

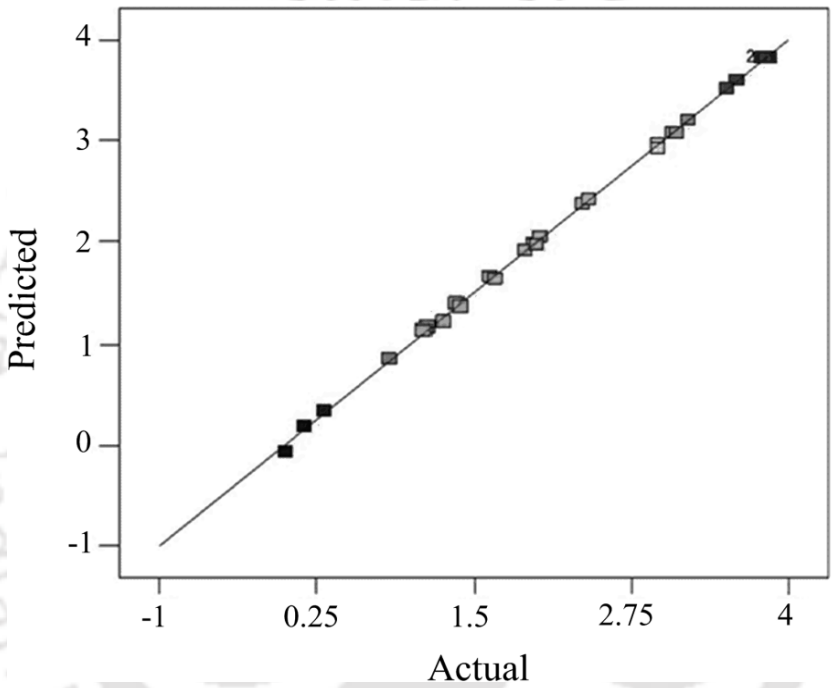

Figure 6.2: Predicted versus Actual plot of response (OOC) for epoxidation of high free fatty acid castor oil

Table 6.2: Regression co-efficients of predicted and quadratic polynomial model for response variable (OOC) for epoxidised high FFA CO

Source	Sum of Squares	Degrees of Freedom	Mean Square	F Value	P-value (prob > F)
Model	42.74	14	3.05	2261.27	< 0.0001
A-Time	0.035	1	0.035	25.56	0.0001
B-Temp	15.99	1	15.99	11843.23	< 0.0001
C- Cat Load	0.83	1	0.83	611.11	< 0.0001
D- H_2O_2	0.11	1	0.11	81.99	< 0.0001
AB	2.24	1	2.24	1660.91	< 0.0001
AC	0.41	1	0.41	305.74	< 0.0001
AD	7.656E-003	1	7.656E-003	5.67	0.0309
BC	0.35	1	0.35	255.64	< 0.0001
BD	1.71	1	1.71	1266.18	< 0.0001
CD	0.39	1	0.39	291.64	< 0.0001
A^2	1.16	1	1.16	858.43	< 0.0001
B^2	8.70	1	8.70	6440.64	< 0.0001
C^2	8.54	1	8.54	6326.76	< 0.0001
D^2	9.32	1	9.32	6906.31	< 0.0001
Lack of Fit	0.018	10	1.812E-003	4.26	0.0616
Pure Error	2.128E-003	5	4.255E-04		

The preciseness of a model is judged by the regression co-efficient (R^2). The R^2 value is always lies in between 0 - 1 and its order of magnitude suggests the aptness of the model (Manivannan and Rajasimman 2011). For a good statistical model, R^2 value should be close to 1, and the regression value for higher epoxide content is presented as 0.9996 which is close to 1 and it signifies that the 99.96% model behaviour can be interpreted for higher epoxide content while only about 0.04% of the full variance can't be explained by the model.

This represents that accuracy and the general ability of polynomial model is good. The predicted R^2 value (0.9982) is in reasonable agreement with the adjusted R^2 (0.9993) which had recommended prominent co-relational statistics between the remarked values and the predicted data. Thus, the regression model provides an excellent explanation of the relationship among the independent process variables and the response variable (OOC).

6.2. Influence of various process variables to maximum OOC

In order to estimate the best reaction condition for maximum epoxide content, the effects of linear, cross and quadratic reaction variables on the epoxidation was studied. Three dimensional response surface plots and two dimensional counter plots which are graphical histrionics of the regression equation are obtained by employing design expert software (trial version 8.0.7.1). These graphical representations of the plots are drawn by varying two process variables at a time while keeping other two variables at a central level (0).

6.2.1 Effect of time (A) and temperature (B)

Figure A.22 (a) and (b) describes two dimensional counter plot and the corresponding three dimensional response surface plot expressing cross effect of time (A) and temperature (B) on maximum OOC with respect to other process variables. Figure A.22 (a) and (b) shows that

OOC increased with an increase in reaction time from 2 h to 4 h, the increasing trend was noticed up to a certain time period of 3 h, beyond which gradual depletion in OOC was observed (Table A.3). Similarly, temperature was altered from 40 ^{o}C to 80 ^{o}C in order to verify the effect of temperature on OOC with respect to time. Results in Figure A.22 (a) and (b) shows that OOC content increased with an increase in temperature up to 60 ^{o}C (Table A.3) and a further increase in the temperature led to decrease in OOC. The behaviour of 2D and 3D figures revealed that longer reaction time and elevated temperature (beyond 60 ^{o}C) lowers OOC due to the oxirane cleavage to form side products (Scheme A.1) (Chavan et al. 2012). The maximum OOC of 3.85 mass% was attained at medium temperature of 60 ^{o}C at 3 h reaction time. Similar behaviour was noticed by Salimon et al. (2011c) during their study on epoxidation of ricinoleic acid. In the present study, lower OOC was obtained due to the higher acid value of castor oil and similar behaviour was noticed by Okieimen et al. (2005) during their study on epoxidation of high acid value rubber seed oil. However, 60 ^{o}C reaction temperature was considered as suitable for epoxidation of CO when the molar ratio of ethylenic un-saturation: acetic acid: hydrogen peroxide was 1:0.5:1.5 and catalysts loading 15 wt% .

6.2.2 Effect of time (A) and catalyst loading (C)

Keeping time (A) and catalyst loading (C) at central levels i.e. 3 h and 15 wt% respectively, combined effect of temperature (B) and hydrogen peroxide (D) was studied aiming at higher epoxide content and results obtained are depicted in Figure A.23 (a) and (b). From figure A.23 (a) and (b), it can be seen that with an increase in time and catalyst loading OOC content increases upto certain level, beyond which OOC decreases (Table A.3). The obtained results attributed to the hypothesis that the availability of enough active surface area of the

catalyst for longer reaction time during the reaction results in cleavage of oxirane oxygen which leads to the formation of side products (Chavan et al. 2012). Hwang and Erhan (2001) reported that the presence of higher FFA content leads to the hydrolysis reaction in acidic media thereby decreases the epoxide content due to oxirane cleavage. Hence within the experimental conditions, the most favorable catalyst loading and reaction duration appeared to be 15 wt% and 3 h.

6.2.3 Effect of time (A) and substrate molar ratio (D)

Figure A.24 (a) and (b) shows the effect of varying substrate molar ratio and reaction time on maximum epoxide content. An increase in the substrate molar ratio from 0.5 to 1.5 mol (Table A.3) leads to a linear increase in epoxide content, due to the formation of more peracetic acid and thereby epoxide. The maximum OOC was attained with the 1.5 molar ratio and the stability of oxirane observed with this ratio was similar to that observed with 1 molar ratio. However, an increase in the final oxirane value was relatively less when the ratio was further increased to 2.5 mol. This may be attributed due to the formation of peracetic acid from organic acid and then it is regenerated after epoxidation of unsaturation sites (Padmasiri et al. 2009). The use of a higher substrate molar ratio raised the additional problem of agitation and decrease mass transfer rate thereby decreases OOC. The maximum substrate ratio and higher reaction time provides an opportunity to react oxirane rings with excess hydrogen peroxide, acetic acid and water as by-product (Sarfaraz et al. 2009). The optimum reaction conditions to obtain maximum OOC for high FFA CO appeared to be 3 h reaction time and 1.5 mol of substrate loading.

6.2.4 Effect of temperature (B) and catalyst loading (C)

The effect of reaction temperature (B) and catalyst loading (C) on maximum OOC was investigated by varying catalyst loading from 5 - 25 wt% (Table A.3) and temperature from 40 ^{o}C to 80 ^{o}C with an interval of 10 ^{o}C. Increase in the temperature (Figure A.25 (a) and (b)) showed a favorable effect on epoxidation reaction and maximum OOC (3.85 mass%) at 60 ^{o}C and catalyst loading of 15 wt%. From Figure A.25 (a) and (b), it can also be seen that beyond 60 ^{o}C decrease in the OOC was observed. Epoxidation at higher temperatures (> 60 ^{o}C) acts as a medium to open the epoxide ring to form a ring opened product, thereby decrease the OOC (Goud et al. 2007). Likewise, altering the catalyst loading from 5 – 25 wt% increases the epoxide content up to 15 wt%. But, beyond 15 wt% catalyst loading inadequate OOC content was noticed, due to the formation of oxirane cleavage. In addition, higher catalyst loading limits the mass transfer rate of epoxidation and due to the availability of high active catalyst surface area, higher reaction time leads to unwanted side reactions which decrease the OOC. However, at 15 wt% of catalyst loading, it was assumed that reaction was free from mass transfer resistance under given conditions and maximum OOC was observed at a moderate reaction temperature of 60 ^{o}C (Dinda et al. 2008). Hence, 15 wt% of catalyst loading and 60 ^{o}C temperature was fixed for subsequent experimentations.

6.2.5 Effect of temperature (B) and substrate molar ratio (D)

The effect of substrate molar ratio (D) on reaction temperature (B) and their combined interaction on epoxidation process at constant catalyst loading of 15 wt% and 3 h of reaction time is represented by 3D response surface plot and its corresponding 2D contour plot in Figure A.26 (a) and (b). From the figure, it can be depicted that increase in OOC with an increase in both temperature and substrate molar ratio indicated that both the variables have

significant interaction between each other, but decrease in OOC was noticed beyond 60 ^{o}C reaction temperature and 1.5 substrate molar ratio. Derawi and Salimon (2010) reported that rate of epoxidation increased as the concentration of hydrogen peroxide in the system increased, but the stability of oxirane ring was very poor at the higher substrate molar ratio's and it leads to production of diol and α-glycol as unwanted side products (Dinda et al. 2011). On the other hand, Dinda et al. (2008) have shown that oxirane ring was quite stable at lower hydrogen peroxide concentrations. Finally, from the interaction of these variables, it can be seen that at medium reaction temperature OOC increases with an increase in the substrate molar ratio. However, higher reaction temperatures and molar ratios had a negative impact on the OOC. Thus, it can be said that the optimum temperature of 60 ^{o}C and 1.5 substrate molar ratios can be used for further experimentations.

6.2.6 Effect of catalyst loading (C) and substrate molar ratio (D)

The influence of catalyst loading on varying hydrogen peroxide molar ratio was investigated at various catalyst loadings and several H_2O_2 substrate molar ratios. The enhanced rate of peracid formation was anticipated with an increase in the catalyst loading and hydrogen peroxide concentration (Mungroo et al. 2008). It was also observed with an increase in the catalyst loading OOC increases. Figure A.27 (a) and (b) describes the effect of catalyst loading and hydrogen peroxide molar ratios on CO epoxidation. Higher selectivity was achieved at 1.5 molar ratio of hydrogen peroxide per mol of double bonds and 15 wt% of catalyst loading. Hydrogen peroxide molar ratio higher than 1.5 leads to a higher rate of oxirane ring decomposition as indicated by most of the researchers (Petrovic et al. 2002) and the same was discussed in the previous section. This observation was in agreement with the

results shown in Figure A.27 (a) and (b). Above all, lower epoxide content for high FFA CO epoxide was due to the hydrolysis reaction in the aqueous phase (Blee et al. 2005).

6.2.7 Process optimization for high FFA CO

The high FFA CO epoxidation reaction was closely monitored to avoid formation of undesired by-products by selecting significant process variables. Therefore, the optimum reaction condition of selected process variables was obtained by solving the polynomial quadratic equation using design expert software. In the current study, this model was aspired to find the epoxidation process for the best fit of variables that gives maximum OOC. The predicted values of process variables for epoxidation reaction obtained from the model equation for the maximum OOC content were substrate ratio (H_2O_2) 1.65 mol, catalyst loading (IR-120) 15.14 wt% and 2.81 h of reaction time at 52.8 ^{o}C reaction temperature. These values were chosen from the optimum solutions proposed by RSM optimization tool. This model expects the maximum OOC that can be obtained at this optimum condition is 4.09 mass%. To confirm the model prediction, the optimum response variables were tested by conducting the laboratory experiment. At the optimized process condition, epoxide content was found to be 3.85 mass% and agrees well with the model predicted value, which suggests that the formulated model is believed to be accurate and reliable. In the present study, all the 30 experiments (Table A.3) including confirmatory experiments were repeated twice at laboratory conditions and the average values are reported here.

6.3. Physico-chemical characterization of prepared high FFA CO epoxide product

6.3.1 Product confirmation by NMR spectroscopy

The epoxidation of high FFA CO was confirmed by ^{1}H-NMR spectroscopy, it is one of the significant techniques to monitor the progress of reaction and product confirmation. The ^{1}H-NMR spectrum of CO and CO epoxide is shown in Figure 6.3 (a) and (b) respectively. Significant signals in the ^{1}H-NMR spectra of CO shows that unsaturation bands (-CH=CH-) were observed from δ 5.25 - 5.58 ppm range (Figure 6.3 (a)). Whereas, the partial disappearance of unsaturation bands were noticed (Figure 6.4 (b)) after completion of the epoxidation reaction which signifies the presence of unsaturation in the end product at optimum condition. Similarly, epoxide peaks (-CH-O-CH-) were found at δ 2.8 - 3.1 ppm which were absent in the CO spectra (Figure 6.3 (a)). Furthermore, characterization of the epoxide product by ^{1}H-NMR revealed that the peak at δ 3.41 ppm represents the presence of ring opening product in a minute quantity. Finally, from the ^{1}H-NMR spectrum of CO and its epoxide, it could be verified and supported that CO conversion into its epoxide was confirmed. But, incomplete conversion of unsaturated double bonds and formation of oxirane cleavage was also noticed which attributed to the hydrolysis reaction in the presence of high FFA in the castor oil, alike results were also reported by Padmasiri et al. (2009) during their study on mee and rubber oil.

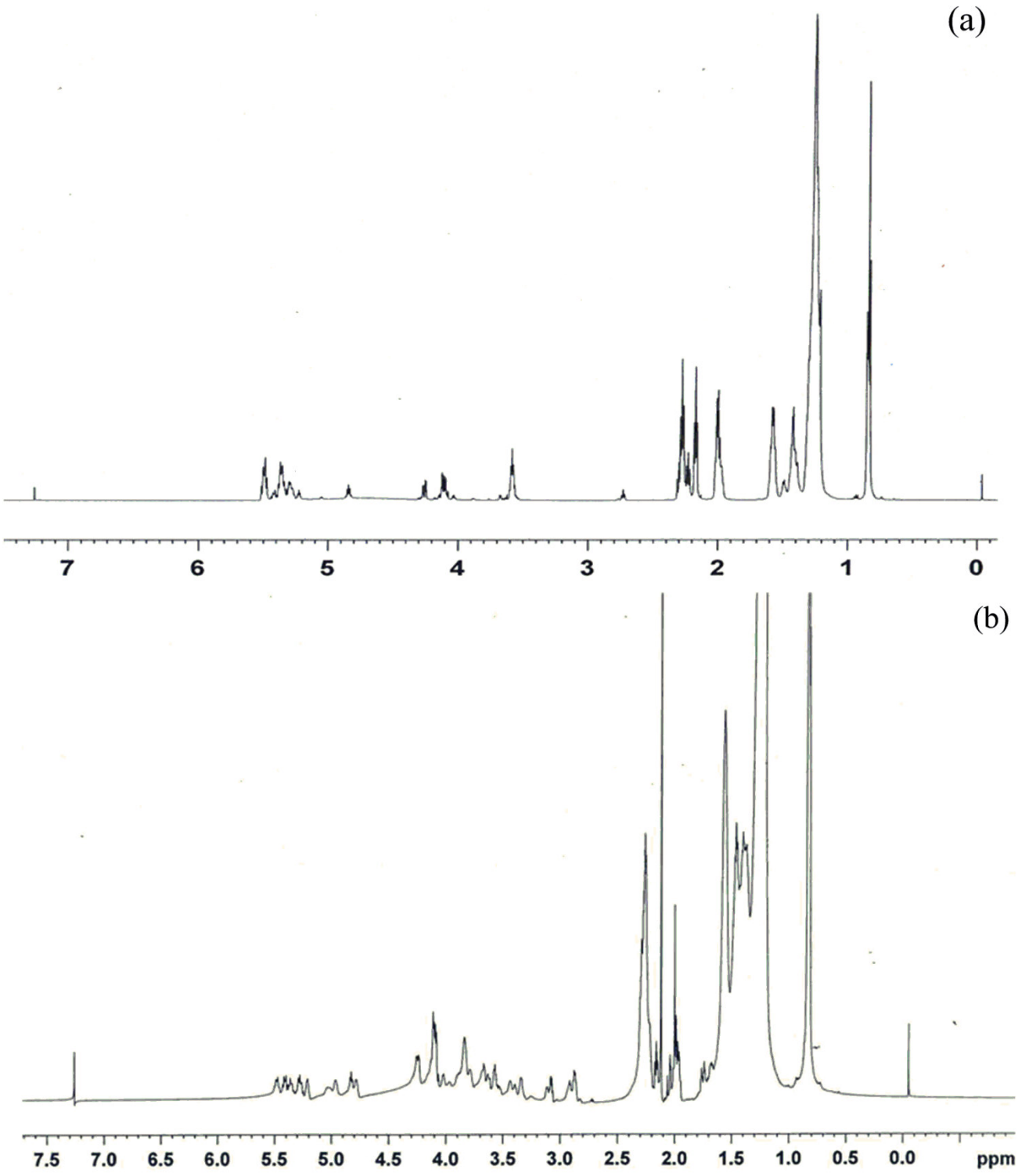

Figure 6.3: ^{1}H-NMR spectra's of CO (a) and CO epoxide (b)

Similarly, Figure 6.4 (a) and (b) shows ^{13}C-NMR spectra of CO and its epoxide. Appearance of peaks at δ 125 - 133 ppm represents the olefinic carbons in CO (Figure 6.4

(a)). The comparison of Figure 6.4 (a) and (b), revealed that formation of epoxy protons were observed at δ 53 – 59 ppm (Figure 6.4 (b)) and similarly disappearance of olefinic carbons peak was also notices at δ 125 - 133 ppm (Figure 6.4 (a)) in the final epoxide product. These additional peaks at δ 53 – 59 ppm which were absent in the CO are due to the epoxidation of high FFA CO. Alike results were noticed by Madankar et al. (2013) during their study on canola oil.

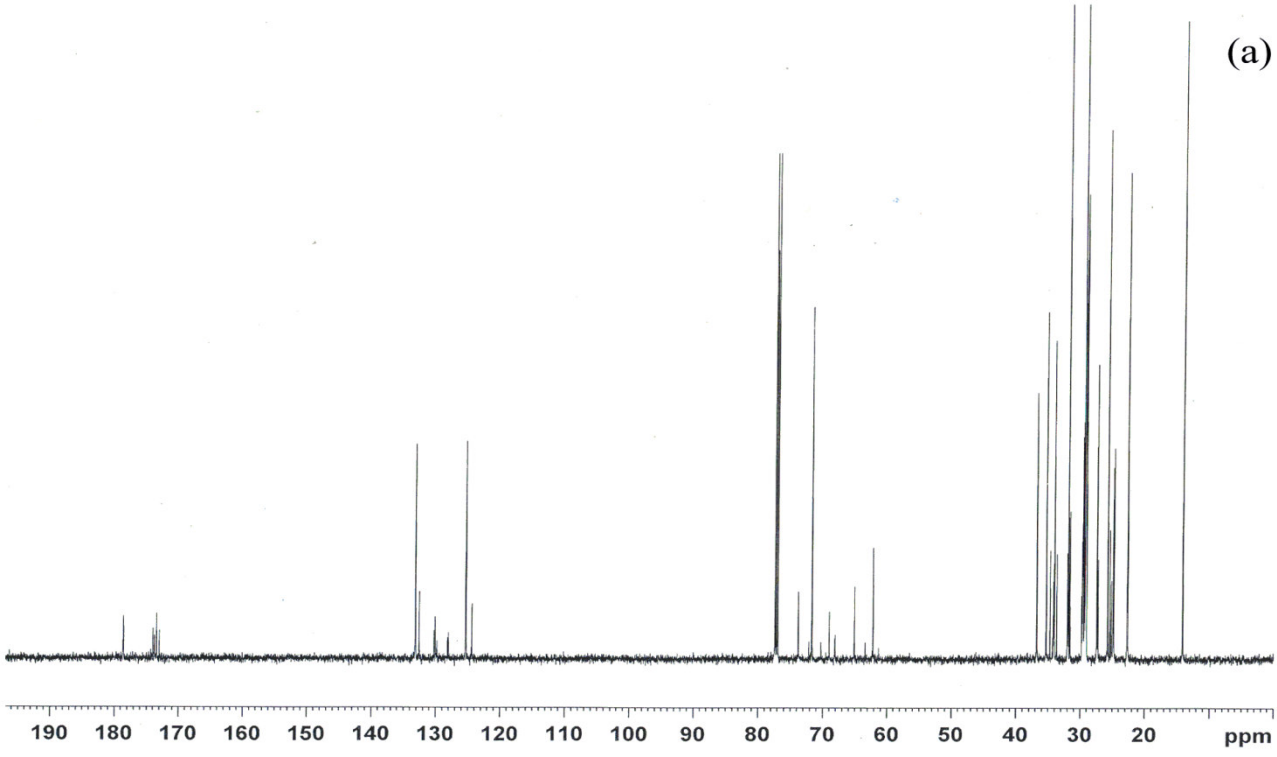

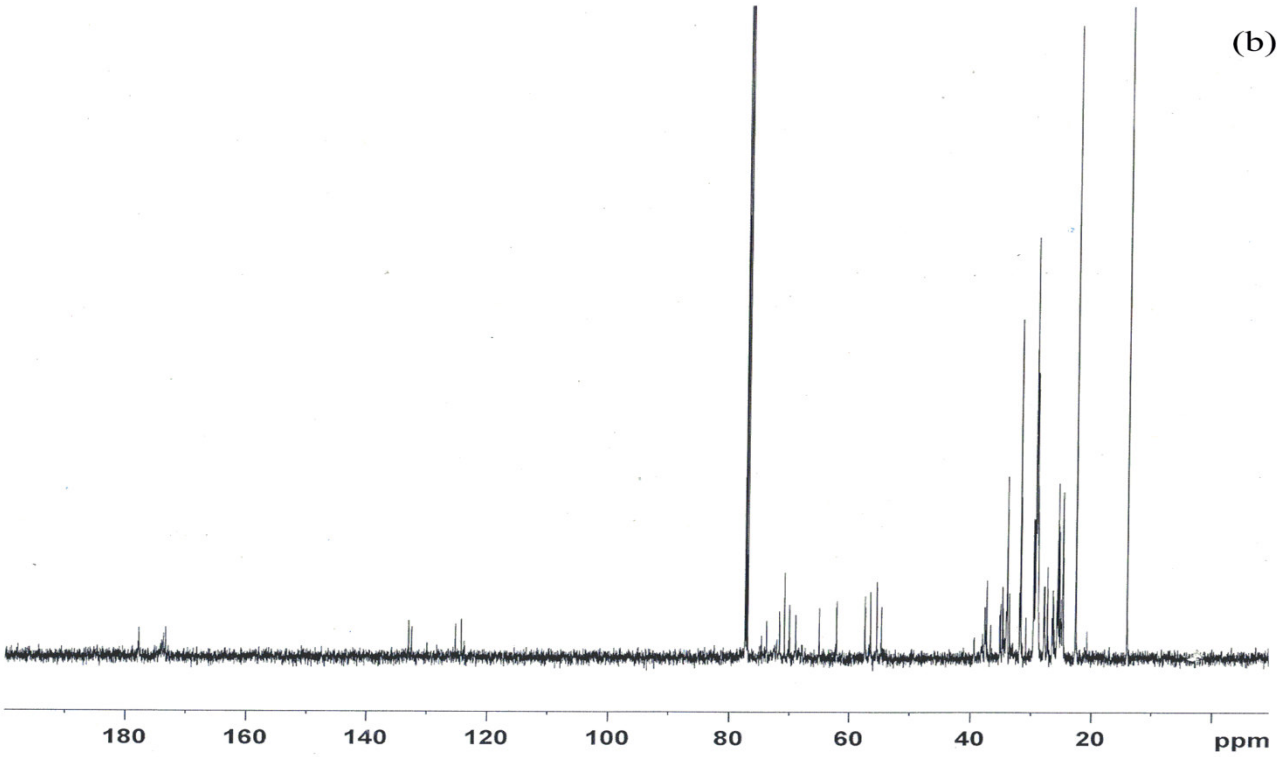

Figure 6.4: ^{13}C-NMR spectrums of CO (a) and CO epoxide (b)

6.3.2 Pour point determination by DSC

Estimation of pour point of the prepared product is important in order to determine the low temperature flow behaviour of modified (i.e. epoxide) and unmodified CO. It is a rough indication of lowest temperature at which epoxide is promptly pumpable (Salih et al. 2013). The DSC thermo-grams of CO and its epoxide are shown in Figures 3.5 and 6.5. From the pour point values of CO (20 ^{o}C) and its epoxide (-15 ^{o}C) it can be seen that after epoxidation (structural modification of CO) PP increased significantly (5 ^{o}C). This behaviour may be due to the conversion of unsaturation into epoxide and absence of double bonds in CO fatty acid composition increased the PP of epoxide. After structural modification, PP of CO epoxide was expected to increase at a higher range (around 8 - 12 ^{o}C), but due to the presence of unsaturation content and hydroxyl groups in CO epoxide no significant difference was encountered. However, Soriano et al. (2006) also observed similar kind of results during the

PP analysis of oils and esters. Elaborate literature survey on vegetable oils cold flow properties revealed that the cold flow property of plant oils is extremely inadequate and this restricts their use at lower operating temperatures. Plant oils have a tendency to form macro crystalline structures at low temperatures through uniform stacking of the triglyceride backbone. The formation of macro crystals restricts the free flow of fluid due to a loss of kinetic energy of individual molecules during the self stacking (Adhvaryu et al. 2005). In general, pour point should be low enough to ensure that the epoxide is pumpable at lower temperatures (Manivannan and Rajasimman 2011). Finally, from this study, it can be seen that the modification in the CO structure can alter the PP which is regarded as one of the major concern for plant oils to be used as an alternative to fossil resources. However, low temperature properties can be improved by additivation.

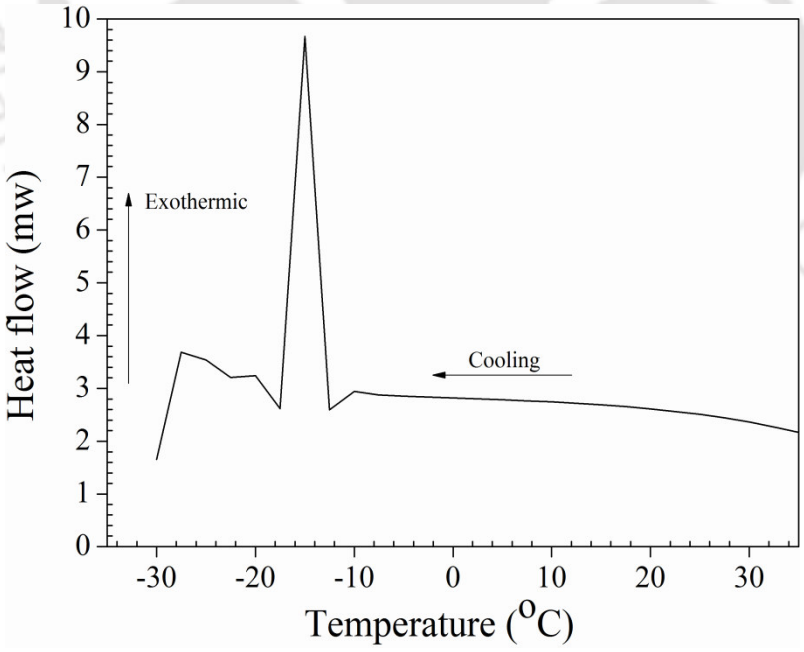

Figure 6.5: DSC thermo-gram for CO epoxide for pour point determination

6.3.3 Thermo-Oxidative Stability

The thermo-oxidative stability of CO and its epoxide was estimated by onset and oxidative onset temperatures. TGA thermo- grams of CO and its epoxide furnish the detailed information related to its degradation behaviour in the presence of inert gas (N_2) and reactive gas (air) (Figure 3.1 and 6.6). The onset temperature was reported as the first perceptible temperature at which the degradation of CO and its epoxides starts. From Figure 3.1, it can be seen that CO and its epoxide were stable up to 310 ^{o}C and 308 ^{o}C (on-set temperatures) respectively in an inert atmosphere. Similarly, maximum decomposition temperature represents the temperature at which utmost weight loss of CO and its epoxide samples occurred i.e. 371.5 ^{o}C and 350.5 ^{o}C. The lower thermal stability of epoxide signifies the degradation of epoxide at lower temperatures than the unmodified CO and the presence of high acid media also responsible for the lower thermal stability of CO epoxide (Blee et al. 2005).

Park et al. (2008) reported that oil with saturated and monounsaturation fatty acids content has a positive influence and more thermally stability than oil with polyunsaturation content. Since the double bonds were converted to epoxide, it was anticipated that epoxide could give higher thermal stability than unmodified CO, but due to the aforementioned reason lower thermal stability was noticed. Thermal stability of epoxide is important for various applications and it depends on chemical the composition and structure of epoxide.

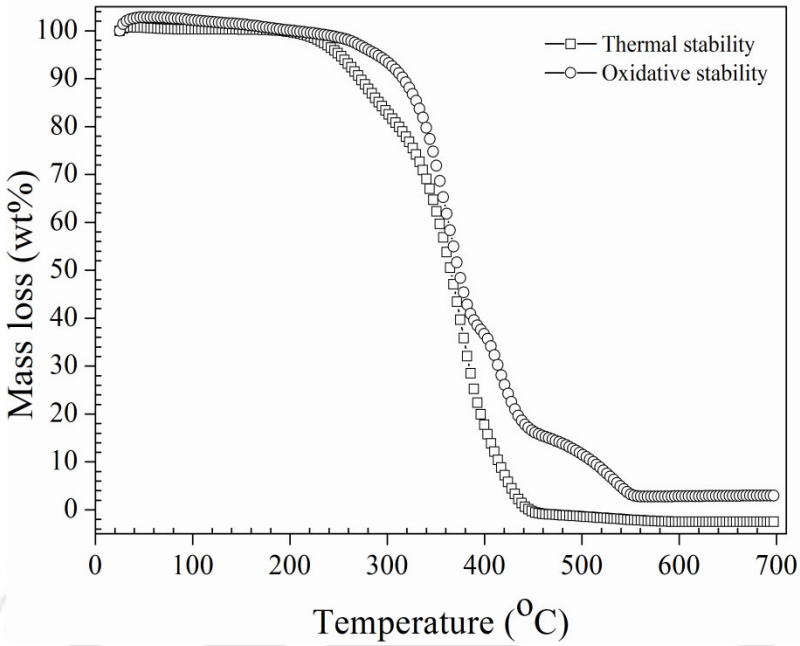

Figure 6.6: TGA thermo-grams for CO and CO epoxide under oxygen atmosphere (Oxidative Stability)

Similarly, oxidative stability was found as a quality indicative parameter under oxygen atmosphere. In the present study, oxidative stability is specified as the resistance of epoxide against oxidation in air atmosphere. Figure 6.6 describes TGA thermo-grams of CO epoxide, from the thermo-grams oxidative onset temperatures was found to be 320 ^{o}C for both modified and unmodified CO (Figure 3.3). Similarly, maximum decomposition temperature was found to be 382 ^{o}C and 354 ^{o}C respectively for CO and its epoxide. From the above discussion it is clear that CO epoxide demonstrated higher oxidative stability than CO. In addition to the aforementioned elucidation, this attitude can be justified by the presence of unsaturation in the epoxide sample. Finally, it can be concluded that CO was thermo-oxidatively more stable than structurally modified CO epoxide.

6.3.4 Viscosity, viscosity index of high FFA CO epoxide

The bulk rheological properties of CO epoxide were estimated using interfacial rheometer by varying shear rates from 0 to 500 s^{-1} at different temperatures such as 28, 40, 60, 80 and 100 ^{o}C. The kinematic viscosities of CO and its epoxide were reported to be 193.13 and 249.84 cSt respectively at 40 ^{o}C. Increase in epoxide molecular weight can be attributed to the addition of the oxygen molecule at the unsaturation sites thereby forming oxirane ring (Okieimen et al. 2005). The CO epoxide viscosity of 249.84 cSt indicates that viscosity was improved over unmodified CO and this signifies that synthesised CO epoxide can serves as an acceptable lubricant basestock with enhanced viscosity to reduce friction. The ability of substance to resist the free flow is one of the highly significant attribute for many heavy duty and industrial materials such as fuels, lubricants and surfactants (Park et al. 2008). Therefore, it is desirable that the viscosity must be high enough all the time to keep the good oil film between the moving parts to reduce friction (Park et al. 2008). Otherwise, due to the loss of lubricant there is a tendency to increase the friction there by resulting in power loss and rapid wear on the parts of the machine (Park et al. 2008). Viscosity is one of the crucial parameter when selecting a lubricant for a specific application, otherwise failure to use the right lubricant with a required viscosity when temperature extremes are expected; it may result in poor lubrication, equipment failure and damage (Anonymous 2009). As discussed above, the acceptable range of viscosity can't be covered by conventional vegetable oils, hence in this study structural modification was attempted to enhance the viscosity and molecular weight. Further, viscosity improvers can be added in the form of additives to improve the viscosity (Quinchia et al. 2009).

Similarly, it is also desirable to check the viscosity in terms of viscosity index (VI) which indicates the lower sensitivity of viscosity variations at higher temperatures. During

this study, CO and its epoxide VI was found to be 99.52 and 188.92 respectively. Higher VI of CO epoxide signifies that addition of an oxygen molecule at the unsaturation sites leads to an overall increase in the molecular weight of final epoxide product and increase in its viscosity index (Salih et al. 2013). Finally from the viscosity and VI data, it can be concluded that the prepared epoxide can act as high temperature lubricant basestock since the VI of epoxide (188.92) was found to be almost double than CO (99.52).

6.3.5 Rheological studies of high FFA CO epoxide

The rheological measurements were carried using interfacial rheometer to study the bulk rheological properties of high FFA CO epoxide by varying the shear rates from 0 to 500 s^{-1} at various temperatures (28, 40, 60, 80 and 100 ^{o}C). From Figure 6.7 and 6.8, it can be seen that in spite of temperature variations, shear stress vs shear rate relation was found to be linear and signifies Newtonian fluid behavior. Similarly, Figure 6.9 illustrates epoxide viscosity variation as a function of temperature over a temperature range varying from room temperature to 100 ^{o}C (28, 40, 60, 80 and 100 ^{o}C). Likewise, Figure 6.9 shows that epoxide viscosity decreased with an increase in the temperature which is due to the higher thermal movement among molecules (Salih et al. 2013). A favourably good agreement was found when the results were compared with the other studies (Soriano et al. 2006).

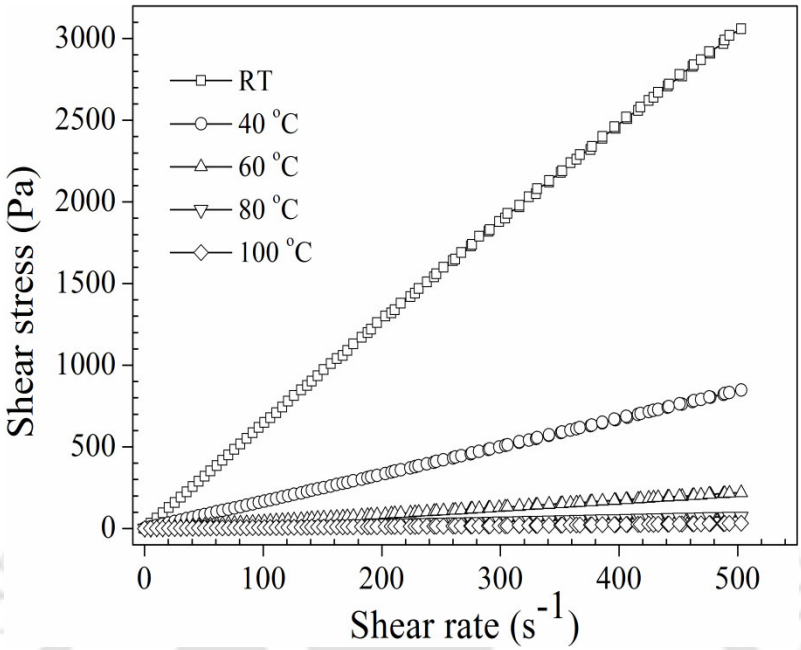

Figure 6.7: Shear stress versus shear rate relation for high FFA CO epoxide

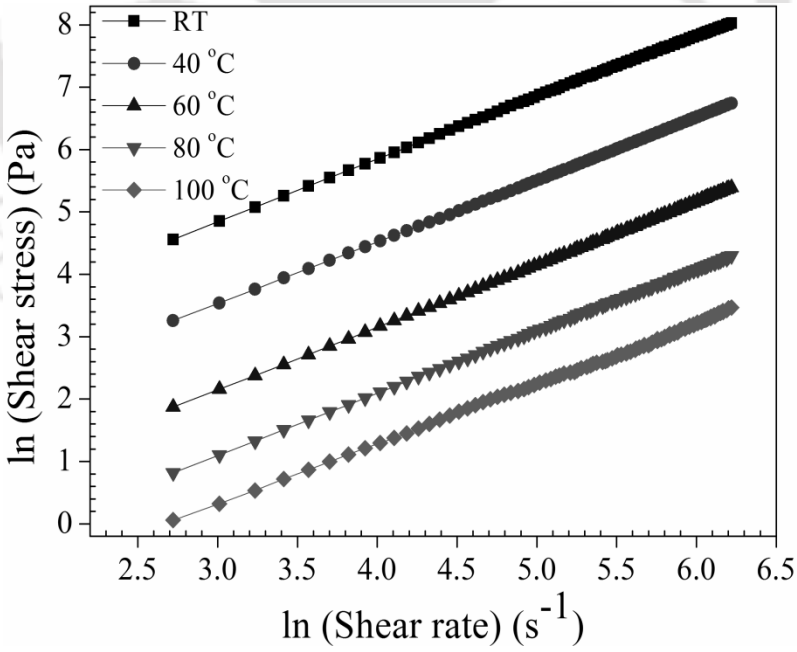

Figure 6.8: Logarithmic plot of shear stress versus shear rate for high FFA CO epoxide

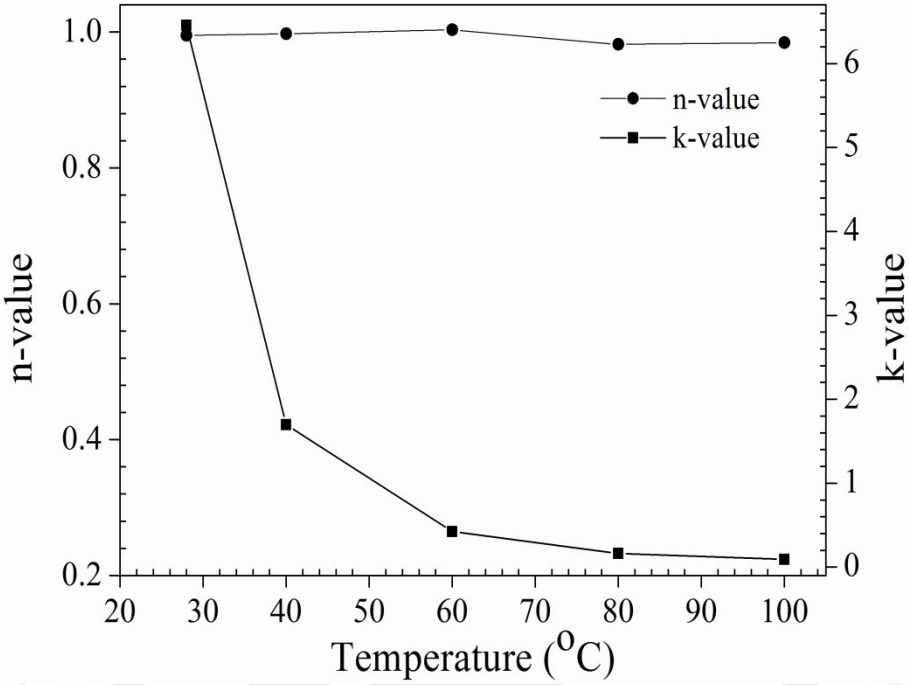

Figure 6.9: Plot of experimental value of n and k for CO epoxide at various temperatures

6.3.6 Physico-chemical characterization

The significant physico-chemical properties of CO and its epoxide were estimated and shown in Table 6.3. Acid value (AV) of CO and its epoxide was found to be 45.6 and 1.46 mg KOH/g respectively. Due to the high acid value of castor oil, we encountered some problem while processing the oil for structural modification as well as during characterization. The lower acid value of CO epoxide signifies the smooth operation and functioning of the equipment during its usage. The obtained FFA value was very less (0.73 mg KOH/g) and signifies trouble free performance of epoxide. During the study, density of CO was found to be 790.74 kg/m^3 and its corresponding epoxide was reported as 837.24 kg/m^3. Improvement in the density was assigned to increase in the molecular weight of epoxide by addition of oxygen molecule in the midst of unsaturation sites. Determination of IV (i.e quantity of the double bonds) after epoxidation reaction is one of the best ways to confirm and support the completion of epoxidation reaction. Initial IV of CO was found to be

89.69 (g I_2/100g of oil), whereas after epoxidation the value was 51.86 (g I_2/100g of epoxide). Higher IV of epoxide signifies that epoxidation reaction was incomplete and the same was noticed and discussed from ^{1}H-NMR spectral analysis. From Table 6.3, it can be seen that 71.96 % relative conversion of unsaturated bonds were converted into epoxide via epoxidation of castor oil (Table 6.3).

Table 6.3: Physico-chemical properties of high FFA CO and CO epoxide

Physico-chemical properties	CO Epoxide	CO
Acid Value (mg KOH/g)	1.46	45.6
Density (kg/m^3)	837.24	790.74
Iodine Value (gI_2/100g)	51.86	89.69
Kinematic Viscosity (cSt) at 40 ^{o}C	249.84	193.13
Moisture Content (wt %)	0.21	0.9
Pour Point (^{o}C)	-15	-20
Refractive Index (at 27.6 ^{o}C)	1.479	1.477
Viscosity Index (VI)	188.92	99.52
Oxirane Content (Experimental, mass%)	3.85	-
Oxirane Content (Theoritical, mass%)	5.35	-
Relative percentage conversion of oxirane (%)	71.96	-
Glycol content (Theoritical, mol/100g)	0.31	-
Glycol content (Experimental, mol/100g)	0.18	-
Relative percentage conversion α-Glycol (mol/100g)	40.67	-

α-glycol content confirms the presence of hydroxyl groups via oxirane cleavage. Theoretical and experimental values of α-glycol content along with the relative percentage conversion of α-glycol are calculated and reported in Table 6.3. Another most significant property of epoxide is moisture content which indicates the presence of water in epoxide

sample. The presence of moisture in epoxide supports the bacterial growth which leads to an undesired performance up on usage thereby increases AV, viscosity and formation of free radical compounds via oxidation. Therefore low moisture content is always preferred for epoxide. In this study, CO epoxide moisture content was found to be 0.21 wt% (Table 6.3) which was very less, indicates the usage of CO epoxide without trouble. The refractive index for both the samples were found to be almost similar 1.477 and 1.479 respectively (Table 6.3), which conveys that very small quantity of heat energy can pass through the CO and its epoxide samples, which is desirable to avoid the thermal degradation of end products during usage and storage.

6.4. Hydroxylation followed by hexanoylation of high FFA CO epoxide

In Chapter-4, a more detailed discussion of WCO epoxide hydroxylation followed by hexanoylation, as a representative example of structurally modified products with preliminary studies is provided. Based on the thorough it was clear that same optimum conditions can be used for high FFA CO hydroxylation and hexanoylation. Therefore, hydroxylation of high FFA CO epoxide was carried out at 10 mol of 2-EH, 3 wt% of H_2SO_4 catalyst loading, 30 min of reaction time at room temperature and 1500 rpm. Further, hexanoylation was also accomplished at 3 mol of hexanoic anhydride, 70 ^oC reaction temperature, 2 wt% of catalyst loading and 9 h of reaction time. During the study it was observed that, irrespective of lower OOC of CO epoxide, 10 mol of 2-EH and 3 mol of hexanoic anhydride required during the hydroxylation and hexanoylation of CO epoxide, which could be due the presence of excess hydroxyl group in the ricinoleic fatty acid structure. Apart from that subsequent transesterification of CO epoxide was also observed during hydroxylation. Hence, during hydroxylation higher amount of 2-EH (alcohol) was consumed for complete conversion of epoxides into hydroxyl groups and for

transesterification of triglycerol. Similarly, hexanoylation at 3 mol of hexanoic anhydride to alter the hydroxyl groups to ester groups. After completion of hydroxylation and hexanoylation reactions, products were purified by washing with sodium bicarbonate followed by diethyl ether and excess solvents (i.e. 2-EH and hexanoic anhydrides) were removed by a short path distillation column at high temperature (80 ^{o}C) and reduced pressure. The end products were dried with sodium sulphate and then used to evaluate their physico-chemical properties.

6.5. Physico-chemical characterization of hydroxylation and hexanoylation derivatives of high FFA CO

6.5.1 Product confirmation by NMR spectral analysis and GPC chromatography

The progress of hydroxylation and hexanoylation of high FFA CO epoxide reaction was monitored by NMR and FTIR analysis. But as disclosed above, due to high FFA content in CO, from the ^{13}C-NMR spectra incomplete conversion of unsaturation into epoxide and further ring opened product was noticed (Figure 6.3). Almost similar ^{13}C-NMR spectra were recorded for epoxide and hydroxylated products and hence it was difficult to identify the products. Therefore, GPC analysis was used to confirm the hydroxylated and hexanoylated product formation. As reported in Table 6.4, molecular weights of hydroxylated and hexanoylated products were increased compared to the epoxide, which signifies that the alkyl and ester groups were functionalized. Similarly, from the following section decreasing trend of pour point also confirmed the formation of hydroxylated and hexanoylated products compared to high FFA CO epoxide.

Table 6.4: Molecular weights of high FFA CO epoxide, hydroxylated and hexanoylated products

Sample	Number Avg. Mol. Wt.	Weight Avg. Mol. Wt.
CO	979	1124
CO epoxide	1197	1320
CO hydroxylation	1488	1770
CO hexanoylation	1780	1920

6.5.2 Viscosity, viscosity index and rheological properties of prepared hydroxylated and hexanoylated products

The kinematic viscosity and viscosity index of prepared hydroxylated and hexanoylated products were evaluated and shown in Table 6.5. From the table it can be seen that, with an increased in branching from hydroxylation to hexanoylation (mono-esters to di-esters), reduction in the viscosity was detected, Mahajan et al. (2013) also noticed alike findings during their study on chemically modified epoxidised mustard oil for bio-lubricant application. The viscosity index which is considered as the measure of change in viscosity with respect to temperature is very much dependent on attached terminal groups. As reported in Table 6.5, it was observed that the viscosity of ring opened product with branching of 2-EH decreases, however viscosity index increases. Yao et al. (2010) stated that, VI increases with molecular weight and in the present study it was found to be 192 for hydroxylated CO derivative, similarly for di-esters it was found to be 30 which indicate that, viscosity variations are high with varying temperature.

The rheological behavior of CO derived di-esters were determined by varying shear rate (0 – 500 s^{-1}) at different temperatures (25, 40, 60, 80 and 100 ^{o}C) and demonstrated in Figures 6.10 (a) and (b). From figures it was noticed that, in spite of increase in the temperature, shear rate increases with respective to shear stress, this linear relation between

shear stress versus shear rate suggests Newtonian behaviour for the sample. Moreover, with an increase in the temperature decrease in the viscosity was also encountered (Figures 6.10(b)).

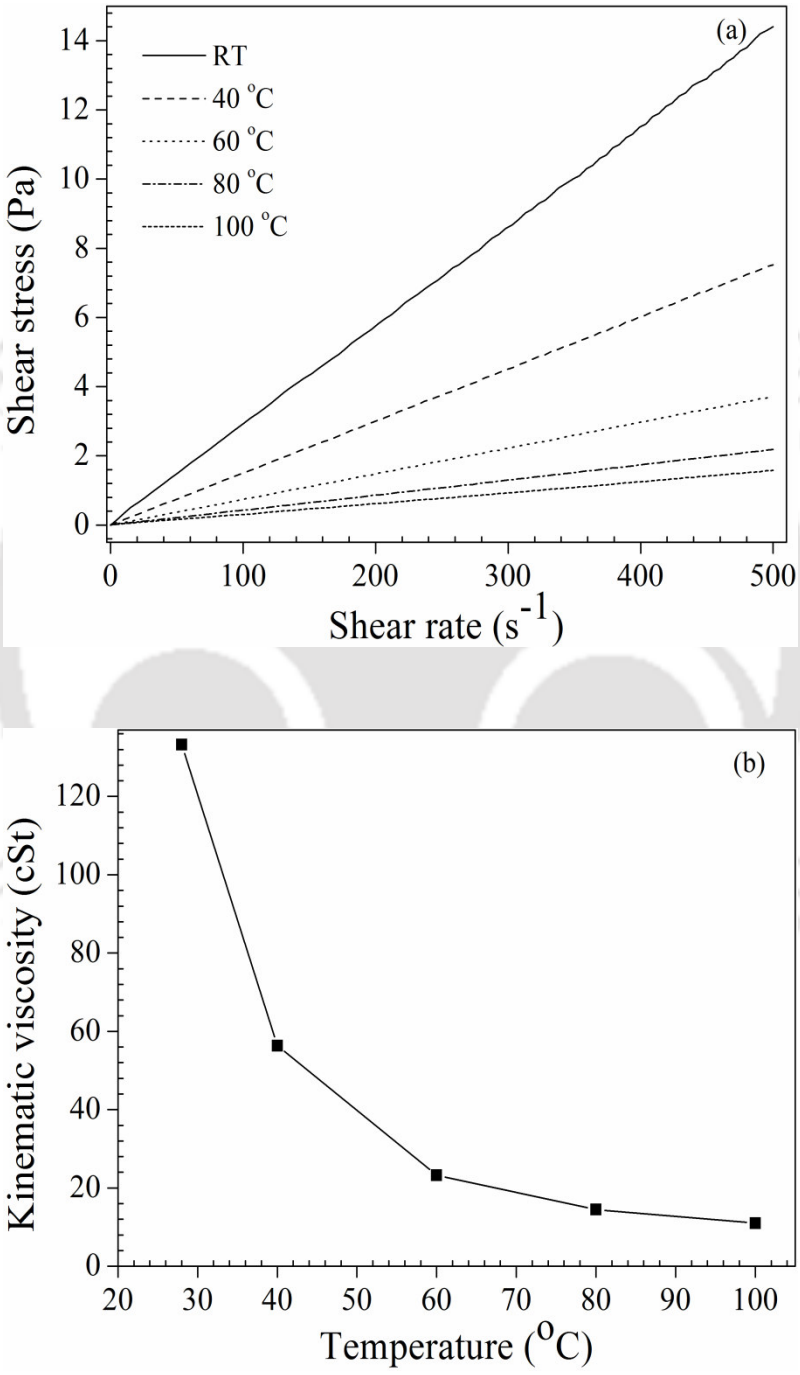

Figure 6.10: Shear stress versus shear rate (a) and temperature versus kinematic viscosity (b) relation for CO derived di-esters

Table 6.5: Kinematic viscosity and viscosity index of hydroxylated and hexanoylated products

Sample	Kinematic Viscosity (cSt)		Viscosity Index
	@40 ^{o}C	@100 ^{o}C	
CO epoxidation	11311	291	128
CO hydroxylation	56.37	11	192
CO hexanoylation	15.54	3.13	30

6.5.3 Thermo-oxidative stability, cold flow properties of CO derived hydroxylated and hexanoylated products

The thermo-oxidative stability and peak temperatures (maximum degradation temperatures) result of the hydroxylated (Figure A.28) and hexanoylated (Figure A.29) products obtained using TG analysis of CO derived products are reported in Table 6.6. From the outcomes of thermal stability data it could be found that via hydroxylation and hexanoylation (chemical modifications), onset temperature decreased significantly. Initially, for high FFA castor oil OT was found to be 308 ^{o}C, whereas, for hydroxylated and hexanoylated product it was found to be 272.8 ^{o}C and 236.6 ^{o}C respectively. Likewise, oxidative stability (OOT) of CO epoxide, hydroxylated and hexanoylated products were found to be 320 ^{o}C, 241.9 ^{o}C and 235.7 ^{o}C respectively. The comparative analysis of OT and OOT results revealed that structural modification of high FFA CO by extending the chain length and branching decreases the thermal and oxidative stability.

Table 6.6: Onset, oxidative onset, peak temperatures and pour points of the prepared CO derived hydroxylation and hexanoylation products

Sample	Thermal stability (^{o}C)		Oxidative stability (^{o}C)		Pour Point (^{o}C)
	OT	PT	OOT	PT	
CO hydroxylation	272.8	348.6	241.9	283.8	-16 ± 0.26
CO hexanoylation	236.6	319.8	235.7	270	-27.65 ± 0.52

Besides stability, CO derived hydroxylated and hexanoylated products pour point were found to be -16 ± 0.26 ^{o}C (Figure 6.11 (a)), -27.65 ± 0.52 ^{o}C (Figure 6.11 (b)) respectively. The hydroxylation of high FFA CO epoxide by 2-EH alkyl group (C_7H_{17}) gave almost identical pour point with epoxide, but increase in the molecular weight was observed compared to epoxide as an indication that hydroxylation reaction taken place (Table 6.6). Nevertheless, hexanoylation step alone showed almost -16 ^{o}C increased in the pour point, this could be attributed to the functionalization of ester group ($CH_3(CH_2)_4CO_3$) by hexanoic anhydride. The functionalization of 2-EH and hexanoic anhydride to ricinoleic fatty acid chains demonstrated the most effective reduction in the PP temperature and this could be attributed to the presence of large branching group at the midst of fatty acid chain and it makes a steric barrier around the individual molecules and suppresses formation of crystal growth which results in lowering samples PP (-27.65 ^{o}C).

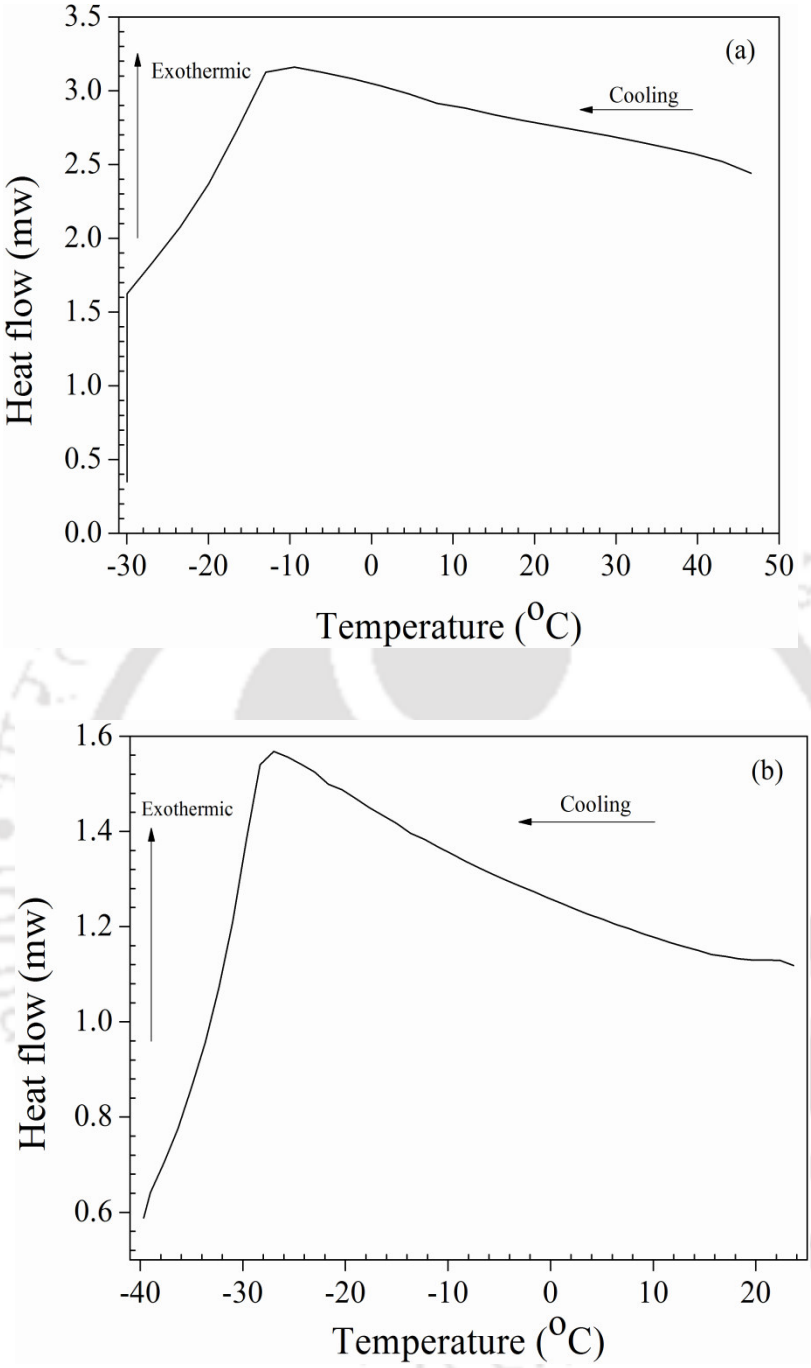

Figure 6.11: DSC thermo-grams for CO hydroxylation (a) and hexanoylation (b)

6.5.4 Tribology and bio-degradability of hexanoylated CO

The anti-wear and friction reducing properties of the prepared hexanoylated high FFA CO was evaluated using HFRR lubricity test. Details about the experimental and analysis part are

well explained in Chapter-2 in section 2.6.14. From the obtained results wear scar diameter was found to be 287 µm, 227 µm, 257 µm (x-axis, y-axis and average, Figure 6.12), with a film thickness of 28 % and co-efficient of friction (CoF) as 0.076. The lower film thickness and co-efficient of friction ascribed to the presence of excess hydroxyl groups in the ricinoleic acid fatty acid structure of castor oil. All the tribological properties are within the acceptable range to use them as lubricant basestocks by comparing with studies conducted by Madankar et al. (2013).

The biodegradation profile of duplicate test run carried out with high FFA CO derived hexanoylated product was found to be 95.45 % ± 1.21. Results of the study revealed that, the prepared high FFA CO derived di-esters was biodegradable and the results obtained are reproducible.

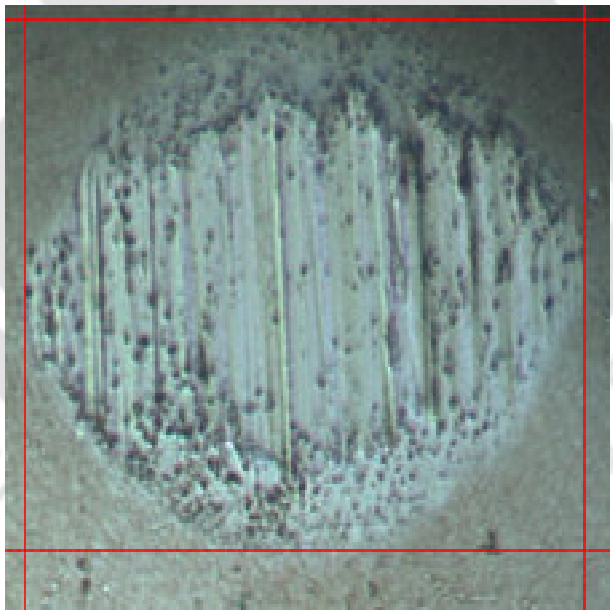

Figure 6.12: Microscopic wear scar image for high FFA CO derived di-esters

6.6. Summary

This chapter highlights the diverse products properties for CO derived bio-lubricant basestocks, when the free fatty acid (FFA) was higher in the feedstock. This chapter also

contributed first report of its kind in the literature on the preparation of bio-lubricant basestock from high FFA CO (45.6 mg KOH/g). The optimum reaction condition for CO epoxidation were; temperature, 52.81 ^{o}C; H_2O_2, 1.65 mol; catalyst loading, 15.14 wt%; and reaction time, 2.81 h. At this condition, maximum epoxide content was found to be 3.85 mass%. Insignificant changes were detected in the epoxidised product compared to CO (OT (2 ^{o}C difference), PP (5 ^{o}C difference), and identical OOT). Further, modification of CO epoxide structure by hydroxylation and hexanoylation showed OT, OOT and PP as 236.6 ^{o}C, 235.7 ^{o}C and -27.65 ^{o}C. Remarkable biodegradability (95.45 %) and tribological performance (WSD - 257 µm, friction co-efficient -0.076, film thickness - 28%) was noticed for hexanoylated CO. But, showed minimum improvement in the thermo-oxidative stability, which may be due to inbuilt hydroxyl groups (i.e., ricinoleic acid) in the CO triglyceride structure. Addition to that, higher FFA based feedstocks are easily susceptible to thermal and oxidative degradation. Hence, from this study, it could be implicit that, feedstocks containing higher FFA are not acceptable for bio-lubricant formulation and application.

CHAPTER-7

Preparation of biodegradable lubricant basestocks from castor oil fatty acid methyl esters

This chapter explores the preparation and characterization of bio-lubricant basestocks from castor oil fatty acid methyl esters originated from high FFA oil feedstock. Series of structural modifications were carried out to enhance the thermo-oxidative stability and cold flow properties of methyl esters by epoxidation, hydroxylation and hexanoylation. Epoxidation of CO methyl esters was optimized to maximize the OOC and to find out the impact of process variables on response. The physico-chemical characterization of COFAME epoxide exhibited poor low temperature properties. Therefore, in order to enhance the low temperature properties, functionalization of 2-EH and hexanoic anhydride to epoxidised methyl ricinoleate was carried out. In summary, thermo-oxidative stability, cold flow properties of hydroxylated product, tribological characteristics and biodegradability of the hexanoylated product has been investigated.

7.1. Optimization of COFAME epoxidation: Statistical analysis

In the present study, to optimize the COFAME epoxidation process parameters, preliminary studies were carried out for four process variables by a single parameter optimization technique (Figure 7.1); the optimum range of each process variables are reported in Table 7.1. Based on the preliminary study data (Table 7.1, Figure 7.1), experimental matrix was generated using CCD optimization technique and presented in the appendix (Table A.4). The CCD model experimental design matrix consists of total 30 runs were carried out at laboratory conditions (Table A.4). To determine whether second order polynomial model is valid or not (Eq. (7.1)), it is necessary to conduct the analysis of variance (ANOVA) (Table

7.2) for maximum OOC. ANOVA table was used to ensure a good model for each term in models; a large F-value and small p-value would imply a more important effect on the respective response variables (Mahmoud et al. 2014). Therefore, in the present study, all linear, quadratic, and cross variables showed a significant effect on OOC maximization. The results in Table 7.2 showed that this regression was statistically significant at an F-value of 5,084.414 and at $p < 0.0001$. There is only a 0.01% chance that an error could occur owing to the noise in the model F-value. The lack of fit F-value of 16.45 implies the lack of fit is significant. Likewise, there is only a 0.32% chance that an error could occur as a result of noise in the lack of fit F-value. The predicted R-squared value of 0.9988 is in reasonable agreement with the adjusted R-squared value of 0.9996. An adequate precision measures the signal to noise ratio, with a ratio greater than four being desirable; in the current study, the adequate precision ratio of 287.372 indicates that the obtained ratio is an adequate signal, and this model can be used to navigate the design. The coefficient of variation (CV) is the ratio of the standard deviation to the mean value of the observed response variable and is a measure of model reproducibility (Borugadda and Goud 2014a). In general, a model can be considered reasonably reproducible if the CV is no greater than 10%, the relatively lower value of CV (0.42%) indicates the better precision, reliability, and reproducibility of the experiments performed.

$$\text{Response (OOC)} = 4.01 - 0.01785\,A - 0.07629\,B + .065875\,C - 0.47916\,D - 0.13569\,A^2 - 0.14292\,B^2 - 0.11705\,C^2 - 0.36494\,D^2 - 0.10274\,AB - 0.02617\,AC - 0.37305\,AD + 0.269238\,BC - 0.32636\,BD + 0.09145\,CD \quad (7.1)$$

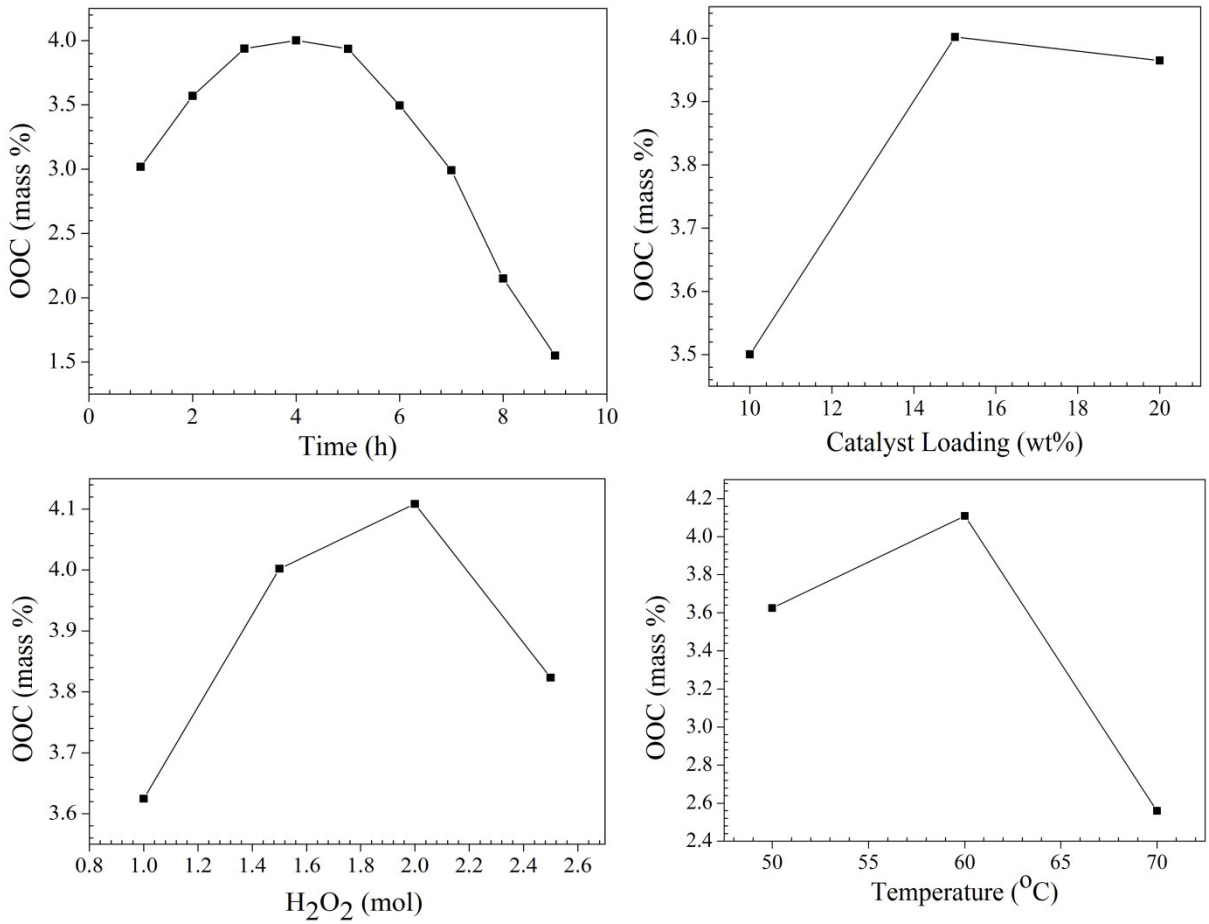

Figure 7.1: Effects of reaction variables time, catalyst loading, hydrogen peroxide and temperature on epoxidation of COFAME (preliminary studies)

Table 7.1: Epoxidation process variables and their levels for response surface design for COFAME epoxidation

Independent variables	Symbol	Unit	Coded levels		
			-1	0	+1
Time	A	h	3.3	4.3	5.3
Catalyst Loading	B	wt%	10	15	20
Oil: Hydrogen Peroxide (H_2O_2)	C	mol	1.5	2	2.5
Temperature	D	^oC	50	60	70

Table 7.2: Regression coefficients of predicted and quadratic polynomial model for response variable (OOC) for epoxidised COFAME

Source	Sum of squares	Degrees of freedom	Mean square	F value	p-value (prob > F)
Model	15.25771	14	1.089836	5084.414	< 0.0001
A-Time	0.007647	1	0.007647	35.67527	< 0.0001
B-Cat Load	0.139672	1	0.139672	651.6106	< 0.0001
C-H_2O_2	0.104149	1	0.104149	485.8872	< 0.0001
D-Temp	5.510187	1	5.510187	25706.68	< 0.0001
AB	0.168896	1	0.168896	787.9522	< 0.0001
AC	0.010954	1	0.010954	51.10238	< 0.0001
AD	2.226601	1	2.226601	10387.76	< 0.0001
BC	1.159821	1	1.159821	5410.915	< 0.0001
BD	1.704147	1	1.704147	7950.36	< 0.0001
CD	0.13381	1	0.13381	624.2622	< 0.0001
A^2	0.504981	1	0.504981	2355.889	< 0.0001
B^2	0.560231	1	0.560231	2613.644	< 0.0001
C^2	0.375765	1	0.375765	1753.055	< 0.0001
D^2	3.653046	1	3.653046	17042.56	< 0.0001
Lack of Fit	0.00312	10	0.000312	16.45199	0.0032

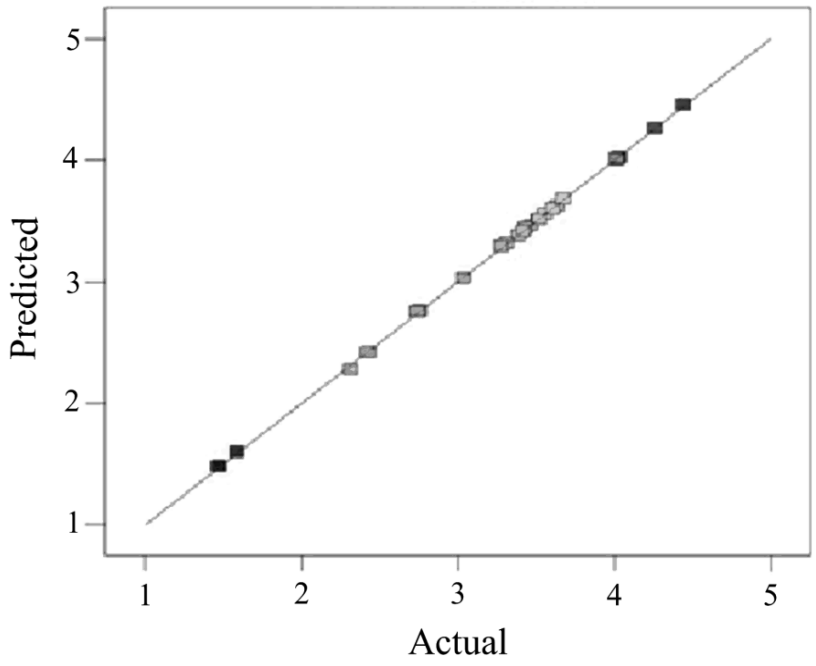

Figure 7.2: Predicted versus Actual plot of response (OOC) for COFAME epoxidation

7.2. Mutual effects of process variables on maximum OOC

During the optimization process of WCO, WCOFAME and CO epoxidation reactions, this thesis has thoroughly studied the interaction among the process parameters to understand their effect to maximize OOC. Therefore, based on earlier studies in Chapters 4, 5 and 6, this chapter directly introduced the optimum condition for COFAME epoxidation by giving a summary on relationship and effect of process parameters for maximum OOC. The actual and predicted OOC plot for maximum oxirane content is displayed in Figure 7.2. The optimum levels of each process variable and their interaction effect on maximum OOC were studied by plotting three dimensional response surface plots and two dimensional counterplots. The response surface and counterplots were plotted against any two independent variables by fixing other variable to a zero level (Figures A.30 – A.35). Figure A.28 shows the effect of time and catalyst loading and their mutual effect, the OOC increased with an increase in the time and catalyst loading up to certain period and then decreased beyond 5.3 h of reaction time and catalyst loading of 20 wt%. Higher catalyst

loading and a longer reaction time led to the formation of undesired products, as reported by Borugadda and Goud (2014a, 2014b). Higher amounts of catalyst and prolonged reaction time provide a platform for oxirane cleavage. Therefore, from RSM study, the optimum time and catalyst loading for maximum OOC was found to be 5.26 h and 19.43 wt%. Similar results were obtained for other interactions with the time and catalyst loading (Figures A.30 - A.35). Alike observations were reported by other researchers during their study on epoxidation of wild safflower oil (Meshram et al. 2011).

The effects of H_2O_2 molar ratio, temperature, and their interaction on maximum OOC are depicted in Figure A.35. The OOC increased with an increase in H_2O_2 molar ratio; similarly, OOC was found to increase without increase in the temperature up to 60 ^oC, beyond which more oxirane cleavage was detected. Mungroo et al. (2008) have shown the formation of oxirane cleavage beyond 60 ^oC, and another study by Mungroo et al. (2011) supports the observations in the present study. Correspondingly, from Figures A.30 – A.35 the optimum H_2O_2 molar ratio and temperature for maximum OOC was found to be 2.54 mol and 50 ^oC. The use of lower operating temperatures also helps in obtaining a higher selectivity of desired product.

7.2.1 Validation of developed model

The main purpose behind validation of the experiments was to corroborate the accuracy of predictive model; for that reason, three validation run tests were performed. The last step of RSM after choosing the optimal parameter combination was to predict and verify the performance characteristics with the chosen optimum process variables. The predicted optimal condition based on the RSM was hydrogen peroxide molar ratio 2.34, catalyst loading 19.43 wt%, temperature 50 °C, and reaction time 5.26 h. Since the fatty acid composition of each feedstock is unique, all the optimum conditions are suitable for the

respective feedstock (local optima). After carrying out the epoxidation at optimum condition for three times, the average OOC was found to be 4.38 mass%, and experimental results confirmed the effectiveness of a response surface model on optimum OOC. The percentage error between the experimental (4.38 ± 0.02 mass%) and predicted (4.44 mass%) values for maximum OOC was found to be 1.35%. The experimental values were closely associated with the result obtained from RSM, and validate the findings of response surface optimization, and ultimately showed that the developed empirical model was accurate and reliable.

7.3. Physico-chemical characterization of prepared COFAME epoxide

7.3.1 Product confirmation by NMR

The ^{1}H-NMR spectra of COFAME and its epoxide are shown in Figures 7.3 (a) and (b). The epoxide product was confirmed by the disappearance of double bonds (unsaturation) at δ 5.3 to 5.6 ppm (Figure 7.3 (b)) and the appearance of epoxy group at δ 2.9-3.2 ppm (Figure 7.3 (b)) region in the epoxidised castor oil fatty acid methyl esters. Similar kind of results was noticed by Salimon et al. (2011) during their study on ricinoleic acid epoxidation.

Similarly, completion of the epoxidation reaction was also confirmed by ^{13}C-NMR spectral analysis. As shown in Figures 7.4 (a) and (b), peaks at δ 125 – 135 ppm were completely removed (unsaturation, Figure 7.4 (a)) and the additional peak of methyl ricinoleate was observed at δ 50 ppm (Figure 7.4 (b)), which confirms the complete removal of glycerol from CO and the formation of methyl esters. Similarly, the complete disappearance of olefinic carbons from the COFAME epoxide (C=C at δ 125 – 135 ppm, Figure 7.4 (b)) and the visual aspect of new peaks at δ 53 – 59 ppm confirmed the complete conversion of double bonds into epoxide (Figure 7.4 (b)).

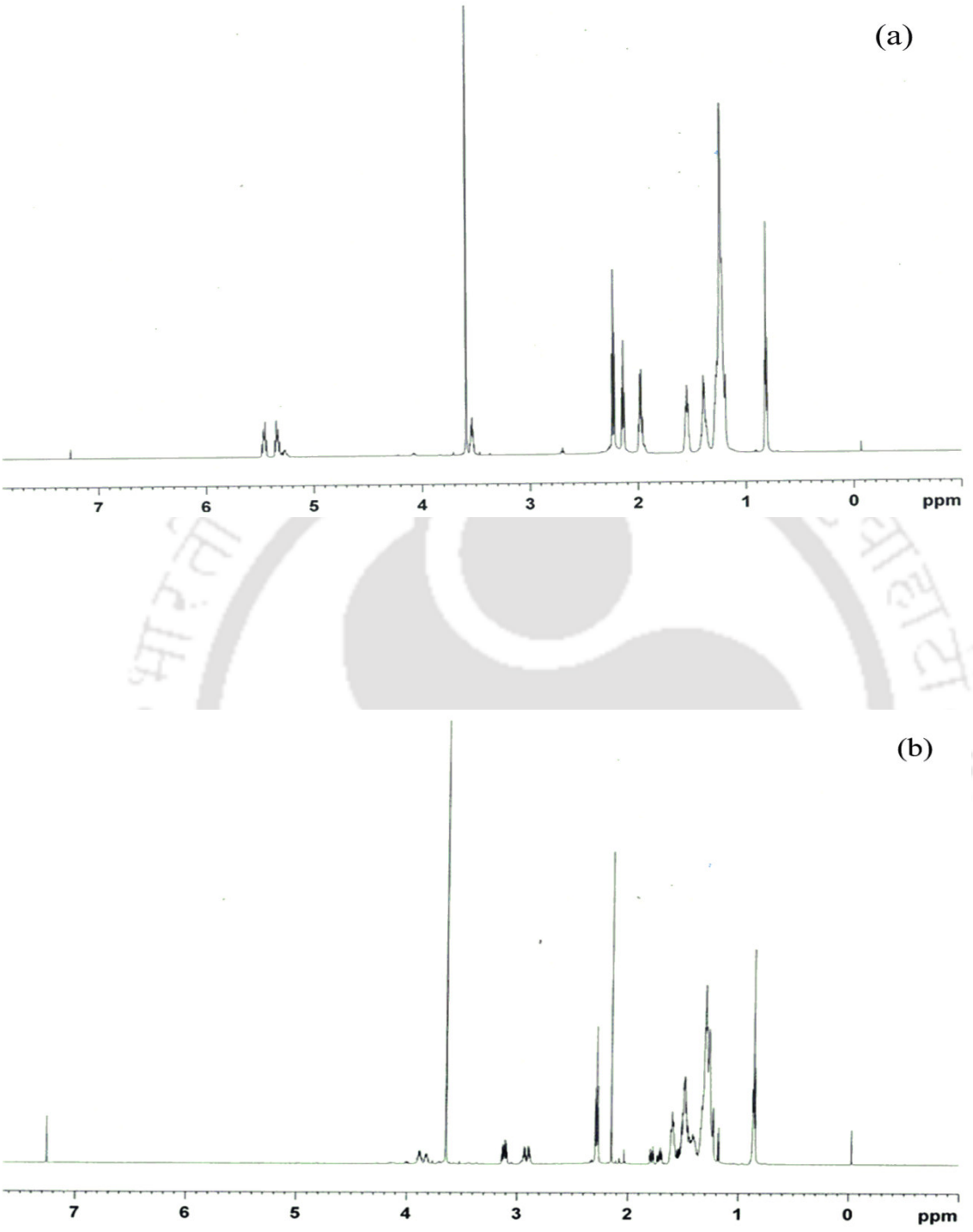

Figure 7.3: ^{1}H-NMR spectrums of COFAME (a) and COFAME epoxide (b)

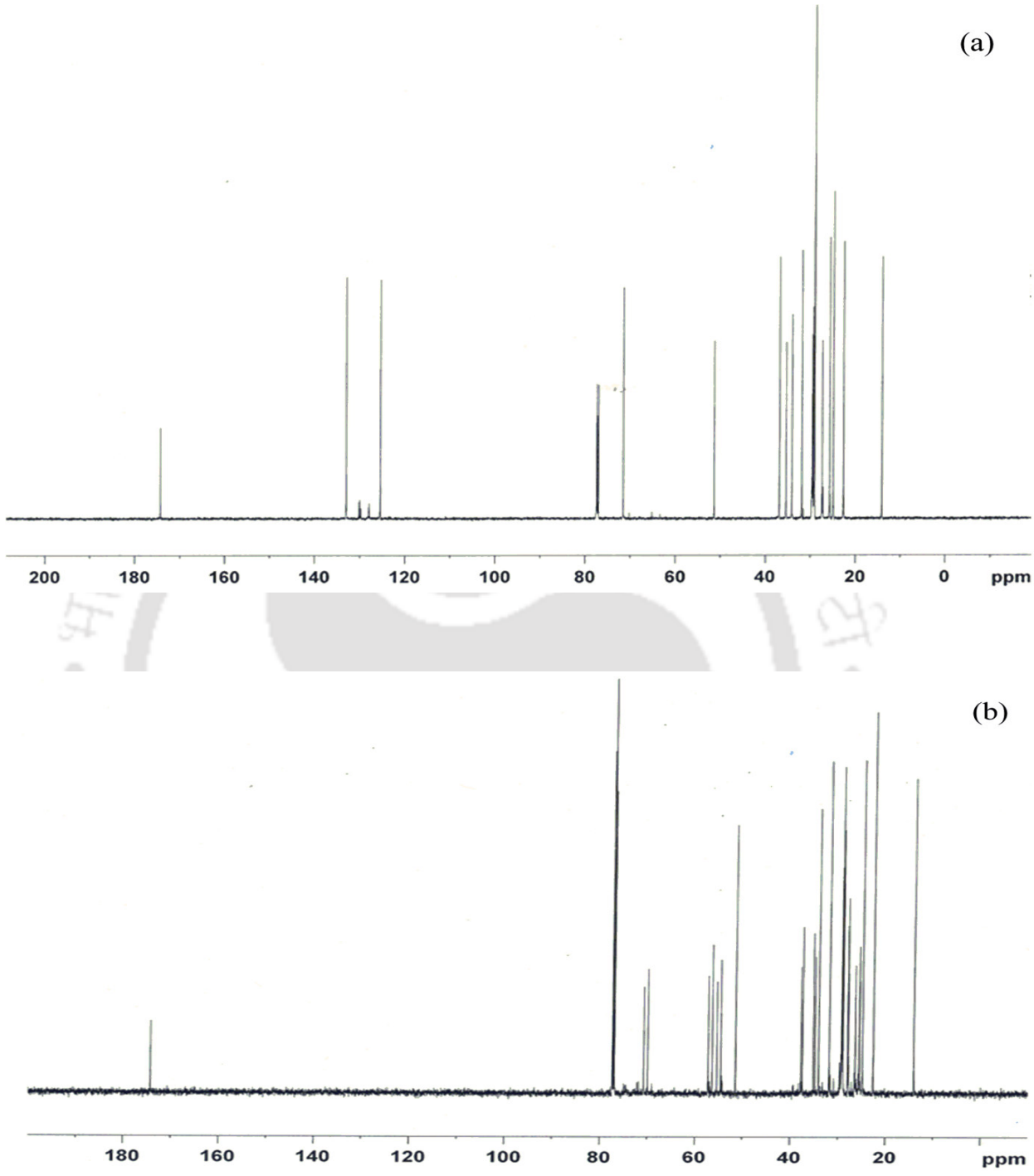

Figure 7.4: ^{13}C-NMR spectrums of COFAME (a) and COFAME epoxide (b)

7.3.2 FTIR Spectroscopy

The FTIR spectrum exhibits several absorption peaks as shown in Figure 7.5. The FTIR peaks of COFAME indicates that there is an unsaturation at 3400 cm^{-1} (C=C). But, after the epoxidation unsaturation peak was disappeared in the same range and an additional peak appeared at 823 - 843 cm^{-1} range. The appearance of epoxy peak at 820 - 843 cm^{-1} provided evidence that epoxidation reaction occurred using ion-exchange resin as catalyst. The change of functionality at this range indicates that all the double bonds were transformed into oxirane rings and the same is highlighted in Figure 7.5. Salimon et al. (2011) described that characteristic signals in the FTIR spectrum of ricinoleic acid at 823 - 843 cm^{-1} represent the quaternary carbons of oxirane ring. The complete disappearance of C=C bonds in the COFAME epoxide spectra (Figure 7.5) further supported almost complete conversion of double bonds in to oxirane (i.e. 98.5%). In this study FTIR spectra exhibited trace of –OH absorption peak at approximately 3000 - 3500 cm^{-1} which represents the presence of hydroxyl groups in the COFAME and its epoxide. These hydroxyl groups are belongs to the ricinoleic acid which is the major fatty acid in COFAME composition.

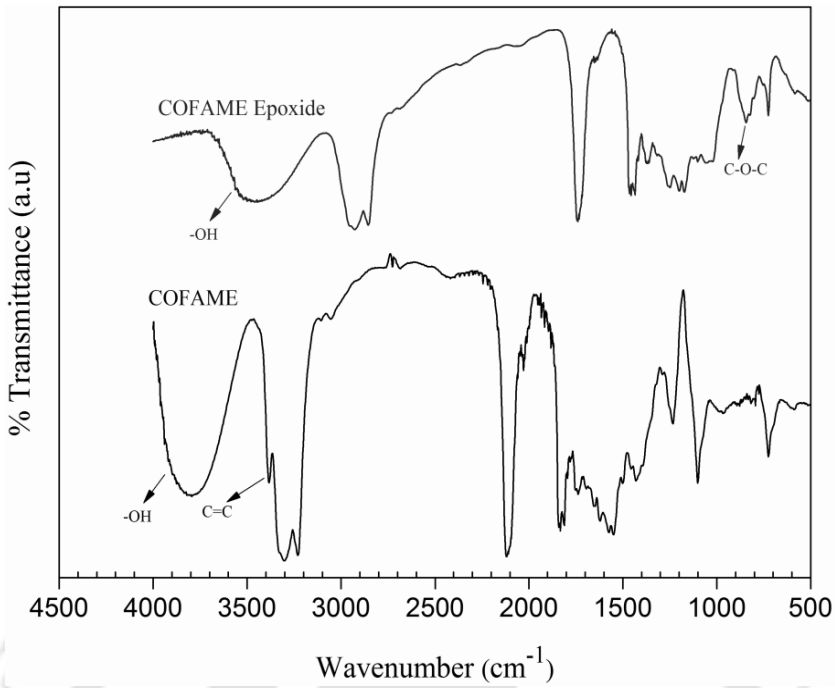

Figure 7.5: FTIR spectra of COFAME and COFAME epoxide

7.3.3 Cold flow properties by DSC

Figures 3.11 and 7.6 represents dynamic DSC plot of COFAME, from Figure 3.11 it can be seen that COFAME has a PP of −13 ± 1.5 ^{o}C, similarly for COFAME epoxide, PP was found to be −10 ± 1 ^{o}C. During epoxidation, unsaturation content in the COFAME was transformed into oxirane (^{13}C NMR spectra, Figures 7.4 (a) and (b)), after epoxidation (structural modification) significant increase in the pour point was observed (i.e. 3 ^{o}C). Difference in the PP attributed to the modification of ricinoleate methyl ester structure. Borugadda and Goud (2013, 2014c) reported that the PP of vegetable oils and methyl esters completely depends on their structure and fatty acid composition. The mono and polyunsaturated fatty acids content plays a major role in the PP value; higher the unsaturated fatty acids content in the sample, lower the PP and vice versa.

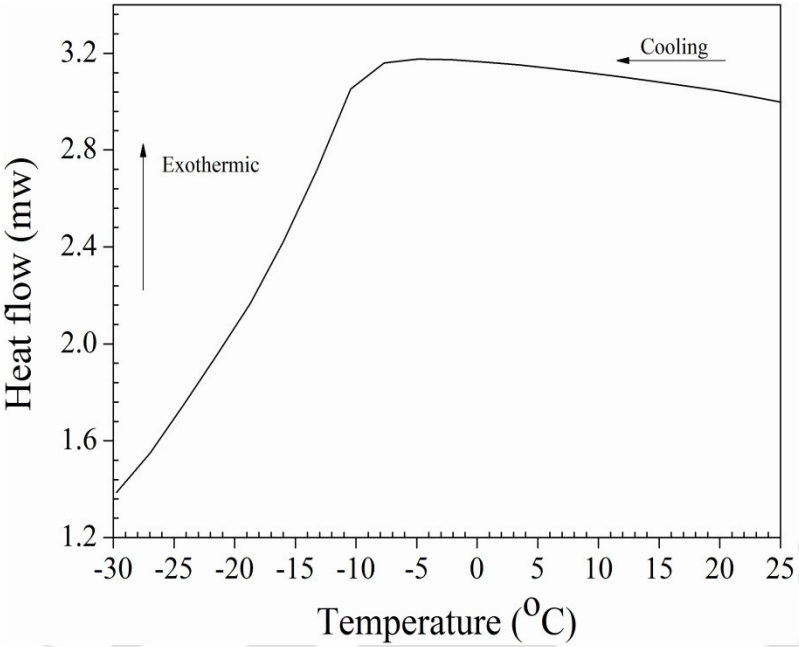

Figure 7.6: DSC thermo-gram for COFAME epoxide for pour point determination

7.3.4 Thermo-oxidative stability

Thermo-oxidative stability of COFAME and epoxidised COFAME was determined from onset temperatures (OT) of thermal decomposition under nitrogen atmosphere. TG curves of COFAME and epoxidised COFAME is shown in Figures 3.7 and 7.7. From figures it can be seen that COFAME and epoxidised COFAME were thermally stable up to 203 and 260 ^{o}C respectively. Beyond the onset temperature decomposition pattern was noticed. The epoxidised COFAME was found to be thermally more stable than COFAME. Higher thermal stability of COFAME epoxide attributed to the removal of unsaturation content in the COFAME fatty acid chain, which improves the thermal stability of epoxide. Alike results were reported by Jin et al. (2008) during their thermal stability study on epoxidised soybean and castor oil.

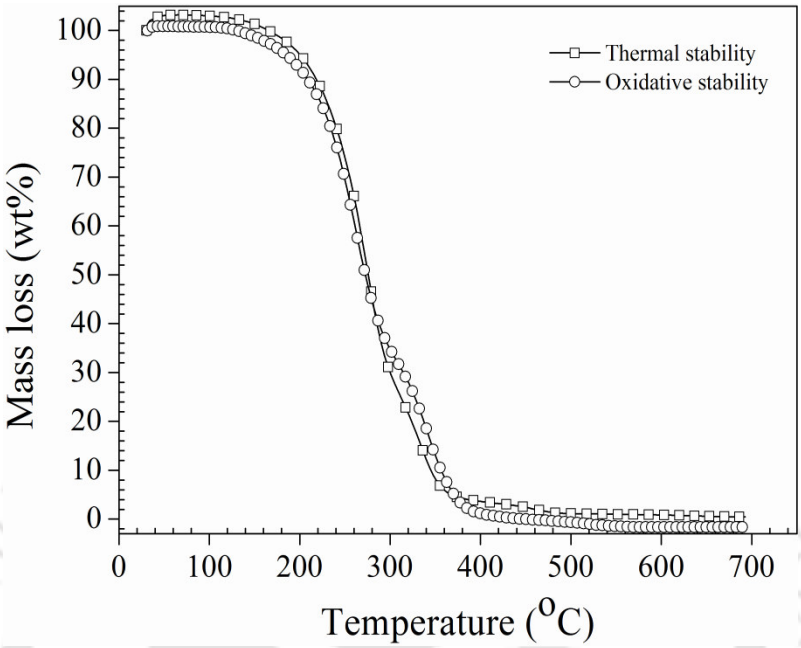

Figure 7.7: TG thermo-grams for COFAME epoxide in N_2 and O_2

Similarly, the oxidative stability of COFAME and epoxidised COFAME were measured from the oxidative on-set temperature under oxygen atmosphere. TG, DTG thermo-grams of COFAME and its epoxide are shown in Figures 3.9 and 7.7. During the analysis single stage degradation pattern was noticed for all the samples. The oxidation onset temperature (OOT) estimated from respective TG curves and was found to be 218 ^{o}C and 250 ^{o}C respectively for COFAME and its epoxide. Beyond OOT, gradual increase in the temperature showed considerable weight loss. From the oxidative onset temperature of epoxidised COFAME and COFAME it was observed that process of decomposition of COFAME initiated and completed within a temperature range inferior to epoxidised COFAME. Altogether, thermo-oxidative stability of epoxidised COFAME (structurally modified ester) was found to be higher compared to COFAME. From this investigation it could be concluded that epoxidised COFAME can act as a potential alternative to

conventional hydraulic lubricant. Higher thermo-oxidative stability was ascribed to the removal of unsaturation from the COFAME fatty acid structure. Several authors (Farias et al. 2002; Park et al. 2008; Kamalakar et al. 2013) reported that plant oil esters with saturated fatty acids and mono un-saturation content has a positive influence, and are thermally and oxidatively more stable than the esters with poly-unsaturation content.

7.3.5 Rheological behaviour of COFAME and COFAME epoxide

The rheological behaviour of COFAME and its epoxide is presented in Figures 7.8-7.10. From the figure it can be seen that shear stress increases with an increase in the shear rate, this linear trend signifies that all samples exhibit Newtonian flow behavior. The rheological behavior of COFAME and its epoxides as a function of temperature is also examined on logarithmic scale and shown in Figure 7.9. From the viscosity plot it can be seen that epoxide viscosity decreased with an increase in the temperature. This behaviour was attributed to the higher thermal moment between molecules, which reduces the intermolecular forces, causing flow among them to be lighter and thereby decreases the viscosity (Santos et al. 2004). Similarly, shear rate vs viscosity of all the samples was determined at 40 ^{o}C in order to obtain the variation in viscosity with respect to shear rate. Figure 7.10 suggests that viscosity does not change with an increase in the shear rate, whereas the plots of shear stress vs shear rate (Figure 7.8) show a straight line passing through the origin.

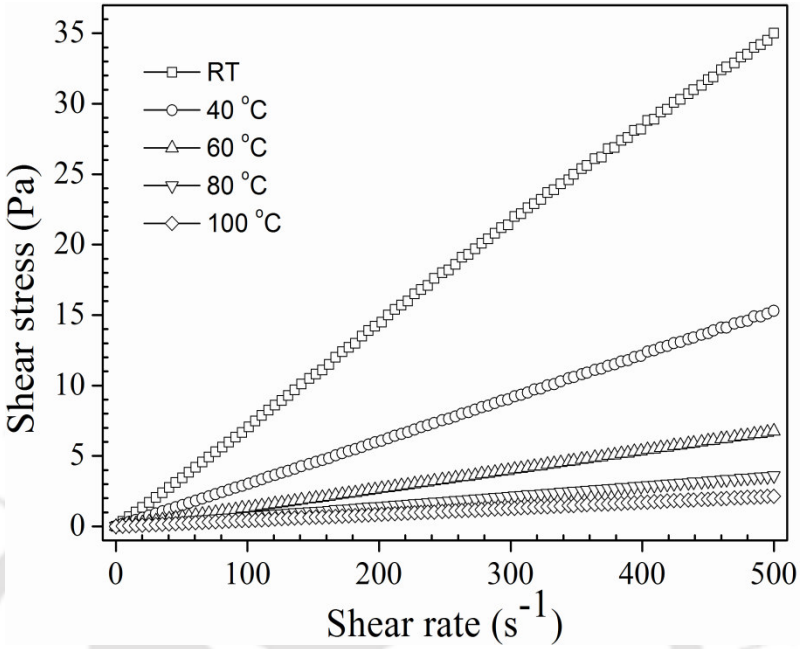

Figure 7.8: Shear stress versus shear rate relation for COFAME epoxide

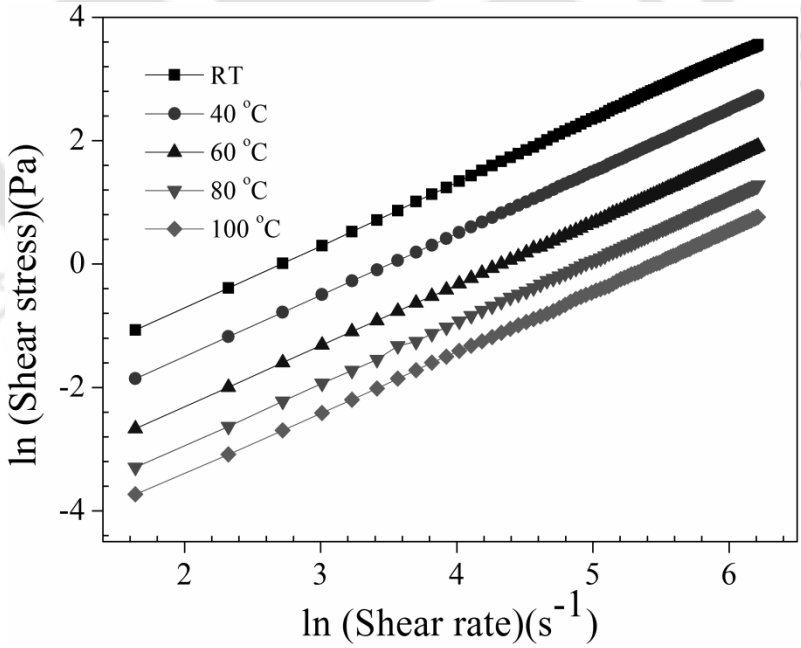

Figure 7.9: Plot of logarithms of shear stress versus shear rate for COFAME epoxide

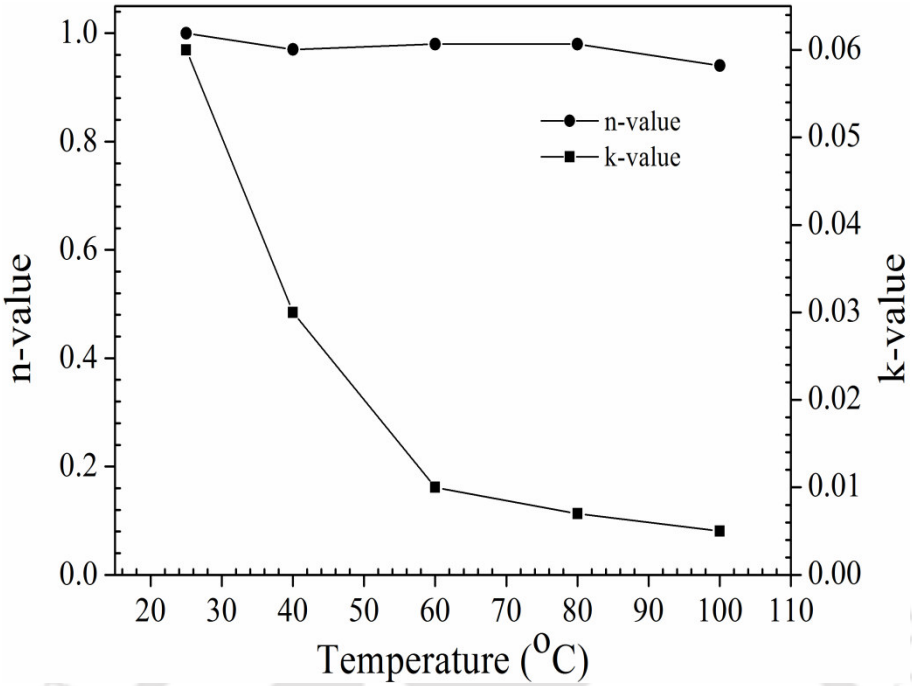

Figure 7.10: Plot of experimental value of n and k for COFAME epoxide at various temperatures

7.3.6 Physico-chemical characterization

The epoxidised oils can be used as lubricant base fluids due to their good lubricity and higher thermo-oxidative stability compared to its structurally unmodified methyl esters (Adhvaryu et al. 2005). Hence, the major emphasis of this study was to modify the ricinoleate fatty acid structure of COFAME by converting unsaturation (indicated by Iodine Value (IV)) into oxirane oxygen ring, so that the thermo-oxidative stability of prepared epoxide can be improved. Lower IV indicates higher thermo-oxidative stability and vice versa. The iodine value of COFAME was found to be 84.6 gI_2/100 g of esters and after epoxidation significant decrease in the iodine value (1.27 gI_2/100 g of esters) was observed (Table 7.3). The decreased iodine value of COFAME epoxide indicates that almost 98.5% (based on IV) of unsaturation was converted into oxirane ring, which results in improved thermo-oxidative stability (Section 7.3.4). The detailed physico-chemical properties of COFAME and its

epoxide are shown in Table 7.3. The lower acid value of epoxide sample (1.08 mg KOH/g) assures smooth functioning of the equipment on usages. During this study density of epoxidised COFAME (956 kg/m^3) was found to be higher than its unmodified COFAME (930 k g/m^3).

Table 7.3: Comparison of COFAME, COFAME epoxide physico-chemical properties

Properties	**COFAME**	**COFAME Epoxide**
Acid value (mg KOH/g)	1.65	1.08
Density (kg/m^3)	930	956
Iodine alue (gI_2/100 g)	84.6	1.27
Kinematic Viscosity (cSt) at 40 ^oC	13.61	35.81
Kinematic Viscosity (cSt) at 100 ^oC	3.86	6.49
Specific Gravity	0.94	0.96
Oxirane Content (Experimental)	-	4.86
Oxirane Content (Theoretical)	-	5.06
Relative percentage conversion to oxirane (%)	-	96.04

Similarly, kinematic viscosity (at 40 ^oC) of COFAME epoxide (35.81 cSt) was two and half times higher than COFAME (13.61 cSt). This may be due to the addition of oxygen molecule in the midst of the double bond, thereby increases the intermolecular forces, molecular weight and polarity. From this study it was also observed that epoxidised esters have higher molecular weight and more polar structure than unmodified methyl ricinoleate esters which results in strong interaction between the molecules. This property of epoxidised COFAME enhances the lubricity in dynamic system. All together these physico-chemical properties have a great significance on the performance of final lubricant basestock and can be used as replacement for conventional hydraulic lube oil.

7.4. Hydroxylation followed by hexanoylation of COFAME epoxide

Chapters - 4, 5 and 6 clearly described hydroxylation followed by hexanoylation in detail by performing preliminary studies for WCO, WCOFAME and CO epoxides. Based on the thorough study, the reaction mechanism, consumption of reactants for complete hydroxylation and hexanoylation was well understood by considering the molecular structure, weight and fatty acid composition of the feedstocks. Therefore, COFAME epoxide hydroxylation and hexanoylation were repeated at the same optimum condition as that of WCOFAME. The chemical structure of CO, COFAME is unique because of the hydroxyl group (ricinoleic acid, which is a fatty acid that contains both a double bond and a hydroxyl group) at 13^{th} carbon position in its fatty acids composition. The hydroxylation of COFAME epoxide was carried out at 8 mol of 2-EH, 3 wt% of H_2SO_4 (catalyst loading), 15 min of reaction time at room temperature and 1500 rpm. Further, hexanoylation was also accomplished at 2 mol of hexanoic anhydride, 50 ^oC reaction temperature, 2 wt% of catalyst loading and 2 h of reaction time. Regardless of the lower OOC in COFAME epoxide (theoretical and experimental), hydroxylation consumed 8 mol of 2-EH and hexanoylation used 2 mol of hexanoic anhydride. The consumption of less 2-EH compared to CO hydroxylation was mainly due to the absence of glycerol in COFAME chemical structure. After completion of the hydroxylation and hexanoylation reactions, products were purified by washing with sodium bicarbonate followed by diethyl ether. The excess 2-EH and hexanoic anhydride were removed by using a short path distillation column at high temperature (80 ^oC) and reduced pressure. At the end, hexanoylated product was dried with sodium sulphate and then analyzed for their physico-chemical properties.

7.5. Physico-chemical characterization of COFAME hydroxylated and hexanoylated derivatives

7.5.1 Product confirmation by NMR spectral analysis and GPC chromatography

The progress of hydroxylation of COFAME epoxide followed by hexanoylation reaction was monitored by ^{13}C-NMR spectra. As shown in Figure 7.4 (b), oxirane oxygen carbons can be observed at δ 50 - 57 ppm range, 1-carboxyl group at δ 177 ppm, aliphatic -CH_3 and -CH at δ 67.8 ppm and δ 14 ppm respectively, and rest all peaks belongs to the aliphatic -CH_2. In the hydroxylated ^{13}C-NMR spectra (Figure 7.11 (a)), the disappearance of oxirane oxygen carbons was observed at δ 50 - 57 ppm range and appearance of new carboxyl peak at δ 172 ppm, aliphatic CH peak at δ 81.2 ppm (Figure 7.11 (a)) confirms the complete hydroxylation of oxirane groups and functionalization of 2-EH alkyl group to oxirane oxygen. Furthermore, during hexanoylation the disappearance of 1-carboxyl group at δ 177 ppm (Figure 7.11 (b)) shows that the ester group of hexanoic anhydride was successfully functionalized into the hydroxyl group of hydroxylated product. Remaining all the aliphatic -CH, -CH_2 and -CH_3 carbons are identical to the hydroxylated ^{13}C-NMR spectra.

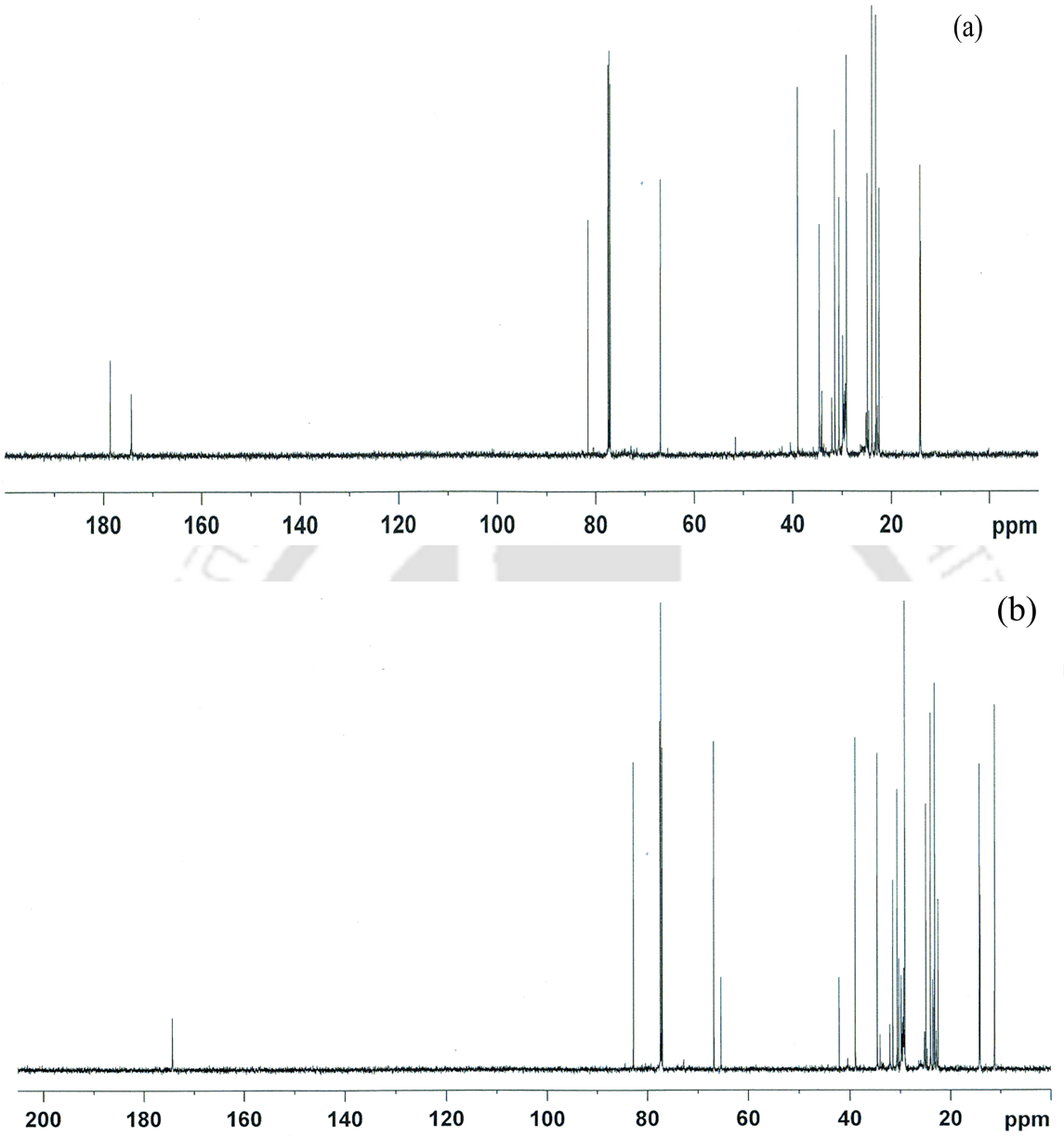

Figure 7.11: Product confirmation by ^{13}C-NMR spectra of COFAME hydroxylation (a) and hexanoylation (b)

In addition to ^{13}C-NMR spectra, GPC was also used to confirm the functionalization of the 2-EH and hexanoic anhydride groups into epoxide and hydroxylated products. The number average molecular weight (MW) and weight average MW of COFAME, COFAME epoxide, hydroxylated and hexanoylated products are depicted in Table 7.4. The molecular weights of hydroxylated and hexanoylated products were increased compared to epoxide,

which signifies that the alkyl and ester groups were functionalized successfully. The same can be observed in the following section with decrease in the PP of hydroxylated and hexanoylated products compared to COFAME epoxide.

Table 7.4: Molecular weights of COFAME, COFAME epoxide, hydroxylated and hexanoylated products

Sample	Number avg. mol. wt.	Weight avg. mol. wt.
COFAME	846	880
COFAME epoxide	907	978
COFAME hydroxylation	1480	1740
COFAME hexanoylation	1750	1865

7.5.2 Viscosity, viscosity index and rheological properties of the prepared hydroxylated and hexanoylated products

The kinematic viscosity and viscosity index of prepared COFAME derived hydroxylated and hexanoylated products were evaluated and depicted in Table 7.5. From the table it can be observed that, with an increase in the branching from hydroxylation to hexanoylation (mono-esters to di-esters), viscosity was found to be decreased and similar observation was recorded by Mahajan et al. (2013) during their study on chemically modified deoxidized mustard oil for bio-lubricant application. Viscosity index is the measure of change in the viscosity with temperature and is very much dependent on attached terminal groups and branching. As reported in Table 7.5, it was observed that viscosity of COFAME derived hydroxylaetd product decreases with the branching of 2-EH, whereas, viscosity index increases. Yao et al. (2010) reported that, viscosity index increases with the molecular weight and same was observed in the present study, where viscosity of hydroxylated COFAME derivative was found to be 306, and for the di-esters it was 166, which signifies that the VI of COFAME hydroxylated and hexanoylated products were higher than COFAME epoxide. Thus, the

prepared COFAME hydroxylated, hexanoylated products can provide better performance during their usage and showed insignificant variation in viscosity with respect to temperature.

The rheological behavior of COFAME derived di-esters determined by interfacial rheometer, by varying shear rate (0 – 500 s^{-1}) at different temperatures (25, 40, 60, 80 and 100 ^{o}C) is demonstrated in Figures 7.12 (a) and (b). From the figures it was noticed that, in spite of increase in the temperature, shear stress vs. shear rate relation was found to be linear and signifies Newtonian fluid behaviour, Figures 7.12 (b).

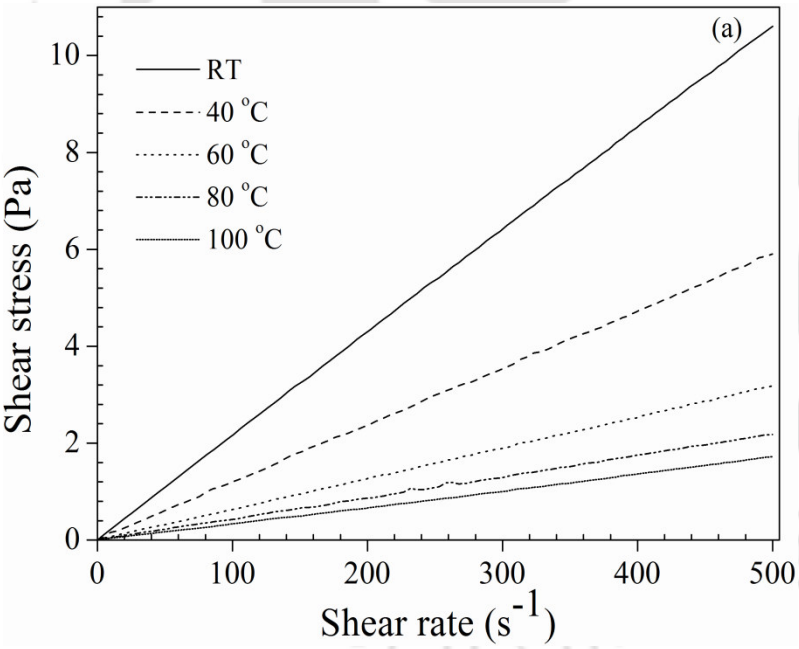

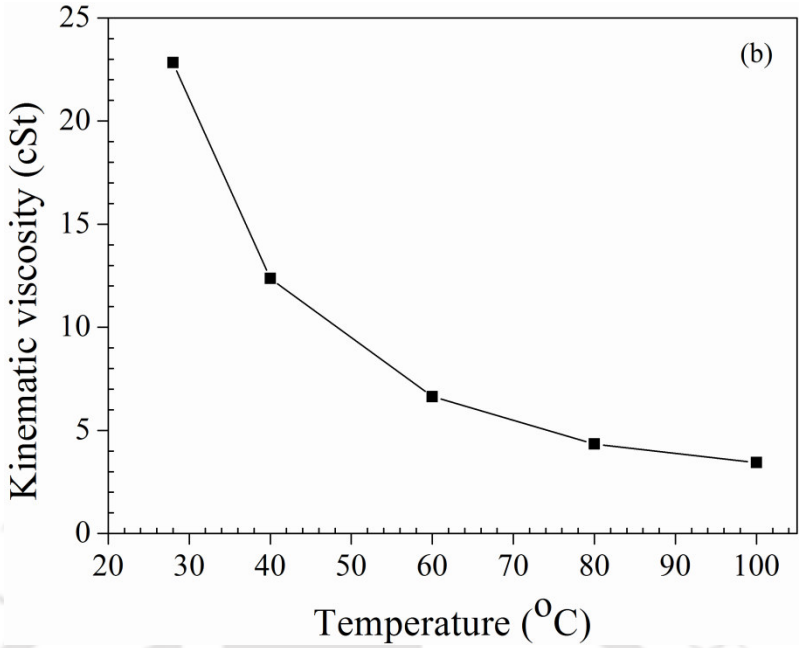

Figure 7.12: Shear stress versus shear rate (a) and temperature versus kinematic viscosity (b) relation for COFAME derived di-esters

Table 7.5: Kinematic viscosity and viscosity index of hydroxylated and hexanoylated products

Sample	Kinematic Viscosity (cSt)		Viscosity Index
	@40 °C	@100 °C	
COFAME epoxidation	39.12	6.49	118
COFAME hydroxylation	33.75	10.06	306
COFAME hexanoylation	12.37	3.44	166

7.5.3 Thermo-oxidative stability, cold flow properties of COFAME derived hydroxylated and hexanoylated products

The thermo-gravimetric analysis of prepared COFAME derived hydroxylated (Figure A.36) and hexanoylated (Figure A.37) products were carried out to determine their stability in an inert and reactive atmosphere. The onset temperature (OT), oxidative onset temperature (OOT) (thermo-oxidative stability) and peak temperature (T_m) (maximum degradation temperatures) of the hydroxylated and hexanoylated products estimated from TGA plot are

reported in Table 7.6. The results indicated that, onset temperatures decreased significantly upon functionalization of alkyl and ester groups by 2-EH and hexanoic anhydride. Likewise, oxidative stability (OOT) data followed the same trend. From the comparative analysis of OT and OOT of COFAME epoxide (Section 7.3.4) and its derivatives, it could be concluded that chemical modification of COFAME epoxide found to have significant influence on the thermal and oxidative stability. However, the highest stability was observed for COFAME epoxide, while the structurally modified products were less stable. This attributes to the loss of some natural antioxidants (Dunn 2009) in the castor oil during various chemical modifications (transesterification, epoxidation, hydroxylation and hexanoylation) along with extending the branching and chain length.

Table 7.6: Onset, oxidative onset, peak temperatures and pour points of prepared COFAME derived hydroxylated and hexanoylated products

Sample	Thermal stability (^{o}C)		Oxidative stability (^{o}C)		Pour Point (^{o}C)
	OT	PT	OOT	PT	
COFAME hydroxylation	287	347.5	254	295	-16.4 ± 0.54
COFAME hexanoylation	233.5	269.9	229.1	292.7	-28.93 ± 0.72

Furthermore, COFAME derived hydroxylated and hexanoylated products pour point was found to be -16.4 ± 0.54 ^{o}C (Figure 7.13 (a)), -28.93 ± 0.72 ^{o}C (Figure 7.13 (b)) respectively. Upon functionalization of COFAME epoxide by 2-EH alkyl group (C_7H_{17}), almost identical pour point were noticed, but molecular weight was found to be increased (Table 7.6). Nevertheless, during hexanoylation alone temperature increased was almost -12.5 ^{o}C, this attributed to the functionalization of ester group ($CH_3(CH_2)_4CO_3$) of hexanoic anhydride to hydroxyl group of COFAME hydroxylated product. The functionalization of 2-EH and hexanoic anhydride to methyl ricinoleate fatty acid chains demonstrated the most effective reduction in PP and this could be attributed to the presence of a large branching

group at the mid-point of a fatty acid chain and it makes a steric barrier around the individual molecules and suppresses the formation of crystal growth, which results in lowering the samples PP' to -28.93 ^{o}C for the end product. Thus the prepared products can be used up to lower temperature of -28.93 ^{o}C.

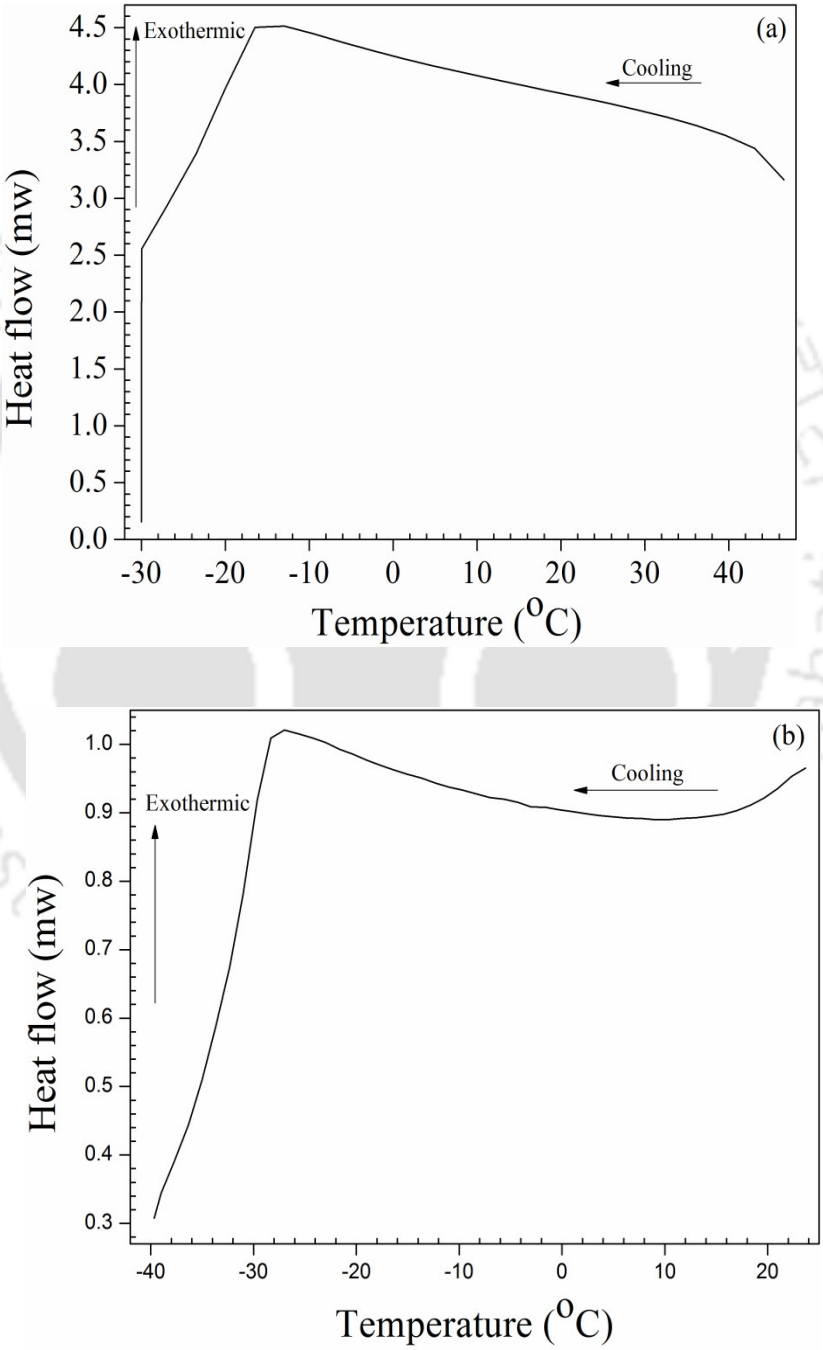

Figure 7.13: DSC thermo-grams for COFAME hydroxylation (a) and hexanoylation (b)

7.5.4 Tribology and bio-degradability of hexanoylaed COFAME

Figure 7.14 shows the wear scar diameter of the hexanoylated COFAME evaluated using HFRR lubricity test. The wear scar diameter was found to be 253 µm, 216 µm, 235 µm (x-axis, y-axis and average, Figure 7.14), with the film thickness of 13 %, and co-efficient of friction (CoF) 0.078. The lower film thickness and co-efficient of friction was mainly due to the presence of excess hydroxyl groups in the methyl ricinoleate acid fatty acid structure and viscosity of the di-ester product. The lower film thickness indicates the formation of protective surface film, promoted by tribochemical processes due to the rubbing action. The comparative analysis of CO and COFAME derived di-ester revealed lower film thickness for COFAME derived di-ester; this could be due to the absence of glycerol molecule in the COFAME composition. Similar observation was reported by Madankar et al. (2013). The estimated tribological properties were within the acceptable range to use them as lubricant basestocks.

Likewise, biodegradability of hexanoylated COFAME derived product was found to be 93.75 % ± 1.35. Compared to the CO derived di-eser, it was slightly less due to the absence of glycerol in its fatty acid structure. The presence of glycerol enhances the process and percentage of degradation. The results of biodegradation study revealed that, prepared hexanoylated COFAME derived product di-esters are biodegradable and showed good reproducibility among the duplicate test runs.

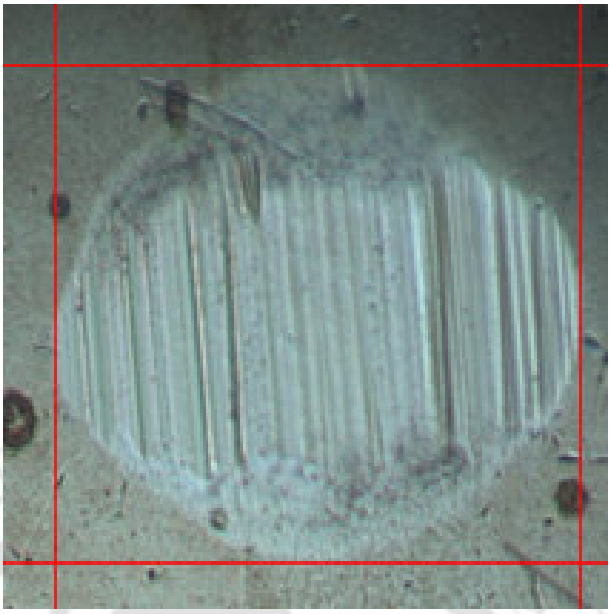

Figure 7.14: Microscopic wear scar image for COFAME derived di-esters

7.6. Summary

The aim of this chapter was to develop COFAME derived bio-lubricant base stock via series of chemical modifications during the absence of glycerol in the feedstock. Like earlier chapter, this chapter also contributed as the first report of its kind in literature on the preparation of bio-lubricant basestock from high FFA castor oil (45.6 mg KOH/g). However, a two-step acid esterification followed by alkali transesterification was performed to synthesize methyl esters from high FFA CO. Esterification was carried out at oil to methanol molar ratio, 1:10; catalyst loading (H_2SO_4), 5 wt%; reaction time, 90 min; at 60 ^oC reaction temperature followed by transesterificaton at identical condition as that of WCOFAME. At the optimum condition oxirane oxygen content of COFAME was found to be 4.38 mass%, with pour point and number average molecular weight (MW) of -10 ^oC and 846 mol/g. Further, via hydroxylation and hexanoylation pour point and molecular weight were improved and observed as -16.4 ^oC, -28.93 ^oC and 1480 mol/g, 1750 mol/g respectively. The onset temperature and OOT (233.5 ^oC, 229.4 ^oC) of COFAME hexanoylated product was

found to be higher (203 ^{o}C, 218 ^{o}C) than COFAME. Similarly, higher biodegradability (93.75 %) and better tribological performance properties (WSD-235 µm, friction co-efficient-0.078, film thickness-13%) of COFAME hexanoylated product indicates that the prepared structurally modified product is in the acceptable range to use them as bio-degradable lubricant basestocks for various industrial applications.

Chapter-8

Comparative analysis of prepared bio-lubricant basestocks with conventional lubricants

Chapters 3-7 clearly described the synthesis and characterization of feedstocks and various products derived from them to enhance the properties (i.e. thermo-oxidative stability, cold flow properties and viscosity, viscosity index). However, in order to find the proper area of application for the prepared products, they need to be compared with the conventional lubricants, which are readily available in the market. Therefore, this chapter is committed to compare the various performance properties of the conventional lubricants with the prepared products and finding the right application for feedstocks and products.

8.1. Comparative analysis of conventional lubricants with bio-lubricant basestocks

8.1.1 Thermo-oxidative stability, Cold flow properties

At the end findings of the entire study was explored by comparing the significant properties of prepared (epoxides, hydroxylated and hexanoylated) products with conventional lubricants. Currently, the Indian lubricant market is occupied with different kind of lubricants supplied by major industries such as Hindustan Petroleum Corporation Limited (HPCL), Castrol, IOCL and Bharat Petroleum Corporation Limited (BPCL) for various practical applications. From the prior arts it was noticed that, bio-lubricants produced from vegetable oils are exactly suitable for hydraulic and transmission applications (Bart et al. 2013). Therefore, during this study, seven conventional lubricant samples (combination of basestocks and additives) were collected which are readily available in the market, the name of lubricant, supplying company and their application is mentioned below in Table 8.1. Thermo-oxidative stability (TG analysis), cold flow properties (ASTM and DSC), viscosity

(Interfacial rheometer) and viscosity index of the conventional lubricants were evaluated at analytical conditions identical that of prepared bio-lubricant basestocks and compared.

Table 8.1: Collected conventional lubricants, their supplying company and application

Sample Name	Supplying Company	Application
Servo Trans Power	Indian Oil	Transmission
Castrol Agri Power Trans	Castrol	Transmission
Castrol Agri TFD	Castrol	Transmission
Castrol Hydra Power	Castrol	Hydraulic
Hydraulic Brake Fluid	Hindustan Petroleum	Hydraulic
Servo Hydraulic Oil	Indian Oil	Hydraulic
MAC Auto XL Engine Oil	Bharat Petroleum	Engine Oil

Comparative summary of thermo-oxidative stability of the collected conventional lubricants with the bio-degradable lubricant basestocks is presented in Tables 8.2, 8.3, 8.4 (a), (b) and 8.5. From Table 8.2, it can be observed that the thermo-oxidative stability of the transmission lubricants and hydraulic lubes is in the range of 271-293 ^{o}C (N_2), 258-287 ^{o}C (O_2); and 188-292 ^{o}C (N_2), 197-299 ^{o}C (O_2) respectively. The relative comparison of thermo-oxidative stability of conventional lubricants with the prepared bio-lubricant basestocks showed that the thermo-oxidative stability of WCO derivatives is superior, and for rest of the derivatives (i.e. CO, COFAME and WCOFAME) thermo-oxidative stability is almost within the acceptable range of conventional hydraulic and transmission lubricants. Similarly, CO and WCO derivatives are oxidatively more stable than conventional lubricants due to the presence of glycerol in their oil derivatives. However, in the absence of glycerol also (i.e. FAME samples) derivatives showed acceptable thermo-oxidative stability (Table 8.2). The higher thermo-oxidative stability of CO and WCO derivatives compare to conventional

lubricants indicates that the prepared bio-lubricant basestocks can be used as a potential alternative to conventional transmission and hydraulic lubricants.

Table 8.2: Comparison of onset and oxidative onset temperatures of conventional lubricants and bio-lubricant basestocks

Lubricant Name	Onset Temperature Range (^{o}C)	Oxidative Onset Temperature Range (^{o}C)
Conventional	**188-314**	**197-299**
CO Derivatives	236-310	235-320
COFAME Derivatives	203-287	218-254
WCO Derivatives	286-360	230-320
WCOFAME Derivatives	178-293	187-247

Table 8.3: Comparison of thermo-oxidative stabilities of conventional and bio-lubricant basestocks

Property	Conventional Lubricants	Bio-Lubricant Basestocks
Thermal Stability (^{o}C)	188 - 314	175 - 360
Oxidative Stability (^{o}C)	180 - 320	197 - 299.5
Pour Point (^{o}C)	(-1) - (-24)	(-1) - (-28.93)

Table 8.4 (a): Thermo-oxidative stabilities of CO and COFAME derivatives

Sample Name	Onset Temperature (^{o}C)	Oxidative onset temperature (^{o}C)
CO	310	308
CO Epoxide	308	320
Hydroxylated CO	272.8	241.9
Hexanoylated CO	236.6	235.7
COFAME	203	218
COFAME Epoxide	260	250
Hydroxylated COFAME	287	254
Hexanoylated COFAME	233.5	229.1

Table 8.4 (b): Thermo-oxidative stabilities of WCO and WCOFAME derivatives

Sample Name	Onset Temperature	Oxidative onset temperature
WCO	360	298
WCO Epoxide	330	320
Hydroxylated WCO	325.5	239.3
Hexanoylated WCO	286.3	230.7
WCOFAME	178	187
WCOFAME Epoxide	187	200
Hydroxylated WCOFAME	265.9	246.8
Hexanoylated WCOFAME	293	247.5

Table 8.5: Thermo-oxidative stabilities of conventional lubricants

Name of Lubricant	Onset Temperature (^oC)	
	N_2	O_2
Castrol Agri Power Trans	285.6	258
Castrol Agri TFD	271.7	265.3
Castrol Hydra Power	257.1	299.5
Hydraulic Brake Fluid	188	197
MAC Auto XL Engine Oil	314.4	266.4
Servo Hydraulic Oil	292.4	280.7
Servo Trans Power	293.7	287.3

8.1.2 Viscosity and viscosity index

A comparative analysis of viscosity and viscosity index of conventional lubricants collected from the market and prepared bio-lubricant basestocks are presented in Table 8.6 and 8.7. The viscosity index (VI) was also calculated in order to indicate the oil viscosity variation with temperature and is normally used as an important parameter to evaluate lubricant oils, higher is the viscosity index, lower is the viscosity variation with temperature. These measurements were performed to evaluate differences in the results obtained, when the bio-

based lubricants was compared with two extreme behaviors (pure vegetable or petroleum based oil). However, the specific application of given lubricant oil is also related to the viscosity value. It may be observed that the bio-based derivatives obtained from castor oil showed much lower viscosity than the castor oil. From the Table 8.6, it can be seen that the viscosity and viscosity index range of transmission lubricants was found to be in the range of 50.1-56.5 cSt (at 40 ^{o}C temperature) and 57-176 for servo trans power, Castrol Agri Power Trans and Castrol Agri TFD; similarly, for hydraulic lubricants (Castrol hydra power, Servo hydraulic oil), it was in the range of 47.9-52.37 cSt and 111-130 respectively. Among all the collected lubricants lower viscosity was observed for the hydraulic brake fluid and higher was found for engine oil from MAC (70.37 cSt). Similarly, viscosity and viscosity index of hydraulic lubricants are below the transmission lubricants range (Table 8.6). Altogether, the collected lubricants viscosity and viscosity indexes was in the range of 18-70 cSt and 57-215.

Table 8.6: Kinematic viscosities and viscosity index of conventional lubricant basestocks

Sample Name	KV @40C	KV @100C	VI
Servo Trans Power	56.49453	7.348094	87
Castrol Agri TFD	52.34294	6.416496	57
Hydraulic Brake Fluid	18.24885	4.914935	215
Servo Hydraulic Oil	52.36944	8.259856	130
Castrol Hydra Power	47.86096	7.241378	111
MAC Auto XL Engine Oil	70.36996	12.56073	180
Castrol Agri Power Trans	50.07541	9.463577	176
Range	**18-70**	**5-12.5**	**57-215**

Table 8.7: Kinematic viscosities and viscosity index of prepared bio-lubricant basestocks

Sample Name	KV @40C	KV @100C	VI
CO	193	21.56	134
CO Epoxide	11311	291	128
Hydroxylated CO	56.37	11	192
Hexanoylated CO	15.54	3.13	30
Range	**15-11311**	**3-291**	**30-192**
COFAME	16.1	5	277
COFAME Epoxide	39.12	6.49	118
Hydroxylated COFAME	33.75	10.06	306
Hexanoylated COFAME	12.37	3.44	166
Range	**12.5-39**	**3.5-10**	**118-306**
WCO	35	8.1	217
WCO Epoxide	282.38	33.33	162
Hydroxylated WCO	29.63	9.65	337.32
Hexanoylated WCO	10.57	2.9	127.98
Range	**10-282**	**3-3.3**	**127-337**
WCOFAME	4.71	2	346
WCOFAME Epoxide	10.42	3.29	213
Hydroxylated WCOFAME	16.76	4.99	257.8
Hexanoylated WCOFAME	8.33	1.09	133
Range	**8.3-16**	**1-4.9**	**133-346**

Correspondingly, the estimated viscosity and viscosity index for bio-lubricant basestocks prepared in the present study are shown in Table 8.7. Analysing the values from Table 8.7, it has been observed that viscosity and viscosity index values of CO, WCO and their derivatives were within the satisfactory range. On the other hand, by considering the viscosity index values; CO, COFAME and WCO derivatives are satisfying the criteria for conventional lubricants. Therefore, from this study it can be concluded that the prepared bio-lubricant basestocks can be used as a potential alternatives to conventional lubricants.

In general, viscosity, viscosity index and tribological properties (CoF, film thickness and wear) show a significant effect on the performance of lubricant. However, as the load increases, film thickness decreases, and nominal film thickness formation is majorly depend upon the lubricant viscosity, but at the same time, rheology of interacting surfaces becomes significant at high contact temperatures. In addition, Masjuki and Maleque (1999) also found that palm-based lubricating oil showed better wear performance compared to mineral oil. According to Havet and Blouet (2001), the length of fatty acid chains tends to increase the adsorbed film thickness, therefore with an increase in the fatty acid length, protected surface area increases. In addition, with an increase in the number of ester groups lead to a better binding of molecules and therefore a greater resistance to shear forces. This phenomenon is probably due to polarity of the attached groups (alkyl and ester). The large amounts of friction increased the temperature and caused wear and seizure.

The experimental results show that the prepared di-ester lubricant basestocks have comparable load carrying capacity and tribological characteristics as that of fully formulated commercial lubricants. Even though this study didn't cover the tribological characteristics for the collected lubricants, but based on the previous reports (Zulkifli et al. 2015) on comparison of tribological characteristics among the vegetable oil based derivatives and conventional lubricants. The pentaerythritol ester showed lowest CoF of around 0.025, even compared to ordinary lubricant at around 0.07. Similarly, in the present study CoF values were found to be in the range of 0.076-0.1, which are on par with the ordinary lubricant. Hence, in order to use the prepared lubricant basestocks as hydraulic and transmission fluids, the essential and required properties are examined in the current study and compared with the conventional lubricant to find out its suitability as bio-lubricant base stock. Finally from the results it could be concluded that the prepared WCO, CO and their methyl esters derivatives can be act as a replacement for aforementioned applications as lubricant

basestocks. However, physico-chemical (performance) properties of the synthesised bio-lubricant basestocks can be further enhanced by adding proper additives (for a specific property or area of application) to bio-degradable lubricant basestocks. Therefore, research to investigate the properties of esters to make them technologically competitive lubricants for various practical applications need to be encouraged.

8.1.3 Other significant properties

In general, the biodegradability of mineral basestocks is strongly related to the presence of aromatic and naphthenic compounds in their composition (the higher the content of these compounds the lower the biodegradability). Similarly, several studies on biodegradability reported that, the biodegradability results are closely related with the samples chemical and physical properties (Haus et al. 2001; 2004) or their chemical composition (Basu et al. 1998). As expected, in the present study the bio-based lubricant basestocks obtained from castor and waste cooking oil, have shown higher biodegradability than the mineral basestocks (Rudnick 2013). Furthermore, a huge difference can be spotted while comparing the biodegradation as a function of time of the synthesized lubricant basestocks with that of the mineral oil. The effective composition for biodegradation (ECB) decides biodegradation time and estimates the percentage of biodegradation as a function of time.

Epoxidation has been carried out to improve the thermo-oxidative stability and low temperature properties, but unsatisfactory cold flow properties are detected after epoxidation of the feedstocks. Nevertheless, further oxirane rings are opened in the presence of 2-EH, followed by functionalization of hexanoic anhydride. The main intension behind the entire study is to assess the performance properties of end products derived from four different feedstocks having unique chemical structure and composition. Altogether, WCOFAME shown highest OT (293 ^{o}C) and OOT (247 ^{o}C) after a series of structural modifications, PP

of all the hexanoylated products are found to be more or less identical. Tribological properties of WCO, CO derived hexanoylated products are higher than their FAME derivatives due to the presence of glycerol or ricinoleic aid in their fatty acid structure. Likewise, hexanoylated products are found to be highly biodegradable i.e., their biodegradability is > 90% in 28 days. In order to improve the OT, OOT of the bio-lubricant basestocks from renewable resources, presence of glycerol/OH should be avoided in the feedstock.

8.2. Summary

The comparison of various performance properties of the prepared bio-lubricant basestocks with conventional hydraulic and transmission lubricants, it could be conclude that the prepared WCO, CO and their methyl esters derivatives (epoxides, hydroxylated and hexanoylated products) can be act as a potential replacement for hydraulic and transmission applications.

Chapter-9

Overall conclusions and future scope

This chapter summarizes the major inferences drawn from the research work presented in this dissertation. The later part of this chapter focuses towards the scope for future research area that can be carried out.

9.1. Significance and salient features of the study

This work dealt with the preparation, characterization and applications of the prepared bio-lubricant base stock from castor oil, waste cooking oil and their fatty acid methyl esters via chemical modification (i.e. epoxidation). The performance limitation properties (thermo-oxidative stability and cold flow properties) and physico-chemical characterization of the prepared epoxides, hydroxylated and hexanoylated products indicated that the prepared basestocks possessed desirable properties to use them as bio-lubricant basestocks, also to replace conventional lubricants for hydraulic and transmission applications in various fields. From the perspective of thesis novelty, the major conclusions obtained from this study are summarized below.

- For the first time, this work reported the preparation and characterization of bio-lubricant basestocks from renewable resources (CO, WCO and their FAME) by a series of chemical modifications along with the physico-chemical characterization.
- The process parameters are optimized to maximize the desired product in epoxidation, hydroxylation and hexanoylation.
- Among all the prepared bio-lubricant basestocks, WCOFAME hexanoylated product exhibits maximum thermo - oxidative stability compared to other derivatives.

- Utmost pour point was obtained for derivatives of WCO (-7 to -28.45 ^{o}C) and WCOFAME (-1 to -27.15 ^{o}C) after a series of structural modifications.
- Rheological study of the feedstocks and all the products after a series of structural modifications showed Newtonian fluid behaviour.
- Tribological characteristics of the hexanoylated products revealed that wear scar diameter, friction co-efficient and film thickness are found to be within the acceptable range to use them for various practical applications.
- Biodegradability of FAME derivatives were found to be 2-3% less biodegradable compared to oil derived bio-lubricant basestocks, however, overall all hexanoylated products are found to be highly biodegradable.
- The comparative analysis of thermo-oxidative stability, viscosity and viscosity index, and pour point of the conventional lubricants (hydraulic and transmission applications) with the bio-lubricant basestocks prepared in this study indicates that the prepared bio-lubricant basestocks can act as a promising alternative to conventional lubricants.
- Further, the elaborate survey on prior arts disclosed that, prepared basestocks performance properties are very much close to ISO grade 15, 22, 32, 46, 68, 100 and ASTM grade 75, 100, 150, 215, 315, 465 food grade lubricants.
- However, all the epoxides, ring opened and hexanoylated products performance properties can be further enhanced by adding suitable additives which are commercially available, depending on the need for a specific application.

In summary, the thesis outlines the efficacy of bio-lubricant basestocks synthesized from low cost feedstocks to substitute conventional lubricants. The obtained data anticipated to serve as a reference data for further research in the field of low cost bio-lubricant basestocks synthesis, characterization and application.

9.2. Future prospects

Research findings in this work provided a good number of insights with respect to preparation, characterization and application of bio-degradable lubricant basestocks synthesized from different renewable feedstocks via chemical modification technique. There are certainly several areas which merit further research attention. Few research areas for future work are presented as follows:

- Epoxidation, hydroxylation and hexanoylation of various feedstocks with IR-15 as heterogeneous strong acid catalyst. Using same catalyst for all the reactions could be an innovative study.
- Tri-esters and tetra-esters formation in the presence of acids rather than in high molecular weight alcohols
- Kinetic study of hydroxylation, hexanoylation and further formation of tri and tetra-esters.
- Studies on the long term storage stability of prepared hydroxylated and hexanoylated products.
- Studies on the use of different additives to improve the performance properties of epoxides, hydroxylated and hexanoylated products.

Anonymous (2009) Lubricant Failure = Bearing Failure, http://www.machinerylubrication.com/Read/1863/lubricant-failure (Accessed on 21st September 2015).

Anonymous (2011) Huge scope for specialty lubricant in Indian market. indiatransportportal.com/2011/05/huge-scope-for-specialtylubricant-in-indian-market/ (Accessed on 10th June 2015).

Anonymous (2013) Indian Lubricant Market. Sectorial Studies and Information. www.businesscoot.com/indian-lubricant-market-204/ (Accessed on 10th June 2015).

Anonymous (2014) Biolubricants – A Global Market Overview. https://www.reportbuyer.com/product/2112733/Biolubricants---A-Global-Market-Overview.html (Accessed on 21st September 2015).

Abdullah BM, Salih N, Slimon J (2014) Optimization of the chemo-enzymatic mono-epoxidation of linoleic acid using D-optimal design. J Saudi Chem Soc 18:276-287.

Abnisa F, Daud WMAW, Sahu JN (2011) Optimization and characterization studies on bio-oil production from palm shell by pyrolysis using response surface methodology. Biomass and bioenergy 35:3604 – 3616.

Adhvaryu A, Erhan SZ (2002) Epoxidized soybean oil as a potential source of high temperature lubricants. Ind Crops Prod 15:247–254.

Adhvaryu A, Liu Z, Erhan SZ (2005) Synthesis of novel alkoxylated triacylglycerols and their lubricant base oil properties. Ind Crops Prod 21:113–119.

Angel P, Abraham C, Carmen MF, Maria JR, Lourdes R (2010) Winterization of peanut biodiesel to improve the cold flow properties. Bioresour Technol 101:7375–7381.

Arbain HN, Salimon J (2009) Synthesis and characterization of ester trimethylolpropane (TMP) based Jatropha curcas oil as biolubricant base stock. J Sci Technol 2:47-58.

Arumugam S, Sriram G, Subadhra L (2012) Synthesis, chemical modification and tribological evaluation of plant oil as biodegradable low temperature lubricant. Procedia Eng 38:1508-1517.

Asadauskas S, Erhan SZ (1999) Depression of pour point of vegetable oils by blending with diluents used for biodegradable lubricants. J Am Oil Chem Soc 76:313-316.

Bart JCJ, Gucciardi E, Cavallaro S (2013) Biolubricants: Science and technology. Woodhead Publishing Limited, UK.

Bastida S, Sanchez MFJ (2001) Thermal oxidation of olive oil, sunflower oil and a mix of both oils during forty discontinuous domestic frying of different foods. Food Sci Technol 7:15–21.

Basu B, Singh MP, Kapur GS, Ali N, Jain SK, Srivastava SP (1998) Prediction of biodegradability of mineral base oils from chemical composition using artificial neural networks. Tribiol Int 31:159–68.

Becker R, Knorr A (1996) An evolution of antioxidants for vegetable oils at elevated temperatures. Lubr Sci 8:95-117.

Biswas A, Adhvaryu A, Stevenson DG, Sharma BK, Willet JL, Erhan SZ (2007) Microwave irradiation effects on the structure, viscosity , thermal properties and lubricity of soybean oil. Ind Crops Prod 25:1–7.

Blee E, Summerer S, Flenet M, Rogniaux H, Dorsselaer AV, Schuber F (2005) Soybean Epoxide Hydrolase. Identification of the catalytic residues and probing of the reaction mechanism with Secondary kinetic isotope effects. J Biological Chem 280:6479-6487.

Bokade VV, Yadav GD (2007) Synthesis of bio-diesel and bio-lubricant by transesterification of vegetable oil with lower and higher alcohols over heteropolyacids supported by clay (K-10). Process Saf Environ Prot 85:372-377.

Brajendra KS, Erhan SZ, Liu Z, Adhvaryu A (2008) One-pot synthesis of chemically modified vegetable oils, J Agr Food Chem 56:3049-3056.

Brophy JE, Zisman WA (1951) Surface chemical phenomena in lubrication. Ann NY Acad Sci 53:836-861.

Borugadda VB, Goud VV (2012) Biodiesel production from renewable feed stocks: Status and opportunities. Renew Sustain Energy Rev 16:4763-4784.

Borugadda VB, Goud VV (2013) Comparative studies of thermal, oxidative and low temperature properties of waste cooking oil and castor oil. J Renew Sustain Energy 5, 063104: 1-14.

Borugadda VB, Goud VV (2014a) Synthesis of waste cooking oil epoxide as a bio-lubricant base stock: characterization and optimization study. J Bioprocess Eng Biorefin 3:57-72.

Borugadda VB, Goud VV (2014b) Thermal, oxidative and low temperature properties of methyl esters prepared from oils of different fatty acids composition: A comparative study. Thermochimica Acta 577:33–40.

Borugadda VB, Goud VV (2014c) Epoxidation of castor oil fatty acid methyl esters (COFAME) as a lubricant base stock using heterogeneous ion-exchange resin (IR-120) as a catalyst. Energy Procedia 54:75-84.

Castro W, Perez JM, Erhan SZ, Caputo F (2006) A study of the oxidation and wear properties of vegetable oils: Soybean oil without additives. J Am Oil Chem Soc 83:47-52.

Campanella A, Fontanini C, Baltanás MA (2008) High yield epoxidation of fatty acid methyl esters with performic acid generated in-situ. Chem Eng J 144:466–475.

Campanella A, Rustoy E, Baldessari A, Baltanas MA (2010) Lubricants from chemically modified vegetable oils. Bioresource Technol 101:245-254.

Chavan VP, Patwardhan AV, Gogate PR (2012) Intensification of epoxidation of soybean oil using sonochemical reactors. Chem Eng Process: Process Intensif 54:22-28.

Choe E, Min DB (2007) Chemistry of deep-fat frying oils. J Food Sci 72:77-86.

Chua SC, Xu X, Guo Z (2012) Emerging sustainable technology for epoxidation directed toward plant oil-based plasticizers. Process Biochemistry 47:1439–1451.

Claudy P, Letoffe JM, Chague B, Orrit J (1988) Crude oils and their distillates: characterization by differential scanning calorimetry. Fuel 67:58-61.

Conceicao MM, Roberlucia AC, Fernando CS, Aline FB, Valter JF, Antonio GS (2007) Thermo-analytical characterization of castor oil biodiesel. Renew Sustain Energy Rev 11: 964–975.

Cronje KJ, Chetty K, Carsky M, Sahu JN, Meikap BC (2011) Optimization of chromium (VI) sorption potential using developed activated carbon from sugarcane bagasse with chemical activation by zinc chloride. Desalination 275:276–284.

Coutinho JAP, Daridon JL (2005) The Limitations of the cloud point measurement techniques and the influence of the oil composition on its detection. Pet Sci Technol 23:1113-1128.

Daniel L, Ardiyanti AR, Schuur B, Manurung R, Broekhuis AA, Heeres HJ (2011) Synthesis and properties of highly branched jatropha curcas L. oil derivatives. European J Lipid Sci Technol 113:18-30.

Derawi D, Salimon J (2010) Optimization on epoxidation of palm olein by using performic acid. E-J Chem 7:1440-1448.

Dinda S, Patwardhan AV, Goud VV, Pradhan NC (2008) Epoxidation of cottonseed oil by aqueous hydrogen peroxide catalysed by liquid inorganic acids. Bioresource Technol 99:3737-3744.

Dinda S, Goud VV, Patwardhan V, Pradhan NC (2011) Selective epoxidation of natural triglycerides using acidic ion exchange resin as catalyst. Asia-Pacific J Chem Eng 6:870-878.

Diniz ZN, Bora PS, Neto VQ, Cavalheiro JMO (2008) Sterculia striata seed kernel oil: characterization and thermal stability. Grasas Y Aceites 59:160-165.

Dweck J, Sampaio CMS (2004) Analysis of the thermal decomposition of commercial vegetable oils in air by simultaneous TG/DTA. J Thermal Analysis Calorimetry.75:385-391.

Dunn RO (1999) Thermal analysis of alternative diesel fuels from vegetable oils. J Am Oil Chem Soc 76:109–115.

Dunn RO (2005a) Cold Weather Properties and Performance of Biodiesel. The Biodiesel Handbook (2nd edition) Edited by Knothe G, Krahl J and Gerpen JV, AOCS Publishing, Chapter 6.3.

Dunn RO (2005b) Effect of antioxidants on the oxidative stability of methyl soyate (biodiesel). Fuel Process Technol 86:1071-1085.

Dunn RO (2006) Oxidative stability of biodiesel by dynamic mode pressurized differential scanning calorimetry (P-DSC). Trans Am Soc Agric Biol Eng 49:1633–41.

Dunn R (2009) Effects of minor constituents on cold flow properties and performance. Progress Energy Combust Sci 35:481-489.

Erhan S Z, Asadauskas S (2000) Lubricant Base Stocks From Vegetable Oils. Ind Crops Prod 11:277-282.

Farias EA, Leles MIG, Ionashiro M, Zuppa TO, Son NRA (2002) Study of thermal stability of vegetable oils and fats by TG / DTA and DTG. Elect Chem 27:111-116.

Farias M, Martinelli M, Bottega DP (2010) Epoxidation of soybean oil using a homogeneous catalytic system based on a molybdenum (VI) complex. Appl Catal A: Gen 384:213-219.

Fiser SS, Jankovic M, Petrovic ZS (2001) Kinetics of in situ epoxidation of soybean oil in bulk catalyzed by ion exchange resin. J Am Oil Chem Soc 78:725–731.

Fiser SS, Jankovic M, Borota O (2012) Epoxidation of castor oil with peracetic acid formed in situ in the presence of an ion exchange resin. Chem Eng Process: Process Intensif 62:106-113.

Fox NJ, Stachowiak GW (2007) Vegetable oil-based lubricants - A review of oxidation. Tribol Intern 40:1035-1046.

Frankel EN, Smith LM, Hamblin CL, Creveling RK, Clifford AJ (1984a) Occurrence of cyclic fatty acid monomers in frying oils used for fast foods. J Am Oil Chem Soc 61:87–90.

Frankel EN (1984b) Chemistry of free radical and singlet oxidation of lipids. Prog Lipid Res 23:197-221.

Garcia JU, Santos HID, Fialho AP, Garro FLT, Filho NRA, Leles MIG (2004) Study of the thermal stability of fish oils in nitrogen atmosphere. Eclet Chem 29:41-46.

Garcia CC, Franco PIBM, Zuppa TO, Filho NRA, Leles MIG (2007) Thermal stability studies of some cerrado plant oils. J Therm Anal Calorim 87:645-648.

Garcia PM, Adams TT, Goodrum JM, Das KC, Geller DP (2010) DSC studies to evaluate the impact of bio-oil on cold flow properties and oxidation stability of bio-diesel. Bioresour Technol 101:6219–6224.

Gawrilow I (2004) Vegetable oil usage in lubricants. Inform: Int News Fats Oils Relat. Mater. 15: 702-705.

Gordon MH, Kourimska L (1995) The effects of antioxidants on changes in oils during heating and deep frying. J Sci Food Agric 68:347–353.

Gorla G, Kour SM, Korlipara PV, Mallampalli KSL, Prasad RBN (2013) Preparation and properties of lubricant base stocks from epoxidized karanja oil and its alkyl esters. Ind Eng Chem Res 52:16598-16605.

Goud VV, Patwardhan AV, Pradhan NC (2006) Studies on the epoxidation of mahua oil (madhumica indica) byhydrogen peroxide. Bioresourc Technol 97:1365-1371.

Goud VV, Patwardhan AV, Dinda S, Pradhan NC (2007) Kinetics of epoxidation of jatropha oil with peroxyacetic and peroxyformic acid catalysed by acidic ion exchange resin. Chemical Eng Sci 62:4065-4076.

Goyan RL, Melley RE, Wissner PA, Ong WC (1998) Biodegradable lubricants. Lubricating Eng 54:10-17.

Guo R, Ma C, Sun S, Ma Y (2011) Kinetic study on on oxirane cleavage of epoxidized palm oil. J Am Oil Chem Soc 88:517-521.

Hajar M, Vahabzadeh F (2014) Modeling the kinetics of biolubricant production from castor oil using Novozym 435 in a fluidized-bed reactor. Ind Crops Products 59:252-259.

Hamilton RJ, Kalu C, Prisk E, Padley FB, Pierce H (1997) Chemistry of free radicals in lipids. Food Chem. 60:193-199.

Haus F, German J, Junter GA (2001) Primary biodegradability of mineral base oils in relation to their chemical and physical characteristics. Chemosphere 45:983–990.

Haus F, Boissel O, Junter GA (2004) Primary and ultimate biodegradabilities of mineral base oils and their relationships with oil viscosity. Int Biodeterior Biodegrad54:189–192.

Havet L, Blouet J, Robbe VF, Brasseur E, Slomka D (2001) Tribological characteristics of some environmentally friendly lubricants. Wear 248:140–146.

Hwang HS, Erhan ZS (2001) Modification of epoxidized soybean oil for lubricant formulations with improved oxidative stability and low pour point. J Am Oil Chem Soc 78:1179-1184.

Hwang HS, Adhyaryu A, Erhan SZ (2003) Preparation and properties of lubricant base stocks from oxidised soybean oil and 2-ethylhexanol. J Am Oil Chem Soc 80:811-815.

Hwang HS, Erhan SZ (2006) Synthetic lubricant basestocks from epoxidised soybean oil and Guerbet alcohols. Ind Crops Prod 23:311-317.

Imahara H, Minami E, Hari S, Saka S (2006) Thermal stability of biodiesel fuel as prepared by supercritical methanol process. Proceedings of the 2nd Joint International Conference on Sustainable Energy and Environment (SEE 2006), Bangkok, Thailand, November, Paper No. C-037:21–23.

Jayadas NH, Nair KP (2006) Coconut oil as base oil for industrial lubricants-evaluation and modification of thermal, oxidative and low temperature properties. Trib Int 39:873–878.

Jin FL, Park SJ (2008) Thermo mechanical behavior of epoxy resins modified with epoxidised vegetable oils. Polym International 57:577-583.

Kamalakar K, Rajak AK, Prasad RBN, Karuna MSL (2013) Rubber seed oil based biolubricant basestocks: A potential source for hydraulic oils. Ind Crops Prod 51:249-257.

Kamalakar K, Gorantla NVT, Manoj S, Prasad RBN, Karuna MSL (2014) Novel acyloxy derivatives of branched mono- and polyol esters of sal fat: Multiviscosity grade lubricant base stocks. J Agri Food Chem 49:11980-11987.

Kaya C, Hamamci C, Baysal A, Akba O, Erdogan A, Saydut O (2009) Methylester of peanut (Arachis hypogeal L) seed oil as a potential feedstock for biodiesel production. Renew Energy 34:1257–1260.

Knothe G (2002) Structure indices in FA chemistry. How relevant is the iodine value? J Am Oil Chem Soc 79:847-854.

Knothe G, Dunn RO (2003) Dependence of oil stability index of fatty compounds on their structure and concentration and presence of metals. J Am Oil Chem Soc 80:1021-1026.

Knothe G (2005) Dependence of biodiesel fuel properties on the structure of fatty acid alkyl esters. Fuel Process Technol 86:1059–1070.

Knothe G (2006) Analyzing biodiesel: standards and other methods. J Am Oil Chem Soc 83:823–833.

Knothe G (2007) Some aspects of biodiesel oxidative stability. Fuel Process Technol 88: 669–677.

Kulkarni RD, Deshpande PS, Mahajan SU, Mahulikar PP (2013) Epoxidation of mustard oil and ring opening with 2-ethylhexanol for biolubricants with enhanced thermo-oxidative and cold flow characteristics. Ind crops prod 49:586-592.

Lang X, Dalai AK, Reaney MJ, Hertz PB (2001) Biodiesel esters as lubricity additives: effects of process variables and evaluation of low-temperature properties. Fuels Int 1-3:207–227.

Lathi PS, Mattiasson B (2007) Green approach for the preparation of biodegradable lubricant base stock from epoxidised vegetable oil. Appl Catals B: Environ 69:207-212.

Lee I, Johnson LA, Hammond EG (1995) Use of branched-chain esters to reduce the crystallization temperature of biodiesel. J Am Oil Chem Soc 72:1155–1160.

Lee PL, Yunus WMZW, Yeong SK, Abdullah DK, Lim WH (2009) Optimization of the Epoxidation of methylester of palm fatty acid distillate. J Palm Res 21:675-682.

Li W, Wang X (2015) Biolubricants derived from waste cooking oil with improved oxidation stability and low temperature properties. J Oleo Sci 64:367-374.

Madankar CS, Dalai AK, Naik SN (2013) Green synthesis of biolubricant basestocks from canola oil. Ind Crops Prod 44:139-144.

Mahajan SU, Kulkarni PR, Kulkarni RD, Mahulikar PP (2013) Synthesis and characterization of chemically modified epoxidised mustard oil for biolubricant properties. Int J Appl Eng Res 17:2023-2030.

Mahalik K, Sahua JN, Patwardhan AV, Meikap BC (2010) Statistical modelling and optimization of hydrolysis of urea to generate ammonia for flue gas conditioning. J Hazard Mater 182:603–610.

Mahmoud Y, Mohammad B, Habibi N, Reza F (2014) Optimisation of ultrasound-assisted extraction of natural pigment from annatto seeds by response surface methodology (RSM). Food Chem 155:319–324.

Manivannan P, Rajasimman M (2011) Optimization of process parameters for the osmotic dehydration of beetroot in sugar solution. J Food Process Eng 34:804-825.

Mang T, Dresel W (2007) Lubricants and lubrication. Wiley Publishers.

Marta MC, Roberlucia AC, Fernando CS, Aline FB, Valter JFJ, Antonio GS (2007) Thermo analytical characterization of castor oil biodiesel. Renew Sustain Energy Rev 11:964–975.

Masjuki HH, Maleque MA, Kubo A, Nonaka T (1999) Palm oil and mineral oil based lubricants their tribological and emission performance. Tribol Int 32:305–314.

Mazumdar P, Borugadda VB, Goud VV, Sahoo L (2012) Physico-chemical characteristics of jatropha curcas L. of north east India for exploration of biodiesel. Biomass Bioene 46:546-554.

Mazza G, Qi H (1992) Effect of after-cooking darkening inhibitors on stability of frying oil and quality of French fries. J Am Oil Chem Soc 69:847–853.

Mercurio P, Burns KA, Negri A (2004) Testing the ecotoxicology of Vegetable Versus Mineral Based Lubricating Oils: 1. Degradation Rates Using Tropical Marine Microbes. Environ Pollut 129:165-173.

Meshram PD, Puri RG, Patil HV (2011) Epoxidation of Wild Safflower (Carthamus oxyacantha) Oil with Peroxy acid in presence of strongly Acidic Cation Exchange Resin IR- 122 as Catalyst. Int J Chem Tech Res 3:1152–1163.

Meyer P, Techaphattana N, Manundawee S, Sangkeaw S (2008) Epoxidation of soybean oil and jatropha oil. Thammasat Intern. J Sci Technol 13:1-5.

Mobarak HM, Mohamad EN, Masjuki HH, Kalam MA, Al Mahmud KAH, Habibullah M, Ashraful AM (2014) The prospects of biolubricants as alternativesin automotive applications. Ren Sustain Energy Rev 33:34–43.

Moser BR, Erhan SZ (2007) Preparation and Evaluation of a Series of α-hydroxy Ethers from 9, 10-epoxystreates. Eur Lipid Sci Technol 109:206–213.

Mubarak NM, Kundu A, Sahu JN, Abdullah EC, Jayakumar NS (2014) Synthesis of palm oil empty fruit bunch magnetic pyrolytic char impregnating with $FeCl_3$ by microwave heating technique. Biomass Bioenergy 61:265 – 275.

Mungroo R, Pradhan NC, Goud VV, Dalai AK (2008) Epoxidation of canola oil with hydrogen peroxide catalysed by acidic ion exchange resin. J Am Oil Chem Soc 85:887-896.

Mungroo R, Goud VV, Naik SN, Dalai AK (2011) Utilization of green seed canola oil for in situ Epoxidation. European J Lipid Sci Technol 113:768–774.

Monono EM, Haagenson DM, Wiesenborn DP (2015) Characterizing the epoxidation process conditions of canola oil for reactor scale-up. Ind Crops Prod 67:364–372.

Nadal MR, Servin JLC, Castellote AI, Rivero M, Sabater MCL (2006) Oxidation stability of the lipid faction in milk powder formulas. Food Chem 100:756–763.

Nagendramma P, Kaul S (2012) Development of ecofriendly/biodegradable lubricants: an overview. Renew Sustain Energy Rev 16:764–774.

Niederhauser WD, Koroly JE (1949) Process for the epoxidation of esters of oleic and linoleic acids, United States Patent Office.

Nik WBW, Ani FN, Masjuki HH (2005) Thermal stability evaluation of palm oil as energy transport media. Energy Convers Manage 46:2198–2215.

Norris S (2007) Trans fats: the health burden, parliamentary information and research service from library of parliament, Retrieved February 7, from the parliament of Canada Web site: http://www.parl.gc.ca/information/library/PRBpubs/prb0521-e.pdf.

Ogunniyi DS, Njikang GN (2000) Preparation and evaluation of alkyd resin from castor oil. Pak J Sci Ind Res 43:378-380.

Okieimen FE, Pavithran C, Bakare IO (2005) Epoxidation and hydroxlation of rubber seed oil: One-pot multi-step reactions. Eur J Lipid Sci Technol107:330-336.

Padmasiri K, Gamage BMO, Karunanayake L (2009) Epoxidation of some vegetable oils and their hydrolysed products with peroxyformic acid - optimised to industrial scale. J. National Sci. Foundation Sri Lanka 37:229-240.

Papadopoulos CE, Dazaridou A, Koutsoumba A, Kokkinos N, Christoforidis A, Nikolaou N (2010) Optimization of cottonseed biodiesel quality (critical properties) through modification of its FAME composition by highly selective homogeneous hydrogenation. Bioresour Technol 101:1812-1819.

Park JY, Kim DK, Lee JP, Park SC, Kim YJ, Lee JS (2008) Blending effects of biodiesels on oxidation stability and low temperature flow properties. Bioresour Technol 99: 1196–1203.

Patchara K, Supawan T (2011) Preparation of cold flow improver property from epoxidized palm oil and 2-ethylhexanol. PACCON, Pure and applied chemistry international conference.

Pathak K (2010) IOC to market bio-lubricant next year by, 2010. Business standard.

Patil PD (2012) Biodiesel production from waste cooking oil using sulfuric acid and microwave irradiation processes. J Environ Prot 3:107–113.

Petrovic Z, Zlatanic A, Lava CC, Fiser SS (2002) Epoxidation of soybean oil in toluene with peroxoacetic and peroxoformic acids-kinetics and side reactions. Eur J Lipid Sci Technol 104:293-299.

Prabhakar C, Raja CA (2012), Screening and optimization of alkaline protease productivity from bacillus sp. Agt from tannery effluent. Int J Pharm Biologic Archives 3:244-248.

Quinchia LA, Delgado MA, Valencia C, Franco JM, Gallegos C (2009) Viscosity modification of high oleic sunflower oil with polymeric additive for the design of new biolubricant formulations. Environ Sci Technol 43:2060-2065.

Quinchia LA, Delgado MA, Franco JM, Spikes HA, Gallegos C (2012) Low-temperature flow behaviour of vegetable oil-based lubricants. Ind Crops Prod 37:383–388.

Ramalho EFSM, Filho JRC, Albuquerque AR, De Oliveira SF, Avalcanti EHS, Stragevitch L, Santos IMG, Souza AG (2012) Low temperature behavior of poultry fat biodiesel: diesel blends. Fuel 93:601-605.

Ramos MJ, Fernandz CM, Casas A, Rodriguez L, Perez A (2009) Influence of fatty acid composition of raw materials on biodiesel properties. Bioresour Technol 100:261-368.

Refaat AA (2009) Correlations between the chemical structure of biodiesel and its physical properties. Int J Environ Sci Technol 6:677–694.

Rodrigues JA, Cardoso FP, Lachter ER, Estevao LRM, Lima E, Nascimento RSV (2006) Correlating chemical structure and physical properties of vegetable oil esters. J Am Oil Chem Soc 83:353–357.

Romeu A, Cuesta C, Sanchez MFJ (1998) Effect of oil replenishment during deep- fat frying of frozen foods in sunflower oil and high-oleic acid sunflower oil. J Am Oil Chem Soc 75:161–167.

Rudnick LR (2013) Synthetics, Mineral Oils, and Bio-Based Lubricants: Chemistry and technology. ISBN 13:978-1-4398-5538-6, CRC Press, Taylor & Francis Group.

Saldaria MDA, Martinez MSI (2013) Oxidative stability of fats and oils measured by differential scanning calorimetry for food and industrial applications." Chapter 19, 445-474, Edited by Amal Ali Elkordy, ISBN 978-953-51-0947-1, InTech publications.

Salih N, Salimon J, Yousif E (2011a) The physicochemical and tribological properties of oleic acid based triester biolubricants. Ind Crops Prod 34:1089-1096.

Salih N, Salimon J, Yousif E (2011b) Synthesis of oleic acid based esters as potential basestock for biolubricant production. Turkish J Eng Environ Sci 35:115-123.

Salih N, Salimon J, Yousif E, Abdullah M (2013) Biolubricant basestocks from chemically modified plant oils: ricinoleic acid based –tetraesters. Chemistry Central J 7, 128-141.

Salimon J, Salih N (2009a) Oleic acid diesters: Synthesis, characterization and low temperature properties. European J Sci Res 32:216-222.

Salimon J, Salih N (2009b) Substituted esters of octadecanoic acid as a potential biolubricants. European J Sci Res 31:273-279.

Salimon J, Salih N (2010) Chemical modification of oleic acid oil for biolubricant industrial applications. Australian J Basic Appl Sci 4:1999-2003.

Salimon J, Abdullah BM, Salih N (2011a) Optimization of the oxirane ring opening reaction in biolubricant base oil production. Arabian J Chem, In press corrected proof.

Salimon J, Salih N, Yousif E (2011b) Synthetic biolubricant basestocks from epoxidised ricinoleic acid: improved low temperature properties. J Chemists Chemical Engineers 60:127-134.

Salimon J, Salih N, Yousif E (2011c) Characterization and physico chemical properties of oleic acid ether derivatives as biolubricant basestocks. J Oleo Sci 60:613-618.

Slimon J, Salih N, Abdullah BM (2012a) Production of chemo-enzymatic catalyzed mono-epoxide biolubricant: Optimization and physico-chemical characteristics. J Biomedicine Biotechnol, Hindwai publishing corporation 2012:1-11.

Salimon J, Salih N, Yousif E (2012b) Biolubricant basestocks from chemically modified ricinoleic acid. J King Saud Uni 24:11-17.

Sahu JN, Acharya J, Meikap BC (2010) Optimization of production conditions activated carbons from Tamarind wood by zinc chloride using response surface methodology. Bioresour Technol 101:1974–1982.

Santana GCS, Martins PF, Da Silva DLN, Batistella CB, Filho MR, Maciel WMR (2010) Simulation and cost estimate for biodiesel production using castor oil. Chem Eng Res Design 88:626-632.

Santos JCO, Antonio GS, Eledir VS, Valter Jr VS, Arilson JNS (2004) Thermoanalytical, kinetic and rheological parameters of commercial edible vegetable oils. J Therm Anal Calorim 75:419-428.

Santos JCO, Santos IMG, Souza AG (2005) Effect of heating and cooling on rheological parameters of edible vegetable oils. J Food Eng 67:401–405.

Sarfaraz A, Sherazi STH, Bhanger MI, Farah NT, Mahesar SA (2009) Oxidative stability assessment of bauhinia pirpurea oil in comparison to two conventional vegetable

oils by differential scanning calorimetry and rancimat methods. Thermochimica Acta 484:1-3.

Saurabh T, Patnaik M, Bhagt SL, Renge VC (2011) Epoxidation of vegetable oils: a review. Intern J Adv Eng Technol 2:491-501.

Schneider M (2006) Plant-oil-based lubricants and hydraulic fluids. J Sci Food Agric 86: 1769–1780.

Schober S, Mittelbach M (2004) The impact of antioxidants on biodiesel oxidation stability Eur J Lipid Sci Technol 106:382-389.

Sharma BK, Adhvaryu A, Erhan SZ (2006) Synthesis of hydroxy thio-ether derivatives of vegetable oil. J Agri Food Chem 54:9866-9872.

Sharma YC, Singh B, Upadhyay SN (2008a) Advancements in development and characterization of biodiesel: A review. Fuel 87:2355-2373.

Sharma BK, Erhan SZ, Liu Z, Adhvaryu A (2008b) One-pot synthesis of chemically modified vegetable oils. J Agri Food Chem 56:3049-3056.

Sharma BK, Doll KM, Erhan SZ (2008c) Ester hydroxy derivatives of methyl oleate : Tribological, oxidation and low temperature properties. Bioresour Technol 99:7333–7340.

Sharma YC, Agrawal S, Singh B, Frómeta AEN (2012) Synthesis of economically viable biodiesel from waste frying oils (WFO). Can J Chem Eng 90:483–488.

Sharma RV, Dalai AK (2013) Synthesis of biolubricant from epoxy canola oil using sulphated Ti-SBA-15 catalyst. Appl catal B: Environ 142-143:604-614.

Sherwin ER (1978) Oxidation and antioxidants in fat and oil processing. J Am Oil Chem Soc 55:809-814.

Siddharth J, Sharma MP (2011) Thermal stability of biodiesel and its blends: A review. Renew Sustain Energy Rev 15:438–448.

Siddharth J, Sharma MP (2010) Review of different test methods for the evaluation of stability of biodiesel. Renew Sustain Energy Rev 14:1937-1947.

Silva MS, Arimateja HJ, Silva GF, Dantas NAA, Castro DTN (2015a) New formulations for hydraulic biolubricants based on epoxidised vegetable oils: Passion fruit (Passiflora edulis Sims f.flavicarpa Degener) and moringa (Moringa oleifera Lamarck). Brazilian J Petroleum Gas 9:27-36.

Silva MS, Foletto EL, Alves SM, Dantas TNC, Neto AAD (2015b) New hydraulic biolubricants based on passion fruit and moringa oils and their epoxy. Ind crops prod 69:362-370.

Small DM (1986) The physical chemistry of lipids: from alkanes to phospholipids. ISBN-13:9780306417634, Plenum Press, New York, USA.

Sricharoenchaikul V, Atong D (2009) Thermal decomposition study on Jatropha curcas L. waste using TGA and fixed bed reactor. J Anal Appl Pyrol 85:155–162.

Suarez PAZ, Perreira MSC, Doll KM, Sharma BK, Erhan SZ (2009) Epoxidation of methyl oleate using heterogeneous catalyst. Ind Eng Chem Res 48:3268-3270.

Sun S, Shan I, Liu JQ, Song Y, Wang X (2009) Solvent free enzymatic synthesis of feruloylated diacylglycerols and kinetic study. J Mol Catal B: Enzym 57:104-108.

Sun S, Ke X, Cui L, Yang G, Bi Y, Song F, Xu X (2011) Enzymatic epoxidation of Sapindus mukorossi seed oil by perstearic acid optimized using response surface methodology. Ind Crops Prod 33:676–682.

Soni S, Agarwal M (2014) Lubricants from renewable energy resources-a review. Green Chem Lett Rev7:359-382.

Soriano NU, Migo VP, Matsumura M (2006) Ozonized vegetable oil as pour point depressant for neat biodiesel. Fuel 85:25-31.

Tabrizi SAH, Nassaj ET (2011) Modeling and optimization of densification of nanocrystalline Al_2O_3 powder prepared by a sol–gel method using response surface methodology. J Sol Gel Sci Technol 57:212-220.

Takeoka GR, Full GH, Dao LT (1997) Effect of heating on the characteristics and chemical composition of selected frying oil and fat. J Agric Food Chem 45:3244–3249.

Tompkins C, Perkins EG (2000) Frying performance of low-linolenic acid soybean oil. J Am Oil Chem Soc 77:223–229.

Tan SG, Chow WS (2010) Biobased epoxidized vegetable oils and its greener epoxy blends: a review. Polym Plast Technol Eng 49:1581–1590.

Tongoona P (1992) Castor (Ricinus communis L.) research and production prospects in Zimbabwe. Ind Crops Prod 1:235-239.

Wadumesthrige K, Salley SO, Simong KYN (2009) Effects of partial hydrogenation, Epoxidation and hydroxylation on the fuel properties of fatty acid methyl esters. Fuel Process Technol 90:1292-1299.

Wu X, Xingang Z, Shengring Y, Haigang C, Dapu W (2000) The study of epoxidised rapeseed oil used as potential biodegradable lubricant. J Am Oil Chem Soc 77:561-563.

Xu XQ, Tran VH, Palmer M, White K, Salisbury P (1999) Chemical and physical analyses and sensory evaluation of six deep-frying oils. J Am Oil Chem Soc 76:1091–1099.

Yao L, Hammond EG, Wang T, Bhuyan S, Sundararajan S (2010) Synthesis and physical properties of potential biolubricants based on ricinoleic acid. J Am Oil Chem Soc 87:937-945.

Yen HY, Yang MH (2003) The effect of metal ions additives on the rheological behavior of polyacrylamide solution. Polym Test 22:389-393.

Zuleta EC, Rios LA, Benjumea PN (2012) Oxidative stability and cold flow behavior of palm, sacha-inchi, jatropha and castor oil biodiesel blends. Fuel Process Technol 102: 96–101.

Zulkifli NWM, Azman SSN, Kalam MA, Masjuki HH, Yunus R, Gulzar M (2015) Lubricity of biobasd lubricant derived from different chemically modified fatty acid methyl ester. Tribology International, Article in Press.

Statistical Analysis

Experimental data obtained by CCD procedure was analysed through RSM by employing a quadratic polynomial equation to predict the response of a process as a function of independent variables and their interactions. In this work, the mathematical relationship relating variables to the response was calculated by the following polynomial equation:

$$Y = \beta_0 + \sum_{i=1}^{n} \beta_i x_i + \sum_{i=1}^{n} \beta_{ii} x_i^2 + \sum_{i=1}^{n} \sum_{j>1}^{n} \beta_{ij} x_i x_j$$

Where Y is the response (OOC), X_i and X_j represent independent variables, β_0 is the constant, β_i is the linear term coefficient, β_{ii} is the quadratic term coefficient, β_{ij} is the cross term coefficient and n is the number of factors studied and optimized in the study. The Design Expert software version 8.0.6 (State-Ease Inc) was opted for multiple regression and graphical analysis of the experimental data. Analysis of variance (ANOVA) was applied to estimate the effects of process variables and their possible interaction effects on the OOC yield of the epoxides in the response surface regression procedure. The goodness of fit of the model was evaluated by the regression coefficient of R^2. Response surface and counter plots were developed using the fitted quadratic polynomial equation obtained from regression analysis, keeping two of the independent variables at a fixed value and varying the other two variables.

Table A.1 Experimental design matrix for optimization of WCO epoxide

Run No	Time (A, h)	Catalyst Loading (B, wt%)	Temperature (C, ^{o}C)	H_2O_2 Molar Ratio (D, mol)	OOC
1.	8	11	45	1.1	4.83
2.	14	11	45	1.1	5.25
3.	8	21	45	1.1	5.14
4.	14	21	45	1.1	5.39
5.	8	11	65	1.1	4.62
6.	14	11	65	1.1	4.50
7.	8	21	65	1.1	5.06
8.	14	21	65	1.1	4.69
9.	8	11	45	2.1	5.16
10.	14	11	45	2.1	5.66
11.	8	21	45	2.1	5.71
12.	14	21	45	2.1	6.03
13.	8	11	65	2.1	5.13
14.	14	11	65	2.1	4.99
15.	8	21	65	2.1	5.67
16.	14	21	65	2.1	5.51
17.	5	16	55	1.6	5.05
18.	17	16	55	1.6	5.28
19.	11	6	55	1.6	5.15
20.	11	26	55	1.6	5.82
21.	11	16	35	1.6	5.10
22.	11	16	75	1.6	4.52
23.	11	16	55	0.6	4.59
24.	11	16	55	2.6	5.62
25.	11	16	55	1.6	6.17
26.	11	16	55	1.6	6.17
27.	11	16	55	1.6	6.17
28.	11	16	55	1.6	6.17
29.	11	16	55	1.6	6.17
30.	11	16	55	1.6	6.17

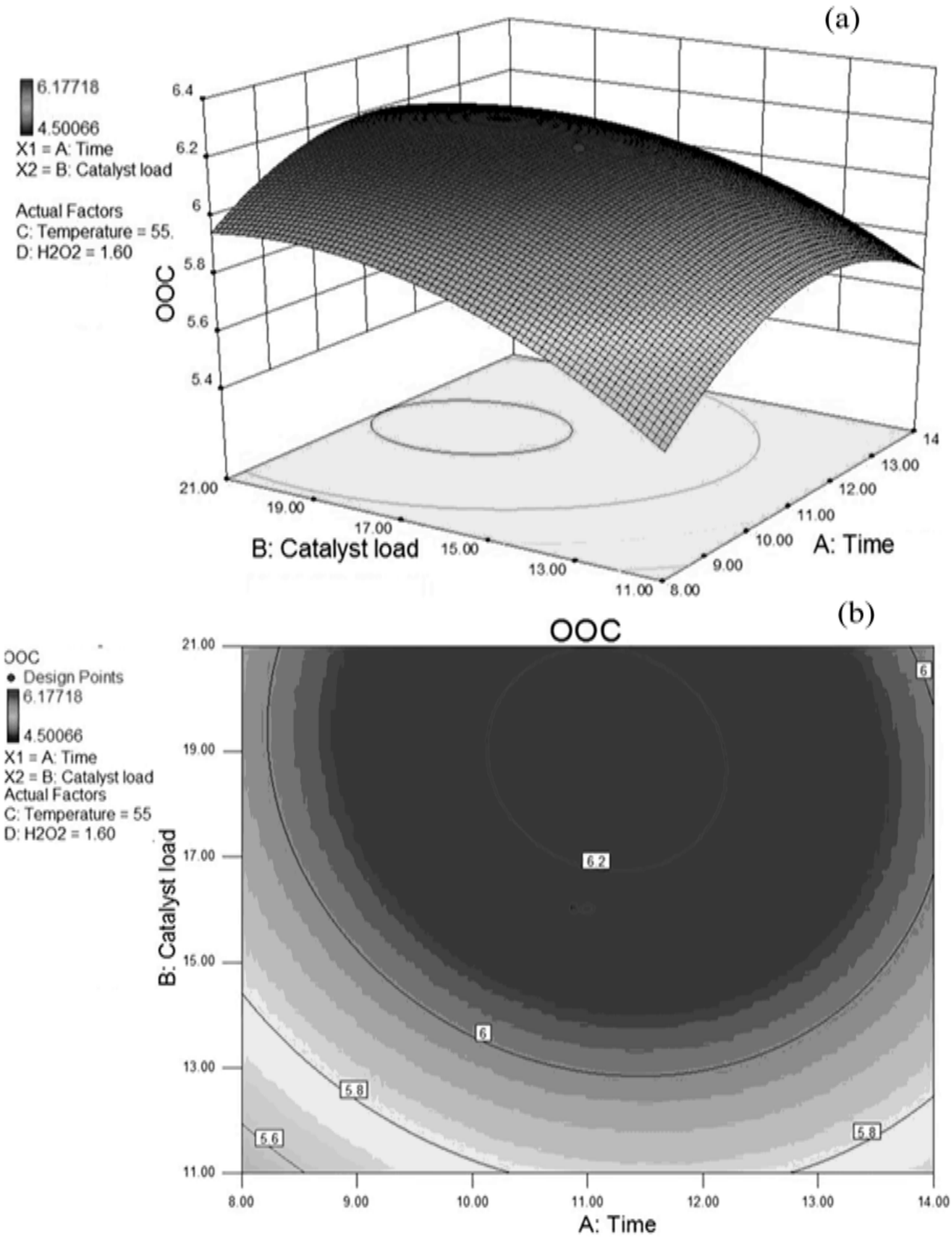

Figure A.1: (a) Response surface and (b) counter plots for the effect of the time (A) and catalyst loading (B) on OOC

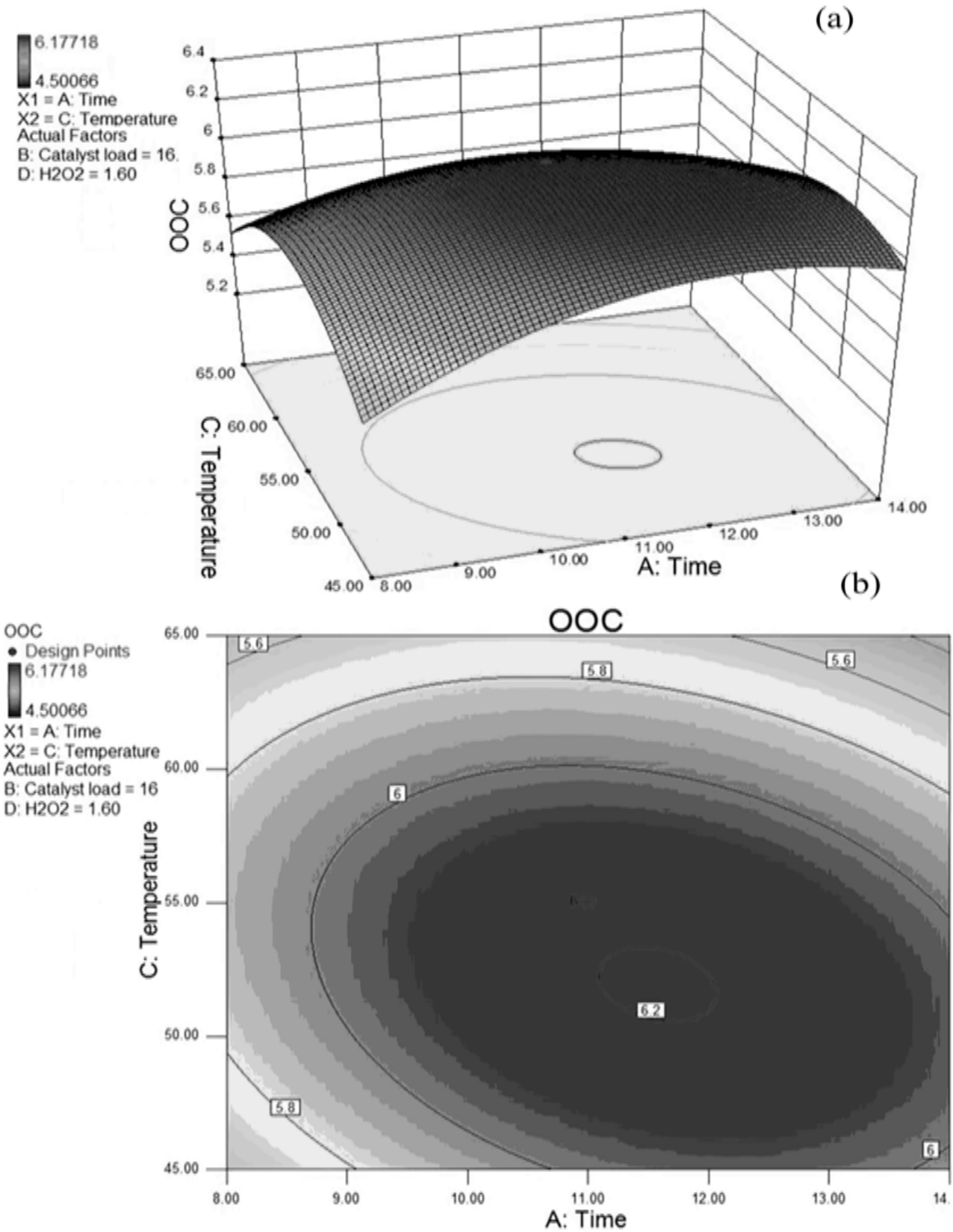

Figure A.2: (a) Response surface and (b) counter plots for the effect of the time (A) and temperature (C) on OOC

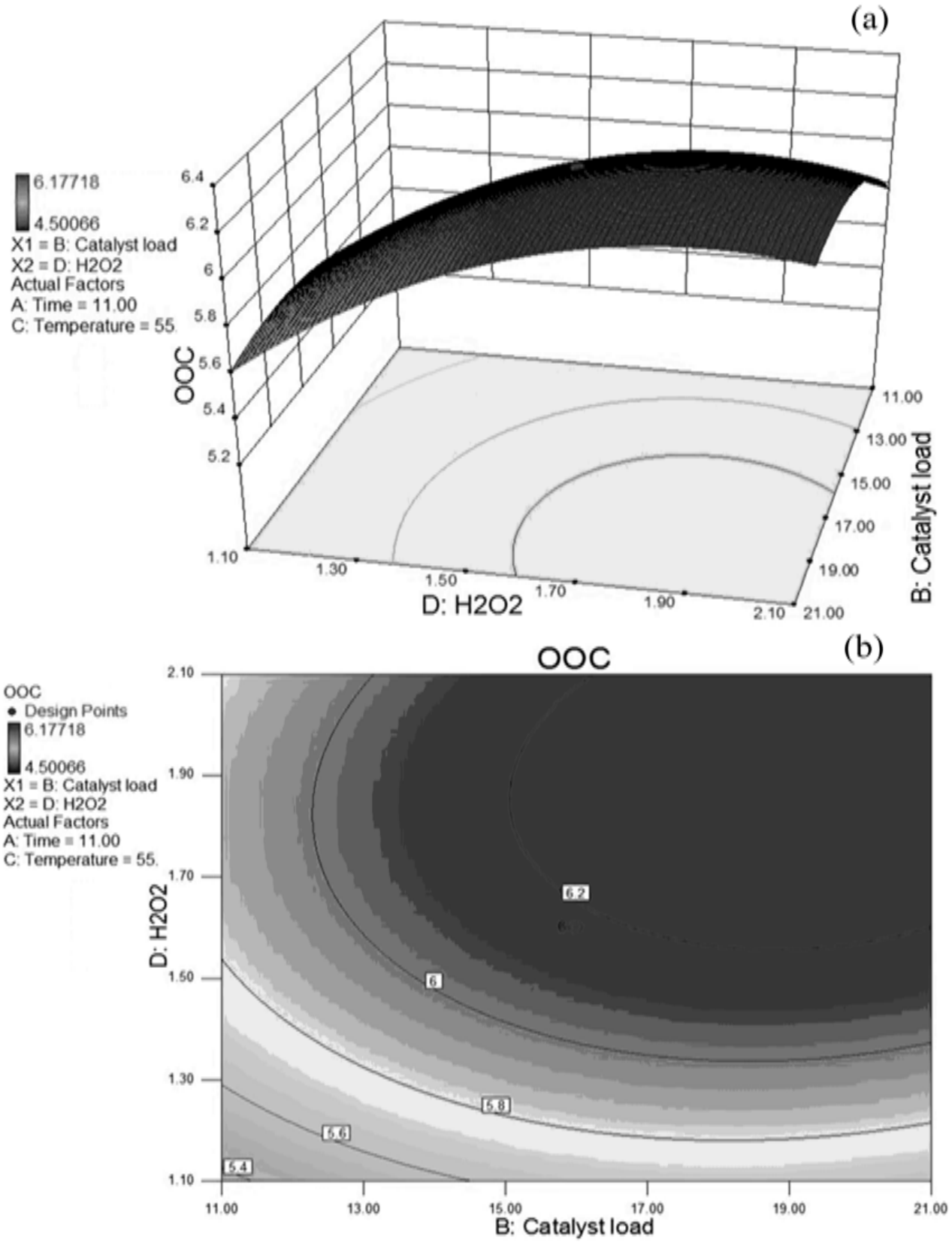

Figure A.3: (a) Response surface and (b) counter plots for the effect of the catalyst loading (B) and hydrogen peroxide molar ratio (D) on OOC

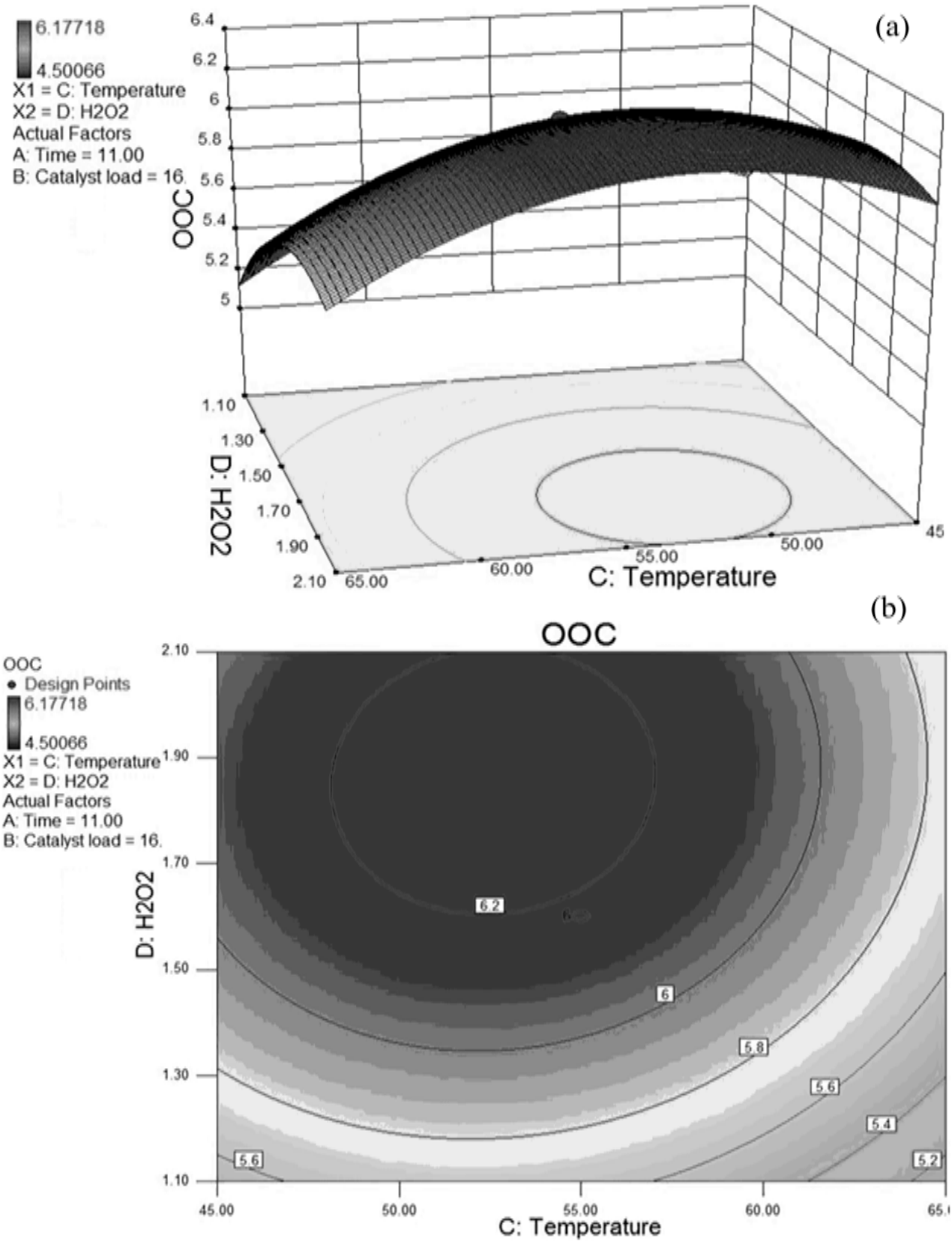

Figure A.4: (a) Response surface and (b) counter plots for the effect of the temperature (C) and hydrogen peroxide molar ratio (D) on OOC

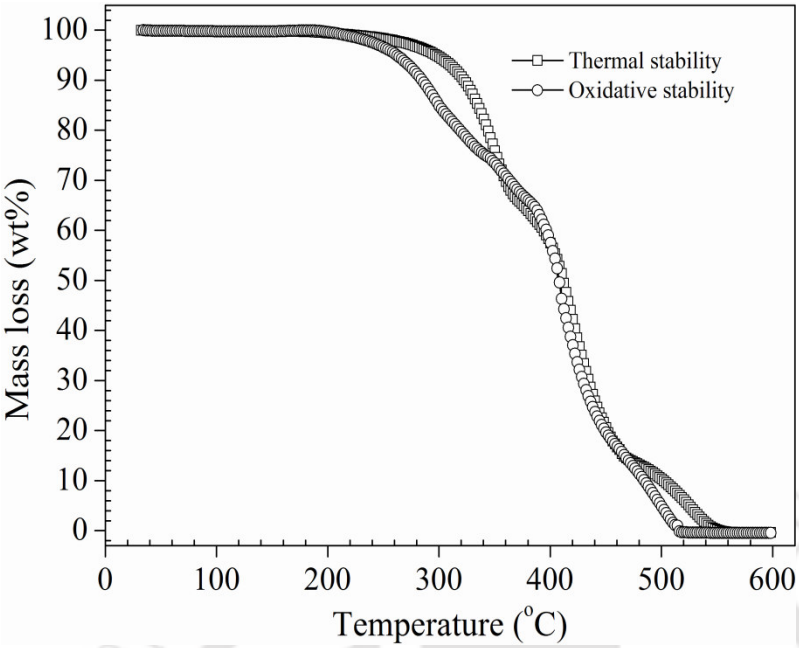

Figure A.5: SBO Thermo-oxidative stability thermo-grams

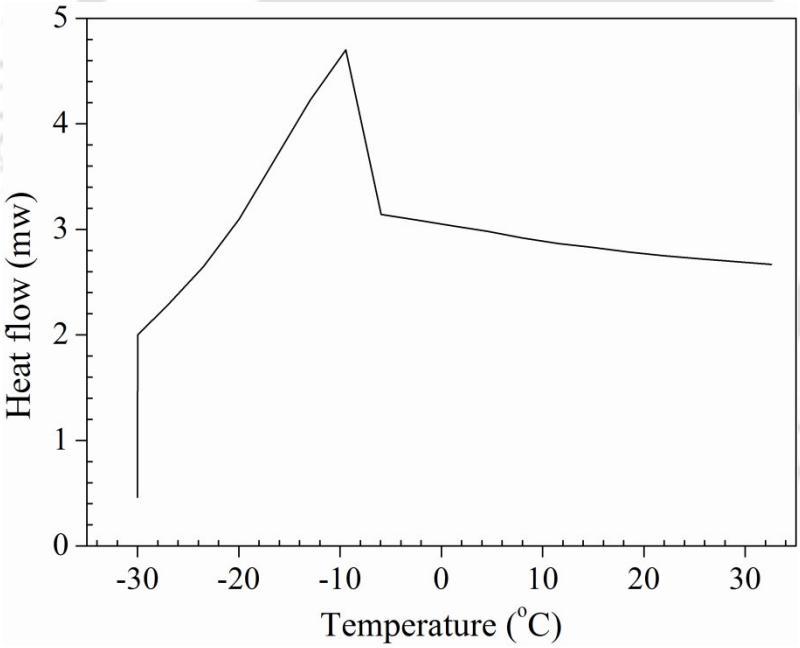

Figure A.6: SBO DSC thermo-gram for PP determination

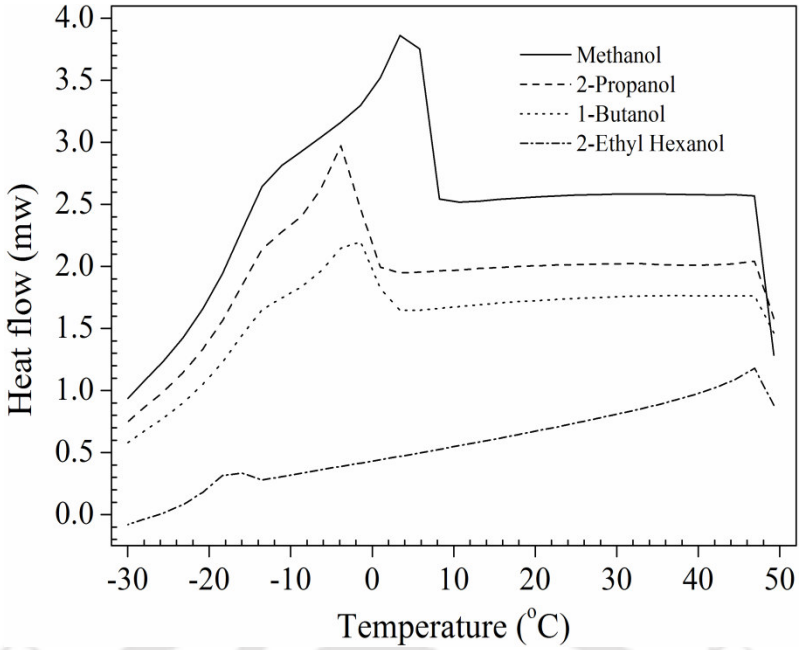

Figure A.7: WCO hydroxylation DSC thermo-grams with different alcohols for PP determination

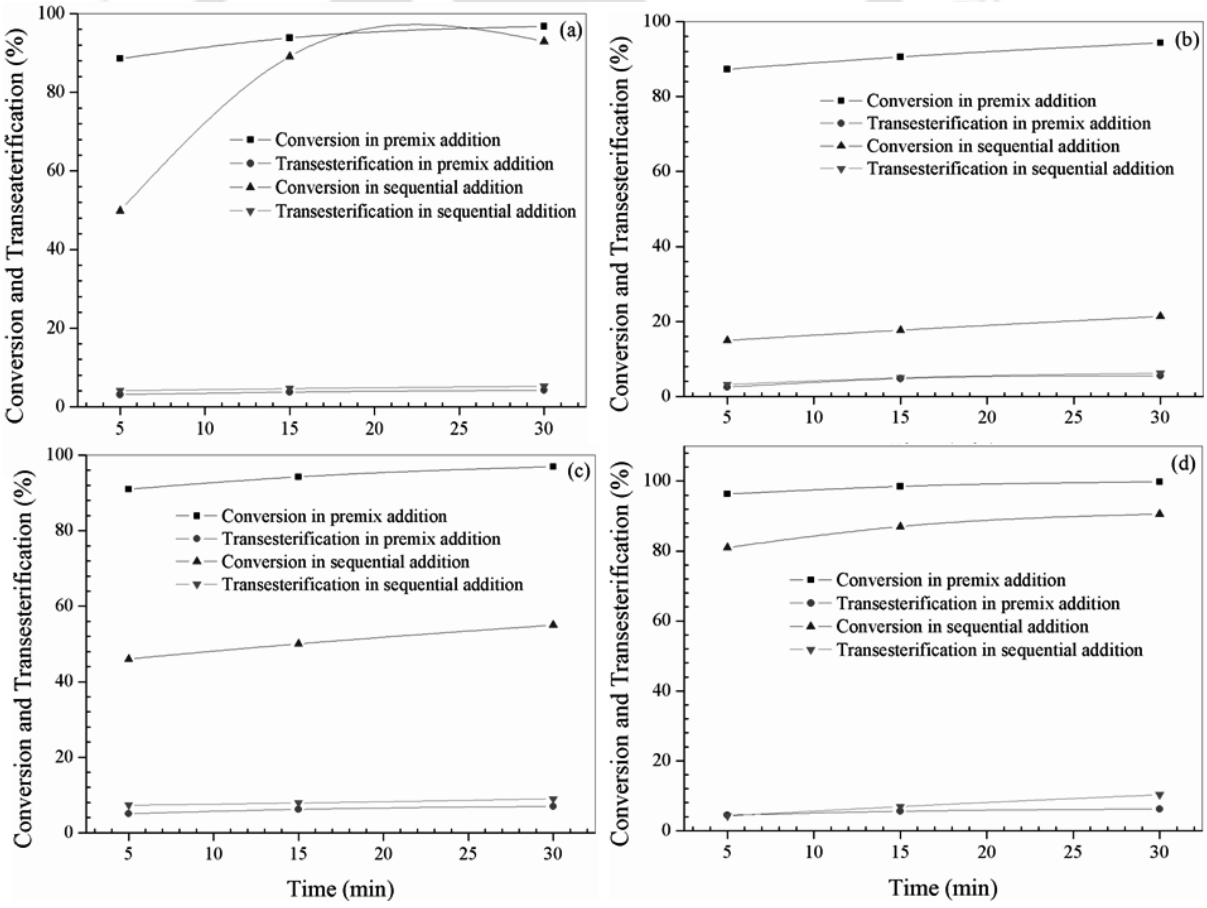

Figure A.8: Conversion and transesterification outcomes of sequential and premix addition for WCO at 8 mol of 2-EH, 3 wt% of H_2SO_4 (a), 10 mol of 2-EH, 1 wt% of H_2SO_4 (b), 10 mol of 2-EH, 2 wt% of H_2SO_4 (c), 10 mol of 2-EH, 3 wt% of H_2SO_4 (d) at room temperature

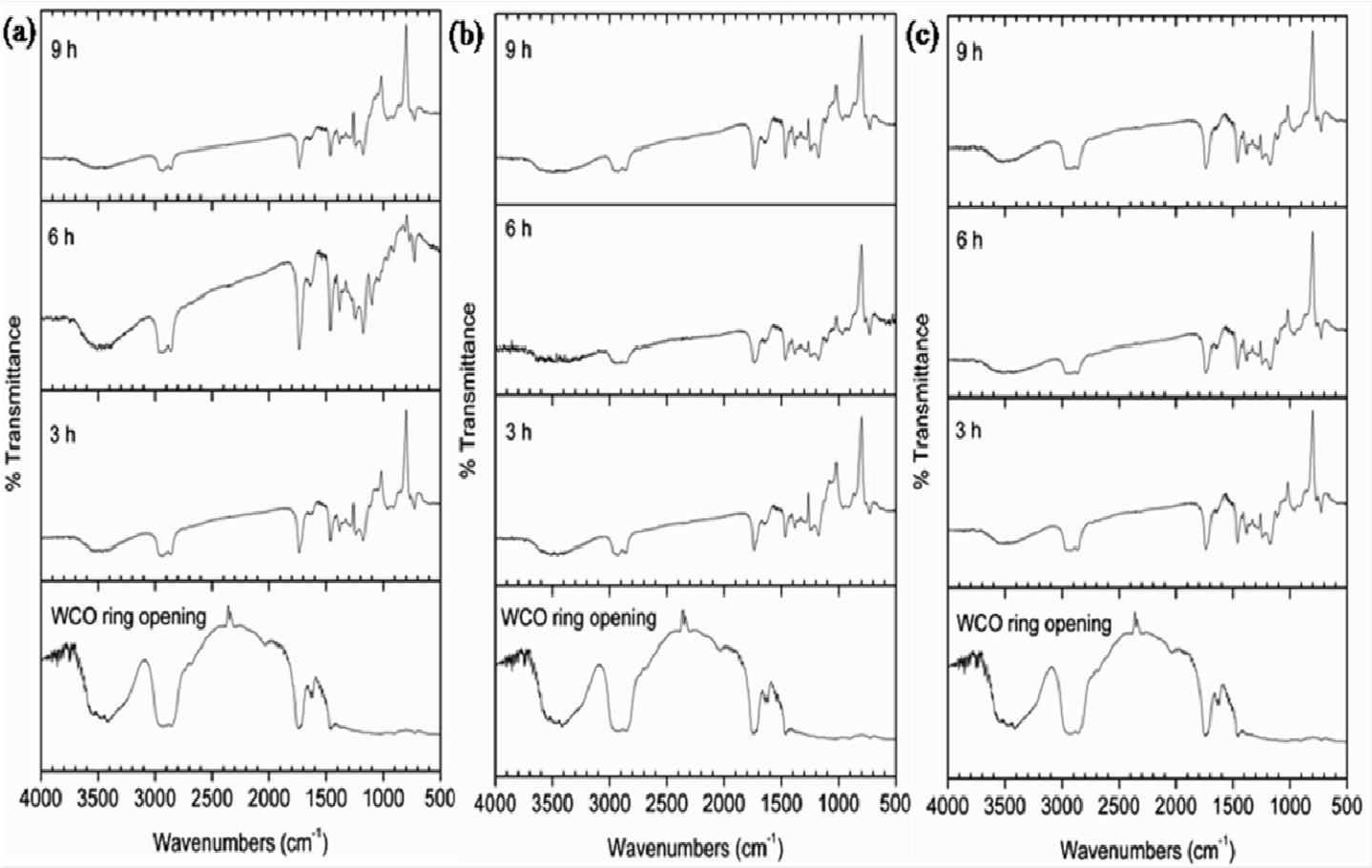

Figure A.9: Product confirmation by FT-IR spectra of various reaction conditions for hexanoylation of WCO ring opened product at (a) 2 mol, 2 wt%, 60 ^{o}C (b) 2 mol, 2 wt%, 70 ^{o}C (c) 2 mol, 2 wt%, 80 ^{o}C

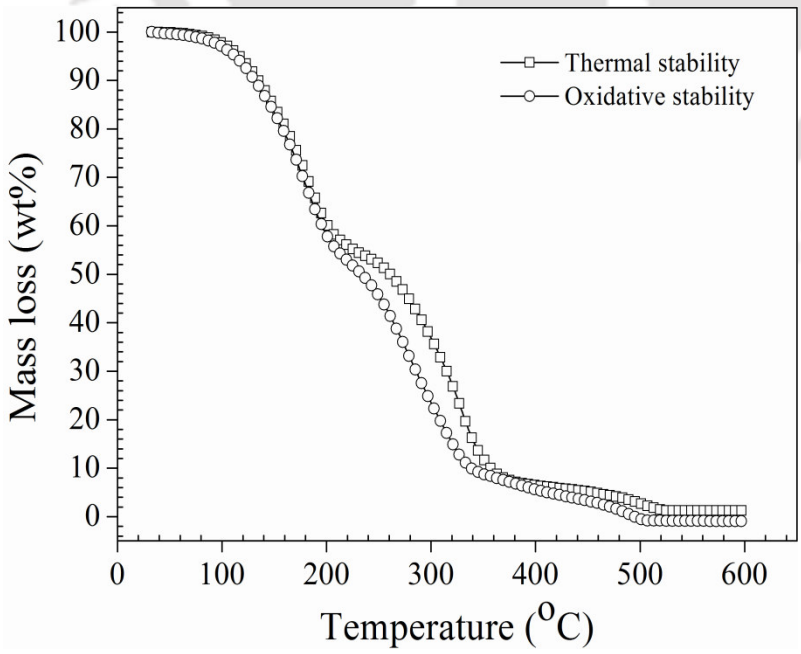

Figure A.10: Thermo-oxidative stability thermo-grams for WCO hexanoylated product

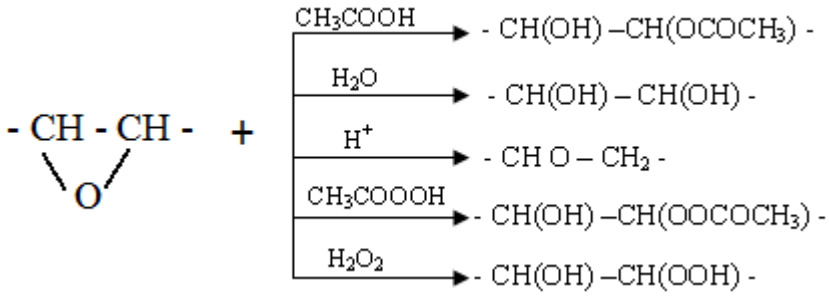

Scheme A.1: Mechanism of excess reagents reaction with the epoxy rings to cause unwanted side reactions

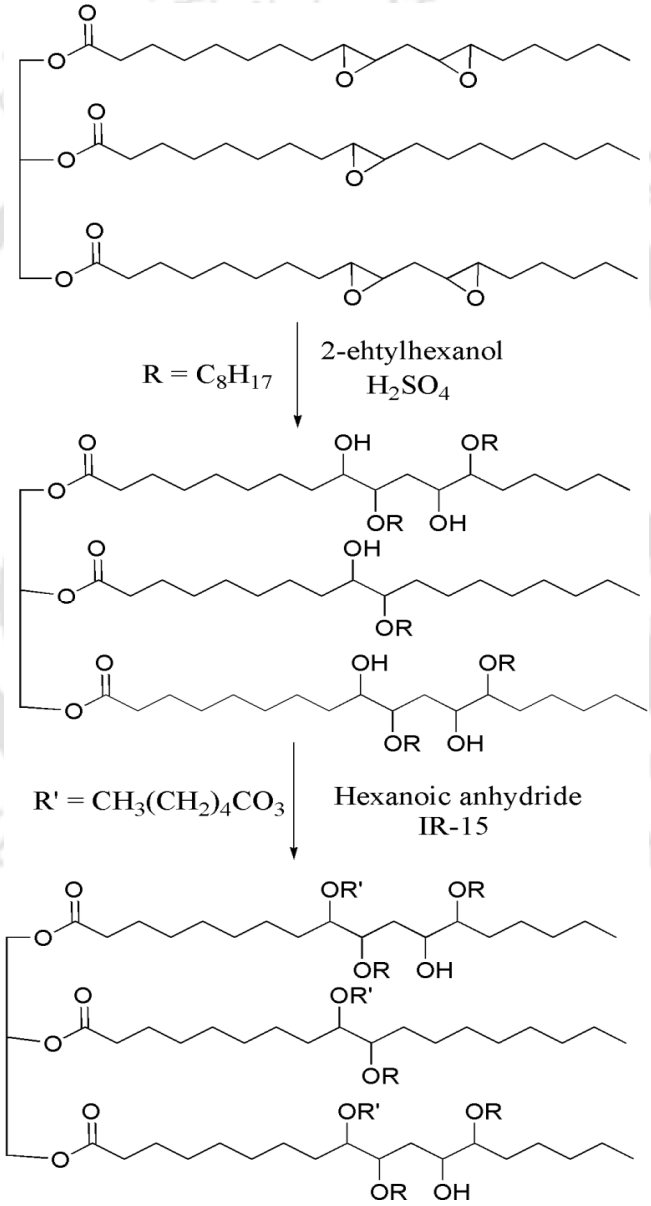

Scheme A.2: Reaction scheme for WCO hydroxylation (ring opening) and hexanoylation

Table A.2: Experimental design matrix for optimization of WCOFAME epoxide

Run No	Time (A, h)	Temperature (B, °C)	H_2O_2 Molar Ratio (C, mol)	Catalyst Loading (D, wt%)	Oxygen oxirane content (OOC)
1.	7	50	1	10	3.76
2.	11	50	1	10	4.37
3.	7	70	1	10	4.1
4.	11	70	1	10	4.2
5.	7	50	2	10	4.06
6.	11	50	2	10	4.73
7.	7	70	2	10	4.21
8.	11	70	2	10	4.47
9.	7	50	1	30	5.46
10.	11	50	1	30	5.11
11.	7	70	1	30	4.98
12.	11	70	1	30	4.23
13.	7	50	2	30	5.6
14.	11	50	2	30	5.44
15.	7	70	2	30	5.03
16.	11	70	2	30	4.46
17.	5	60	1.5	20	5.1
18.	13	60	1.5	20	5.03
19.	9	40	1.5	20	4.53
20.	9	80	1.5	20	3.8
21.	9	60	0.5	20	3.89
22.	9	60	2.5	20	4.32
23.	9	60	1.5	0	4.44
24.	9	60	1.5	40	6.04
25.	9	60	1.5	20	5.82
26.	9	60	1.5	20	5.84
27.	9	60	1.5	20	5.83
28.	9	60	1.5	20	5.845
29.	9	60	1.5	20	5.829
30.	9	60	1.5	20	5.836

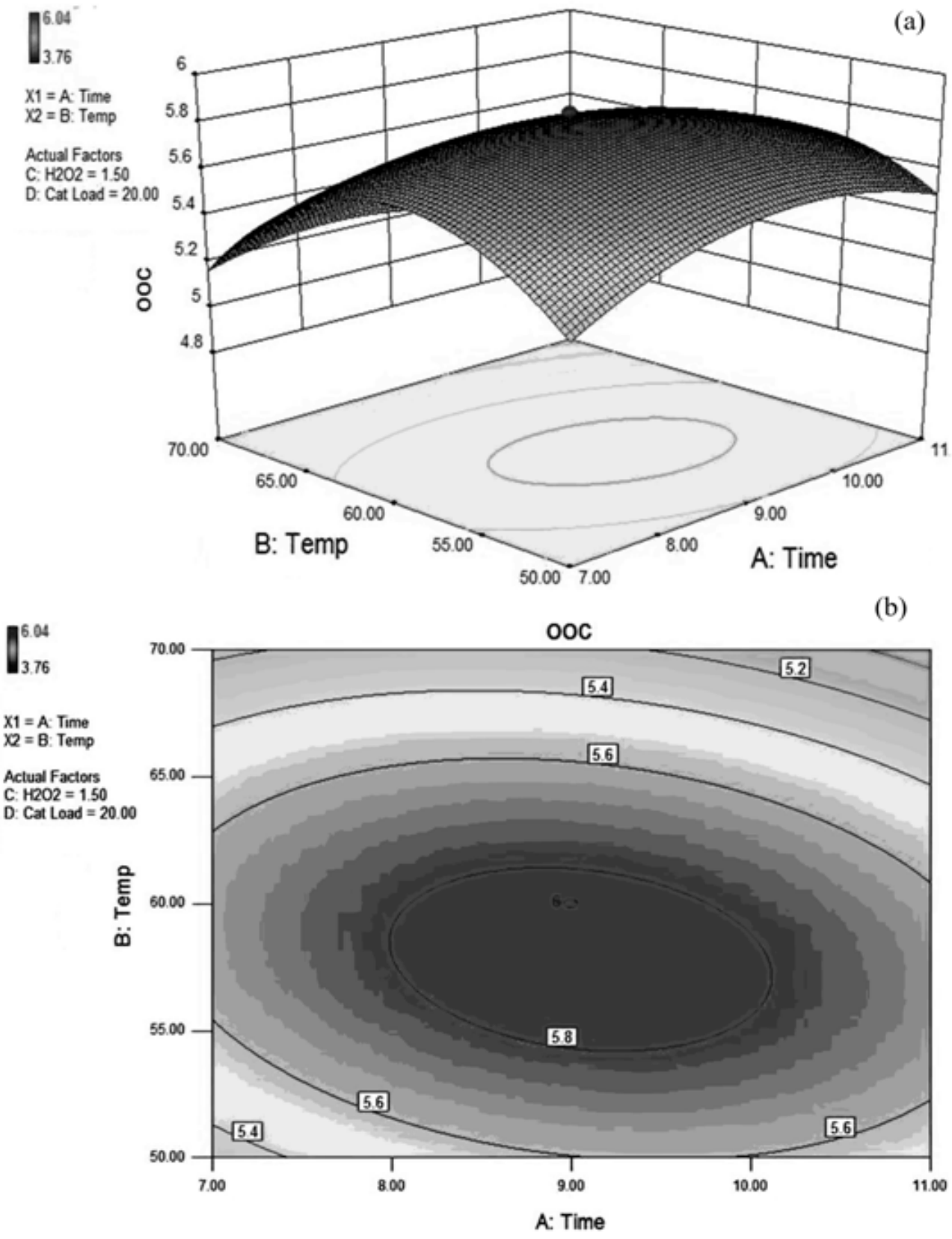

Figure A.11: Response surface (a) and counter (b) plots for the effect of the time (A) and temperature (B) for maximum OOC

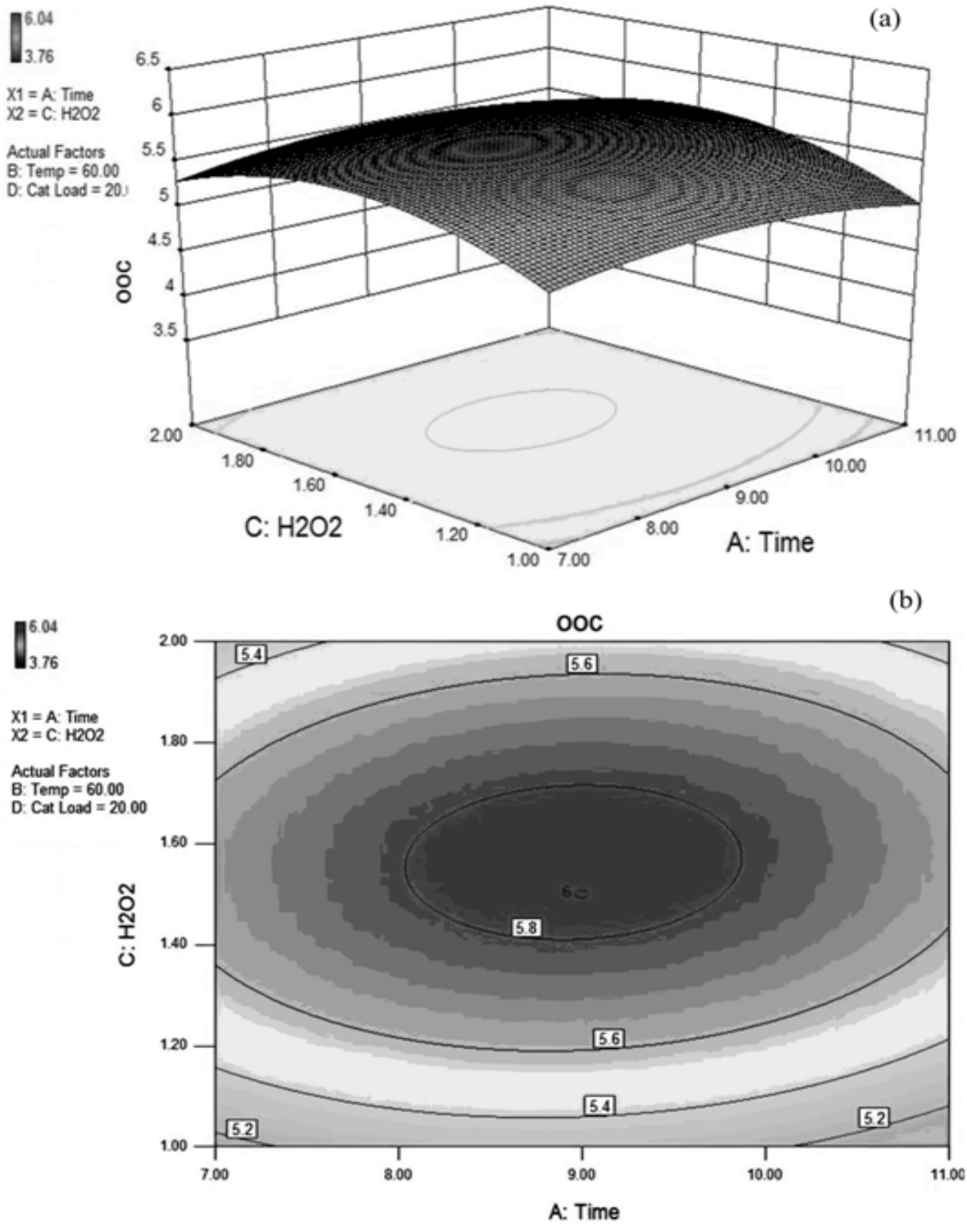

Figure A.12: Response surface (a) and counter (b) plots for the effect of the time (A) and hydrogen peroxide molar ratio (C) for maximum OOC

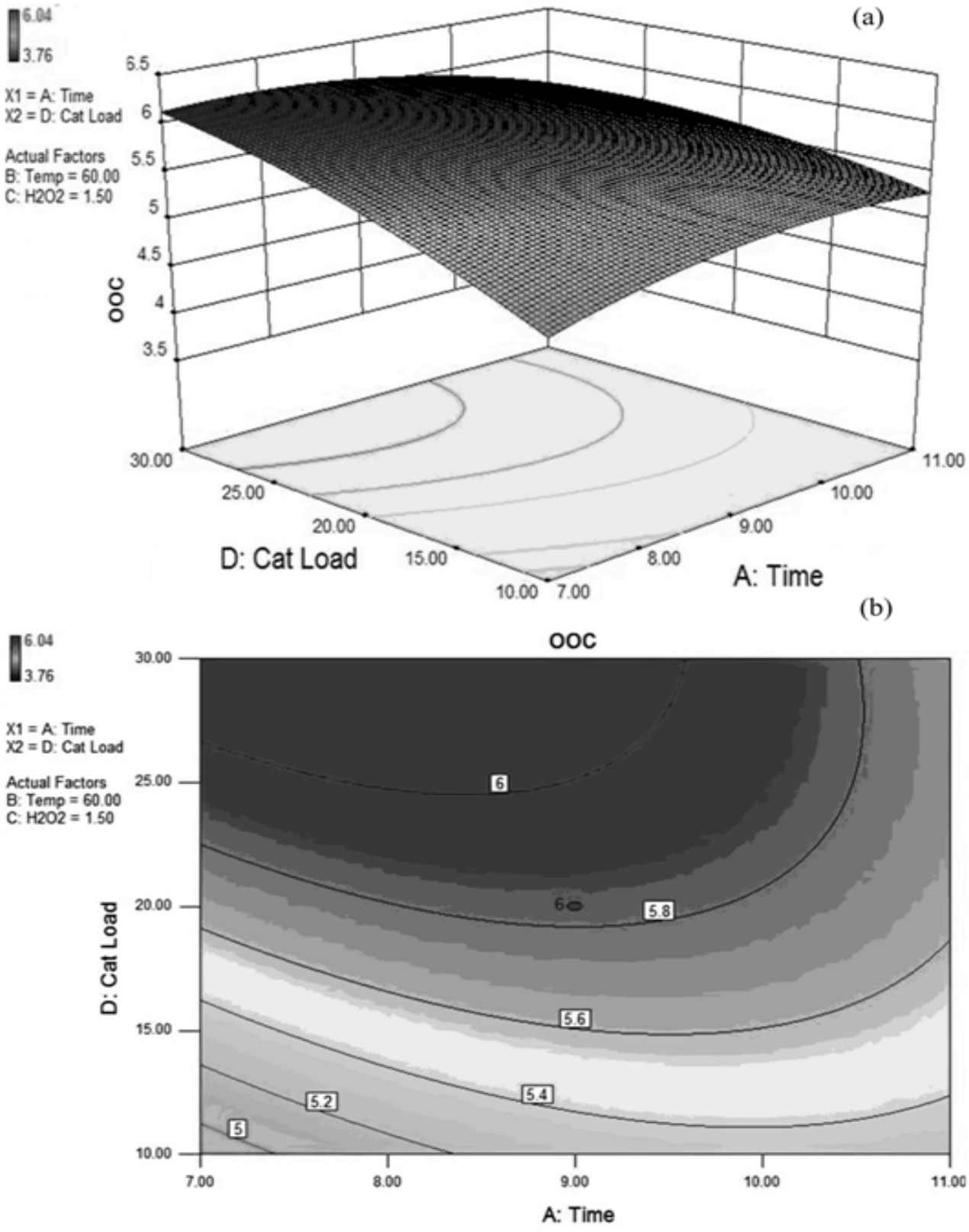

Figure A.13: Response surface (a) and counter (b) plots for the effect of the time (A) and catalyst loading (D) for maximum OOC

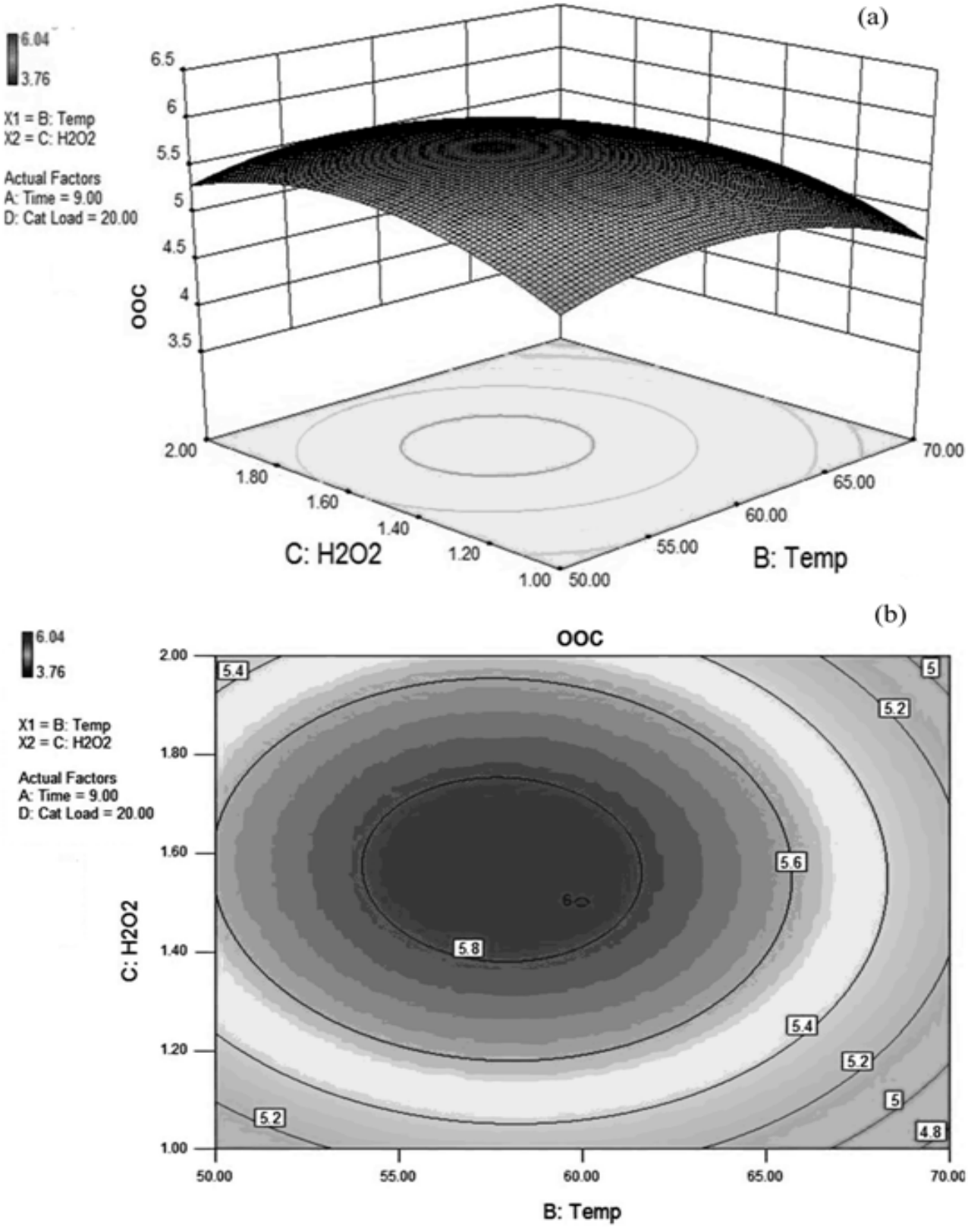

Figure A.14: Response surface (a) and counter (b) plots for the effect of the temperature (B) and hydrogen peroxide molar ratio (C) for maximum OOC

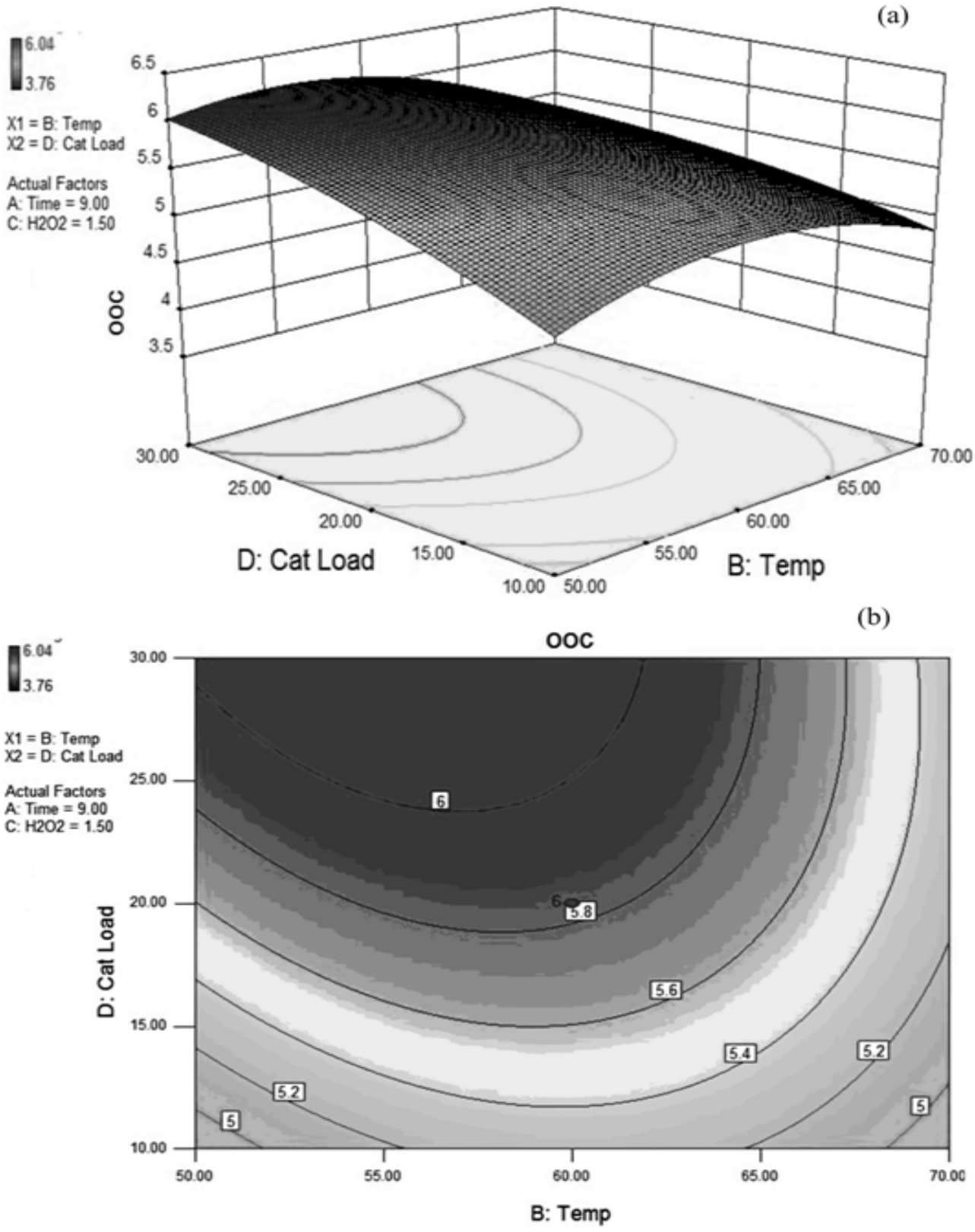

Figure A.15: Response surface (a) and counter (b) plots for the effect of temperature (B) and catalyst loading (D) for maximum OOC

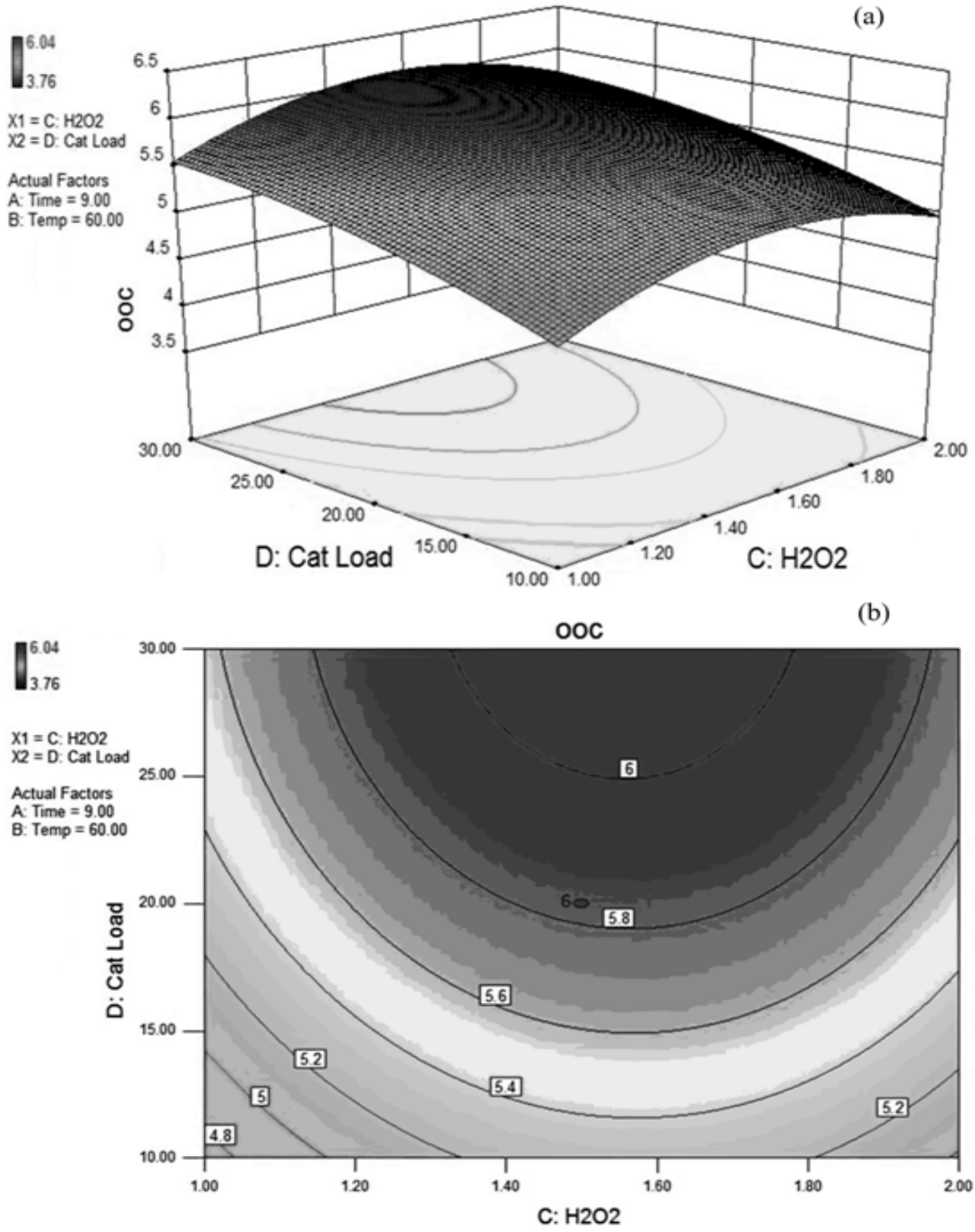

Figure A.16: Response surface (a) and counter (b) plots for the effect of hydrogen peroxide molar ratio (C) and catalyst loading (D) for maximum OOC

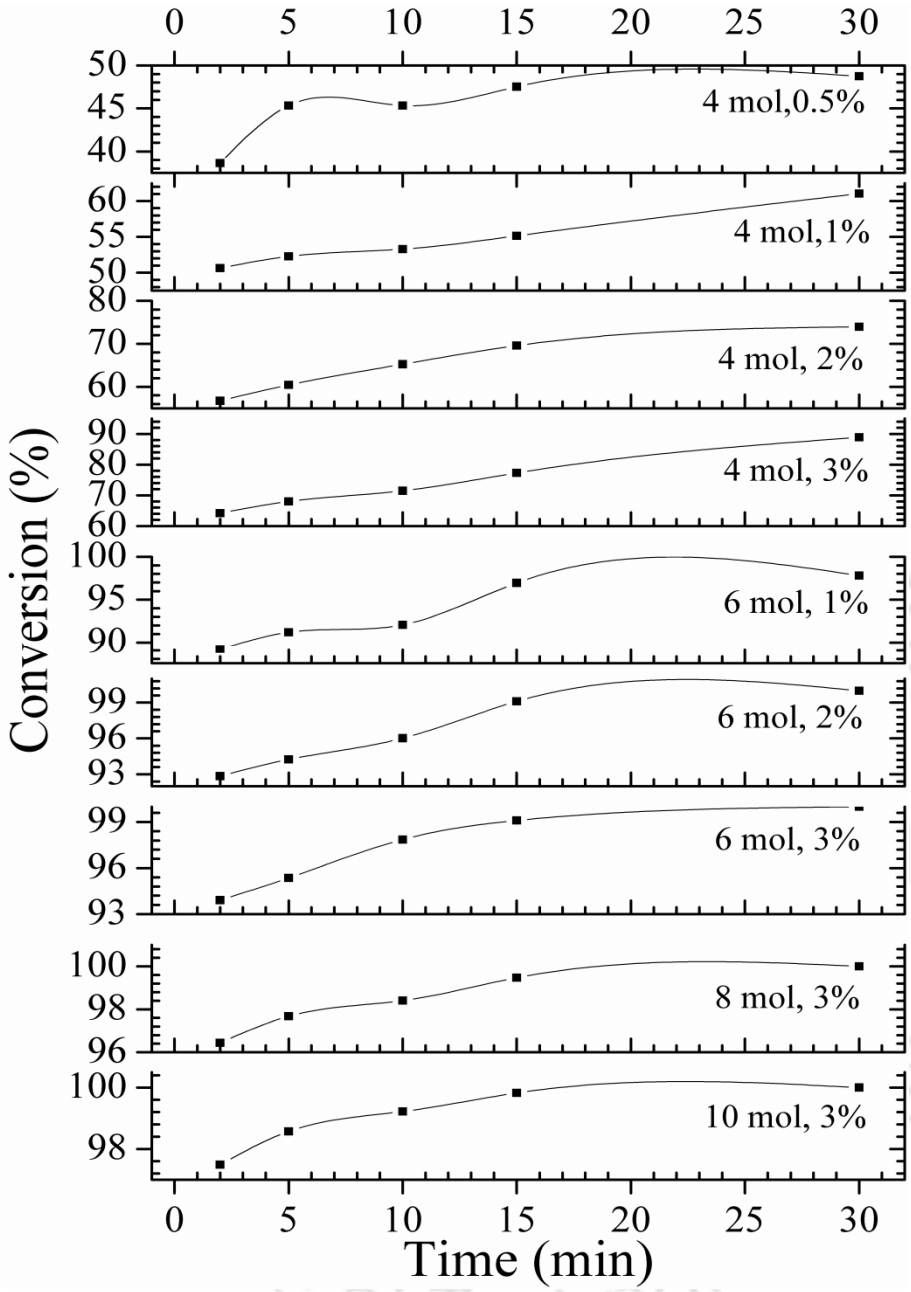

Figure A.17: Conversion in premix addition for WCOFAME hydroxylation at ambient temperature by varying catalyst loading and alcohol moles

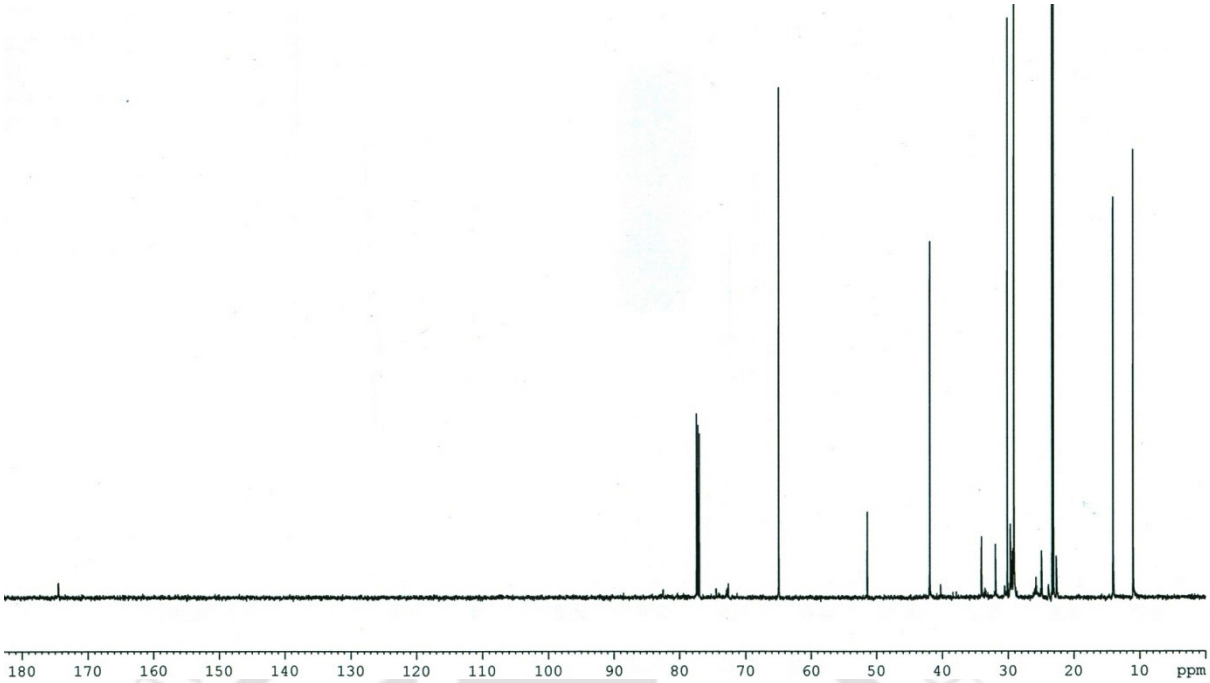

Figure A.18: ^{13}C-NMR spectra of WCOFAME hydroxylation

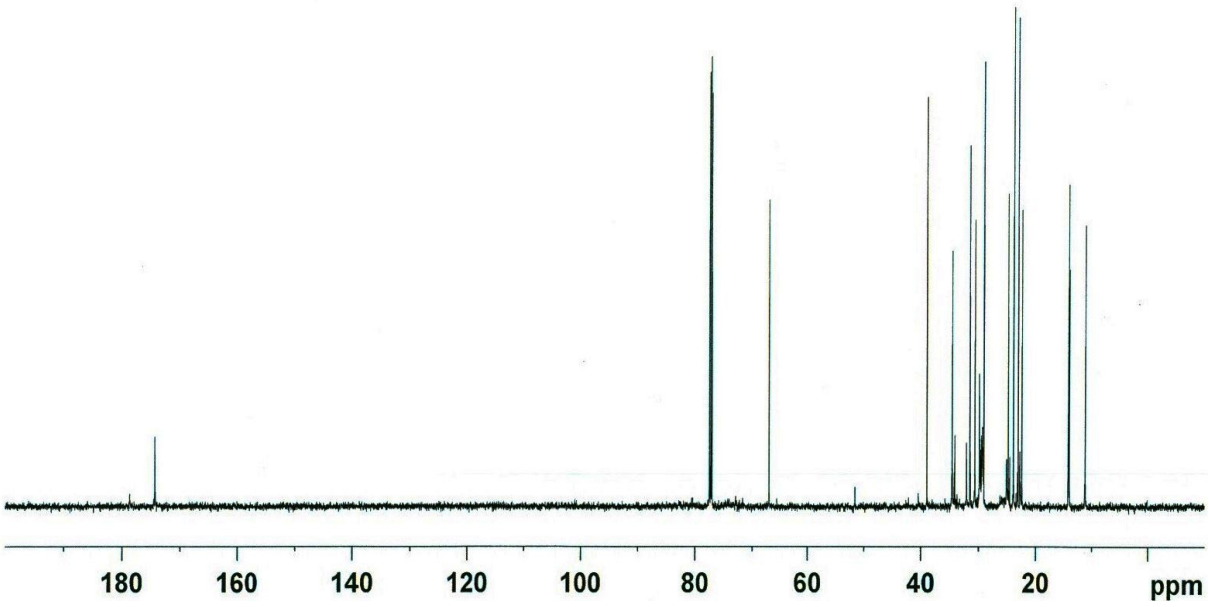

Figure A.19: ^{13}C-NMR spectra of WCOFAME hexanoylation

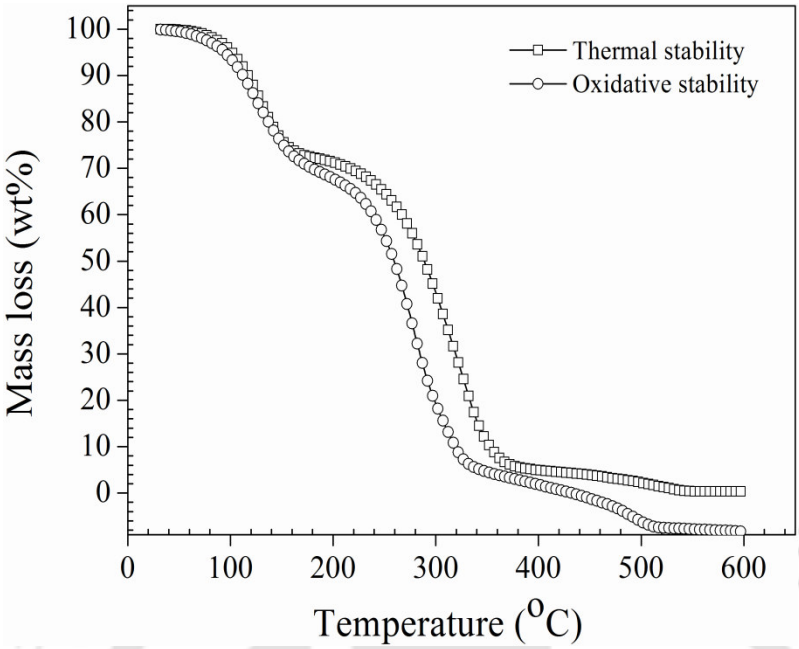

Figure A.20: Thermo-oxidative stability thermo-grams for WCOFAME hydroxylated product

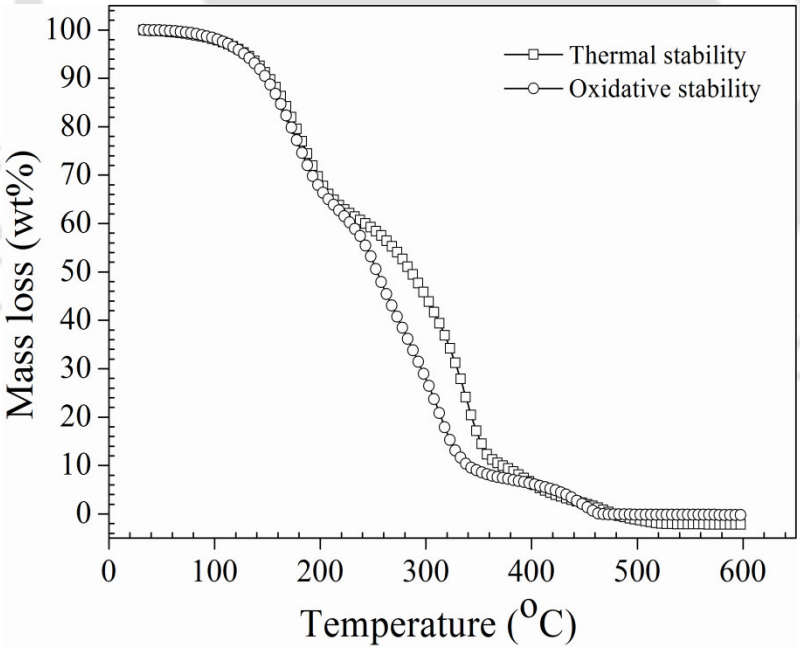

Figure A.21: Thermo-oxidative stability thermo-grams for WCOFAME hexanoylated product

Table A.3: Experimental design matrix and results of high FFA CO epoxidation

Run No	Time (hr)	Temperature (^oC)	Catalyst Loading (wt%)	H_2O_2 Molar Ratio (mol)	Oxygen Oxirane Content (OOC)
1.	2	50	10	1	1.97
2.	4	50	10	1	3.08
3.	2	70	10	1	2.02
4.	4	70	10	1	1.62
5.	2	50	20	1	1.9
6.	4	50	20	1	2.36
7.	2	70	20	1	1.36
8.	4	70	20	1	0.32
9.	2	50	10	2	2.41
10.	4	50	10	2	3.59
11.	2	70	10	2	1.14
12.	4	70	10	2	0.84
13.	2	50	20	2	2.96
14.	4	50	20	2	3.51
15.	2	70	20	2	1.11
16.	4	70	20	2	0.16
17.	1	60	15	1.5	2.96
18.	5	60	15	1.5	3.11
19.	3	40	15	1.5	3.2
20.	3	80	15	1.5	0.01
21.	3	60	5	1.5	1.99
22.	3	60	25	1.5	1.26
23.	3	60	15	0.5	1.39
24.	3	60	15	2.5	1.66
25.	3	60	15	1.5	3.82
26.	3	60	15	1.5	3.84
27.	3	60	15	1.5	3.82
28.	3	60	15	1.5	3.85
29.	3	60	15	1.5	3.79
30.	3	60	15	1.5	3.821

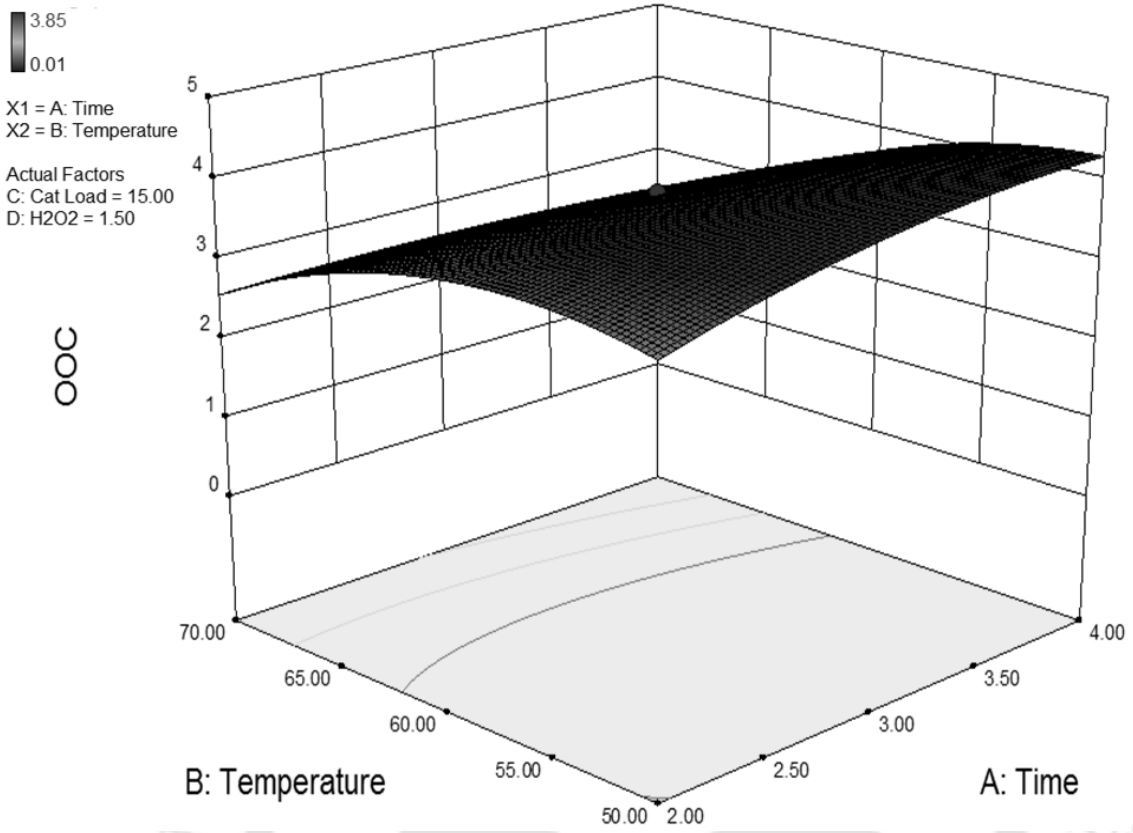

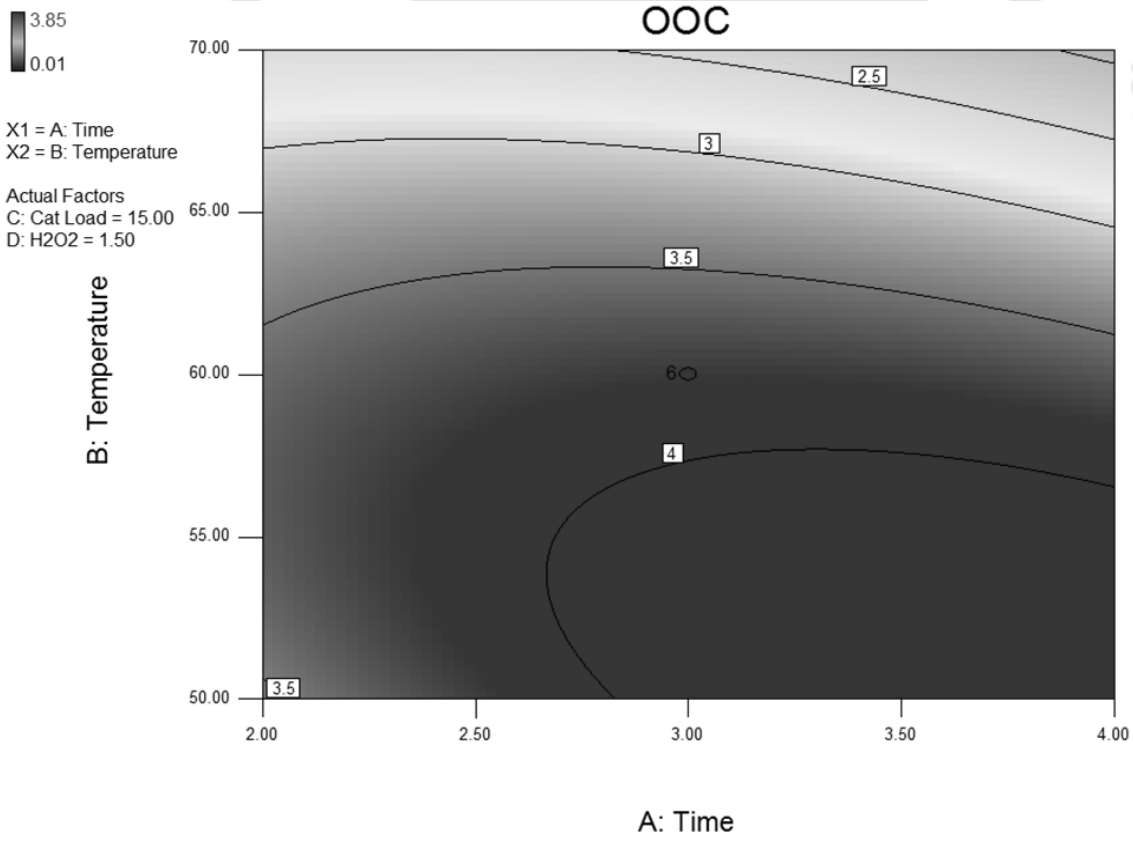

Figure A.22: Response surface (a) and counter (b) plots for the effect of time (A) and temperature (B) for maximum OOC

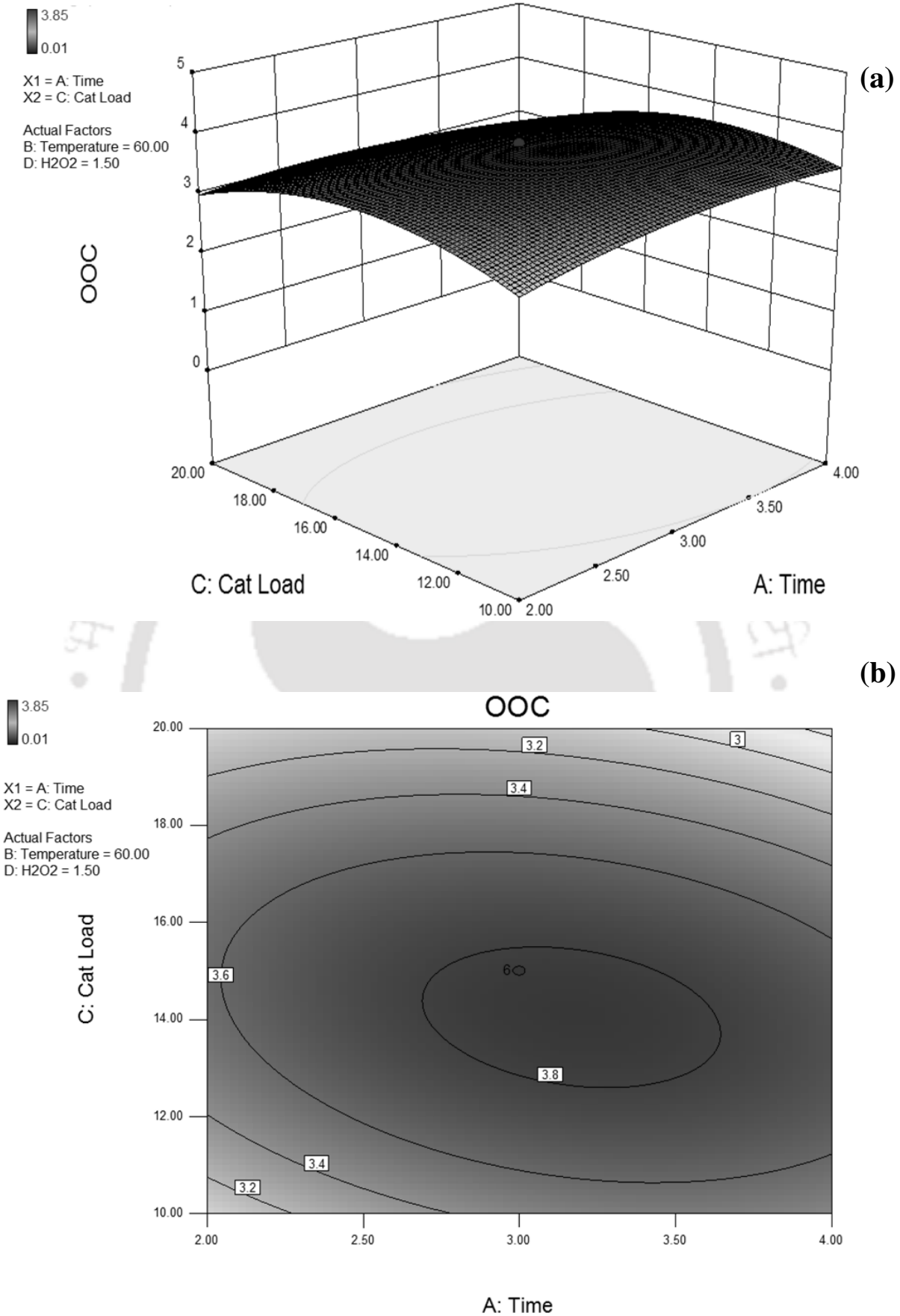

Figure A.23: Response surface (a) and counter (b) plots for the effect of time (A) and catalyst loading (C) for maximum OOC

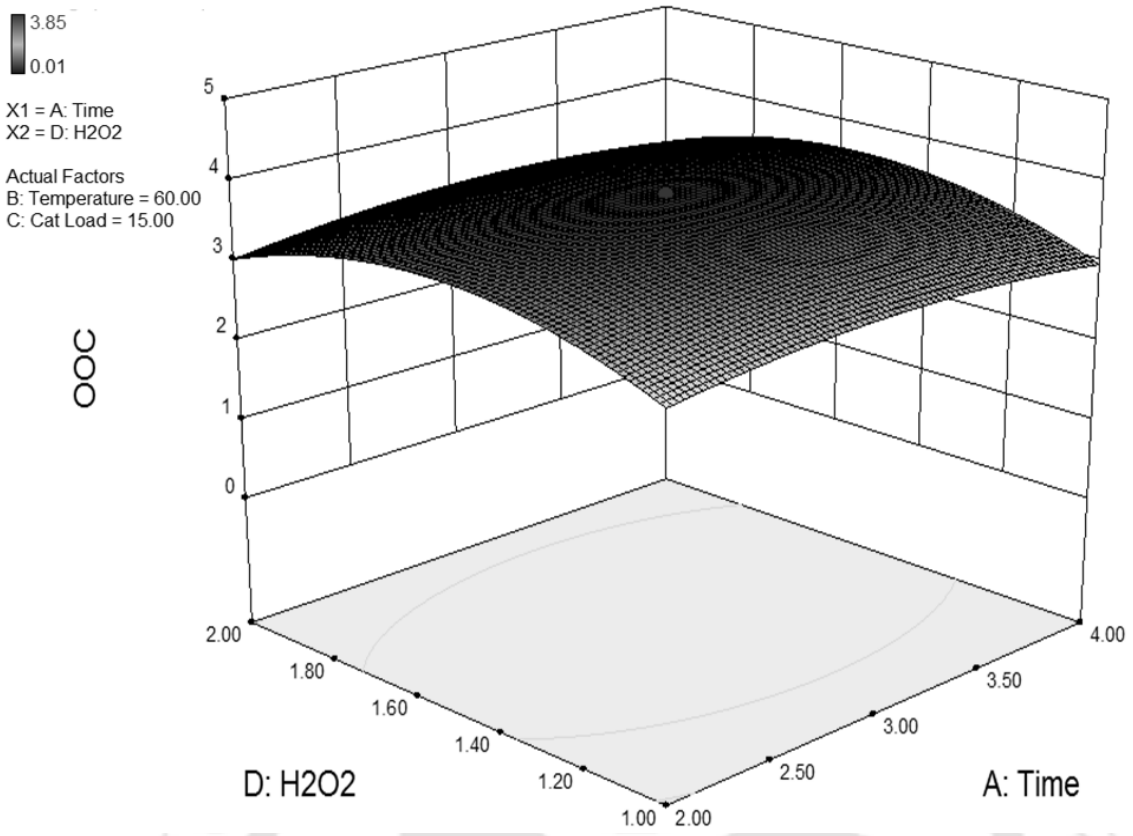

(a)

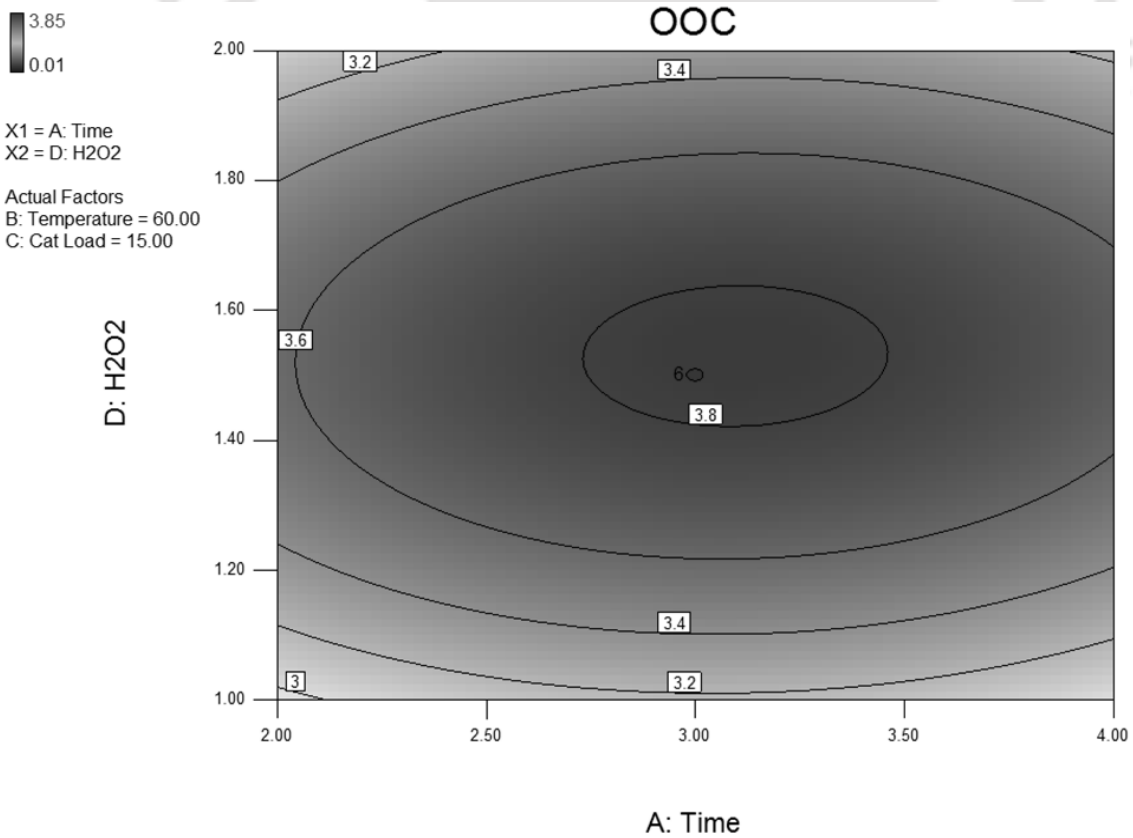

(b)

Figure A.24: Response surface (a) and counter (b) plots for the effect of time (A) and hydrogen peroxide molar ratio (D) for maximum OOC

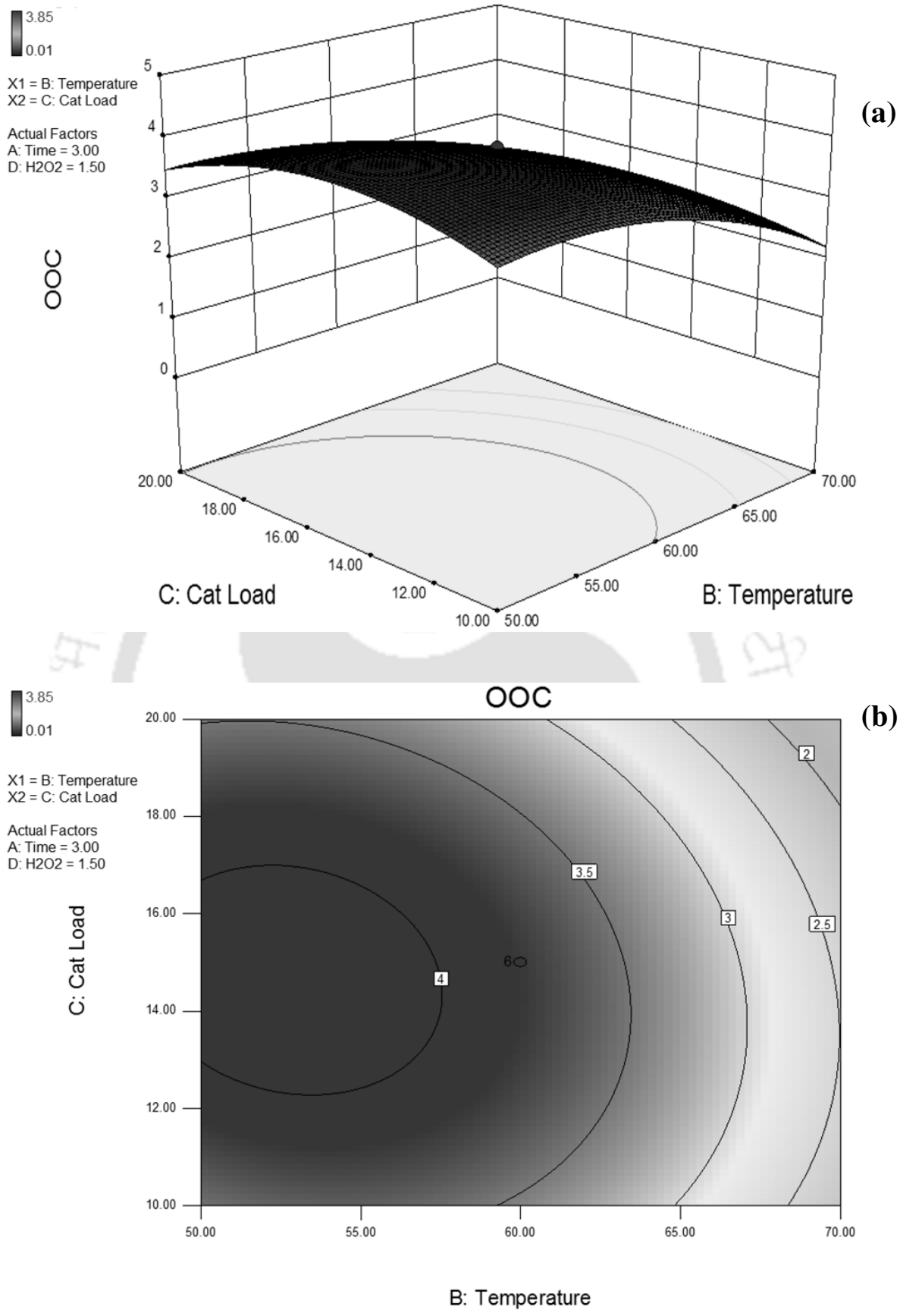

Figure A.25: Response surface (a) and counter (b) plots for the effect of temperature (B) and catalyst loading (C) for maximum OOC

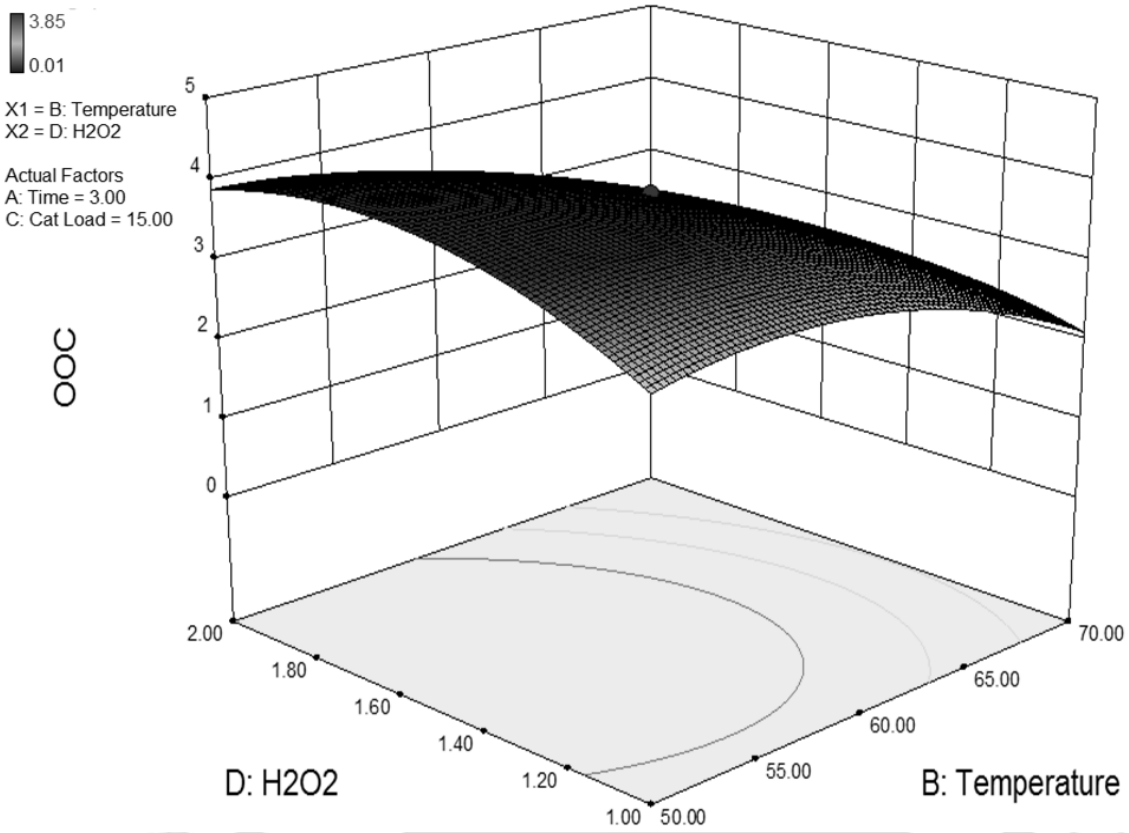

(a)

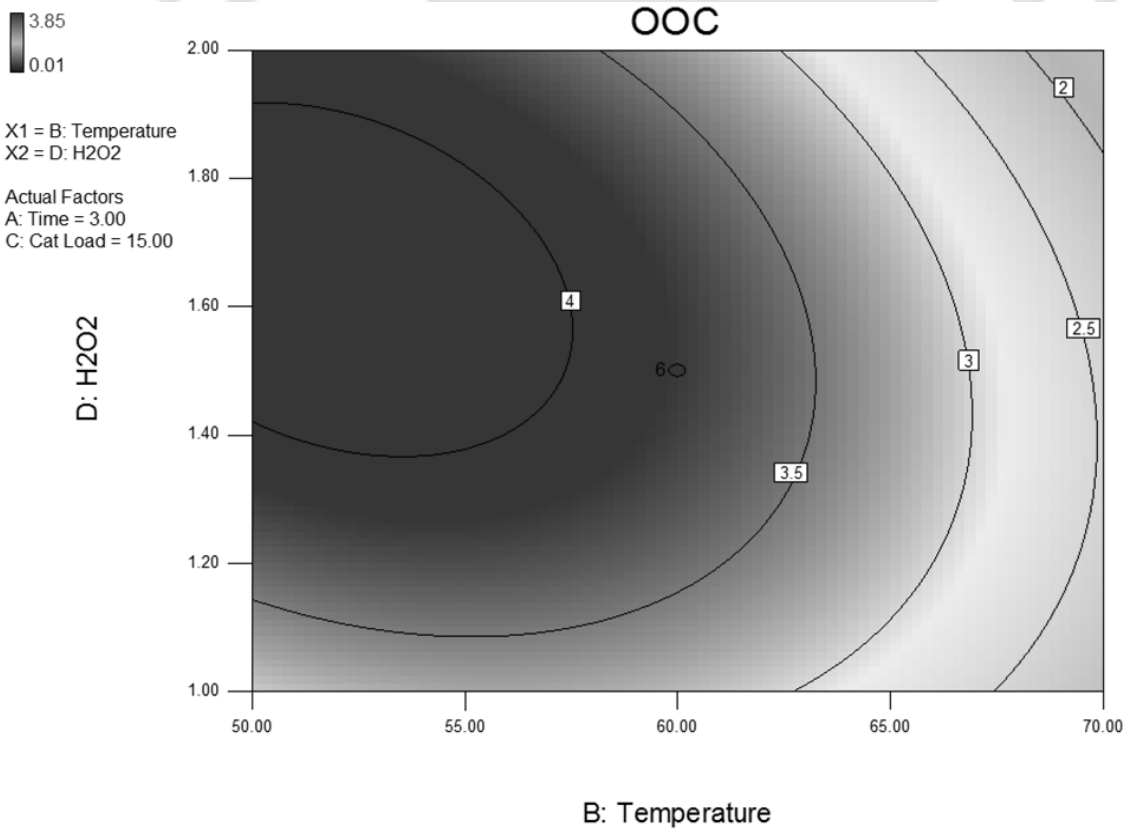

(b)

Figure A.26: Response surface (a) and counter (b) plots for the effect of temperature (B) and hydrogen peroxide molar ratio (D) for maximum OOC

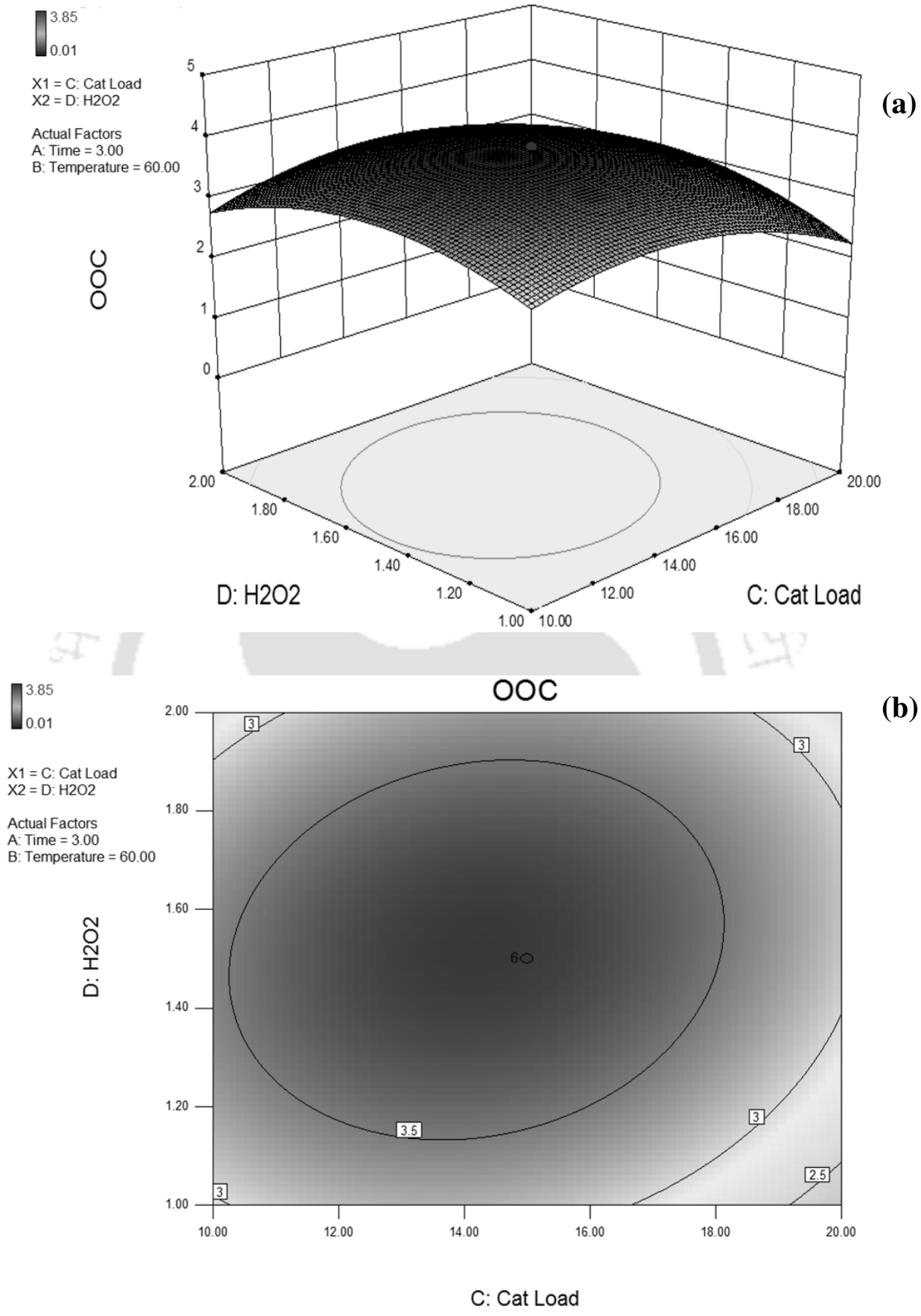

Figure A.27: Response surface (a) and counter (b) plots for the effect of catalyst loading (C) and hydrogen peroxide molar ratio (D) for maximum OOC

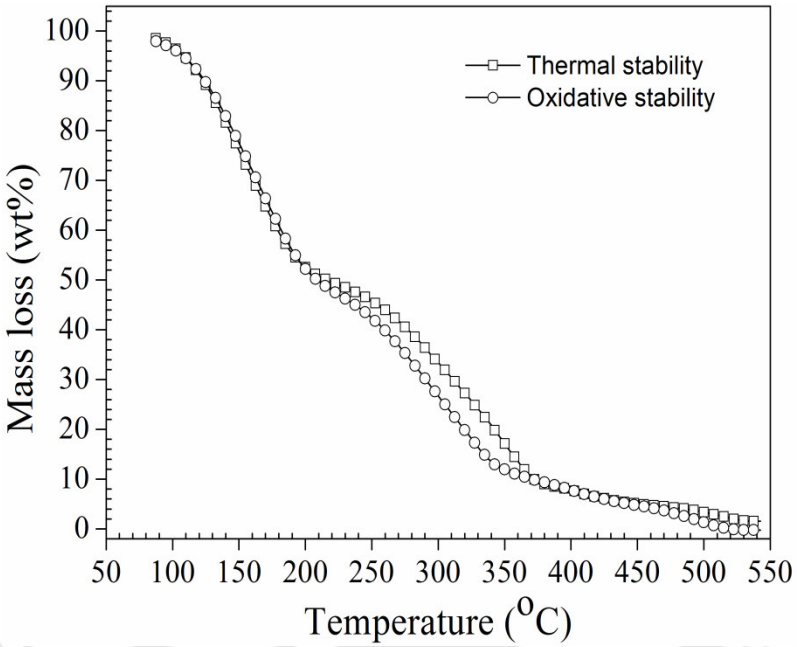

Figure A.28: Thermo-oxidative stability thermo-grams of CO hydroxylated product

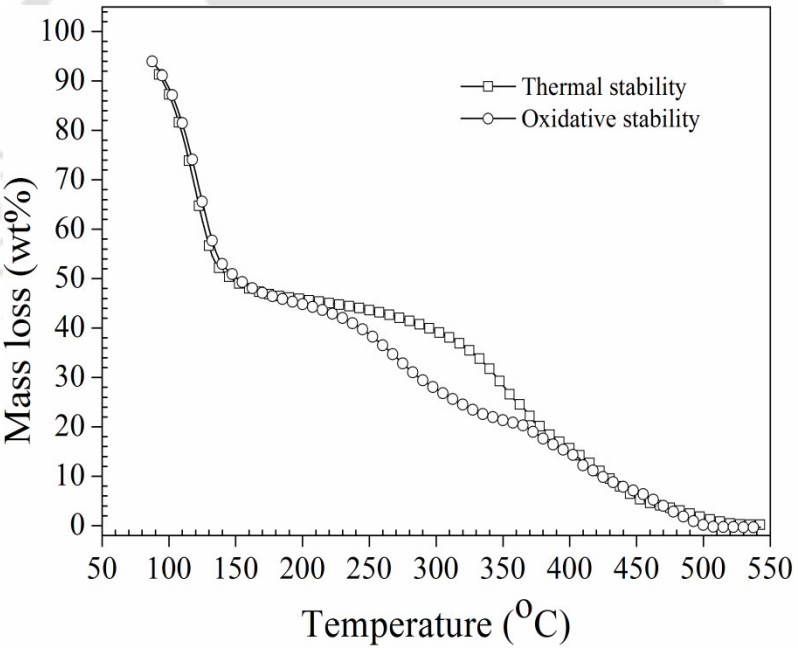

Figure A.29: Thermo-oxidative stability thermo-grams of CO hexanoylated product

Table A.4: Experimental design matrix for optimization of COFAME epoxidation

Run No	Time (A, h)	Catalyst Loading (B, wt%)	H_2O_2 Ratio (C, mol)	Temperature (D, ^oC)	Oxirane Oxygen Content (OOC)
1.	3.3	10	1.5	50	3.27
2.	5.3	10	1.5	50	4.26
3.	3.3	20	1.5	50	3.46
4.	5.3	20	1.5	50	4.03
5.	3.3	10	2.5	50	2.75
6.	5.3	10	2.5	50	3.63
7.	3.3	20	2.5	50	4.01
8.	5.3	20	2.5	50	4.44
9.	3.3	10	1.5	70	3.55
10.	5.3	10	1.5	70	3.03
11.	3.3	20	1.5	70	2.42
12.	5.3	20	1.5	70	1.47
13.	3.3	10	2.5	70	3.38
14.	5.3	10	2.5	70	2.74
15.	3.3	20	2.5	70	3.31
16.	5.3	20	2.5	70	2.31
17.	2.3	15	2	60	3.51
18.	6.3	15	2	60	3.43
19.	4.3	5	2	60	3.60
20.	4.3	25	2	60	3.27
21.	4.3	15	1	60	3.41
22.	4.3	15	3	60	3.67
23.	4.3	15	2	40	3.52
24.	4.3	15	2	80	1.59
25.	4.3	15	2	60	4.01
26.	4.3	15	2	60	4.01
27.	4.3	15	2	60	4.02
28.	4.3	15	2	60	4.01
29.	4.3	15	2	60	4.01
30.	4.3	15	2	60	4.01

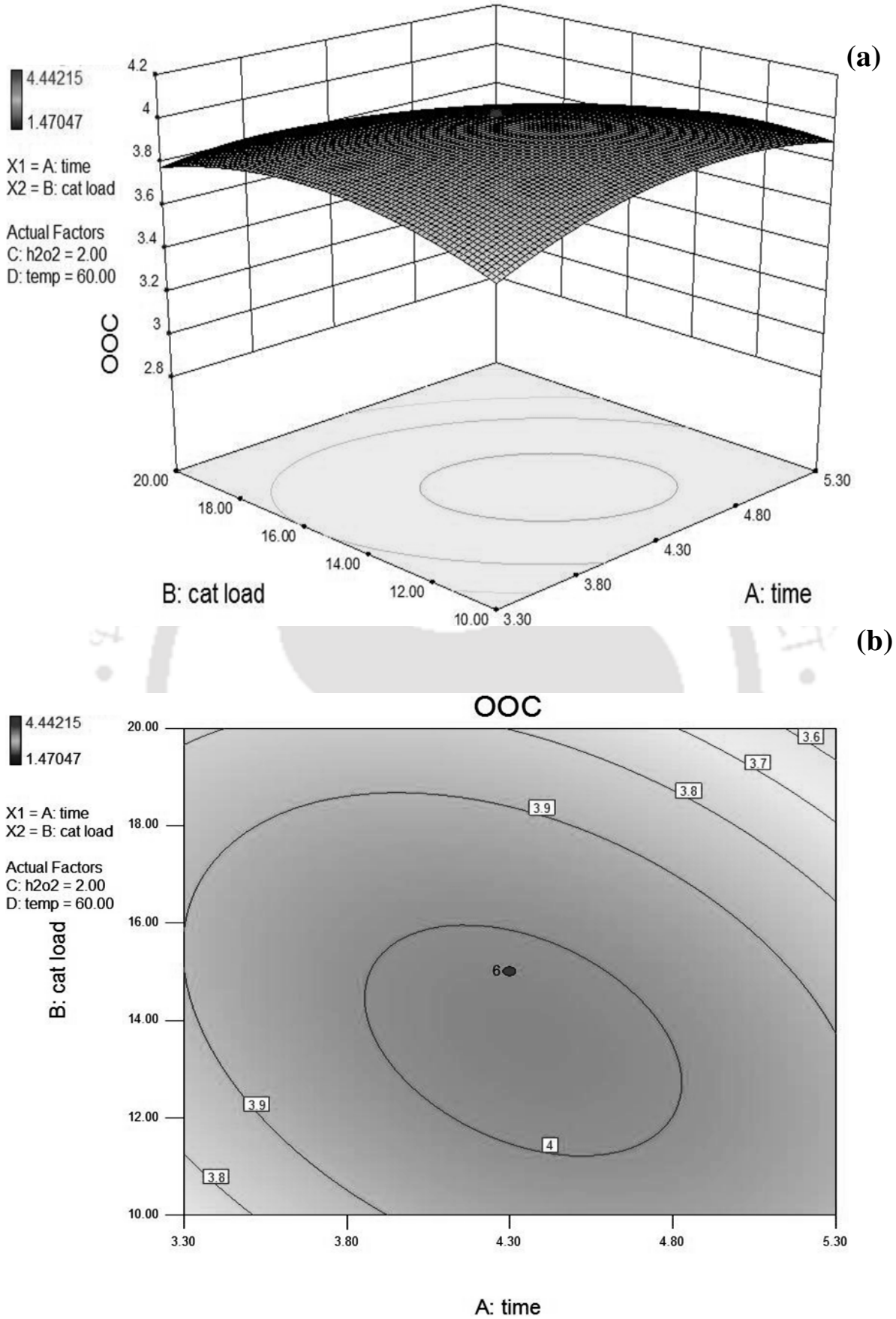

Figure A.30: Response surface (a) and counter (b) plots for the effect of time (A) and catalyst loading (B) for maximum OOC

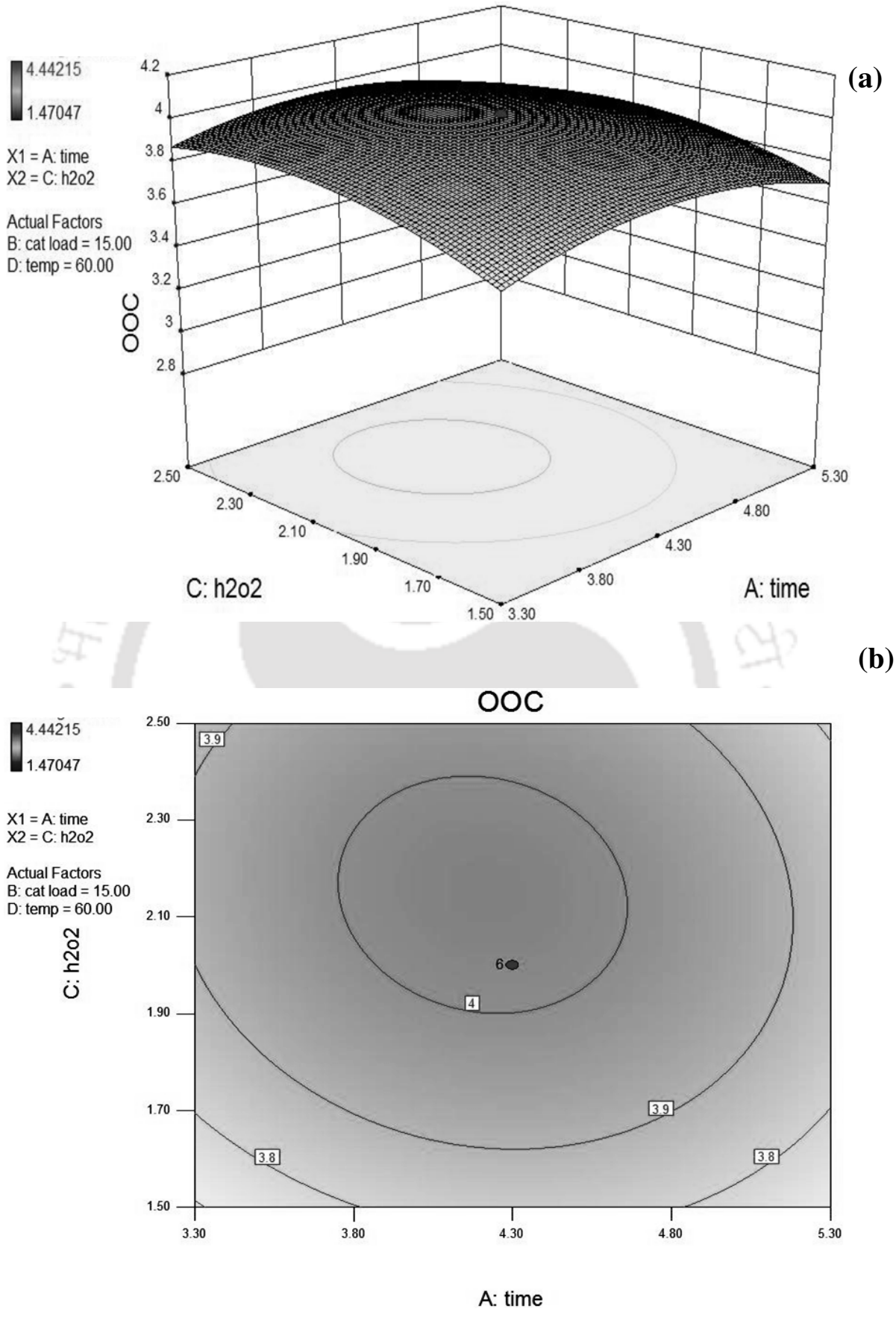

Figure A.31: Response surface (a) and counter (b) plots for the effect of time (A) and hydrogen peroxide molar ratio (C) for maximum OOC

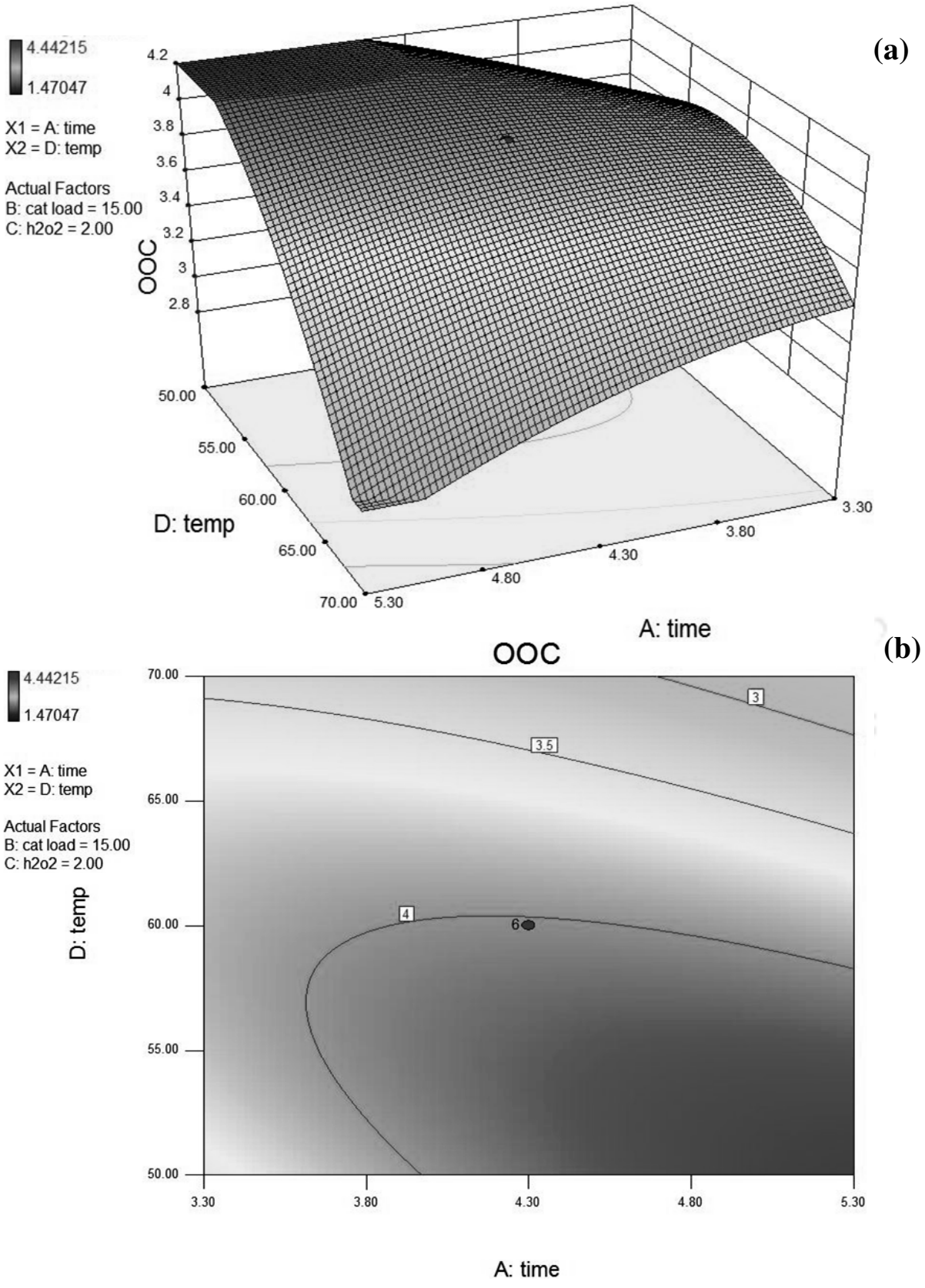

Figure A.32: Response surface (a) and counter (b) plots for the effect of time (A) and temperature (D) for maximum OOC

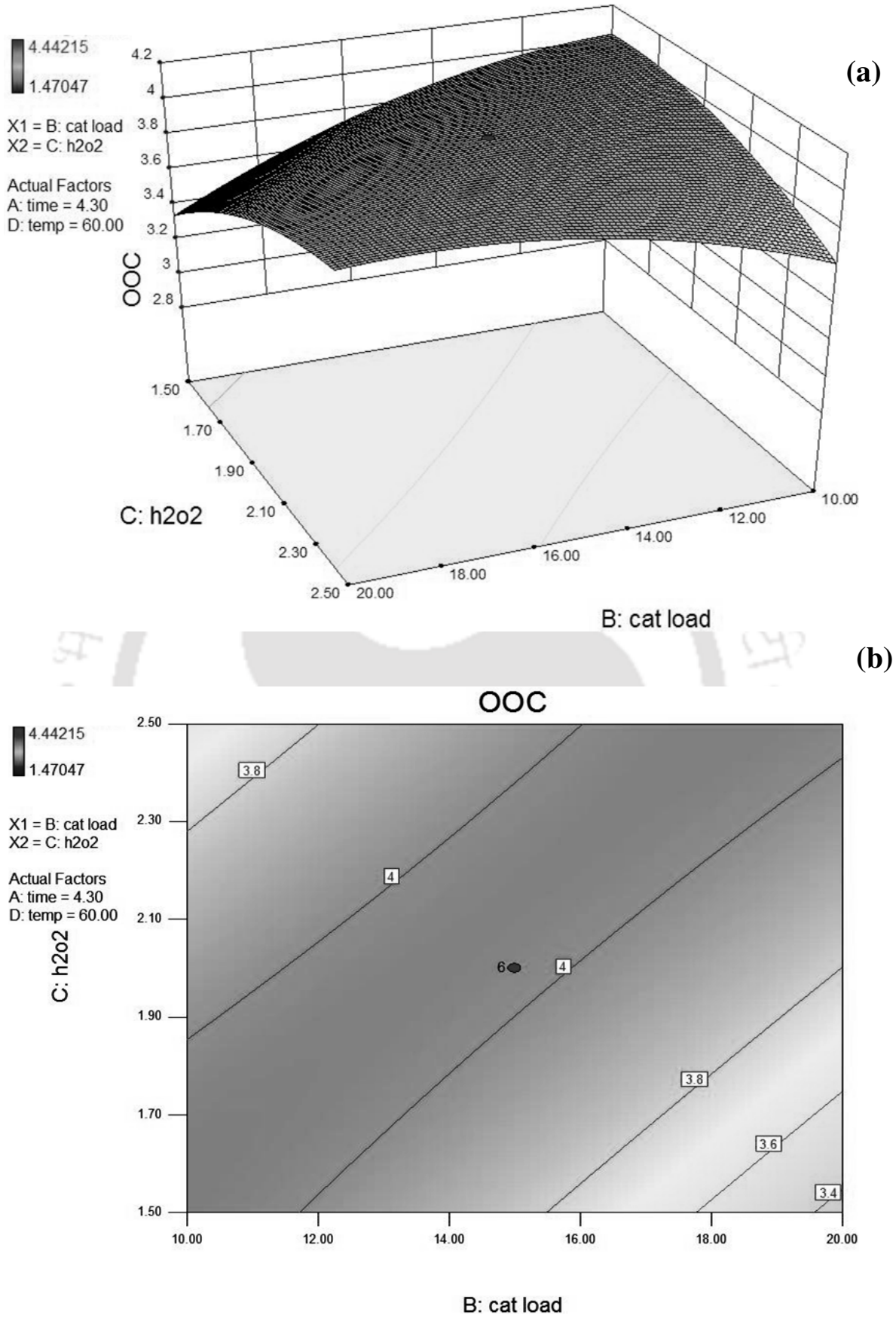

Figure A.33: Response surface (a) and counter (b) plots for the effect of catalyst loading (B) and hydrogen peroxide molar ratio (C) for maximum OOC

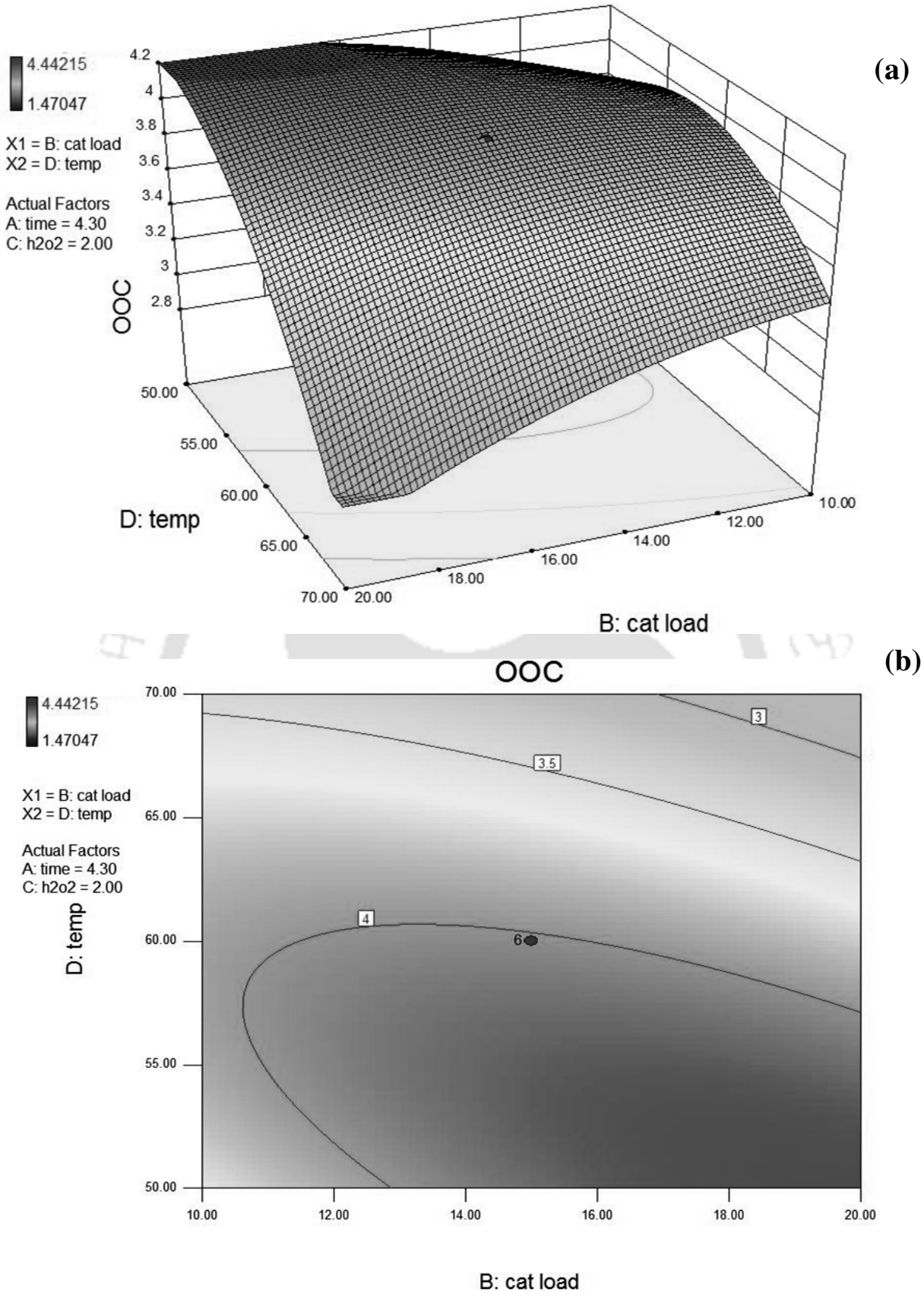

Figure A.34: Response surface (a) and counter (b) plots for the effect of catalyst loading (B) and temperature (D) for maximum OOC

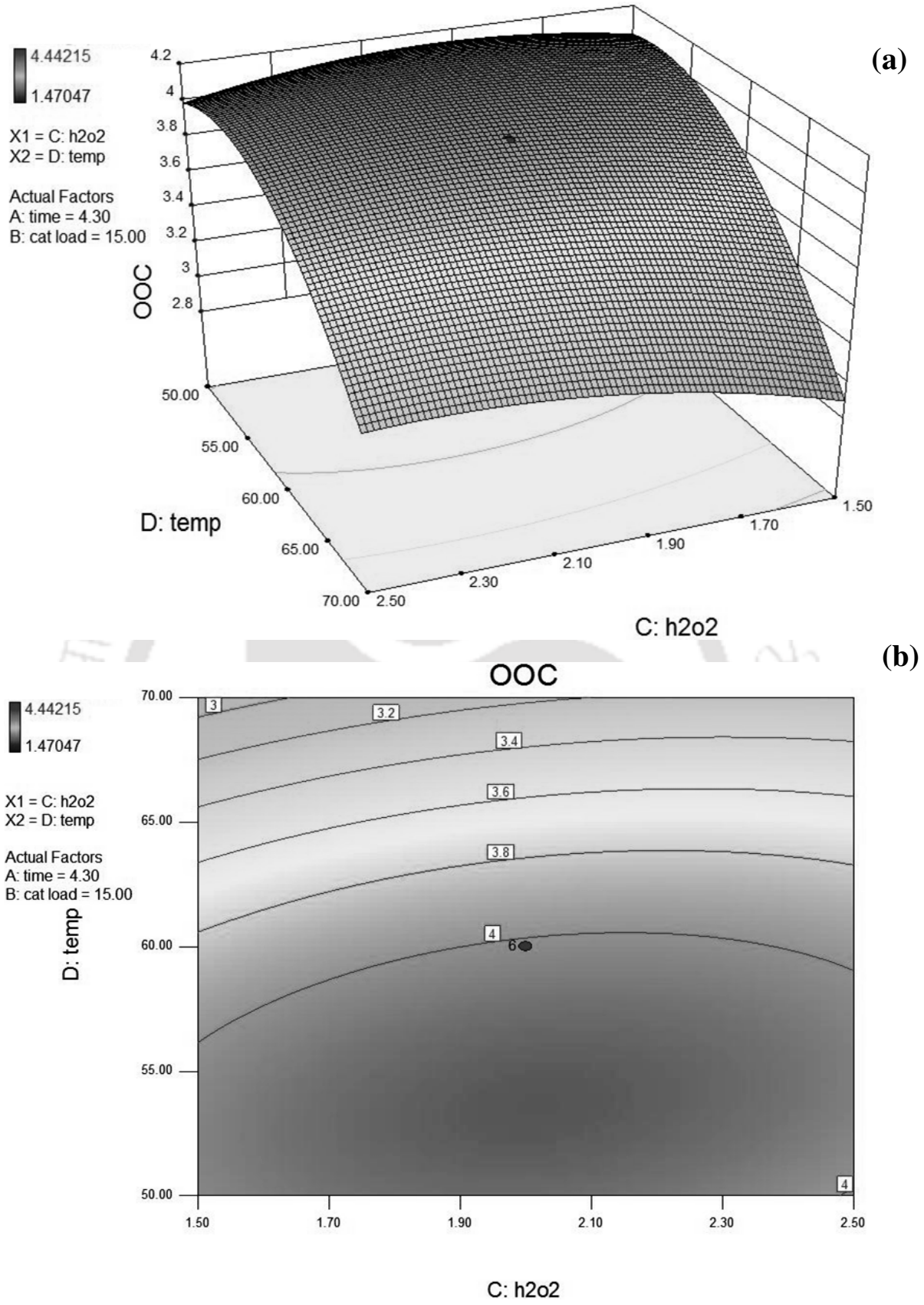

Figure A.35: Response surface (a) and counter (b) plots for the effect of hydrogen peroxide molar ratio (C) and temperature (D) for maximum OOC

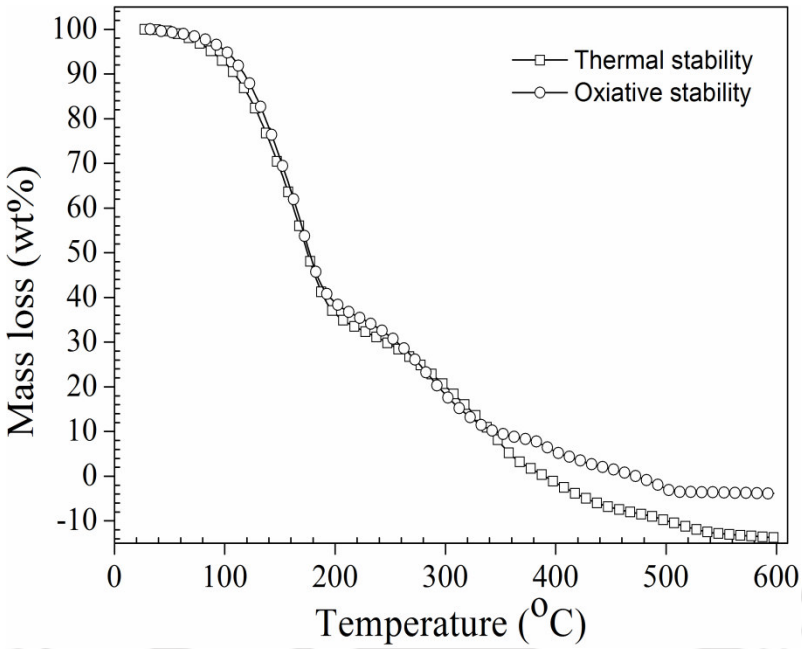

Figure A.36: Thermo-oxidative stability thermo-grams for COFAME hydroxylated product

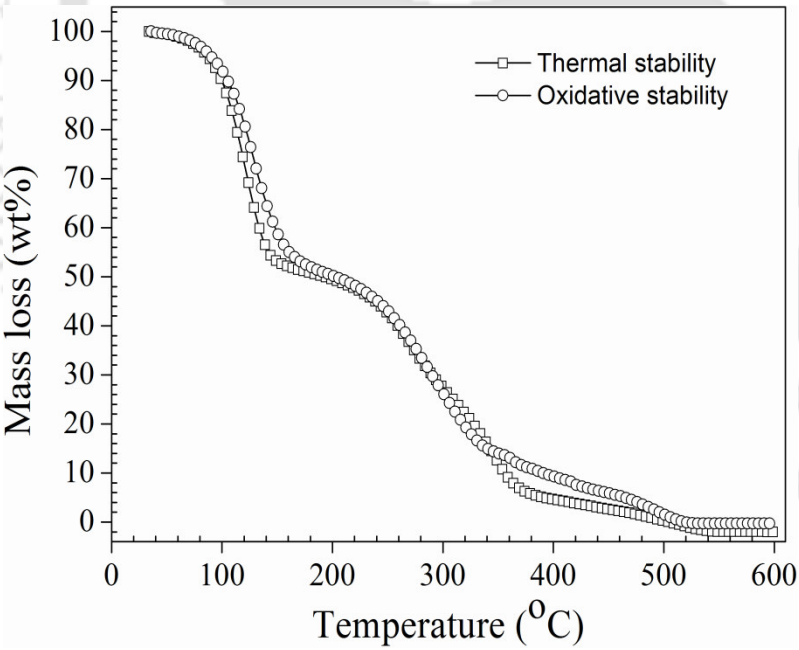

Figure A.37: Thermo-oxidative stability thermo-grams for COFAME hexanoylated product

Book Chapters:

1. Swapan K. Achar, **Venu Babu Borugadda**, Vaibhav V. Goud (2013) Feedstocks: Production Practices, Technologies and Environmental Impacts (Energy Science, Engineering and Technology). Chapter 2. Ultrasonic-Assisted Transesterification of High Free Fatty Acid Karanja Oil. NOVA publishers, ISBN: 978-1-62948-156-2, 47-72.

2. Swapan K. Achar, Swaroopa Rani Dasari, **Venu Babu Borugadda**, Vaibhav V Goud. Environmental Sustainability - Role of green technologies, P.Thangavel, Sridevi G, Comparative studies on thermal, oxidative and low temperature properties of biodiesel prepared from oils of different origin, Springer (Accepted).

Journal Publications:

1. **Venu Babu Borugadda**, Vaibhav V Goud (2012) Biodiesel production from renewable feedstocks: Status and opportunities. Renew Sustain Energy Rev 16:4763–4784.

2. **Venu Babu Borugadda**, Vaibhav V. Goud (2013) Comparative studies of thermal, oxidative and low temperature properties of waste cooking oil and castor oil. J Renew Sustain Energy 5:1-14.

3. **Venu Babu Borugadda**, Vaibhav V. Goud (2014) Thermal, oxidative and low temperature properties of methyl esters prepared from oils of different fatty acids composition: A comparative study. Thermochimica Acta 577:33–40.

4. **Venu Babu Borugadda**, Vaibhav V. Goud (2014) Epoxidation of castor oil fatty acid methyl esters (COFAME) as a lubricant base stock using heterogeneous ion-exchange resin (IR-120) as a catalyst. Energy Procedia 54:75-84.

5. **Venu Babu Borugadda**, Vaibhav V. Goud (2014) Synthesis of waste cooking oil epoxide as a bio-lubricant base stock: characterization and optimization study. J Bioprocess Eng Biorefinery 3:57-72.

6. **Venu Babu Borugadda**, Vaibhav V. Goud (2015) Response surface methodology for optimization of bio-lubricant base stock synthesis from high free fatty acids castor oil. Energy Sci Eng 3:371-383.

7. **Venu Babu Borugadda**, Vaibhav V. Goud (2015) Improved Low Temperature Properties of Chemically Modified High Free Fatty Acid Castor Oil Methyl Esters: Blending and Optimization Study. J Energy Eng 04015020:1-10.

8. **Venu Babu Borugadda**, Vaibhav V. Goud (2015) Improved thermo-oxidative stability of structurally modified waste cooking oil methyl esters for bio-lubricant application. J Clean Prod (Accepted).

9. **Venu Babu Borugadda**, Vaibhav V. Goud (2015) In-situ epoxidation of castor oil using heterogeneous acidic ion-exchange resin catalyst (IR-120) for bio-lubricant application. Tribol. Online 10:1-6.

10. **Venu Babu Borugadda**, Vaibhav V. Goud (2015) Physico-chemical and rheological characterization of waste cooking oil epoxide and their blends. Waste and Biomass Valorization (Accepted).

11. Purabi Mazumdar, **Venu Babu Borugadda**, Vaibhav V. Goud, Lingaraj Sahoo (2012) Physico-chemical characteristics of Jatropha curcas L. of North East India for exploration of biodiesel. Biomass and Bioenergy 46:546-554.

12. Purabi Mazumdar, **Venu Babu Borugadda**, Vaibhav V. Goud, Lingaraj Sahoo (2013) Effect of storage parameters on stability of Jatropha-derived biodiesel. Int J Energy Environ Eng 4:13.

13. Purabi Mazumdar, Swaroopa Rani Dasari, **Venu Babu Borugadda**, Garima Srivasatava, L. Sahoo, Vaibhav V. Goud (2013) Biodiesel production from high free fatty acids content Jatropha curcas L. oil using dual step process. Biomass Convers Biorefinery 3:361-369.

Manuscripts to be communicated:

1. **Venu Babu Borugadda**, Ashish J. Chaudhary, Vaibhav V. Goud (2015) Experimental study on exhaust emissions and diesel engine performance fuelled with blends of waste cooking oil biodiesel (Under Review).
2. **Venu Babu Borugadda**, Vaibhav V. Goud (2015) Bio-lubricants derived from waste cooling oil and its methyl esters with improved thermo-oxidative stability and cold flow properties: Tribological and Bio-degradability study.
3. **Venu Babu Borugadda**, Vaibhav V. Goud (2015) Long term storage stability of epoxides derived from vegetable oils and their methyl esters.
4. **Venu Babu Borugadda**, Vaibhav V. Goud (2015) Synthesis di-estersd from castor oil and its methyl esters with improved cold flow properties: Tribological and Bio-degradability study**.**
5. **Venu Babu Borugadda**, Atanu Kumar Paul, Vaibhav V. Goud (2015) Optimization of the

product parameters for waste cooking oil lubricant basestock and physico-chemical characterization of the product.

Conference Presentations (National/International):

1. **Venu Babu Borugadda**, Vaibhav V Goud (2011) "Biodiesel production from high free fatty acid karanja and jatropha curcas oil" 3rd International Congress on Green Process Engineering, 5 - 8th December, University of Malaya, Malaysia.

2. **Venu Babu Borugadda**, Vaibhav V Goud (2011) "Evaluation and comparison of thermal, oxidative and low temperature properties of vegetable oils (WCO, CO) as base oil for lubricant application" Indian Chemical Engineering Congress (CHEMCON-2011), 27-29th December, M. S. Ramaiah Institute of Technology, Bangalore, India.

3. **Venu Babu Borugadda**, Vaibhav V. Goud (2012) "Synthesis of biodegradable lubricant basestock from epoxidised used cooking oil" Recent Advances in Chemical Engineering, 4th Febraury, Maharashtra University, Jalgaon, India (First Prize and Best Paper).

4. **Venu Babu Borugadda**, Vaibhav V. Goud (2013) "Process optimization of WCO Epoxidation using Liquid inorganic acid as catalyst (H_2SO_4)" Bioenergy, Environment and Sustainable Technologies (BEST-2013) 27-30th January, Arunai Engineering College, Tiruvannamalai, India.

5. **Venu Babu Borugadda**, Swaroopa Rani Dasari and Vaibhav V. Goud (2013) "Comparative Studies of Thermo-oxidative and cold flow Properties of Methyl Esters Prepared from Waste cooking oil and castor oil" Reflux-1, Annual chemical engineering festival, 6-7th April, 2013, IIT Guwahati, Guwahati, India (First Prize and Best Paper).

6. **Venu Babu Borugadda**, Vaibhav V. Goud (2013) "Castor oil fatty acid methyl esters (FAME) epoxidation by RSM design using heterogenous catalyst (IR-120)" 9th World Chemical Engineering Congress, WCCE9 & APCChE, 18-23rd August, Seoul Korea.

7. **Venu Babu Borugadda**, Vaibhav V. Goud (2013) "Synthesis of Castor oil Bio-diesel and evaluation of thermo-oxidative stability intended to use as base oil for lubricant application" Student's Chemical Engineering Congress (SCHEMCON-2013), 14-15th September, MVGR College of Engineering, Vizianagaram, India.

8. **Venu Babu Borugadda**, Vaibhav V. Goud (2013) "Synthesis of bio-lubricant base stock via epoxidation of waste cooking oil using ion-exchange resin as a catalyst" Presented for MP Chary Memorial Award, Student's Chemical Engineering Congress (SCHEMCON-2013), 14-15th September, MVGR College of Engineering, Vizianagaram, India.

9. **Venu Babu Borugadda**, Vaibhav V. Goud (2013) "Synthesis of epoxidised castor oil fatty acid methyl esters (COFAME) as a lubricant base stock using ion exchange resin (IR-120) as a catalyst" 4th International Conference on Advances in Energy Research, 10-12th December, IIT Mumbai, Mumbai, India.

10. **Venu Babu Borugadda**, Vaibhav V. Goud (2014) "Epoxidation of castor oil using IR-120 as heterogeneous catalyst and process optimization" Advances in sustainable polymers (ASP-14), 10-11th January, IIT Guwahati, Guwahati, India.

11. **Venu Babu Borugadda**, Vaibhav V. Goud (2014) "In-situ epoxidation of castor oil using heterogeneous acidic ion-exchange resin catalyst (IR-120) for Bio-lubricant application" Asiatrib – 2014, Tribology Society of India, 17-20th Febraury, Agra, India.

12. **Venu Babu Borugadda**, Vaibhav V. Goud (2014) "Waste cooking oil as an inexhaustible raw material for biodiesel production: characterization, optimization and engine study"

Reflux-2 2014, Annual chemical engineering festival, 29-30th March, IIT Guwahati, Guwahati, India.

13. **Venu Babu Borugadda**, Vaibhav V. Goud (2014) "In-situ epoxidation of waste cooking oil methyl esters and assessment of thermal and oxidative stability" GPE-4th International Congress on Green Process Engineering, 7-10th 2014, April, Sevilla, Spain.

14. **Venu Babu Borugadda**, Vaibhav V. Goud (2014) "Structural modification of waste cooking oil using heterogeneous catalyst (IR-120) for Bio-lubricant application" WasteEng Conference 2014, 24 -29th August, Rio de janeiro, Brasil.

15. **Venu Babu Borugadda**, Vaibhav V. Goud (2015) "Synthesis of lubricant base stock from high free fatty acid based castor oil: Process optimization and product characterization" Advances in Sustainable Polymers (ASP- 2015), 21-22nd January, IIT Guwahati, Guwahati, India.

16. **Venu Babu Borugadda**, Vaibhav V. Goud (2015) "Synthesis of bio-degradable lubricant base stock from high free fatty acid castor oil: Process optimization and product characterization" Annual chemical engineering festival, Reflux-3 2015, 27-29th March, IIT Guwahati, Guwahati, India.

17. **Venu Babu Borugadda**, Vaibhav V. Goud (2015) "Long term storage stabilityof Jatropha derived biodiesel: Effect of environment" workshop on Frontier energy research with industry academia partnership Centre for energy, 20-21st March, IIT Guwahati, Guwahati, India.

18. Atanu Kumar Paul, **Venu Babu Borugadda**, Vaibhav V. Goud (2015) "Study of rheological property of rubber seed oil (RSO) with its methyl ester and blends" Science, Technology and Innovation, 10-11th Sept. 2015, Guwahati University, Guwahati, India.

Chapter 1:

Introduction and Literature Review

Background;

State-of-the-art;

Objectives;

Organization of thesis;

Borugadda VB and Goud VV (2012) Renew Sustain Energy Rev 16:4763-4784

Chapter 2:

Experimental and Characterization

Feedstocks preparation;

Physico-chemical characterization methods;

Chapter 3:

Estimation of Thermo-oxidative Stability and Cold Flow Properties of Feedstocks

Feedstocks characterization;

Evaluation of performance properties;

Borugadda VB and Goud VV (2013) J Renew Sustain Energy 5:1-14

Borugadda VB and Goud VV (2014) Thermochimica Acta 577:33–40

Chapter 4:

Formulation of Bio-lubricant Basestocks via Structural Modifications of Waste Cooking Oil

Bio-lubricant basestocks from WCO;

Optimization of WCO epoxidation process parameters;

Physico-chemical characterization of prepared basestocks;

Borugadda VB and Goud VV (2014) J Bioprocess Eng Biorefin 3:57-72

Borugadda VB and Goud VV (2015) Waste Biomass Valor (Accepted)

Chapter 5:

Modifications of Waste Cooking Oil Methyl Esters for the Production of Bio-lubricant Basestocks

Bio-lubricant basestocks from WCOFAME;

Optimization of WCOFAME epoxidation process parameters;

Physico-chemical characterization of prepared basestocks;

Borugadda VB and Goud VV (2015) J Clnr Prod (Accepted)

Chapter 6:

Synthesis of Bio-lubricant Basestocks from Castor Oil Containing High Levels of Free Fatty Acids

Bio-lubricant basestocks from high FFA CO;

Optimization of high FFA CO epoxidation process parameters;

Physico-chemical characterization of prepared basestocks;

Borugadda VB and Goud VV (2015) Energy Sci Eng 3:371-383

Borugadda VB and Goud VV (2015) Tribol Online 10:1-6

Chapter 7:

Preparation of Biodegradable Lubricant Basestocks from Castor Oil Fatty Acid Methyl Esters

Bio-lubricant basestocks from COFAME;

Optimization of COFAME epoxidation process parameters;

Physico-chemical characterization of prepared basestocks;

Borugadda VB and Goud VV (2014) Energy Procedia 54:75-84

Borugadda VB and Goud VV (2015) J Energy Eng 04015020:1-10

Chapter 8:

Comparative Analysis of the Prepared Bio-lubricant Basestocks with Conventional Lubricants

Bi-lubricant basestocks versus conventional lubricants;

Through study on performance properties;

Chapter 9:

Overall Conclusions and Future Scope

Concluding remarks;

Appendix

List of Publications

References